Universitat Ramon Llull

DOCTORAL THESIS

Title TRANSTHYRETIN FAMILIAL AMYLOID POLYNEUROPATHY: NOVEL THERAPEUTICS DERIVED FROM DRUG REPURPOSING AND NEW INSIGHTS IN DIAGNOSIS THROUGH PROTEOMIC ANALYSIS OF CLINICAL SAMPLES

Presented by Marta Vilà Rico

Centre IQS School of Engineering

Department Bioengineering

Directed by Dr. Francesc Canals and Dr. Antoni Planas

C. Claravall, 1-3
08022 Barcelona
Tel. 936 022 200
Fax 936 022 249
E-mail: urlsc@sec.url.es
www.url.es

“Everything will be okay in the end. If it’s not okay, it’s not the end”

John Lennon

ACKNOWLEDGEMENTS

En primer lloc m'agradaria donar les gràcies als meus directors de tesi, el Dr. Antoni Planas i el Dr. Francesc Canals. Toni, gràcies per haver confiat en mi des del principi i haver-me permès entrar al projecte TTR per realitzar la meva tesi de màster i, més tard, per embarcar-me en l'aventura del doctorat. Gràcies pels teus raonaments crítics i comentaris al llarg de la tesi, amb ells he pogut créixer no només professionalment sinó també de manera personal. Francesc, gràcies per obrir-me les portes del teu laboratori i del teu despatx, per estar sempre disponible als meus dubtes i preguntes, pels teus consells i per escoltar-me sempre amb un somriure pacient. Amb tu he après tot el que sé sobre proteòmica.

Gràcies a tots els membres del laboratori de proteòmica de Vall d'Hebron amb els qui he tingut el gran plaer de coincidir. Núria, des del primer dia em vas introduir al món de la proteòmica i sempre has estat allà amb un somriure per recolzar-me en els moments més difícils i celebrar amb mi les alegries i bons resultats. Gràcies per la paciència i per estar sempre disponible per donar-me un cop de mà, aquesta tesi també és teva. Luna, gracias por tu constante apoyo y alegría, por mostrarte siempre disponible para ayudarme, por tus ganas y por los momentos de risas. Al igual que Núria, esta tesis también es tuya. Marta, gràcies a tu també, perquè tot i no treballar juntes en el mateix projecte ha estat un gran plaer poder coincidir amb tu al laboratori. Gràcies pels teus consells, per escoltar-me i pels bons moments viscuts. Núria, Luna i Marta, perquè a part de companyes de laboratori heu estat amigues, em sento molt agraïda d'haver-vos conegut i de saber que tot i que la meva tesi ha acabat vosaltres continuareu formant part de la meva vida! Gràcies també al Joanjo, la Gemma, la Laura, l'Anna i la Carolina, pels moments de riure al voltant de la cafetera i el calaix de xocolata!

Gràcies també al laboratori de bioquímica de l'IQS. Magda, gràcies per escoltar-me i per ser sempre allà amb un somriure. Patri, gràcies per tota l'ajuda durant aquests anys de màster i de doctorat. Xevi, gràcies pels teus comentaris sempre útils i per estar sempre disponible a ajudar-me. Carles, Sergi, Victòria, Cristina, Marta M, Estela, Hugo, Ellen, Isadora, Tania, Anabella... gràcies pels moments de riure, els moments spotify, els dinars a la terrassa i els moments de teràpia! Perquè sempre és més fàcil treballar quan el riure està assegurat! Ha estat un plaer haver coincidit amb vosaltres. Gràcies també a tota la resta de membres del laboratori amb els que he coincidit, ha estat un plaer.

Un especial agraïment als membres del consorci TTR, per introduir-me al món de la TTR i per permetre'm formar part d'aquest grup tant especial. Gemma, Gregori, Jordi, Dani, Nuria, gràcies pels vostres comentaris, aportacions i reflexions, amb vosaltres he après tot el que sé de la que jo anomeno, "la meva proteïna", la TTR. Ha estat un plaer poder treballar amb vosaltres.

Gràcies també al servei d'espectrometria de masses de l'IRB, dirigit per la Dra. Marta Vilaseca, per permetre'm venir al vostre laboratori pels experiments de top-down. Gràcies Marta pel temps que m'has dedicat pacientment i per introduir-me al món del top-down. Gràcies també a la Marina i la Mar per tota l'ajuda rebuda!

Carles, Bego y Kiko gracias por los momentos de risas, las horas de terapia y nuestro humor negro sobre la vida del doctorando. Con vosotros ha sido más fácil vivir estos años: tapas, pádel, catán, juegos en general, voley playa, fallas, mudanzas con calor asfixiante, bailes en la alfombra, karaoke... Mil gracias chicos! Carles y Bego, espero con ganas vuestro gran día! Y a los tres, ya lo sabéis, tenéis casa allí dónde yo vaya!

Biotecs!! Gràcies a vosaltres també, perquè en el fons, tots junts vam començar l'aventura ja fa molt… el 2005!!! Gràcies pels bons moments viscuts i per les trobades al llarg del temps tot i que a vegades és difícil coincidir o estem temps sense veure'ns, els retrobaments (o els e-mails jeje) són sempre insuperables!

Finalment, i no per això menys importants, tot el contrari, m'agradaria donar les gràcies a la meva família. Mama, gracias por estar siempre a mi lado, por darme fuerzas, escucharme y apoyarme siempre, por tus ánimos, tus consejos y tu fuerza. Sin ti no habría llegado hasta aquí ni sería quien soy, de eso estoy segura. Esta tesis es también tuya. Abuela, gracias por preocuparse siempre por mi, por darme siempre ánimos y cuidarme tanto. Xavi, gràcies per les teves bromes i el teu bon humor. Per ajudar-me sempre en tot el que has pogut, preocupar-te per mi i pel teu suport. Emilio, aunque quizás no lo sepas, gracias por enseñarme que la vida no se debe tomar tan en serio y que es mejor no preocuparse demasiado por las cosas. Michaël, thank you for your support during the last 5 years, for accepting my dreams and for helping me to achieve them. Thanks for being patient with me, for listening to me and for making me forget about my worries each time I'm with you.

SUMMARY

Transthyretin (TTR) is an amyloidogenic tetrameric protein (55kDa) present in human plasma, transporting T4 hormone and retinol, through the retinol binding protein (RBP). TTR is associated with several amyloidosis, namely familial amyloidotic polyneuropathy (FAP), familial amyloidotic cardiomyopathy (FAC) and senile systemic amyloidosis (SSA). Variability of TTR is not only due to point mutations in the encoding gene but also to post-translational modifications (PTMs) at Cys-10, the most common PTMs being the S-Sulfonation (S-Sulfo), S-Glycinylcysteinylation (S-CysGly), S-Cysteinylation (S-Cys) and S-Glutathionylation (S-GSH). It is thought that PTMs at Cys-10 may play an important biological role in the onset and pathological process of amyloidosis related to TTR.

We have aimed TTR amyloidosis from two different perspectives i) Therapeutic interventions and ii) FAP diagnosis and monitoring. Regarding the first part of the project, we have performed the screening of a library of 41 possible fibrillogenesis inhibitors selected by a bioinformatic repurposing workflow, finding 4 new TTR tetramer stabilizers and thus, new potential candidates for TTR amyloidosis treatment.

Concerning the diagnostic approach of this work, we have developed a methodology for quantification of PTMs in serum samples, as well as for the determination of serum TTR levels, from healthy (wt) and TTR-amyloidotic (V30M mutation) individuals. It involves an enrichment step by immunoprecipitation followed by mass spectrometry analysis of (i) the intact TTR protein and (ii) targeted LC-MS analysis of peptides carrying the PTMs of interest. Analysis of serum samples by the combination of the two methods affords complementary information on the relative and absolute amounts of the selected TTR PTM forms. It is shown that methods based on intact protein are biased for specific PTMs since they assume constant response factors, whereas the novel targeted LC-MS method provides absolute quantification of PTMs and total TTR variants. The reported methodology has been applied to two different sets of clinical samples. As a result of the study of human samples of FAP patients at different disease stages, we preliminary pointed out S-GSH and S-CysGly isoforms as biomarkers of disease progression, allowing the differentiation between FAP stage 0 and 1 and therefore indicating disease onset. Through the analysis of a time series from FAP patients having undergone liver transplantation (LT) and from domino liver transplantation (DLT) recipients from V30M carriers, we have characterized the progression of the wt:V30M ratios, as well as the evolution of the Cys-10 PTMs, from transplantation and up to 9 years after. Additionally, we have observed significant differences in the levels of S-GSH and S-CysGly when comparing liver and domino liver transplanted patients, analogous to the results obtained in the comparison of wt individuals and FAP stage 0 patients.

SUMARI

La transtirretina (TTR) és una proteïna tetramèrica amiloidogènica (55 kDa) present al plasma humà i responsable del transport de la hormona T4 i del retinol a través de la proteïna d'unió a retinol (RBP). La proteïna TTR està associada amb diverses amiloïdosis, concretament la polineuropatia amiloide familiar (FAP), la cardiomiopatia amiloide familiar (FAC) i l'amiloïdosi senil sistèmica (SSA). La variabilitat associada a la TTR es deu tant a mutacions puntuals al gen codificant per aquesta com a modificacions post-traduccionals (PTMs) al residu Cys-10. Les PTMs més comuns associades a la Cys-10 de la TTR són la S-Sulfonació (S-Sulfo), la S-Glicinilcisteinilació (S-CysGly), la S-Cisteinilació (S-Cys) i la S-Glutationilació (S-GSH). Es creu que dites PTMs associades a la Cys-10 podrien jugar un paper biològic important en l'inici i procés patològic de les diferents amiloïdosis lligades a TTR.

Hem tractat les amiloïdosis lligades a TTR des de dues perspectives diferents i) Intervencions terapèutiques i ii) Diagnòstic i monitorització de FAP. Referent a la primera part del projecte, hem portat a terme el cribratge de 41 possibles inhibidors de fibril·logènesis seleccionats mitjançant estratègies bioinformàtiques de *repurposing* de fàrmacs. Com a resultat de l'estudi, s'han trobat 4 nous estabilitzadors del tetràmer de TTR i, per tant, nous candidats pel tractament d'amiloïdosis lligades a TTR.

Pel que fa a l'aproximació diagnòstica d'aquest treball, hem desenvolupat una metodologia per a la quantificació de PTMs en mostres de sèrum, així com per a la determinació dels nivells de TTR en aquest, tant en individus sans (wt) com en individus portadors de TTR amiloïdogènica (mutació V30M). Dita metodologia consisteix en una primera etapa d'enriquiment en TTR mitjançant immunoprecipitació, seguit de l'anàlisi de la TTR per espectrometria de masses de i) la proteïna intacta i ii) els pèptids de TTR portadors de les PTMs d'interès mitjançant l'anàlisi dirigit per LC-MS. L'anàlisi de les mostres de sèrum per la combinació d'ambdues estratègies aporta informació sobre la quantificació relativa i absoluta de les diferents PTMs presents a la TTR. Ha sigut possible mostrar que els mètodes basats en proteïna intacta es troben esbiaixats per algunes de les PTMs, donat que assumeixen un factor de resposta constant per les diferents isoformes. Contràriament, el nou mètode de LC-MS dirigit permet la quantificació absoluta de les diferents PTMs i els nivells totals de TTR (wt i mutant). La metodologia reportada ha sigut aplicada en l'anàlisi de dos grups de mostres clíniques. Com a resultat de l'estudi de mostres humanes de pacients de FAP en els diferents estadis de la malaltia, suggerim de forma preliminar les isoformes S-GSH i S-CysGly com a biomarcadors de progressió de la malaltia, permetent la diferenciació entre pacients en estadi 0 i 1 i, per tant, indicant l'aparició de la malaltia. Mitjançant l'anàlisi de mostres de pacients de FAP a diferents temps després de sotmetre's a un transplantament de fetge (LT) i de pacients receptors de transplantament de fetge dominó provinent d'individus portadors de la mutació V30M, hem caracteritzat la progressió de la relació wt:V30M, així com l'evolució dels nivells de PTMs a la Cys-10, des de la intervenció fins a 9 anys després. Addicionalment, hem observat diferències significatives en els nivells de S-GSH i S-CysGly en comparar pacients de LT i DLT, resultats anàlegs als obtinguts en la comparació d'individus wt (sans) i pacients de FAP en estadi 0.

SUMARIO

La transtirretina (TTR) es una proteína tetramérica amiloidogénica (55 kDa) presente en el plasma humano y la responsable del transporte de la hormona T4 y el retinol, a través de la proteína de unión al retinol (RBP). La proteína TTR está asociada con varias amiloidosis, concretamente la polineuropatía amiloide familiar (FAP), la cardiomiopatía amiloide familiar (FAC) y la amiloidosis senil sistémica (SSA). La variabilidad encontrada en la TTR se debe tanto a mutaciones puntuales encontradas en el gen que codifica para ésta como a modificaciones post-traduccionales (PTMs) en el residuo Cys-10. Las PTMs más comunes asociadas a la Cys-10 de la TTR son la S-Sulfonación (S-Sulfo), la S-Glicinilcisteinilación (S-CysGly), la S-Cisteinilación (S-Cys) y la S-Glutationilación (S-GSH). Se cree que dichas PTMs asociadas a la Cys-10 podrían jugar un papel biológico importante en el inicio y proceso patológico de las distintas amiloidosis ligadas a TTR.

Hemos abordado las amiloidosis ligadas a TTR desde dos perspectivas distintas i) Intervenciones terapéuticas y ii) Diagnóstico y monitorización de FAP. Respecto a la primera parte del proyecto, hemos llevado a cabo el cribado de 41 posibles inhibidores de fibrilogenesis seleccionados mediante estrategias bioinformáticas de *repurposing* de fármacos. De este modo, se han encontrado 4 nuevos estabilizadores del tetrámero de TTR y por tanto, nuevos candidatos para el tratamiento de amiloidosis ligadas a TTR.

En relación a la aproximación diagnóstica de este trabajo, hemos desarrollado una metodología para la cuantificación de PTMs en muestras de suero, así como para la determinación de los niveles de TTR en éste, tanto en individuos sanos (wt) como en individuos portadores de TTR amiloidogénica (mutación V30M). Dicha metodología consiste en una primera etapa de enriquecimiento en TTR mediante immunoprecipitación, seguido por el análisis de ésta mediante espectrometría de masas de i) la proteína TTR intacta y ii) de los péptidos de TTR portadores de las PTMs de interés mediante análisis dirigido por LC-MS. El análisis de muestras de suero mediante la combinación de ambas estrategias aporta información sobre la cuantificación relativa y absoluta de las distintas PTMs en TTR. Ha sido posible mostrar que los métodos basados en proteína intacta se encuentran sesgados para algunas de las PTMs, dado que asumen un factor de respuesta constante para las distintas isoformas. Por el contrario, el nuevo método de LC-MS dirigido permite la cuantificación absoluta de las distintas PTMs y los niveles totales de TTR (wt y mutante). La metodología reportada ha sido aplicada en el análisis de dos grupos de muestras clínicas. Como resultado del estudio de muestras humanas de pacientes de FAP en los distintos estadios de la enfermedad, sugerimos de forma preliminar las isoformas S-GSH y S-CysGly como biomarcadores de progresión de la enfermedad, permitiendo la diferenciación entre pacientes en estadio 0 y 1 y, por lo tanto, indicando la aparición de la enfermedad. Mediante el análisis de muestras de pacientes de FAP a distintos tiempos después de someterse a un trasplante de hígado (LT) y de pacientes receptores de trasplante de hígado dominó proveniente de individuos portadores de la mutación V30M, hemos caracterizado la progresión del ratio wt:V30M así como la evolución de los niveles de PTMs en la Cys-10, des de la intervención hasta 9 años después. Adicionalmente, hemos observado diferencias significativas en los niveles de S-GSH y S-CysGly en comparar pacientes de LT y DLT, resultados análogos a los obtenidos en la comparación de individuos wt (sanos) y pacientes de FAP en estadio 0.

INDEX

PREFACE

This doctoral thesis is structured into a general introduction, four independent chapters, general concluding remarks, and conclusions. Each chapter can be read independently and presents its own introduction, materials and methods, results and discussion, and conclusion. All the references cited within each chapter appear in the References section at the end of each chapter. The general concluding remarks section summarizes the main results and conclusions reached in the four different chapters.

The present dissertation has been possible thanks to the project grant 101431/32 from la Fundació Privada de la Marató de TV3 and the corresponding fellowship from the granted project to the author.

INTRODUCTION

I.1 AMYLOIDOSIS

Amyloidosis is a group of diseases wherein soluble extracellular proteins become insoluble due to folding problems. As a result, those proteins are deposited in form of aggregates in different organs and tissues throughout the body. The misfolding of a protein can take place in parallel or as an alternative pathway to its physiological folding (Fig. I-1) (Knowles et al. 2014, Merlini and Bellotti 2003). This dynamic process generates fibrillar and non-fibrillar aggregates of various sizes that are toxic for the tissue of deposition. Those fibrils are rigid and non-branched and can range from 7.5 to 10 nm in diameter. Amyloid deposits are rich in β-sheet structures and present unique tinctorial properties like apple-green birefringence when viewed under polarised light after staining with Congo red (Fig. I-2) (Westermark et al. 2002).

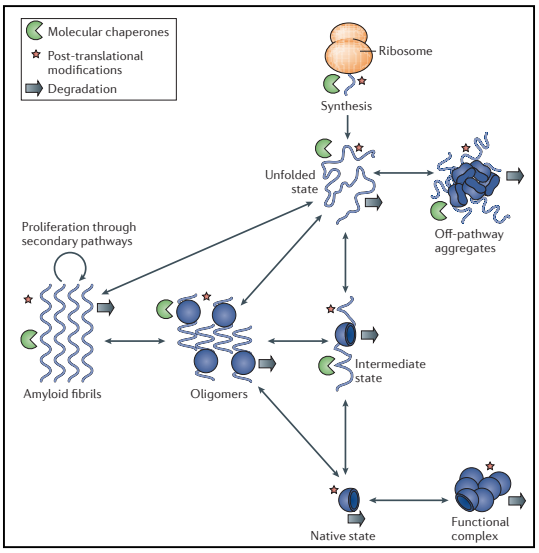

Figure I-1. Different states that a protein can adopt. Many proteins adopt various other biologically relevant conformational states in addition to their native structures. These different conformational states can take place alternatively or in parallel to the native state folding process (Knowles et al. 2014).

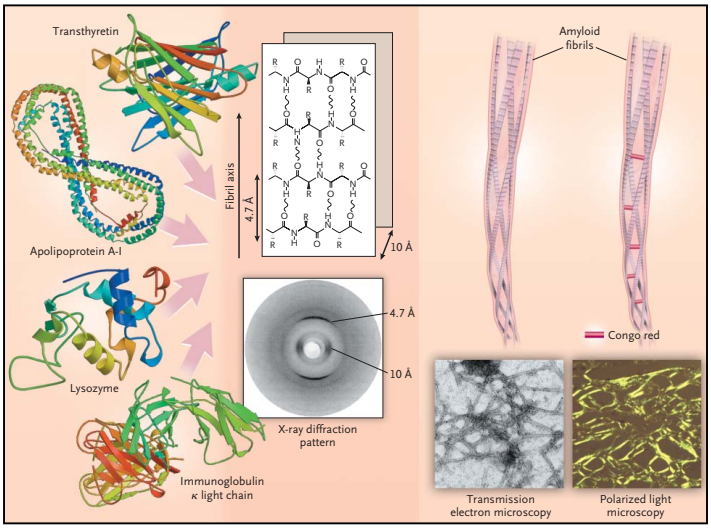

Figure I-2. Structural features of amyloid. The three-dimensional structures of lysozyme, transthyretin, apolipoprotein A-I and immunoglobulin α light chain are shown on the left. In the middle, cross-beta super-secondary structure characterized by x-ray diffraction with prototypical inter-strand and inter-sheet distances of 4.7 and 10 to 13 Å, respectively. Contiguous β-sheet polypeptide chains form a protofilament. Several protofilaments form an amyloid fibril, as shown on the right, with diameters of 7.5 to 10 nm, visible on transmission electron microscopy (x100.000) as seen on the bottom right. In addition, after Congo red staining, amyloid fibrils present apple-green birefringence under polarized light microscopy (bottom right). (Merlini and Bellotti 2003).

There are several proteins associated to amyloid processes leading to high social impact pathologies such as Alzheimer's disease, affecting more than 12 million people all over the world (Merlini and Bellotti 2003). Table I-1 shows the relationship between the different amyloid proteins and its associated disease as well as the affected tissue.

Table I-1. Amyloid proteins and their precursors (Merlini and Bellotti 2003)

Amyloid Protein	Precursor	Distribution	Type	Syndrome or Involved Tissues
Aβ	Aβ protein precursor	Localized Localized	Acquired Hereditary	Sporadic Alzheimer's disease, aging Prototypical hereditary cerebral amyloid angiopathy, Dutch type
APrP	Prion protein	Localized Localized	Acquired Hereditary	Sporadic (iatrogenic) CJD, new variant CJD (alimentary?) Familial CJD, GSSD, FFI
ABri	ABri protein precursor	Localized or systemic?	Hereditary	British familial dementia
ACys	Cystatin C	Systemic	Hereditary	Icelandic hereditary cerebral amyloid angiopathy
Aβ2M	$Beta_2$-microglobulin	Systemic	Acquired	Chronic hemodialysis
AL	Immunoglobulin light chain	Systemic or localized	Acquired	Primary amyloidosis, myeloma-associated
AA	Serum amyloid A	Systemic	Acquired	Secondary amyloidosis, reactive to chronic infection or inflammation including hereditary periodic fever (FMF, TRAPS, HIDS, FCU, and MWS)
ATTR	Transthyretin	Systemic Systemic	Hereditary Acquired	Prototypical FAP Senile heart, vessels
AApoAI	Apolipoprotein A-I	Systemic	Hereditary	Liver, kidney, heart
AApoAII	Apolipoprotein A-II	Systemic	Hereditary	Kidney, heart
AGel	Gelsolin	Systemic	Hereditary	Finnish hereditary amyloidosis
ALys	Lysozyme	Systemic	Hereditary	Kidney, liver, spleen
AFib	Fibrinogen Aα chain	Systemic	Hereditary	Kidney

The conversion of a native structure protein into a predominantly antiparallel β-sheet structure is a pathological process highly related to the physiological protein folding. As it occurs with the native protein, the folding process evolves through a funnel shaped thermodynamic folding energy landscape exploration (Fig. I-3A). The misfolded protein arrives to a conformational state corresponding to a minimum of energy similar to that one reached by the native protein. Therefore, the protein achieves a relatively stable misfolded state, which is prone to aggregation. In addition, once the folding process is completed and the native protein secreted, in many cases, there is a dynamic equilibrium with a partially folded conformation, from which they retrace the final part of the folding pathway to give either the native protein or the misfolded one.

The amyloid state of a protein is also characterized by special thermodynamics. In the native state of a protein amino acid residues interact mainly intramolecularly, while in the amyloid state interactions are generally intermolecular. As it has already been mentioned, the free energy (G) of the peptide or protein molecule in the amyloid state has to be lower than in the native state, since a protein will not spontaneously transition from a state of lower free energy to a state of higher free energy. In the case of the amyloid state, stability is dependent on protein concentration, whereas in the native state is not, unless it exists in a functional complex. For this reason, there is a concentration at which the stability of the amyloid state is the same as that of the native state; that concentration is known as the critical concentration. At concentrations above the critical one, a protein is more stable in the amyloid state than in its native state. In those cases, the native state can only exist if there are high free energy barriers that hinder the transition into the more stable

amyloid state. In such cases, the native state is said to be kinetically metastable (Fig. I-3B) (Knowles et al. 2014).

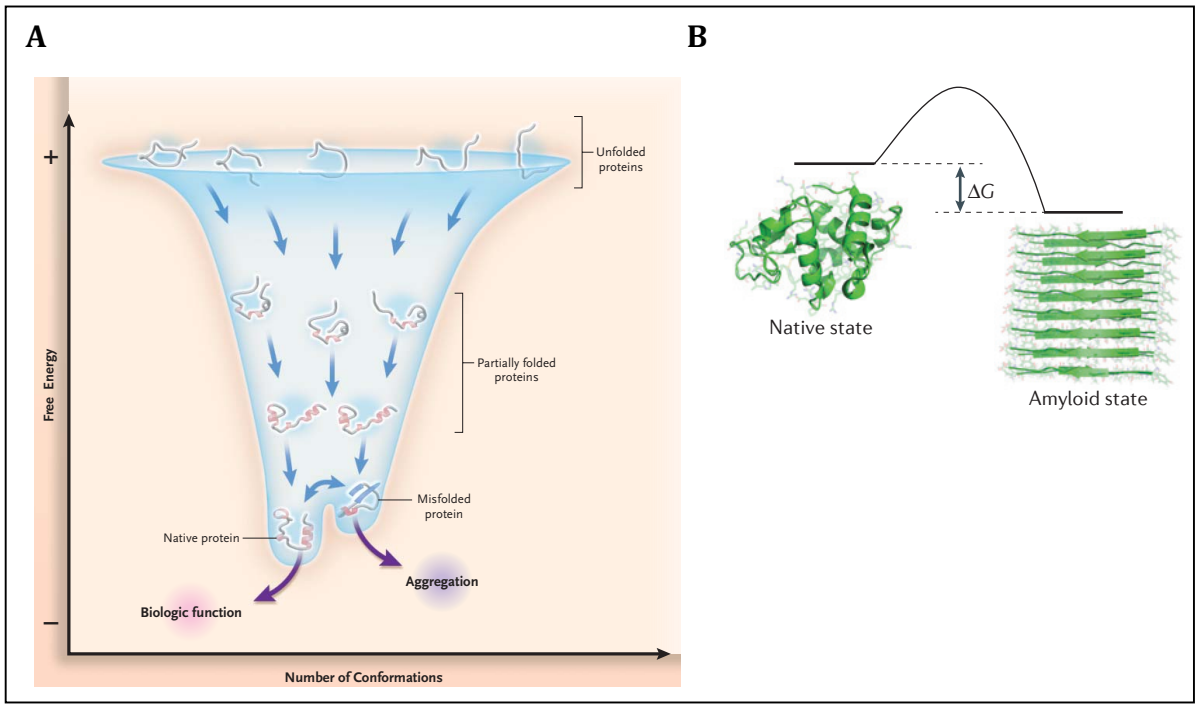

Figure I-3. Amyloid formation. A) The process of protein folding. From a random coil conformation, the unfolded polypeptide enters a funnel-like pathway in which the conformational intermediates become progressively more organized as they merge, resulting in the most stable native state. In this state, there is a minimum of free energy, resulting from the balance between the level of enthalpy (internal energy in folded protein) and the level of conformational entropy (level of randomness of the polypeptide in solution) (Merlini and Bellotti 2003). **B) Thermodynamics of the amyloid state**. At concentrations exceeding the critical concentration, a protein is more stable in the amyloid state than in its native state (lower free energy). (Knowles et al. 2014)

There are three different mechanisms by which a misfolded protein can be produced. Those mechanisms can act independently but also in cooperation with one another. The first mechanism considers that the protein itself has an intrinsic propensity to misfold, a characteristic that could be triggered by aging and also by the presence of high concentrations of the protein in serum. The second mechanism explains the misfolding of a protein by single point mutations in its sequence. Finally, the third mechanism consists in proteolytic remodelling of the protein precursor (Merlini and Bellotti 2003).

In order to shed light on the molecular mechanisms that explain protein aggregation, experimental kinetic studies have been performed. Chemical kinetics provides an opportunity to approach the fibril formation process in a quantitative manner. However, its application to the process of amyloid formation has been highly challenging because of the difficulties in obtaining reproducible experimental kinetic data and because of the nonlinear nature of the differential equations that describe protein aggregation reactions. Nevertheless, those complications can be overcome and recent progress, both experimental and theoretical, has been achieved (Knowles et al. 2014). In order to understand and describe amyloid formation kinetics, we need to connect the microscopic and macroscopic manifestations underlying fibril formation by considering the different ways in which new aggregates can be formed (Fig. I-4A). For instance, amyloid formation can be explained by

primary nucleation (spontaneous assembly of monomeric species), by fragmentation of existing fibrils or through secondary nucleation (nuclei formation is catalysed by existing aggregates in combination with monomers). The integration of both microscopic and macroscopic manifestations explains the typical sigmoidal reaction time course of the process (Fig. I-4B); an initial lag phase (τ_{lag}) is observed followed by a rapid growth phase (r_{max}). This behaviour is typical of nucleated polymerization and when the total quantity of protein is limited, the growth phase is followed by a plateau phase in which the reaction rate declines as a result of the depletion of the soluble species that is being monitored as it converts into fibrils (Knowles et al. 2014).

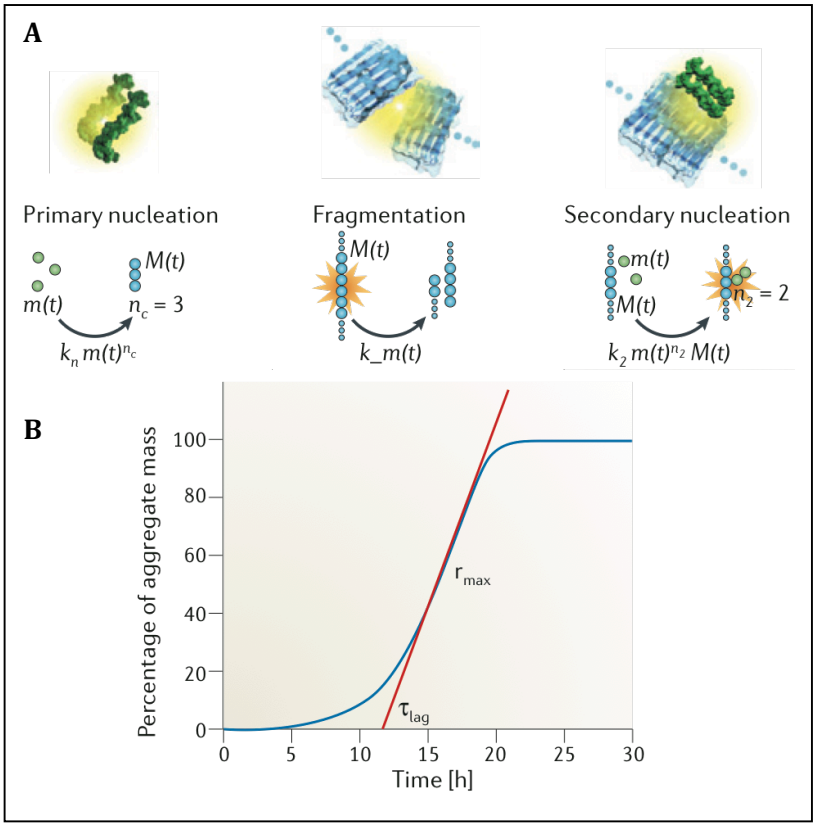

Figure I-4. Kinetics of amyloid formation. **A) Three different amyloid formation mechanisms.** On the left, fibril formation through primary nucleation (monomers are shown in green); on the centre, from existing fibrils through fragmentation (fibrils are shown in blue); on the right, from a combination of both monomeric and aggregated species through secondary nucleation. **B) Sigmoidal function representing filament growth.** Filament growth is characterized by a lag time and a maximal growth rate. Adapted from (Knowles et al. 2014).

There is an extraordinary diversity in the target organ for amyloid deposition. Usually, a specific protein aggregates in a specific tissue, like the fibrinogen Aα chain in kidney or the V30M transthyretin in peripheral nerves. However, there are other cases where the deposits can appear virtually in any organ, like it is the case for light-chain amyloidosis. It is thought that the specificity in the deposition could be given by different physiological conditions, for instance, a high local concentration for a given organ, a low pH in the zone, the occurrence of proteolytic processing, the presence of fibril seeds and specific interactions with tissue or cell-surface receptors (Merlini and Bellotti 2003).

Fibril deposition in a certain tissue or organ is closely related to tissue damage and lastly, organ dysfunction. The mechanisms by which this dysfunction takes place remain unclear. Nevertheless, there are several hypotheses to explain this process. Organ failure could be explained by the fact that

protein aggregation can affect organ architecture. In addition, fibrils may interact with local receptors, triggering a strong inflammatory reaction in the region (Merlini and Bellotti 2003). Finally, and more recently, it is thought that damage in tissues is closely related to the presence of oligomeric intermediates that would be cytotoxic through different mechanisms (Fändrich 2012, Knowles et al. 2014).

I.2 HEREDITARY TRANSTHYRETIN AMYLOIDOSIS

Hereditary transthyretin amyloidosis are a group of diseases associated with mutations in the gene codifying for the protein named transthyretin (TTR) (Saraiva et al. 1984).

There are several related transthyretin amyloidosis namely familial amyloidotic polyneuropathy, familial amyloidotic cardiomyopathy, central nervous system selective amyloidosis and senile systemic amyloidosis, the first three classified as rare diseases (Saraiva 2002). While the first three are caused by single point mutants, the last one is associated to the wild-type TTR (Westermark et al. 1990).

Senile systemic amyloidosis (SSA) is related to the deposition of wild-type TTR and affects around 25% of the population older than 80 years (Westermark et al. 1990). SSA presents a late age of onset and amyloid TTR deposits are found in several organs. There is not a characteristic symptomatology associated to the disease and it is usually considered as benign. However, some kindred, especially men, are severely affected by important amounts of amyloid deposits in the myocardium, ending in some cases in cardiomegaly and congestive heart failure (Westermark et al. 1990).

Familial amyloidotic cardiomyopathy (FAC) is related in the vast majority of the cases to V122I TTR, a TTR variant found in people with African origins. It is thought that around 4% of Afro-Americans (1.3 million people) are heterozygote for V122I TTR mutation. Age of onset is usually around 60 years and carriers of the mutation are prone to cardiac failure, a fact usually observed in homozygote individuals for this mutation (Jiang et al. 2001).

Central nervous system selective amyloidosis (CNSA) is related mainly to variants A25T and D18G and it is characterized by an age of onset in the fifth decade of life and low serum variant TTR levels. Those low TTR plasmatic levels could be explained by a decreased secretion of variant TTR from liver or by rapid degradation of TTR postsecretion, seeming the last one the most plausible option. Finally, it is characterized by highly unstable homotetramers but yet, a quite late age of onset, probably due to its low serum concentration (<25% of wt TTR) since the self-assembly of the amyloidogenic intermediate is a concentration-dependent process (Benson 1996, Sekijima et al. 2003).

The present work is directly related to the last kind of TTR amyloidosis, familial amyloidotic polineuropathy (FAP), associated mainly to V30M TTR mutation. For this reason, a deeper insight into the disease is going to be next addressed.

FAP is an autosomal dominant neurodegenerative disorder with endemic character in specific geographical areas (Fig. I-5). The disease was first described by Andrade in 1952, in the Portuguese city of Porto. However, other endemic areas have been described since then, mainly Sweden, Japan and Mallorca island (Andersson 1976, Andrade 1952, Coutinho et al. 1980, Munar-Ques et al. 1988). The most relevant clinical manifestation is systemic extracellular deposition of amyloid fibrils

throughout the connective tissue, with the exception of the brain and liver parenchyma, and special affection of the peripheral nervous system (PNS). The progression of the disease leads, finally, to organ dysfunction and lastly, to death (Sousa and Saraiva 2003).

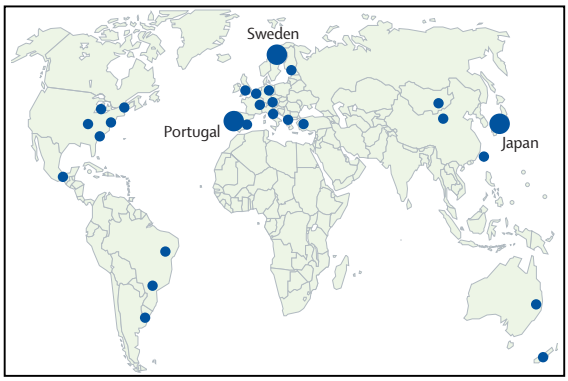

Figure I-5. Geographic distribution of transthyretin familial amyloid polyneuropathy. Geographical areas where FAP has an endemic character (Planté-Bordeneuve 2014).

FAP presents important heterogeneity both in clinical manifestation and age of onset, this last one varying geographically. Whereas there is an early onset of the disease (<50 years) in Portugal (Coutinho et al. 1980), a late age of onset is generally observed both in Sweden and Japan (Koike et al. 2012) (Table I-2). Despite the high heterogeneity, different stages have been established to describe and classify the disease progression. The first classification consists of three stages (Coutinho et al. 1980), taking into account both symptomatology and walking disability progression. The second classification (Yamamoto et al. 2007) is based only in the progression of walking disability. Both classifications are summarized in Table I-3.

Table I-2. Clinical presentations of early onset and late onset TTR FAP (Adapted from (Adams 2013))

	Early onset V30M TTR FAP	Late onset V30M TTR FAP
Age of onset	<50 years	>50 years
Country	Portugal, Japan, Brazil	Sweden, France, UK, Italy, Japan
Positive family history	94%	48%
Peripheral neuropathy	57%	81%
Autonomic neuropathy	48%	10%
Weight loss	5%	0
Mean delay for aid for walking	>5.6 years	3 years
Cardiac	Progressive conduction disorders	Restrictive cardiomyopathy, cardiac insufficiency
Median survival	11 years	7.3 years
Causes of death	Cachexia, infections	Cardiac insufficiency, sudden death, cachexia or secondary infection

Table I-3. Classification of FAP progression according to Coutinho et al. (1980) and Yamamoto et al. (2007) (Adams 2013)

	Coutinho *et al.* (1989)	Duration of stage		Yamamoto *et al.* (2007)
Stage 1	The disease is limited to the lower limbs Walking without help Slight weakness of the extensors of the big toes	**5.6 ± 2.8 years**	**PND I**	Sensory disturbances in extremities Preserved walking capacity
Stage 2	Motor signs progress in lower limbs with steppage and distal amyotrophies, the muscles of the hands begin to be wasted and weak The patient is by then obviously handicapped but can still move around, although needing help	**4.8 ± 3.6 years**	**PND II**	Difficulties walking but without the need for a walking stick
			PND IIIa	One stick or one crutch required for walking
			PND IIIb	Twho sticks or twho crutches required for walking
Stage 3	The patient is bedridden or confined to a wheelchair, generalized weakness and areflexia	**2.3 ± 3.1 years**	**PND IV**	Patient confined to a wheelchair or a bed

Pathological features linked to FAP are still quite unknown. Most reports on FAP agree that axonal fiber degeneration begins in the unmyelinated and low diameter myelinated fibers and only in advanced cases are the heavy myelinated fibers affected (Sousa and Saraiva 2003). The reason why unmyelinated fibers are so heavily affected remains unclear. The same happens with the causes of neurodegeneration in FAP, though several hypotheses to explain it have been formulated.

Some of those hypotheses correlate directly amyloid formation to neurodegeneration progression. This relationship could be explained by several mechanisms such as lesions to sensory and sympathetic neurons, compression of the nervous tissue and finally, ischemia. In all cases, amyloid formation would be the triggering factor (Sousa and Saraiva 2003).

However, all those theories present several weaknesses. For instance, it has never been clearly demonstrated the effect of amyloid deposition on the biochemical functions and physicochemical structure of the PNS in FAP. In addition, it is difficult to establish a cause-effect correlation between amyloid deposition, structural nerve changes and degeneration. Moreover, most of the pathological analyses performed were based on sural nerve biopsies and little information is available on more proximal nerves or ganglia. Finally, the ischemic mechanism wouldn't be valid for those cases were no amyloid deposition has been observed in blood vessels (Sousa and Saraiva 2003).

This apparent lack of cause-effect relationship between amyloid deposition and neurodegeneration points to the existence of another factor as the main responsible for degeneration and neuronal loss in FAP. Recent studies strongly suggest that non-fibrillar TTR aggregates may play a key role in cell toxicity in other amyloid-related disorders like Alzheimer's disease, Parkinson's disease and Huntington's disease. It has been demonstrated that physical fragmentation of preformed fibrils into small fragments exacerbated the effects of fibrils on cells, confirming the concept of smaller species being more effective as toxic agents. In addition, several studies *in vitro* showed that specific aggregates perturb the integrity of lipid bilayers, affecting cellular ion homeostasis, ending, in last term, in cell death (Fändrich 2012). Confirming these results, it was seen *in vitro* that oligomers were able to induce the release of dye molecules placed inside liposomes. In addition, they also increased ion permeability, causing an influx of Ca^{2+}, which at increased intracellular levels affects several enzymes, causing synaptic degeneration and cell death (Fändrich 2012).

In the specific case of FAP it has recently been demonstrated the deposition of TTR in the form of non-fibrillar aggregates before amyloid formation. Those deposits were found both in asymptomatic TTR V30M carriers and in later stages of FAP, coexisting with mature fibrils. The deposited non-fibrillar aggregates were negative for Congo red staining, but positive for immuno-electronmicroscopy with anti-TTR antibodies labelling (Sousa and Saraiva 2003). It has been lately described that TTR fibrils are unable to cause cellular damage and that are TTR aggregates the ones causing toxicity to cells, and thus, being potentially able to induce neurodegenerative changes (Sousa and Saraiva 2003).

There are several mechanisms proposed to explain toxicity of non-fibrillar TTR aggregates at the molecular level, though it remains unknown how peripheral nerve axons of asymptomatic TTR V30M carriers are able to survive this injury. Among the mechanisms suggested there is the induction of oxidative stress through the enhancement of inducible nitric oxide synthase (iNOS) expression by TTR aggregates. In addition, it has been shown that caspase-3 activation occurs *in vitro* when Schwann

cells were exposed to TTR aggregates, suggesting the triggering of programmed cell death. Finally, and following the idea that amyloid related proteins could perturb cellular properties by engaging cellular receptors, the receptor for advanced glycation end products (RAGE) was studied. It was seen that RAGE expression increased along with disease progression and, in addition, the distribution of RAGE correlated with TTR deposits. *In vitro*, RAGE has proved to bind TTR aggregates, promoting the transcription of some pro-inflammatory cytokines and oxidant-stress related molecules among others (Fig. I-6) (Sousa and Saraiva 2003).

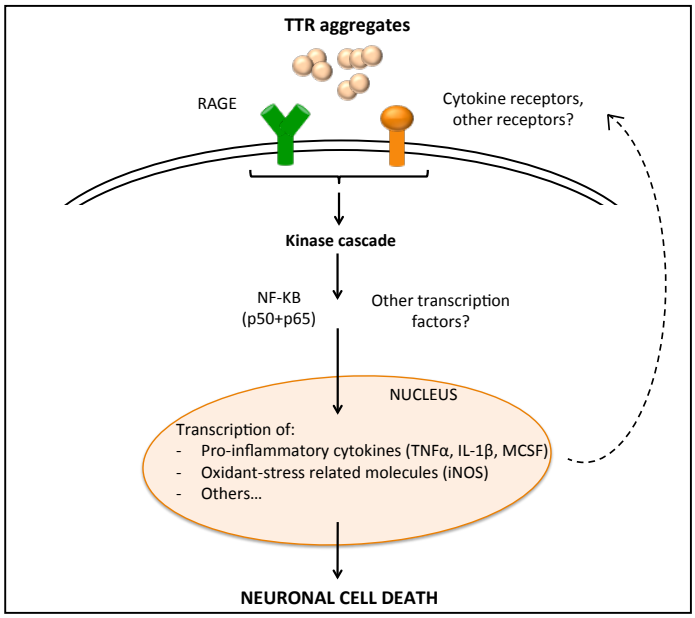

Figure I-6. Hypothesis for neurodegenerative molecular signaling in FAP. Interaction of TTR non-fibrillar aggregates with cellular receptors triggers intracellular signaling pathways that result in neuronal degeneration. Adapted from (Sousa and Saraiva 2003).

I.3 TRANSTHYRETIN

I.3.1 Sequence and protein structure

Human transthyretin (TTR; MIM#176300) is a tetrameric protein (≈55kDa) formed by four identical subunits (≈14 kDa). The codifying gene for TTR is found in chromosome 18 (Wallace et al. 1985) with a size of 6.9 kb, consisting of 4 exons of about 200 pb and 3 introns.

It occurs to be a highly heterogeneous protein, with about 100 described point mutations in the TTR encoding gene, some of them playing important roles in the development of several kinds of hereditary amyloidosis (Connors et al. 2003, Saraiva 2001). In Annex Table A-1, amyloid-related TTR mutations are shown while in Annex Table A-2, non-pathogenic mutations are listed. Most of those mutations occur in the CpG islands, DNA regions with high content of C and G nucleotides.

Several mutations can take place at the same time, being of special relevance cases of patients with more benign clinical courses. In those cases, the combination of a pathogenic mutation with a non pathogenic one has been found, suggesting a protective effect of some mutations, for instance, V30M TTR individuals with the additional mutation of T119M (Saraiva 2001, Sousa and Saraiva 2003).

Even though the majority of individuals affected by V30M TTR are heterozygotes, some homozygote cases have been reported in Sweden and Japan, presenting a surprisingly late age of onset, without the typical FAP symptomatology nor the presence of amyloid deposits (Sousa and Saraiva 2003).

In terms of secondary structure, TTR presents a high content in β-sheet, with a small fragment of α-helix. Almost all the residues conforming the protein possess a structural implication, the 10 amino acids conforming the N-term part of the protein and the 5 amino acids configuring the C-term being an exception, which do not present a direct implication in the folding of the protein, acting just as a "head and tail" (Hamilton and Benson 2001).

Dimers forming the tetrameric conformation present identical sequences but small conformational variations, especially in the A-B loop region. The union of two monomers is possible through an extensive β-sheet contact region, rich in hydrogen bonds. The dimer resulting from these interactions is highly stable. At the same time, each monomer is organized in 8 β-chains, A-H, connected by loops, conforming the well-known β-barrel. β-chains are placed conforming an inner and outer β-sheet, CBEF and DAGH respectively (Fig. I-7). As observed, all chains but A and G present antiparallel interactions (Hamilton and Benson 2001).

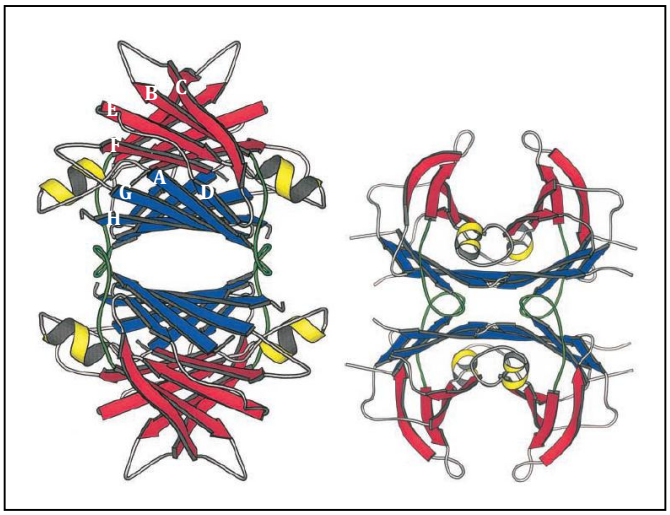

Figure I-7. TTR tetramer representation. In blue, inner β-sheet, DAGH and H'G'A'D'. In red, outer β-sheet, CBEF and F'E'B'C'. The α-helix regions are shown in yellow and in green, the loops contributing to the formation of the functional tetramer (Hamilton and Benson 2001).

As mentioned above, the interaction between monomers is very strong, on the contrary, the contact region between dimers, which gives place to the functional tetramer, is weak and constituted by hydrophobic and hydrophilic interactions between the loop AB of one monomer and the H chain from the other monomer. Taking all these reasons into account, the TTR dimer instead of the monomer is considered as the basic TTR structural unit (Hamilton and Benson 2001); SDS-PAGE gels corroborate this idea, where the dimer is still visible despite the denaturing conditions (Robbins et al. 1978).

I.3.2 Synthesis and function

TTR is synthesised in the liver and the choroid plexus of the brain (Soprano et al. 1985), the first one being the main responsible for plasmatic TTR production. Its main biological role is thyroxine (Fig. I-8A) transport as well as retinol, through the formation of a complex 1:1 with the retinol binding protein (RBP) (Fig. I-8B) (Raz and Goodman 1969, Raz et al. 1970). Whereas TTR transports nearly all the circulating RBP in serum and it is the main thyroxine transporter in cerebrospinal fluid (CSF) through the blood-brain barrier, it only transports around 15% of the serum circulating thyroxine (Schreiber et al. 1990). Additionally, between 1-2% of the circulating TTR in plasma travels in association with high density lipoproteins (HDLs). TTR is a highly abundant protein in plasma with concentrations around 0.2-0.4 µg/µL in healthy individuals. However, lower TTR levels have been described for TTR-amyloidotic patients (Buxbaum et al. 2010, Saraiva et al. 1984).

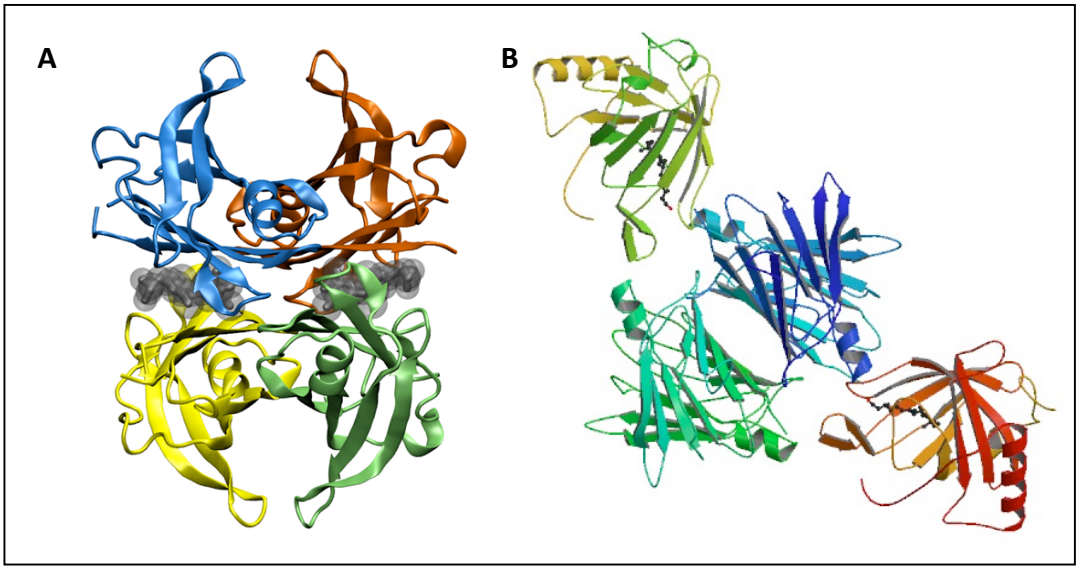

Figure I-8. Main biological TTR roles. A) hTTR complex with T4 hormone, PDB accession number 2ROX**. B)** hTTR complex with RBP, PDB accession number 1RLB

Several studies with knockout transgenic mice for TTR have been carried out. Despite those mice presented depressed levels of retinol and thyroxine, they had a normal phenotype. Absence of TTR did not affect thyroxine transport to the brain and did not produce hypothyroidism (Saraiva 2002). As a consequence, the role of TTR in the thyroxine transport from blood into the brain is put into question. Alternatively, it is thought that compensatory mechanisms for thyroxine metabolism may act in the absence of TTR. A similar situation is found in humans, where V30M TTR individuals are euthyroid even though in that case TTR binds virtually no thyroxine (Saraiva 2002).

The main TTR degradation regions in rat are liver, kidney, muscle and skin, though the cellular TTR uptake mechanism remains still unclear. Several works have been performed in order to elucidate the process using different cell lines, describing megalin as the main responsible for TTR uptake in kidney. In the case of the liver, and in addition other tissues, it has been reported that TTR uptake is inhibited by RAP (Receptor-Associated Protein) and lipoproteins, proposing a RAP-sensitive uptake (Fig. I-9).

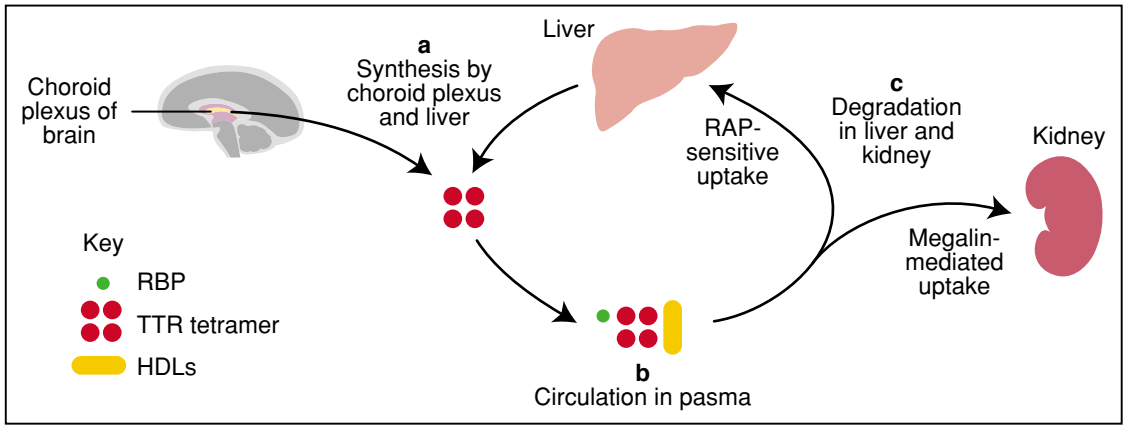

Figure I-9. Synthesis, circulation and uptake of TTR. TTR tetramers are represented by red circles, RBP by a green circle and HDLs by a yellow bar. TTR is synthesized by the choroid plexus of the brain and by the liver. The tetramer circulates in plasma bound to RBP and in a small proportion, bound to HDLs. TTR degradation takes place in kidney and liver mainly, as well as muscle and skin (not shown). In the kidney tubules, TTR is taken up by megalin, remaining still not identified its receptor in liver (Saraiva 2002).

I.3.3 Fibril formation mechanism

The mechanism by which TTR leads into fibril formation and thus aggregation remains still unknown. In order to find a correlation between the different TTR mutations, structural changes and onset of fibril and aggregate formation, the effect of those single point mutations was studied through X-ray crystallography. As a result of those studies, it has been proposed that the presence of the different mutations destabilize the TTR tetramer. The aforesaid destabilization would be produced by important secondary structural changes, giving rise to the exposure of certain parts of the protein related to aggregation (Saraiva 2002). On the basis of the study of those exposed surfaces the construction of the Y78F TTR mutant, a highly amyloidogenic TTR variant able to form fibers at almost neutral pH (Dolado et al. 2005, Redondo et al. 2000), was proposed. This same mutant was found later on *in vivo* in a FAP patient (Magy et al 2003).

Despite the uncertainty in the fibril formation mechanism *in vivo*, it has been possible to induce the fibril formation *in vitro* by lowering the pH (Bonifacio et al. 1996, Chakrabartty 2001, Colon and Kelly 1992, Lai et al. 1996). Under mild acidic conditions (pH=5.75), tetramer dissociation can be induced by protein dilution in the solution. Monomers obtained under these conditions preserve its original conformation. On the contrary, when pH is lowered (pH=4.5), monomer dissociation is favoured, with the resulting monomers presenting conformational changes related to its partial unfolding. Those partially unfolded monomers are known as amyloidogenic intermediates. In this way, at pH=4.5, if temperature and protein concentration are high enough, fibril formation is observed. On the contrary, under strong acidic conditions the fibril formation rate decreases, favouring the formation of amorphous aggregates (Fig. I-10).

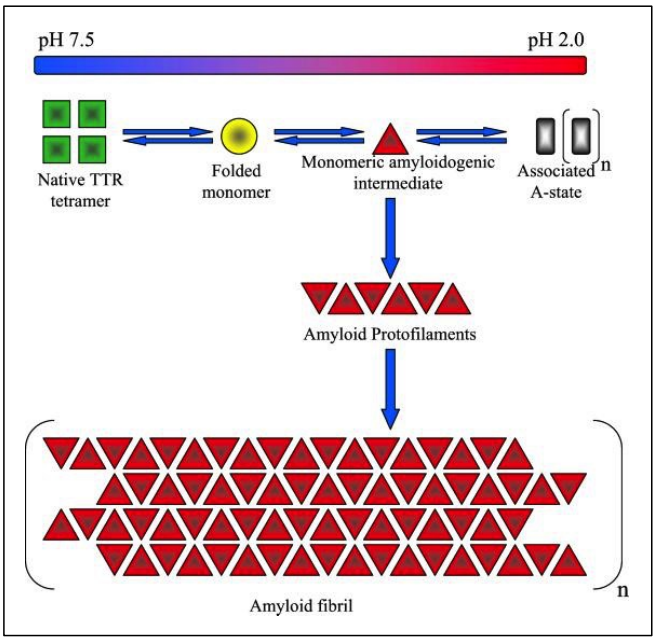

Figure I-10. Acid-induced denaturation/fibrillogenesis pathway of TTR. Under mild acidic conditions (pH 5.75) tetrameric wt TTR can be induced to partially dissociate into monomers by dilution. Further acidification to pH 4.5 induces greater monomer formation and structural changes (partial unfolding of monomers) leading to amyloid fibril formation (Chakrabartty 2001).

As a result of all the structural studies performed, a relationship between the amyloid TTR potential and the weakening of the interaction between monomers has been established. In this way, amyloid fibril formation is determined by the kinetics of tetramer dissociation into monomers. In particular, it is suggested that TTR tetramers would dissociate into monomers with non-native conformation and low stability. Those partially folded monomers would be highly prone to aggregation and as a consequence, to amyloid fibril formation (Saraiva 2002). Fig. I-11A represents in a schematic way the mentioned theory for TTR fibril formation *in vivo*. The specific process for protofibrils formation is illustrated in Fig. I-11B. The proposed pathway (resulting from *in vitro* studies) is that TTR tetramers dissemble into amyloidogenic subunits, predominantly monomers but also, in smaller quantities, dimers, from which annular oligomers with octameric symmetry assemble. A single annular oligomer could act as a scaffold for the continuous addition of subunits up to the formation of an annular doublet, conformed of up to 16 monomers, further stacking being unlikely. Association of annular TTR oligomers seems more likely in order to form the first lineal aggregates. However, the most plausible phenomenon might be the structural reorganization of the annular oligomers into spheroid oligomers containing between 8 and 16 units. It was seen that spheroid oligomers coalesce in a dynamic equilibrium with the growing protofibrils, which are abundant in the first week of incubation (Pires et al. 2012).

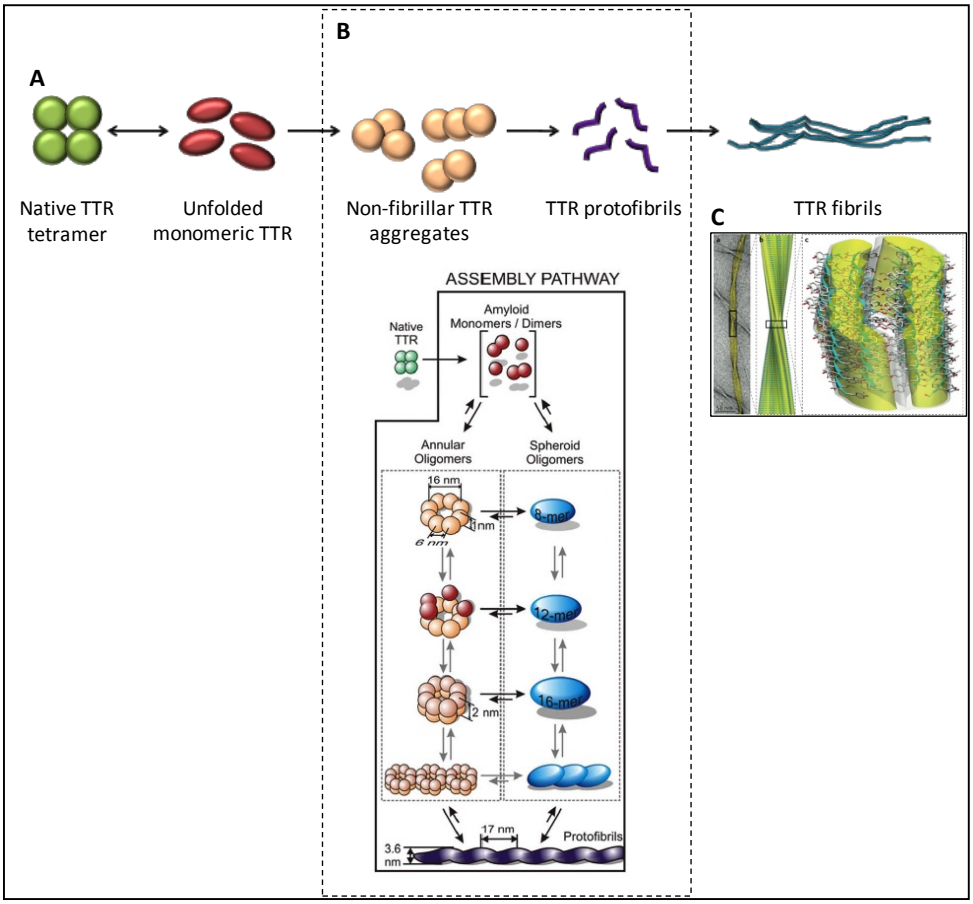

Figure I-11. Schematic representation of the hypothetical pathway of TTR fibril formation. A) Proposed mechanism for TTR fibril formation. TTR tetramers dissociate into partially folded monomers that interact to give non-fibrillar aggregates, resulting in TTR protofibril and finally, TTR fibril formation. **B) Assembly pathway for protofibril formation.** The non native monomers resulting from tetramer dissociation present amyloid characteristics. Those monomers assemble into annular oligomers that coalesce with spheroid oligomers, ending in both cases into protofibril formation (Pires et al. 2012). **C) Structure of TTR fibrils.** Left, cryo-electron microscopy imaging of TTR fibrils. Center, solid-state NMR analysis. Right, hierarchical organization of this amyloid fibril, formed by 3 filaments (each one formed by pairs of cross-β protofilaments) (Knowles et al. 2014).

Recently, it has been possible to determine using several biophysical methods the complete structure of a mature amyloid fibril, formed through the hierarchical self-assembly of cross-β filaments (Knowles et al. 2014). This structure shows the existence of component protofilaments, each having a cross-β structure composed of pairs of nearly flat β-sheets, which interact with other protofilaments through specific interactions of side chains and through water-filled interfaces (Fig. I-11C).

Nevertheless, wt TTR tetramers are relatively stable and, as seen for SSA, they can also be amyloidogenic. For this reason, it is thought that another mechanism may act in those cases. In fact, there are studies where C-terminal TTR fragments have been found in amyloid of SSA patients, pointing to the hypothesis of fibril formation triggered by proteolytic activity (Bergström et al. 2005). As a matter of fact, two different amyloid patterns in mutant and wild-type TTR associated amyloidosis have been found. The first one is related to the incorporation of full-length TTR monomers into the fibrils (in FAP patients), and the second one is mainly due to the formation of fibrils by C-terminal fragments (in SSA patients and some FAP patients). It is unknown whether TTR proteolysis takes place locally at the place of deposition or elsewhere. However, it is likely to be

locally since small amounts of N-terminal fragments were found in the amyloid pattern related to TTR fragments. On the same way, the fact that C-terminal TTR components are predominant in the amyloid deposit suggests that fragmentation cannot be a post-fibrillogenic event (Bergström et al. 2005).

Finally, it is important to highlight the utility of pH induction of fibril formation *in vitro* since it allows the study of the fibrillogenesis potential of different mutants. The most amyloidogenic mutations will be those ones lowering the most the kinetic barrier of tetramer dissociation and thus, allowing fibril formation at higher pH values. Moreover, it is possible to perform studies about fibril formation inhibition *in vitro*, *in vivo* and *ex vivo*, allowing the screening of compounds in the search of drug candidates for the treatment of TTR-associated amyloidosis (Arsequell and Planas 2012).

I.4 THERAPEUTIC STRATEGIES IN FAP

Therapy for FAP is complex and requires approaches from different perspectives. Three main branches for FAP therapy can be highlighted. First, symptomatic treatment of peripheral and autonomic neuropathy; second, anti-amyloid treatments; finally, therapies aimed to solve organ insufficiency problems. All these approaches are summarized in Fig. I-12 (Adams 2013).

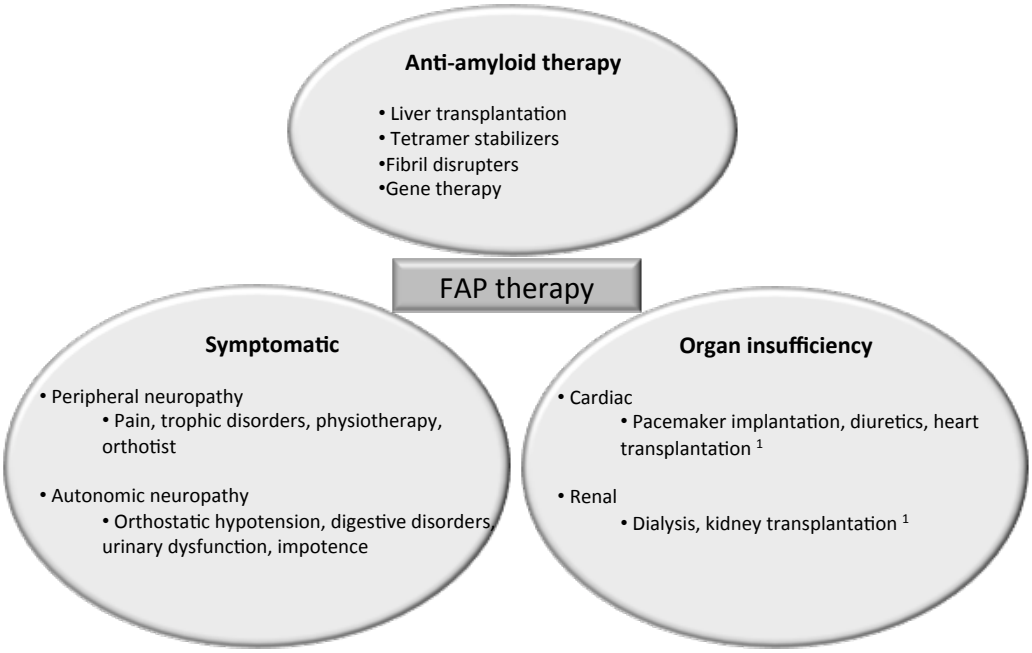

Figure I-12. Principles of therapy for familial amyloid polyneuropathy. [1] In the cases where organ insufficiency is observed and heart/kidney transplantation is required, it is in association with liver transplantation (adapted from (Adams 2013)).

I.4.1 Symptomatic treatment of peripheral and autonomic neuropathy

Treatment at this level is important for FAP patients in order to improve their quality of life. It includes treatment of manifestations of sensorimotor polyneuropathy, prevention and cure of trophic disorders, physiotherapy, help of an orthesis, control of autonomic dysfunction (at digestive, urinary and orthostatic hypotension levels), treatment of associated ophthalmologic manifestations and cardiac disorders (Adams 2013).

I.4.2 Anti-amyloid therapies

I.4.2.1 Liver transplantation (LT)

Until recently, liver transplantation (LT) was the only considered anti-amyloid therapy for FAP patients. LT was proposed 20 years ago, since it allows the suppression of the main source of mutant TTR and thus, prevents the formation of amyloid deposits and the disease progression. According to data in the Familial Amyloidotic Polyneropathy World Transplant Registry (FAPWTR), more than 2000 LT were performed until 2012 in 19 countries, half of the LT being performed in Portugal. Success of LT is tightly related to the TTR gene mutation, the age of the patient and the stage of the disease progression. The main causes of death after LT are cardiac related affections (21%), septicemia (21%) and liver related complications (14%), according to FAPWTR data. After the first year, however, patients die from progress of the amyloid disease (50%), affecting specially the heart or peripheral nervous system. In addition, the rate of survival at 5 years for V30M FAP patients is 20% higher than for other FAP mutations. After LT, 98% of the mutated TTR is reduced in the following days and thus, disease progression is stopped in 70% of patients at mid term. Despite all this facts, LT does not allow clinical or functional recovery, since autonomic dysfunctions are unchanged. In some cases, worsening of walking ability is possible after LT, explained by the fact that wt TTR may continue accumulating in the nerve after LT. It is recommended to perform LT as soon as possible in the disease progression, and thus, acting before the onset of walking difficulties that require aid. In the case of patients with cardiac involvement, the effect of LT depends on the type of initial cardiopathy and the genotype, early or late onset or TTR variant. Again, in some cases, worsening of cardiopathy may be observed after LT due to deposition of wt TTR in the myocardium. Finally, regarding renal function and ocular manifestations, while the first one remains stable in most patients after LT, the last one presents the risk of developing glaucoma or vitreous opacities in 8% and 12% of the patients respectively, due to the retinal source of mutated TTR (Adams 2013).

I.4.2.1.1 Domino liver transplantation (DLT)

Since there is a clear shortage in donors for LT, it was proposed the use of livers from FAP patients as a subsequent graft in a second liver transplant. In fact, livers from FAP patients are anatomically and functionally normal, the production of mutant TTR being the only problem associated to them. In addition, donors are usually young and the ischemic time is short. This procedure (Fig. I-13) is called domino liver transplantation (DLT) and was first performed in 1995 in Portugal. Since then, more than 1000 DLT have been performed worldwide (FAPWTR data).

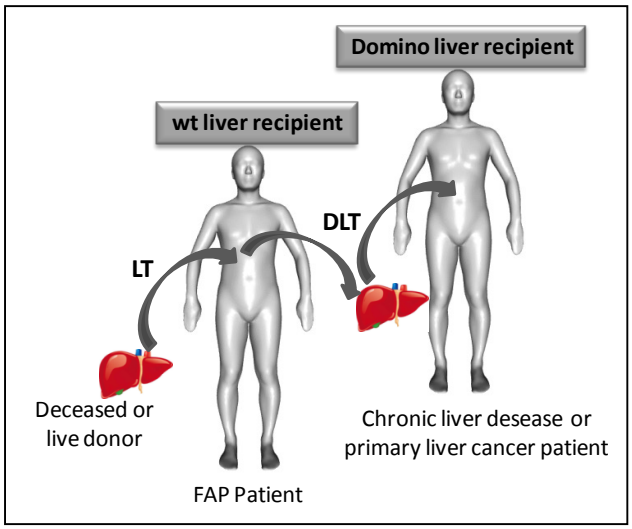

Figure I-13. Schematic representation of LT and DLT transplants. FAP patients receive wt livers from deceased or live donors**.** On the contrary, domino liver recipients receive the V30M livers from the FAP patients.

Short-term and long-term graft and patient survival rates have been shown to be similar to those of standard LT with cadaveric donors (Azoulay et al. 2012, Lladó et al. 2010). The main indications for DLT are patients with primary hepatic malignancy, metastatic hepatic malignancy, cirrhosis secondary to hepatitits B and C, alcoholic cirrhosis and retransplantation. In fact, since FAP livers were considered as marginal livers, they were offered to patients with marginal indications for liver transplantation or to patients over 60 years old (Samuel and Adams 2007). The main causes of death after DLT are tumor recurrence (24%), septicemia (16%), cardiac related deaths (7%) and preoperative deaths (5%), according to FAPWTR data.

Despite all the advantages discussed previously, the main drawback of DLT is the risk of developing acquired amyloid neuropathy, since the mutant TTR is produced by the liver. Nevertheless, since FAP is usually not symptomatic during the first 20 years of life, it was considered that the FAP liver recipient was not supposed to develop FAP symptoms before 20 years after transplantation. On the contrary, in a prospective study to assess the risk-benefit ratio of DLT, systemic amyloidosis developed earlier than expected, with amyloid deposits on labial salivary gland 5 years after DLT in half of patients or on rectal biopsy in one third of patients. The delay to declare polyneuropathy ranged from 3.5 to 9 years (Adams 2013). On this way, *de novo* amyloid neuropathy mimics FAP of early onset putting into question DLT transplantation. The reason explaining why those patients develop symptoms earlier than expected is not known, although several explanations have been proposed. It is thought that the recipient's age may have a possible role, since amyloid deposition may depend on unknown age-related mechanisms that promote amyloid fibrillogenesis. Other proposed factors are, for instance, the fact that the presence of amyloid fibers in the graft may trigger the disease or the fact that inflammatory reactions related to the liver transplantation may promote the production of amyloid, accelerating the development of the disease (Lladó et al. 2010). Despite all the problems related to *de novo* amyloid neuropathy, it is considered that the shortage of graft from cadaveric donors still justifies the DLT in selected patients. However, DLT recipients must be fully informed prior to the procedure as well as undergo prospective and focused follow-up. Moreover, the appearance of FAP symptoms in the recipient of domino liver may be an indication for a second transplantation with a non-FAP liver (Lladó et al. 2010, Samuel and Adams 2007).

I.4.2.2 Tetramer stabilizers

Although LT is the current standard therapeutic strategy to ameliorate familial TTR amyloidosis it has a number of limitations, already pointed out, such as shortage of donors, requirement of surgery, and the need for long-term post-transplantation immunosuppressive therapies. In addition, as it has already been said, TTR deposition may continue in eye and CNS since the retinal pigment epithelium and choroid plexus also synthesize TTR. Moreover, cardiac amyloidosis progresses in some patients after LT because of wt TTR deposition. Finally, LT is not a valid option for SSA, since the deposits are formed of wt TTR. Therefore, it is desirable to develop a general, convenient and non-invasive alternative therapeutic strategy to ameliorate TTR amyloidosis (Adamski-Werner et al. 2004, Westermark et al. 1990).

New therapeutic strategies are being developed, taking advantage of the current understanding of the mechanism of TTR amyloidogenesis. Tetramer dissociation to a misfolded monomeric subunit is rate-limiting for amyloid formation *in vitro* and most likely *in vivo*. Increasing the kinetic barrier associated with TTR dissociation, referred to as kinetic stabilization, is known to prevent the TTR amyloid disease FAP. The design of small molecules able to act as TTR ligands and, at the same time, as inhibitors of fibril formation, finds its fundamentals in the interaction between TTR and its natural ligand, the hormone T4. Through *in vitro* experiments it was observed that the hormone T4 was able to stabilize TTR tetramer and therefore, inhibit fibril formation (Miroy et al. 1996). Each of the two thyroxine binding sites is characterized by a small inner cavity and a larger outer cavity (Fig. I-14A) with three pairs of symmetric depressions distributed throughout (Fig. I-14B), termed halogen binding pockets (HBPs), wherein the iodine atoms of T4 reside (Johnson et al. 2005). The innermost pockets are HBP3 and HBP3', and the outermost are HBP1 and HBP1' (Cotrina et al. 2013). Thyroxine binds to these two sites with negative cooperativity since its binding to the first site causes TTR conformational changes that render the second site less suitable for binding (Johnson et al. 2005). Over the past decades, a wide variety of families of compounds able to act as tetramer stabilizers (Fig. I-15) through the binding to the T4 hormone sites have been discovered and studied. Two different mechanisms for interaction between those small molecules and TTR have been described, the forward and the reverse modes (Fig. I-14C-D). In the forward mode the interaction takes place through the outer binding pocket, with an electrostatic interaction with Lys15. In the reverse mode the interaction takes place through the inner pocket by hydrogen bonds with Ser117 (Adamski-Werner et al. 2004). Small molecule TTR ligands are typically composed of two aromatic rings, either linked directly as a biaryl or separated by linkers of variable chemical structure. Typically, one aromatic ring is substituted with a polar substituent while the other ring displays halogenated substituents, alkyl groups, or a combination thereof. Polar substituents can make important electrostatic interactions with the Lys-15 and to some extend with the Glu-54 when positioned in the outer binding site. The halogenated or alkylated aryl rings complement the hydrophobicity of the inner binding pocket by occupying a subset of the HBPs. As a consequence, small molecules typically bind to TTR in the forward mode, wherein the aromatic ring bearing an anionic substituent prefers the outer binding pocket owing to electrostatic interactions with the Lys-15 (Johnson et al. 2005). Many of the compounds studied belong to the nonsteroidal antiinflammatory drugs category (NSAIDS), which have proven to be effective in the increase of the kinetic barrier for TTR tetramer dissociation. Some examples are flufenamic acid (Baures et al. 1999), diclofenac (Oza et al. 2002) or diflunisal (Adamski-Werner et al. 2004). Even though all those compounds bind to the T4 sites, it is

possible to administer them without major side effects since TTR is a T4 tertiary transporter in blood plasma with more than 99.5% of the two T4 binding sites unoccupied (Sekijima 2014).

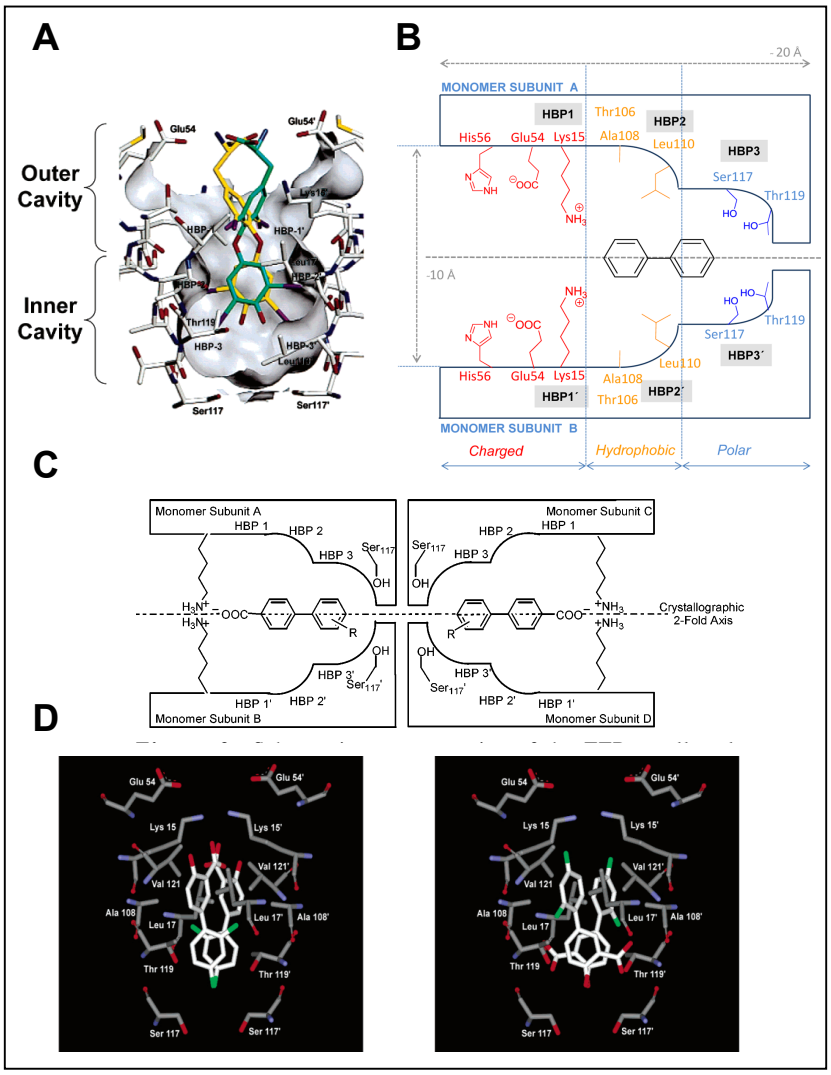

Figure I-14. Interaction of TTR with small ligands. (A) Expanded view of one T_4 binding pocket. T_4 hormone is shown in its two symmetry-related binding modes (green and yellow) with the binding site surface shown in grey (Johnson et al. 2005). **(B) Schematic representation of a TTR binding site.** The three chemical regions in which TTR binding sites can be divided are shown, as well as the halogen binding pockets (HBPs) location (Cotrina et al. 2013). **(C) Representation of the forward binding mode of a TTR ligand.** The inhibitor carboxylate participates in electrostatic interactions with the ε-amonium of Lys15 and 15' (Adamski-Werner et al. 2004). **(D) X-ray crystal structure of diflunisal bound to TTR.** Left, forward binding mode. Right, reverse binding mode (Adamski-Werner et al. 2004).

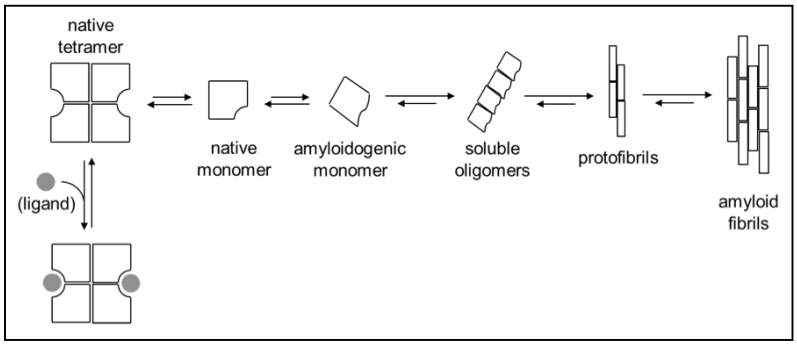

Figure I-15. Inhibition of fibril formation by small ligands. Ligands bind to TTR tetramer avoiding its dissociation and thus, fibril formation, through kinetic tetramer stabilization (Dolado et al. 2005).

In addition, fewer compounds have been reported to stabilize TTR tetramer by binding to different regions than the T_4 binding sites (Ferreira et al. 2009).

I.4.2.2.1 Evaluating the inhibition of TTR fibrillogenesis induced by small ligands

In order to evaluate TTR amyloidosis inhibitors, large libraries of compounds and molecules derived from rational design have been evaluated by means of a great variety of assays including *in vitro* (using isolated recombinant TTR protein), *ex vivo* (plasma selectivity), and *in vivo* (cellular assays and animal models) strategies. Assays can be grouped in 2 main classifications according to what do they measure: those ones monitoring the end products (formation of protein aggregates or fibrils) and those ones measuring binding to and stabilization of the native tetramer. To be able to evaluate the inhibition of TTR fibrillogenesis by small ligands, a combination of different assays has to be used, since different properties along the fibrillogenesis pathway need to be measured. Table I-4 summarizes and classifies most of the methods reported in the bibliography for the evaluation of TTR fibrillogenesis inhibitors (Arsequell and Planas 2012).

Table I-4. Assays to monitor TTR fibrillogenesis and aggregation for the screening and evaluation of inhibitors. Primary screening (A,B), secondary screening (C,D), *in vitro* validation (E), and *in vivo* pre-clinical validation (F) (Arsequell and Planas 2012)

ASSAY	Evaluated property	Instrumentation
A) *In vitro* assays that monitor protein aggregation and/or fibril formation		
- Turbidimetric assays	Aggregation under acidic conditions	UV/vis spectrophotometer
- Thioflavin T and dye binding assays	Fluorescence upon binding to fibrils	Fluorimeter
- TEM and AFM monitoring of fibril formation	Imaging of fibrils and aggregates morphology	Electron and atomic force microscopes
B) *In vitro* assays that monitor binding to native protein. ***B.1. Non-competitive assays***		
- Isothermal titration calorimetry (ITC).	Ligand binding constants	Microcalorimeters. Binding in solution
- Surface plasmon resonance (SPR).	Ligand binding constants	SPR instrument. TTR immobilization on sensor
- Affinity Capillary Electrophoresis	Ligand binding constants	Capillary electrophoresis
- Ligand complexes by mass spectrometry	Protein-ligand complexes and stability	Mass spectrometer
B.2. Competitive assays		
- T4 binding competition assay.	Displacement of bound T4 (radiolabeled) by ligand	Gel filtration chromatography / scintillation counting
- SPR biosensor competitive inhibition assay.	Displacement of ligand from TTR-ligand complex by immobilized T4	SPR instrument. T4 immobilized on sensor
- Fluorescence conjugate competition assay.	Ligand competition for a fluorescent probe covalently binding to TTR	Fluorimeter
- Fluorescence polarization displacement binding	Displacement of a fluorescent probe bound to TTR by ligand	Fluorimeter. Fluorescence polarization
C) *Ex vivo* TTR plasma selectivity assays		
- Plasma binding selectivity by T4 displacement.	Displacement by ligands of labeled T4 bound to plasma proteins	Gel electrophoresis, autoradiography
- Plasma binding selectivity by immunoprecipitation.	Stoichiometry of ligand binding to TTR in the presence of plasma proteins	Immunoprecipitation, HPLC of captured ligand
D) *In vitro* assays for tetrameric TTR stabilization		
- Native TTR stabilization under partially denaturating conditions.	Tetramer stabilization by ligands in the presence of denaturants (SDS, urea)	Gel electrophoresis, isoelectrofocusing
- TTR stabilization to thermal unfolding.	Increase of Tm (thermal stability) by ligands	Differential scanning calorimeter (DSC)
E) Cellular assays		
- Cellular assay for TTR deposition	Amyloid inhibition by ligands on transfected cells expressing TTR	Filter assay to separate aggregates. Immunodetection
- Cellular assay for TTR-induced cytotoxicity	Cytotoxicity due to TTR oligomerization	Cell viability assays
F) Animal models to evaluate amyloidosis inhibitors		
- Mouse models	Transgenic mouse. Amyloid deposits	Histology. Marker assays
- Drosophila models	Transgenic Drosophila. Amyloid deposits	Histology. Marker assays
- Monkey model	Vervet monkey. Amyloid deposits	Histology. Marker assays

Among all the small ligands designed to stabilize TTR tetramer that have been tested, two of them deserve a special treatment in this section:

I.4.2.2.2 Diflunisal

Diflunisal is a well-known non-steroidal anti-inflammatory drug already approved for that indication as a prescription drug in more than 40 countries. Phase I and II clinical trials were performed based on repurposing *in vitro* analysis showing the capability of diflunisal to inhibit amyloid fibril formation by binding to the T4 binding sites. The studies showed that at a dose of 250 mg twice a day, TTR stability in TTR amyloidosis patients increased beyond the level of normal controls without adverse effects. The treatment would be effective for both wt TTR and variant TTRs. In addition, clinical efficacy of diflunisal has been demonstrated recently in a randomized double-blind placebo-controlled phase II trial (Sekijima 2014).

I.4.2.2.3 Tafamidis

Tafamidis meglumine (Vyndaquel®) is a newly developed small molecule able to stabilize TTR tetramer also by binding to the T4 binding sites. It stabilizes both wt TTR and TTR variants and its efficiency has been shown *in vitro* in the serum of treated patients. Moreover, it was tested later in a multicenter international clinical phase II/III trial in 128 patients (Fx-005) showing the absence of progression of neuropathy in 60% of patients in the tafamidis group *versus* 38% in the placebo group and also by a better preserved total quality of life (TQOL). Its most frequent side effects (very common, at least one in ten patients) are urinary tract infections and diarrhea, and the long-term side effects or its potential drug-drug interactions are still unknown (Adams 2013).

Tafamidis is preferable for treating early stage symptomatic FAP, with amyloidogenic mutant TTR. However, physicians should continue to assess the need for other therapies, including LT (Adams 2013).

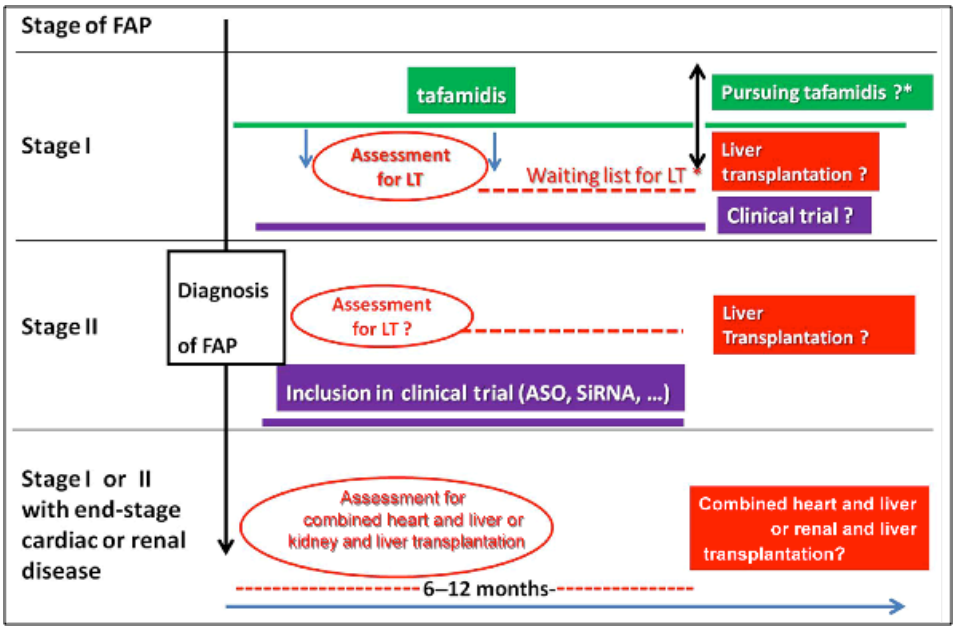

Figure I-16. Therapeutic strategy in patients with familial amyloid polyneuropathy (FAP) according to the stage of the disease. Stage III is a contraindication for any transplantation. ASO, antisense oligonucleotide; LT, liver transplantation; siRNA, small interfering RNA (Adams 2013).

Tafamidis was approved by the European Medicines Agency in 2011 for the treatment of early stage (stage I) FAP (Fig. I-16) and by the Japanese Pharmaceuticals and Medical Devices Agency in 2013 for the treatment of FAP at any stage.

I.4.2.3 Fibril disrupters

As mentioned, the knowledge acquired in the last years concerning the identification of intermediate species and the mechanisms underlying amyloidosis opened the possibilities for the investigation of drugs capable of interfering with the amyloidogenic pathway at different stages. Apart from the kinetic tetramer stabilization previously discussed, another strategy could be the disruption of the already formed amyloid fibrils. However, TTR stabilizers seem to be more interesting since they would impair very early the process of amyloid formation and could also have a prophylactic effect. On the contrary, and in favor of fibril disrupters, there is the fact that they are expected to function in all amyloid fibril types, independently of their protein/peptide precursor and therefore, could represent a treatment for a broad range of amyloidosis. Nevertheless, in the case of fibril disrupters it is of special interest the assessment of the toxicity not only of the putative drug itself but also of the sub-products created by means of the fibril disruption (Cardoso et al. 2010).

I.4.2.3.1 Doxycycline-taurodesoxycholic acid

A combination of doxycycline and taurodesoxycholic acid (TUDCA) has been tested on transgenic mice allowing suppression of TTR deposits in most of the old mice. The combination appears to have a synergistic action that acts during many steps of amyloidogenesis and tissular-induced damage. Doxycycline acts primarily as a fibril disrupter in vitro. TUDCA, a biliary acid, acts as a potent antiapoptotic and antioxidant with the ability to reduce the toxic aggregates of TTR by 75% in young transgenic mice for human V30M TTR in a TTR null background. A phase II study enrolling 20 patients was performed in 2012, with a total of 7 patients completing 1 year of treatment. Safety was good and several patients were stable at 1 year (Adams 2013, Cardoso et al. 2010).

I.4.2.3.2 Antiserum amyloid P monoclonal antibodies

Another possible strategy is based on enhancing the clearance of amyloid deposits with a monoclonal antibody against human serum amyloid P component (hu-SAPMab). Amyloid P component is a ubiquitous nonfibrillar plasma glycoprotein in amyloid deposits. After administration of hu-SAPMab to mice with amyloid deposits containing hu-SAP, massive visceral amyloid deposits are removed. Such a removal is explained by the triggering of a potent complement-dependent, macrophage-derived giant cell reaction that swiftly removes massive visceral amyloid deposits. The strategy has not yet been tried for TTR FAP but good results have been obtained in an experimental model of human systemic amyloid A (AA) amyloidosis with splenic and hepatic AA protein mouse model (Adams 2013).

I.4.2.4 Gene therapy

Apart from LT, stabilization of TTR tetramer or amyloid fibril disruption there are other mechanisms to fight against TTR amyloidosis (Fig. I-17). Gene silencing has been developed to block hepatic synthesis of both mutant and wild type TTR. Some of the strategies to this aim are considered as promising and some clinical trials are currently underway.

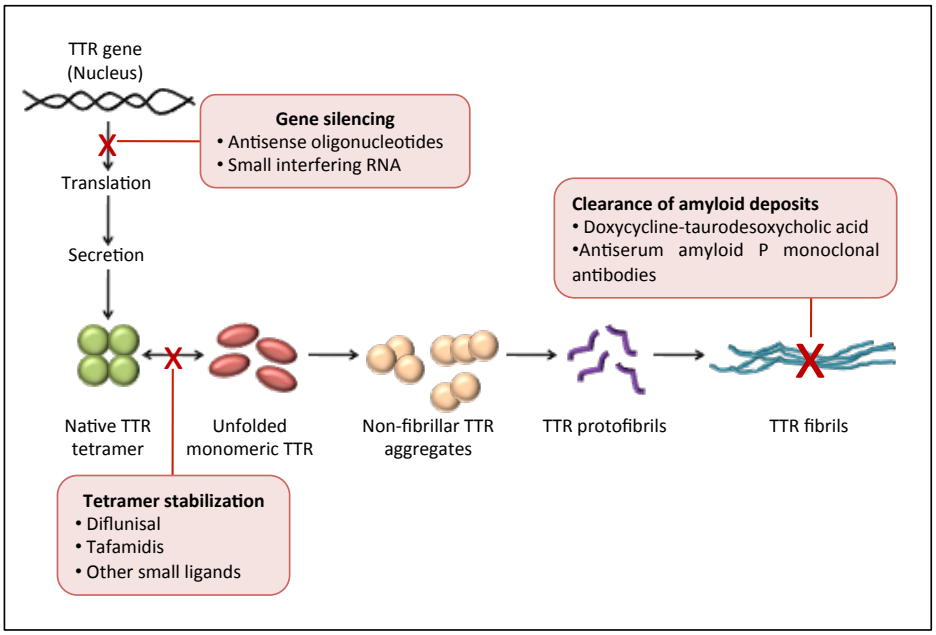

Figure I-17. Sites of action of potential therapeutic strategies for FAP. Indicated in red boxes are the different levels of action for newly developed strategies: gene silencing, tetramer stabilization and clearance of amyloid deposits.

I.4.2.4.1 Antisense oligonucleotides

Antisense oligonucleotides (ASOs) are short synthetic single strands of oligonucleotides designed to prevent the expression of a targeted protein by selectively binding to the mRNA encoding the target protein and therefore, preventing translation. Several recent clinical studies have reported that the antisense concept works in humans and indeed, several drugs have been approved by the U.S. Food and Drug administration.

In the particular case of TTR amyloidosis, ISIS-TTR_{RX} is a second-generation antisense drug targeting TTR. It is designed to bind to the 3' non-translated portion of the human TTR mRNA, which results in degradation of TTR mRNA by RNase H and therefore, avoids TTR production in all its variants. It has been tested in a human TTR transgenic mouse model achieving up to 80% reduction in a dose dependent manner of human TTR production (both liver TTR mRNA levels and circulating plasma TTR levels) after twice weekly subcutaneous injections with ISIS-TTR_{RX} for 4 weeks (Benson et al. 2006). Suppression of choroid TTR expression was also observed more recently, a dose-dependent reduction of human TTR in cerebrospinal fluid after intraventricular administration of ASO was described (Benson et al. 2010). Finally, studies in monkeys using subcutaneous injection showed reduction levels of liver TTR mRNA and plasma TTR around 80% after 12 weeks of treatment. The good tolerance observed both in rodents and monkeys encouraged a first phase I clinical trial involving healthy volunteers. ISIS-TTR_{RX} was administrated subcutaneously in single and multiple-dose (50-400mg) achieving up to 80% reduction. In general, the subjects treated with the ASO tolerated well the drug, however, mild-to-moderate adverse events were observed; for instance, injection site pain and somnolence. In February 2013, a clinical phase II/III randomized double-blind placebo-controlled study to evaluate the efficacy of ISIS-TTR_{RX} in patients with FAP was started (Sekijima 2014).

I.4.2.4.2 Small interfering RNA

Small interfering RNAs (siRNAs) are a class of double stranded RNA molecules with a length of around 21-23 base pairs. siRNAs play many roles but are most important in the RNA interference (RNAi) pathway, affecting the expression of specific genes with complementary nucleotide sequence.

ALN-TTR01 and ALN-TTR02 (Patisiran) are first- and second-generation formulations of lipid nanoparticles who act as vehicules for siRNA delivery. Despite presenting similar physicochemical properties they are formed by different ionizable lipid components. In both cases, the encapsulated molecule is an identical siRNA that targets a conserved sequence in the 3' untranslated region of mRNA in TTR, both wt and mutant forms. A single-dose phase I clinical trial was carried out for both formulations. The intravenous administration of ALN-TTR01 (1mg/kg) suppressed serum TTR levels on day 7 up to 38%. On the contrary, for ALN-TTR02 (0.15-0.3mg/kg) the reduction of TTR protein levels was up to 86%, with reductions up to 67% on day 28 (Coelho et al. 2013). Based on those results, a phase III randomized double-blind placebo-controlled study (APOLLO Phase III study) was planned for 2014 to evaluate the efficacy and safety of ALN-TTR02 in FAP patients (Sekijima 2014).

I.4.3 Solving organ insufficiency problems

Organ insufficiency is sometimes observed in FAP patients, depending on the severity and manifestations of the disease. The systems typically affected are cardiac and renal systems. For this reason, assessment of cardiac function must be systematic in patients with FAP, with regular cardiac checkups. It is highly important to evaluate cardiac function and impact of myocardial amyloid infiltration on ventricular function. In addition, combined heart and liver transplantation may be considered, despite the fact that severe cardiac injury may constitute a contraindication for liver transplantation. In those cases with renal injury due to amyloidosis, first hemodialysis and later renal transplantation could be required.

I.5 POST-TRANSLATIONAL MODIFICATIONS IN TTR

Proteome's variability in nature can be increased by modification reactions that take place once proteins have been synthetized. Such modifications are known as post-translational (PTMs) and can be the result of different cellular reactions, environmental factors and cellular and physiological cycles.

In the particular case of TTR, each monomer contains a cysteine residue at position 10 (Cys-10) in the sequence. This Cys-10 residue is exposed to the surface under native folding tetramer conditions at the beginning of helix α regions (Lim et al. 2003). On this way, the heterogeneity described for TTR is not only found at the mutational level but also at the post-translational one, associated to Cys-10 (Table I-5). In fact, Cys-10 PTMs in TTR cannot be taken as an exception since it has been found that only 10-15% of plasmatic or cerebrospinal fluid TTR remains unmodified at this level (Lim et al. 2003). The most common modifications found *in vivo* are S-sulfonation (S-Sulfo), S-glycinylcysteinylation (S-CysGly), S-cysteinylation (S-Cys) and S-glutathionylation (S-GSH) (Poulsen et al. 2012).

These different Cys-10 forms are believed to reflect the redox balance of the *in vivo* environment and may suggest that TTR participates in the defence against oxidative stress through thiol conjugation, buffering the redox balance (Poulsen et al. 2012). It is thought that PTMs at Cys-10 may play an

important biological role in the onset and pathological process of TTR-related amyloidosis, though its implications are still badly understood. Several studies have been performed aiming to elucidate whether Cys-10 isoforms have a significant influence on protein stability and tetramer dissociation or not, ending in not clear conclusions (Altland et al. 1999, Bergquist et al. 2000, Nakanishi et al. 2010, Suhr et al. 1999, Takaoka et al. 2004, Zhang and Kelly 2003, 2005). In general, it is suggested that the presence of modifications in Cys-10 may result in more amyloidogenic protein variants. In addition, this increment in the amyloidogenic capability of the protein has been found to be higher when combining the presence of Cys-10 variants with destabilizing TTR mutations. This last observation suggests that it might be necessary to accomplish both requisites (Cys-10 mixed disulfides and destabilizing mutation) to develop TTR related amyloidosis. However, it has not been possible to establish a direct relationship between Cys-10 PTMs and the pathogenesis of FAP since many of those studies were carried out *in vitro*.

Table I-5. Cys-10 PTMs in TTR. Theoretical calculated Δ masses (free thiol as reference) (Poulsen et al. 2012)

Modification on Cys10	Chemical structure	Theoretical mass (Da)	Theoretical Δ mass (Da)
Cys → Gly	TTR—H	13706.901	−45.988
Cys → dehydroalanine	TTR=CH$_2$	13718.901	−33.988
None = free thiol	**TTR—C(H$_2$)—SH**	**13752.888**	**0**
Cysteine sulfenic acid	TTR—C(H$_2$)—S—OH	13768.883	15.995
Cysteine sulfinic acid	TTR—C(H$_2$)—S(=O)—OH	13784.878	31.990
Cysteine sulfonic acid	TTR—C(H$_2$)—S(=O)$_2$—OH	13800.873	47.985
S-sulfonate	TTR—C(H$_2$)—S—S(=O)$_2$—OH	13832.845	79.957
S-Cys	TTR—C(H$_2$)—S—S—C(H$_2$)—C(H)(NH$_2$)—C(=O)—OH	13871.892	119.004
S-CysGly	TTR—C(H$_2$)—S—S—C(H$_2$)—C(H)(NH$_2$)—C(=O)—N(H)—C(H$_2$)—C(=O)—OH	13928.920	176.026
S-glutathione	TTR—C(H$_2$)—S—S—C(H$_2$)—C(H)(NH$_2$)—C(=O)—N(H)—C(H$_2$)—C(=O)—N(H)—C(H)(CH$_2$CH$_2$C(=O)OH)—C(=O)—OH	14057.956	305.068

Moreover, homodimers of TTR linked via Cys-10-Cys-10 have been found in cardiac amyloid deposits (Kingsbury et al. 2007). Nevertheless, the origin, function and relevance at the pathologic level of those disulfide bridges remain unknown. It has also been suggested that there is a link between Cys-10 conjugation and aging and, therefore, with the development of SSA (Kingsbury et al. 2007). In addition, there are crystallographic studies with wt and V30M TTR revealing how in the case of wt TTR there is a hydrogen bond formation between Cys-10 and Gly57 that it is not observed in V30M TTR due to small conformational changes. Finally, studies performed in transgenic mice support the evidences of the importance of Cys-10 residue since when performing Cys10Ser substitution, while maintaining V30M mutation (Ser10/Met30 mice), a suppression of amyloid deposition is observed (Takaoka et al. 2004).

For all those reasons Cys-10 residue is thought to be important in the pathogenic process of TTR related amyloidosis. Nevertheless, since in plasma a high heterogeneity at the tetrameric level is

observed (not all are post-translationally modified) (Lim et al. 2003), it is risky to conclude which is the real role of those modifications. In addition, most of the hypotheses performed come from *in vitro* studies, which may not mimic the real physiological conditions. Therefore, all that information should be complemented with studies performed with plasma patient samples, taking into account the clinical evolution of their disease as well as the age of onset of the amyloidosis.

I.6 PROTEOMICS

The term proteomics is defined as the large-scale study of the proteome and it is the linguistic equivalent of the word genomics, with the study of the genome. A proteome has been defined as the protein complement expressed by the genome of an organism or in the case of multicellular organisms, as the protein complement expressed by a tissue or differentiated cell (Wilkins et al. 1996), at a given moment under specific conditions.

Proteins are responsible for most of the biochemical processes that take place in cells and organisms. Therefore, the study of its expression levels, distribution, post-translational modifications, structure, and function is of extreme importance in order to understand cellular processes in health and disease. Despite the great amount of information obtained by genomic techniques, there are several reasons that highlight the importance of performing proteomic studies as well. Firstly, protein expression levels are not predictable from the mRNA expression levels. Secondly, proteins are dynamically modified and processed in ways which are not necessarily apparent from the gene sequence and thirdly, proteomes are dynamic and reflect the state of a biological system (Wilkins et al. 1996).

I.6.1 Utility of proteome analysis for biological research

I.6.1.1 The proteome as a database

The use of proteomics as a database or data archive consists mainly in the enumeration of all the components of a proteome. It is an attempt to identify all the proteins in a cell or species and to annotate each protein with its known biological information. This approach could be compared to all the efforts put into genomic studies, where large datasets of lists of genes have been produced. However, the proteome is difficult to define since unlike the genome, it is highly dynamic. Processes such as differentiation, cell activation and disease can all change the proteome of a species. Thus, while describing a proteome, it is important to provide all the information comprising the state and the type of the cells from which the proteins were extracted.

In the last years, a lot of effort has been put in the characterization of the 20.300 genes of the known human genome and the consequent generation of the map of the protein based molecular architecture of the human body. Obtaining such information will help to elucidate biological and molecular function and thus, advance diagnosis and treatment of diseases. This large project is organized within the Human Proteome Project (HPP) and it is organized at the chromosome level (Chromosome-Based Human Proteome Project, C-HPP) and at the Biology/Disease level (Biology/Disease Human Proteome Project, B/D-HPP). The goal of the HPP is to have high-quality, extensive proteome maps by 2022. In addition, it is intended to make proteomic technologies and knowledge practical and accessible for wide use across the life sciences and biomedical research communities and to complete a gene-centric parts list for proteins and their isoforms. The HPP

project biggest challenge is to use proteomics to bridge major gaps between evidence of genomic variation and diverse phenotypes. To this aim, 14 different countries and almost 50 teams participate within the project by studying a given chromosome. The working schema for this branch of the HPP, the C-HPP, is summarized in Fig. I-18. In addition, within the B/D-HPP project, several groups have begun to assemble prioritized lists of proteins relevant to several different diseases and biological systems, making them publicly accessible (Aebersold et al. 2014).

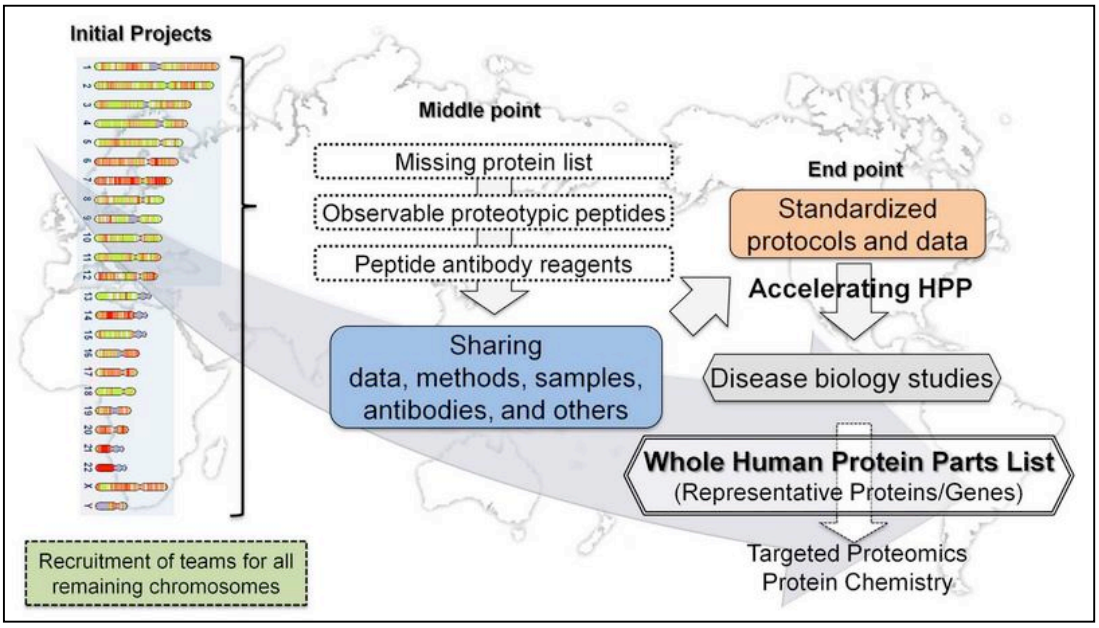

Figure I-18. Working strategy for the C-HPP. The main goal is to map the human protein subset or parts list coded by genes on each chromosome. The starting point is the missing proteins (>30%) mapping and the end point is to complete a list of all proteins coded by genes in all human chromosomes. The mapping will be complemented by studies of cellular and organ expression, subcellular distribution, functions, PTMs, interactions and disease biology studies (The Human Proteome Project).

I.6.1.2 The proteome as a clinical tool/assay

In this approach, the main goal is to detect dynamic changes in the proteome following external/internal perturbations. In the case of classical biological assays, the state of a system is studied through the quantitative or qualitative measurement of one or more variables. Most classical biochemical assays allow the study of one variable of a single component, for example, a particular enzyme activity. In the case of proteomic assays, multiple variables can be measured on many proteins in a sample, for example, the expression level, rate of synthesis and phosphorylation state measured in all the proteins of a given sample. However, there are some technical limitations in the detection of all proteins in a sample due to its high dynamic range. For this reason, prior fractionation steps or enrichment in less common proteins must be done in order to increase the number of proteins detected in a sample (Haynes et al. 1998).

I.6.2 Expression proteomics

Expression proteomics tries to identify and quantify the proteins found in a specific tissue, cell or body fluid under specific conditions. To this aim, different separation and identification techniques are used in order to perform qualitative and quantitative large-scale characterization studies. Those

techniques are constantly in renovation, being more and more automatic and allowing higher sensitivity.

Different classifications of those techniques can be performed according to different criteria. For example, taking into account the separation techniques used we can speak about gel-based or gel-free proteomic techniques. They can also be classified according to the aim of the study as discovery or targeted proteomics. Depending on the type of quantification performed, they can be classified as relative or absolute quantification techniques.

I.6.2.1 Mass spectrometry in protein characterization

Nowadays, protein characterization by mass spectrometry (MS) is an indispensable tool in the proteomics field, thanks to the creation of databases with information coming from genetic studies (gene and genome sequences) and to the improvements in the protein and peptide ionization methods (Aebersold and Mann 2003, Colomé 2012).

Mass spectrometers consist of three main parts: the ion source, the analyzer and the detector (Fig. I-19).

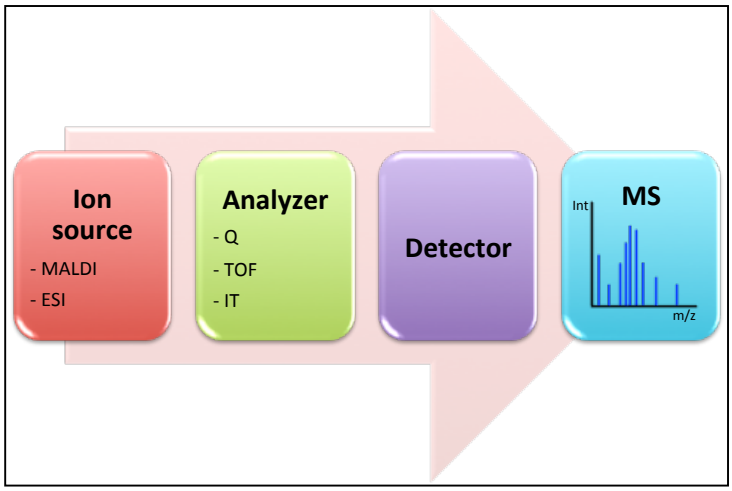

Figure I-19. Schematic representation of a mass spectrometer. Matrix-assisted laser desorption/ionization (MALDI), electrospray (ESI), quadrupole (Q), time-of-flight (TOF), ion trap (IT), mass spectra (MS).

There are several types of ion sources (MALDI, ESI) and analyzers (quadrupole, time-of-flight, ion trap). The selection of a given combination over another is defined by the kind of experiment or analysis that will be performed. Table I-6 shows the performance and characteristics of the most used mass spectrometers in proteomics (Domon and Aebersold 2006).

Table I-6. Summary of performance and characteristics of mass spectrometers

Characteristic	MALDI-TOF	ESI-IT	ESI-Q-TOF	ESI-QqQ	ESI-Orbitrap
Mass precission	+++	+	++++	+	++++
Resolution	+++	++	+++	+	++++
Sensitivity	+++	++	+++	++++	++++
Dynamic range	++	++	+++	++++	+++

+ means bad or low, ++++ means good or high

A mass spectrometer with a high mass accuracy avoids false positive identifications. In addition, the higher the resolution, the lower is the overlapping between peaks and the better is the assignment of the number of charges of a peptide. Other characteristics not taken into account in the table are their ability to measure low masses or the possibility of identifying PTMs. MALDI-TOF is the usual choice for the identification of proteins after their separation by bidimensional gels by means of peptide mass fingerprinting (PMF). However, for high troughput identification of proteins by LC-MS/MS (liquid chromatography coupled to tandem mass spectrometry) after protein digestion, the usual procedure is ESI-IT or Orbitrap mass spectrometry. Finally, for the validation of biomarkers, where targeted quantitative measures with high specificity and sensitivity are needed, ESI-QqQ instruments are the most commonly used, although other types of targeted LC-MS/MS analysis are possible in Orbitrap or Q-TOF instruments.

I.6.2.1.1 Protein identification

Generally, while speaking about protein identification by mass spectrometry, there are two main approaches. The first one, known as top-down proteomics, is based in the analysis of an intact protein. Under this approach, intact proteins are ionized and introduced in the analyzer without any previous enzymatic digestion. The second one, known as bottom-up proteomics, is based in the analysis of the peptide mixture resulting from enzymatic digestion of a protein. Through the analysis of those peptides it is possible to identify proteins by peptide mass fingerprinting or tandem mass spectrometry.

I.6.2.1.1.1 Protein identification by peptide mass fingerprinting (PMF)

The digestion of a given protein by a specific protease results in a collection of peptides specific for that pair of protein-protease. The molecular mass of those peptides can be determined by MS, resulting in a list of masses (mass spectra) known as peptide fingerprint.

The identification of a protein from its peptide fingerprint is possible thanks to bioinformatic tools. First, the protein or genomic sequence for the studied protein needs to be in a database (SwissProt, NCBI, IPI). Second, we need to use a search motor (MASCOT, Phenyx), that will generate the *in silico* peptide mass fingerprint for all the proteins listed in the database depending on the selected protease, among other parameters. Finally, the selected search motor will compare the *in silico* and experimental peptide fingerprints, giving as a result a list of possible candidate proteins, sorted according to the level of confidence in the identification (score) (Fig. I-20).

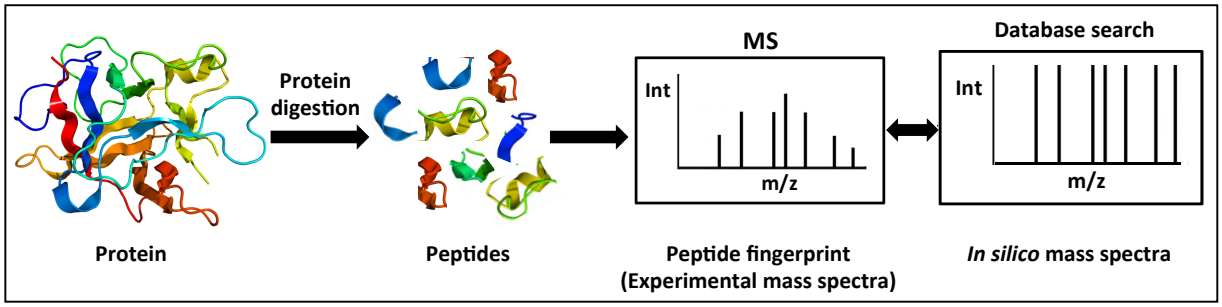

Figure I-20. Workflow of protein identification by peptide mass fingerprinting (PMF)

PMF is only used in the identification of purified proteins or for low complex samples. It is the most common identification procedure in bidimensional electrophoresis and MALDI-TOF is usually the mass spectrometry technique applied.

I.6.2.1.1.2 Tandem mass spectrometry (MS/MS)

Tandem mass spectrometry or MS/MS consists in the fragmentation of a peptide in the mass spectrometer thanks to the collision of its ions with an inert gas. Each peptide has a characteristic fragmentation pattern (fragmentation spectra) that allows the determination of its amino acid sequence. The fragmentation pattern depends on the sequence of the peptide, the number of charges of the fragmented ion, the collision energy and the kind of collision gas used.

The fragmentation of a peptide takes place mainly on the peptide bonds in its linear backbone chain. The resulting fragments can be of different nature and there is a specific nomenclature to distinguish them (Biemann 1992, Roepstorff and Fohlman 1984). Fig. I-21 shows those fragments and the specific nomenclature. Only fragments with at least one charge can be detected. When that charge is retained in the fragment containing the N-terminus of the peptide, fragments are referred as type a, b or c. If the charge is retained in the fragment containing the C-terminus of the peptide, the ions are defined as x, y or z. The number of amino acid residues contained in the fragment is expressed with a subscript. In addition, inner fragments can be obtained. The most commonly observed are the immonium ions, derived from a single amino acid.

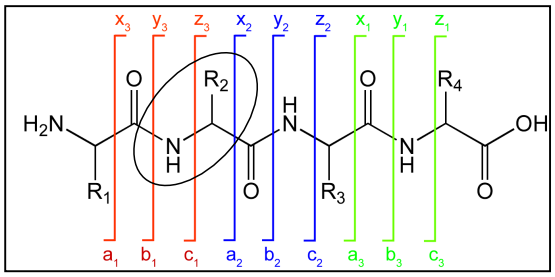

Figure I-21. Peptide fragmentation notation using the scheme of Roepstorff and Fohlman. The circle shows the inner fragment immonium.

There are also different kinds of collision energy, depending mainly of the mass spectrometer used. In the specific case of TOF and IT instruments, low collision energies are applied in order to induce dissociation (CID). The typical fragments obtained in those cases are type y and b, as a result of breaking of the amide bond. In addition, in IT instruments it is also possible to work with collision energies based in fragmentation by transference (ETD) or capture (ECD) of electrons, resulting in

fragments c, y and z. The advantage of these fragmentations is that week bonds such as the ones in PTMs are not broken, allowing their detection. Finally, in MALDI-TOF instruments, fragmentation is based in post-source decay (PSD) and the types of fragments obtained are mainly y and b.

As it occurs in PMF, MS/MS protein identification is based in the comparison of experimental data to *in* silico results from databases. It is not necessary that the fragmentation spectra matches the whole sequence. Therefore, identifications can be performed from partial sequences and the molecular mass of the parental peptide (Fig. I-22).

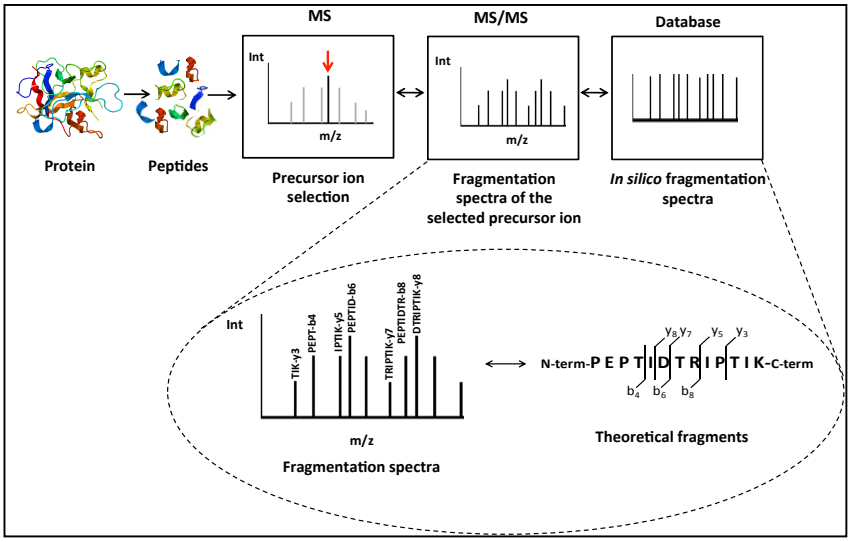

Figure I-22. Workflow of protein identification by MS/MS. Circled in the image there is a theoretical example for the experimental-*in silico* comparison performed in the identification.

I.6.2.1.2 Sample preparation

Proteins are part of a complex network of interacting biomolecules that regulate their function and localization within the cell. Therefore, extraction and isolation of proteins from chemical and physical interactions with other biomolecules from specific cellular sub-compartments is a critical step for their global analysis in a biological context (Zhang et al. 2013).

The choice and optimization of sample preparation protocols is critical for the quality of the final mass spectrometry results. There is no universal rule of thumb for sample preparation, since it is tightly related to the kind of experiment to be performed or its main goal, as well as the nature of the sample itself.

Usual challenges found are related to cell disruption, subcellular fractionation, protein enrichment, elimination of interfering substances, dynamic range of samples, solubilization and denaturation of proteins and quantification of proteins.

Subcellular fractionation allows the reduction of sample complexity and the enrichment of proteins from a certain cell compartment. Another way to reduce sample complexity is protein enrichment and more specifically, PTMs enrichment. On this way, it is possible to fractionate the proteome according to certain biochemical pathways or biological events. In addition, one of the main drawbacks while working in proteomics is the large dynamic range of samples, which causes that just the most abundant proteins are detected and measured in the mass spectrometer, masking changes

involving less abundant proteins. Indeed, all steps within an LC-MS proteomics approach are protein abundance-dependent. In order to solve this problem, apart from reducing sample complexity, depletion or elimination of most abundant proteins is a good solution. Moreover, in order to be able to label proteins, separate them by mono or bidimensional electrophoresis, digest them or analyze them by LC-MS, proteins must be soluble and totally disaggregated. To this purpose, it is common to work with solutions containing neutral chaotropic agents, detergents and reducing agents. Finally, a common way to concentrate proteins and separate them from interfering contaminants is protein precipitation by organic solvents, acids, salts or a combination of some of them.

A common way to enrich a given protein and dramatically reduce sample complexity is immunoprecipitation. We will give special attention to this technique, since it was the one selected in the present work.

I.6.2.1.2.1 Immunoprecipitation

Classical immunoprecipitation protocols required the presence of bi- or multivalent antibodies and an antigen with at least two antigenic determinants per molecule. Cross-linking of antigen molecules resulted in the formation of a lattice that gradually increased its size until its precipitation from the solution. In order to enable the formation of lattices, it was necessary to find the optimal proportion of antigen:antibody (equivalence zone) in order to achieve maximum immunoprecipitation of the antigen (Fig. I-23). The time course of the immunoprecipitation varied dramatically depending on the affinity, avidity, and valence of the antibody; the size and number of antigenic determinants of the antigen; the reaction temperature, ionic strength, and viscosity of the medium; the interactions between the medium and reactants; among other factors (McClatchey 2002).

However, modern immunoprecipitation techniques have evolved to more easily optimizing protocols, being no longer necessary to take into account the equivalence zone. There are two different approaches depending on when the immobilization of the antibody takes place, either before or after antigen-antibody recognition (Fig. I-24). In the first case, an antibody (monoclonal or polyclonal) against a specific protein is pre-immobilized onto an insoluble support, such as agarose or magnetic beads, and then incubated with a cell lysate containing the target protein. The immobilized immune complexes are then collected from the lysate, eluted from the support and analyzed. In the second case, free antibody forms immune complexes in the lysate and then the complexes are pulled down by the insoluble support. This second approach is beneficial if the target protein is present in low concentrations, the antibody has a weak binding affinity for the antigen or the binding kinetics of the antibody to the antigen are slow. In general, antibodies are immobilized to the different supports either by interaction with protein A or G, either by covalent immobilization strategies that chemically bind the antibody to the beaded support.

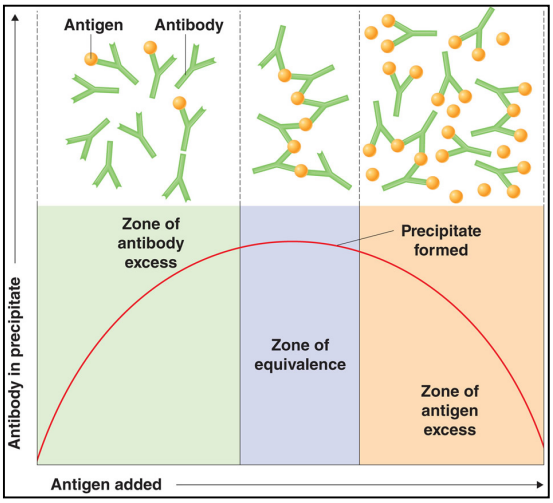

Figure I-23. Immunoprecipitation reaction as a function of antigen concentration
From http://classes.midlandstech.edu/carterp/Courses/bio225/chap18/lecture2.htm

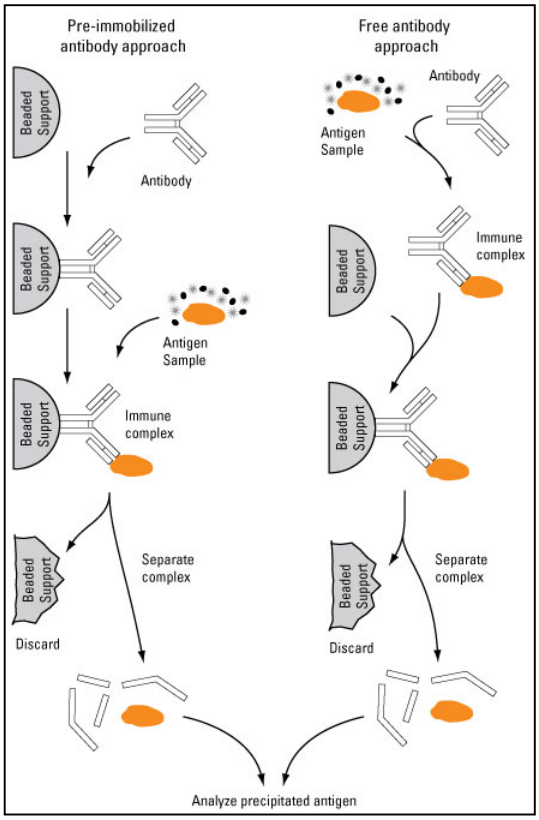

Figure I-24. Schematic representation of immunoprecipitation (IP). Left, IP using pre-immbolized antibodies. Right, IP using free antibodies and immobilization after antigen recognition. From http://www.piercenet.com/method/immunoprecipitation

The decision regarding whether to use a polyclonal or monoclonal antibody depends on its use and its commercial availability. Polyclonal antibodies can be generated much more rapidly, are less expensive and require less technical skills. Nevertheless, monoclonal antibodies are mono-specific, a useful characteristic while evaluating changes in molecular conformation, protein-protein interactions, phosphorylation states or identifying single members of protein families. However, that high specificity may represent a drawback in some cases. For example, small changes in the structure

of an epitope, such as genetic polymorphism, glycosylation or denaturation, may lead to no recognition by the antibody. Those changes, in contrast, do not affect polyclonal antibodies recognition, since they are heterogeneous and recognize a host of antigenic epitopes (Lipman et al. 2005).

I.6.2.1.3 Shotgun/Discovery proteomics

Shotgun proteomics refers to the use of bottom-up strategies on a mixture of proteins, the term was first used by the Yates lab, based on its analogy with shotgun genomic sequencing. Shotgun proteomics provides an indirect measurement of proteins through peptides derived from proteolytic digestion of intact proteins. The obtained peptide mixture is usually fractionated by liquid chromatography and then analyzed by MS/MS. Identification of peptides is performed by comparison to *in silico* data from databases (Fig. I-25). Nevertheless, notable success has been achieved by top-down approaches, measuring up to 200 kDa proteins and performing a large scale study for the identification of more than 1000 proteins by multi-dimensional separations from complex samples. Despite this progress and the fact that the top-down approach has some potential advantages for PTM and protein isoform determination, it has significant limitations compared with shotgun proteomics. Those limitations are mainly related to difficulties in protein fractionation, ionization, and fragmentation in the gas phase, making shotgun proteomics more universally adopted for protein analysis (Zhang et al. 2013).

In the past decade shotgun proteomics have been widely used by biologists for many different research experiments. Some of those applications include proteome profiling, protein quantification, protein modification, and protein-protein interaction. In addition, with the advances in sample preparation, protein/peptide fractionation, sensitivity, and accuracy in modern mass spectrometry, the proteome map of a certain organisms can now be routinely obtained in reasonable depth using shotgun methods (Zhang et al. 2013).

Finally, bioinformatics is an essential aspect of shotgun proteomics, since increasingly complex data sets from increasingly comprehensive MS-based proteomic analyses are being produced. The integration of bioinformatic tools into proteomics pipelines has begun to help standardize and simplify proteomic analysis.

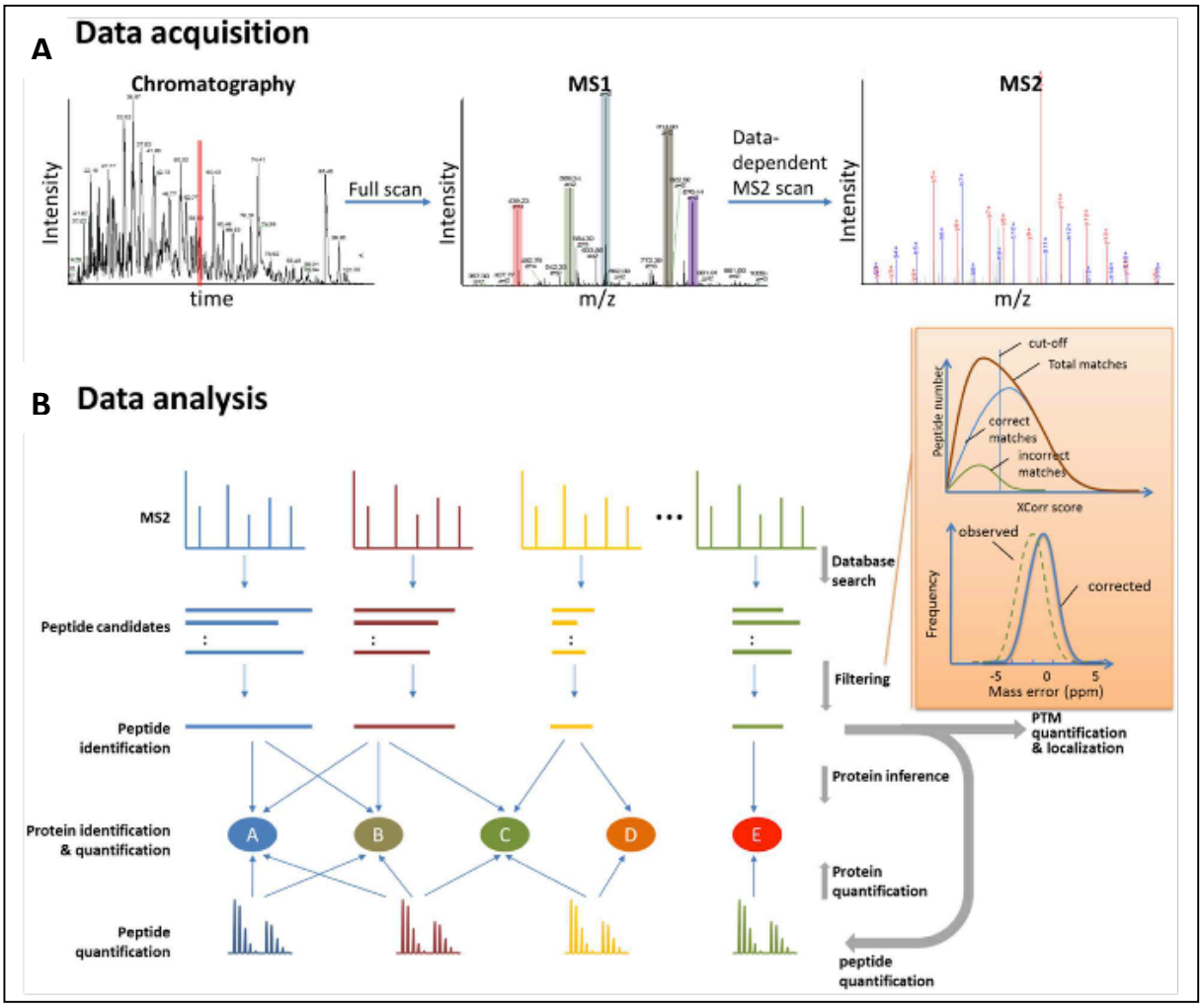

Figure I-25. Representative LC-MS/MS data and bioinformatic analysis pipeline for protein identification and quantification in shotgun proteomics. (A) Data acquisition and fragmentation spectra obtention. **(B)** The acquired data is processed through a bioinformatics pipeline. Database search is used to match theoretically generated peptide fragmentation spectra to experimental MS/MS fragmentation spectra, allowing protein identification and quantification (Zhang et al. 2013).

I.6.2.1.4 Targeted proteomics

In the past decade, most of the proteomic studies were based on shotgun proteomics in order to maximize the amount of information obtained in an experiment. However, it has been pointed out that those experiments present several limitations such as instrumental scanning speed, stochastic selection of ions for fragmentation, poor reproducibility, and a relatively narrow dynamic range. Moreover, and despite the improvements in current instrumentation, the number of peptides in a biological digest may be many times larger than the number of ions that can be sequenced in an experiment. Therefore, most of the information would still be inaccessible due to under-sampling. Finally, as a consequence of the bias for the most abundant species that those methods present, low abundance peptides are unlikely being sequenced in a complex biological sample (Law and Lim 2013).

In addition, the ability to detect and quantify proteins or sets of proteins with high precision across multiple samples has become an essential task in biological and biomedical research. To this purpose, targeted proteomics have emerged recently. Proteomic techniques based on targeted

proteomics offer specificity, reproducibility, sensitivity, and linearity, allowing quantitative studies. Moreover, high-throughput genomics and proteomics platforms have accelerated the discovery of biomarker candidates as indicative of disease states. Those candidates need to be further confirmed before entering expensive validation studies. The conventional approach based on immunoassays (for example, ELISA) to measure proteins in body fluids is at present the gold standard methodology. Nevertheless, developing ELISAs for new targets requires substantial efforts and cost. Thus, there is a need of alternate solutions offering cost-effective and high-throughput analysis. On this sense, targeted proteomics have also emerged as an effective approach to evaluate protein biomarkers (Kim et al. 2013).

However, and despite all these advantages, targeted proteomics have not been the preferred method for many studies. This can be explained by the fact that a prior knowledge of the targeted proteins in the sample is required and that the number of proteins that can be monitored is limited, in practice, up to 100. Finally, method development process in targeted approaches is sometimes laborious and time consuming (Kim et al. 2013).

We will here discuss about three different targeted proteomic approaches. First, we will focus on selected reaction monitoring (SRM) based proteomics since it is the main and first targeted approach used in this kind of experiments. Second, we will center in parallel reaction monitoring (PRM) as a recent alternative to SRM experiments. Finally, we will explain targeted approaches based on MS information and the high resolution of the new instruments. We will give special interest to this last point since it has been the method of choice in the present study.

I.6.2.1.4.1 Selected Reaction Monitoring (SRM)

SRM is used most effectively in a liquid chromatography-coupled mass spectrometry (LC-MS) system, where a capillary chromatography column is connected in-line to the electrospray ionization source of the mass spectrometer. SRM profits from the unique characteristic of triple quadrupoles (QQQ) mass spectrometers to act as mass filters and to selectively monitor a specific analyte molecular ion and one or several fragment ions generated from the analyte by collisional dissociation (Picotti and Aebersold 2012). The number of fragment ions that reach the detector is counted over time, resulting in a chromatographic trace where signal intensity is represented versus the retention time (Fig. I-26). Each pair of precursor-fragment ion is called transition, and can be sequentially and repeatedly measured at a periodicity that is fast compared to the analyte's chromatographic elution, yielding chromatographic peaks for each transition and allowing the quantification of multiple analytes. This multiplexing capability has led to the term multiple reaction monitoring (MRM), often used as a synonym for SRM experiments (Picotti and Aebersold 2012).

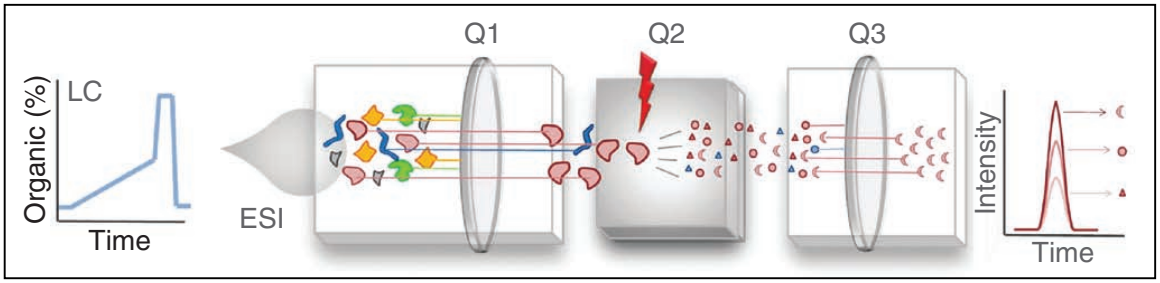

Figure I-26. Schematic representation of the selected reaction monitoring technique. Molecular ions of a specific analyte are selected in Q1 and fragmented in Q2. A specific fragment ion from the target analyte (transition) is selected in Q3 and guided to the detector (Picotti and Aebersold 2012).

SRM experiments are based on the analysis of peptide mixtures resulting from enzymatic digestion of proteins. Specifically, molecular ions within a mass range centered around the mass of the targeted peptide are selected in the first mass analyzer (Q1), fragmented at the peptide bonds by collision-activated dissociation (in Q2), and one or several of the fragment ions uniquely derived from the targeted peptide are measured by the second analyzer (Q3). If the suitable heavy isotope-labeled reference standards are added to the peptide mixture, absolute quantification of targeted peptides is possible and thus, absolute quantification of the corresponding proteins (Picotti and Aebersold 2012).

A typical SRM experiment consists of four different steps: selection of the target peptides, selection of the optimal transitions and its validation, data acquisition and finally, confirmation of the peptides detected. Desirable target peptides are unique to the target protein and easily detectable by mass spectrometry. The choice of peptides with favorable mass spectrometry properties (high signal intensity and low level of interfering signals) is crucial since it determines the sensitivity of the assay. In order to validate the selected transitions, Q2-fragment ion spectra of the target peptide are acquired on a QQQ instrument and assigned via sequence database searching, with the corresponding statistical filtering of the data to an acceptable error rate. Referring to SRM data acquisition, there is a physical limit to the number of transitions that can be measured in the same analysis. Monitoring too many transitions in an SRM run results in too long a cycle time and hence an insufficient number of data points to reconstruct the chromatographic elution profile of the targeted peptide, compromising accurate quantification. As a partial solution to this problem, scheduled SRM methods have been developed. A scheduled SRM method monitors the transitions for a given peptide in a small time window centered around the expected peptide elution time. Consequently, the cycle time is spent measuring the peptides actually eluting in the selected time window, increasing the number of peptides measured in a LC-MS run without reducing the limit of detection or the quantitative accuracy. Typically, in order to confirm if the peptides detected are the desired ones, 3-5 transitions are measured and usually, heavy isotope-labeled standards are added to the sample, simplifying the peptide detection step (Picotti and Aebersold 2012).

In addition, as it has already been mentioned, one of the main advantages of targeted approaches is that they allow quantification, absolute or relative, of several proteins. In the case of relative quantification, the purpose is to express the amount of a protein in a given state relative to that of another state. A summary of the quantification strategies than can be included in a SRM experiment is shown in Table I-7. We can differentiate between label-free and label-based approaches, being the first ones more simple and straightforward but less precise than the second ones.

Table I-7. Protein quantification strategies used with SRM. Adapted from (Picotti and Aebersold 2012)

Quantification	Labeling	Quantification strategy
Relative	Labe-free	Label-free
	Metabolic stable-isotope labeling	[15N] ammonium sulfate
		SILAC
	Chemical stable-isotope labeling	ICAT
		iTRAQ
		mTRAQ
	Enzymatic stable-isotope labeling	[18O] water
Absolute	Metabolic stable-isotope labeling	QconCAT
		PSAQ
	Chemical stable-isotope labeling	AQUA synthetic peptides

SILAC, stable-isotope labeling by amino acids in cell culture; ICAT, isotope-coded affinity tags; iTRAQ, isobaric tags for relative and absolute quantificaition; mTRAQ, non-isobaric tags for relative and absolute quantification; QconCAT, quantification concatamers; and PSAQ, protein standard absolute quantification

I.6.2.1.4.2 Parallel Reaction Monitoring (PRM)

As a result of the analytical advantages offered by SRM, mainly high sensitivity and multiplexing, this technique has been more and more used in biomarker evaluation. Nevertheless, while working with very complex samples, analyzers are prone to loss of selectivity introduced by the presence of background signals. In order to overcome those difficulties, more accurate analyzers were needed and high-resolution and accurate-mass (HR/AM) analyzers appeared. Lately, hybrid instruments such as fast quadrupole-TOF (Q-TOF) and quadrupole-Orbitrap (Q-Orbitrap) mass spectrometers were applied to quantify peptides in biological samples, demonstrating their effectiveness for the development of more robust methods in biomarker evaluation (Kim et al. 2013).

State-of-the art LC-MS instruments can measure easily biomarkers circulating in several body fluids at very low concentrations, without interference of background signals. However, in practice, nonspecific background from co-eluting peptides interferes with the measurement. This phenomenon is translated in higher values for the limits of detection and quantification, which are more related to sample complexity than to the intrinsic sensitivity of the instrument.

Recently, significant progress in quantitative analysis has been achieved thanks to high-performance instruments such as Q-Orbitrap spectrometers. Advances in quantitative methodologies have been done thanks to HR/AM measurements with fast acquisition rate (Kim et al. 2013). One of those methods is PRM that unlike SRM, it acquires full MS/MS spectra of selected precursor ions from the quadrupole in the Orbitrap, providing highly accurate m/z values of fragment ions. The signals of fragment ions are extracted to construct a series of extracted ion chromatograms (XICs), alike the traces of multiple transitions in SRM methods, being used for quantification (Fig. I-27).

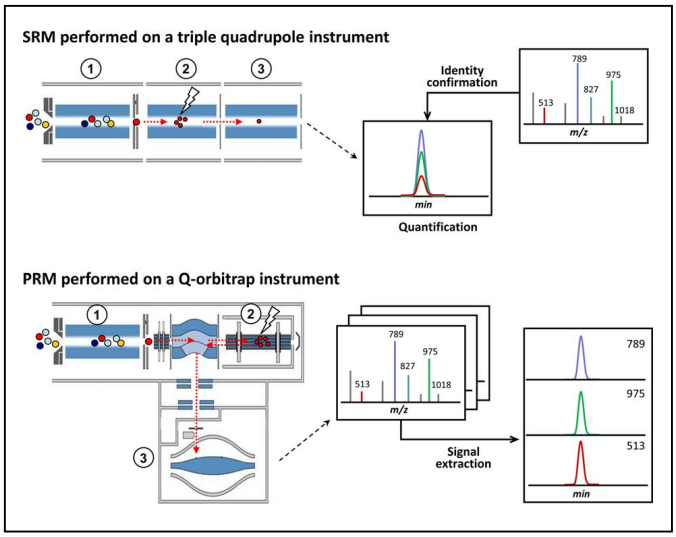

Figure I-27. Targeted analysis of proteins. Upper part shows targeted analysis performed in a triple quadrupole in SRM mode. Lower part shows targeted analysis in a Q-Orbitrap performed in PRM mode. In SRM, peptide ions enter Q1 (1) where a targeted precursor is selected and transferred to Q2 (2) and fragmented. Selected fragments are filtered in Q3 (3) and the ions measured by the detector directly reflect the amount of peptide in the sample. In PRM, precursors are selected in the quadrupole (1) and transferred to the collision cell (2) via the C-trap in order to perform fragmentation. The fragmented ions are transferred to the orbitrap via the C-trap, and analyzed in HR/AM mode (3). Ion chromatograms (XICs) are generated from the MS/MS spectra (Kim et al. 2013).

The markedly reduction in background interference is explained by the fact that narrow extraction window for XICs can be used (e.g., a tolerance of ≈10 ppm), improving the selectivity of the assays. It has been demonstrated that the improving in the selectivity is directly related to an improvement in the sensitivity. Moreover, the experimental design in a PRM experiment is simplified compared to a SRM one, since only m/z values of selected precursor ions are required instead of all the predefined transitions with SRM. Therefore, the traces used in data analysis can be selected post-acquisition because the signals of all fragment ions are already recorded in the PRM experiment, without the need for validation or selection of transitions. In addition, as many signals as possible can be introduced without any compromise in throughput, PRM assays are more robust compared to SRM experiments. However, local spectral libraries generated from the analysis of reference compounds under well-controlled conditions are required to exploit this strategy, since fragmentation patterns are strongly dependent on instrumental and experimental parameters. Such spectral libraries can be further exploited to determine the peptide-specific optimal acquisition parameters, such as the collision energy generating the most abundant fragment ions (Kim et al. 2013).

I.6.2.1.4.3 Targeted High-Resolution extracted ion chromatogram (HR-XIC)

Another alternative to the time-consuming SRM experiments that does not require detailed knowledge of the fragmentation of the target peptides is HR-XIC. HR-XIC is a targeted proteomics approach based on extracted ion chromatograms at the level of MS using the high-resolution, dynamic range and accuracy at all acquisition speeds offered by an Ultrahigh Resolution (UHR) Q-TOF system. Stable signal intensities and high mass accuracy are achieved in this kind of platform, providing the robustness, speed, sensitivity and selectivity required for an MS-based quantification. Moreover, the high-resolution based approaches supported by the Q-TOF architecture enable all detectable ions to be recorded, therefore allowing retrospective data mining. For HR-XIC, data

acquisition is accomplished in the full-scan MS mode without any fragmentation events. Therefore, identification and quantification is based on the MS1 signals from the m/z value and retention time (Fig. I-28). In this way, the instrument is set up so that the highest sensitivity in MS mode can be obtained without compromising the number of data points that characterize the chromatographic peak. HR-XIC offers a very simple way to proceed to targeted proteomics experiments, with virtually no method development and a full compatibility with very sharp UHPLC peaks. However, its main limitation is the potential of interferences from isobaric co-eluting ions in very complex sample digests.

Data processing automation is a very important step in targeted approaches and fully contributes to the robustness and ease of use of these strategies. In this line, Skyline Software is a freely available tool for targeted proteomics developed by the MacCoss lab (University of Washington). Initially, it was designed to support method creation and data analysis for triple quadrupole instruments. Nevertheless, it supports now chromatography-based quantitative proteomics approaches for QTOF instruments, like the HR-XIC strategy.

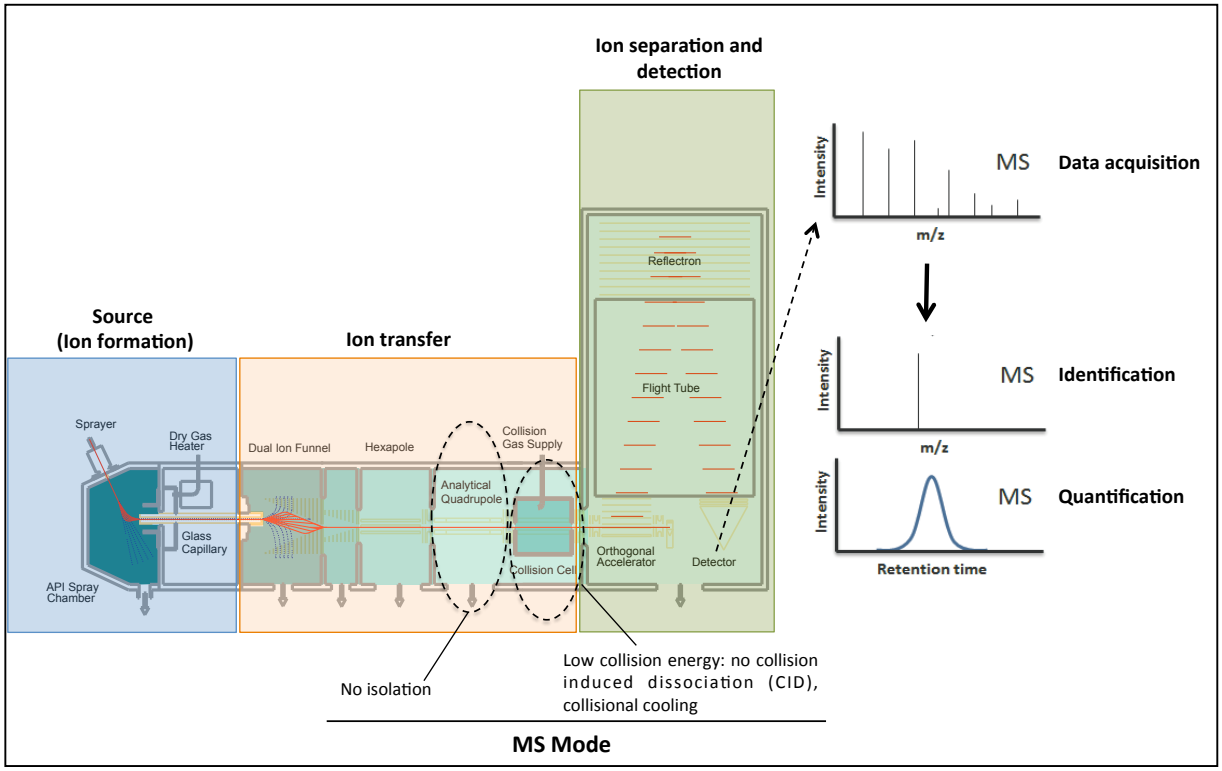

Figure I-28. Schematic representation of targeted HR-XIC. Data acquisition is accomplished in the full-scan MS mode without any fragmentation events. Identification and quantification is based on the MS1 signals from the m/z value and retention time

For identification of target peptides, an identification run is required where acquisition is performed using a shotgun method with a dynamic MS/MS acquisition speed. A spectral library is built in Skyline software based on this MS/MS run, in order to provide target information needed for the later quantification, like m/z value and retention time. Skyline software allows the configuration of several parameters that enable a better data filtering of m/z precursors. Afterwards, data sets (MS runs) are imported into Skyline. The software provides detailed graphical information regarding retention times and peak areas, helping to quickly evaluate peak picking of targeted peptides. Some of this

graphical information is the expected precursor area isotopic distribution and the dot product. Expected precursor area isotopic distribution can be directly compared to the observed precursor ion peak area distribution for a selected precursor ion. In addition, Skyline can also display, through the dot product (idopt) representation, the comparison of observed and theoretical isotopic distributions. The idopt value provides an addition step for verification of correct peak picking especially if no MS/MS data is available, like in the case of HR-XIC. For an ideal peak match and therefore a correct peak picking, the idopt value is 1.0 (Fig. I-29). Retention times and peak areas are displayed throughout all samples giving a fast overview about peak picking and allowing interaction with regard to the picked peak and retention times across samples (Kaspar et al. 2014).

As in the previous targeted approaches, HR-XIC also allows quantitative measurements of several peptides. Absolute quantification can be performed by means of adding isotope-labeled reference standards. Skyline filters the m/z signals for both heavy (standard) and light (endogenous) peptides (co-eluting in the chromatogram), allowing the comparison of their areas and thus, the determination of the absolute quantification of the endogenous peptides in the samples (Kaspar et al. 2012).

In conclusion, it has been shown that the combination of HR-XIC approaches together with Skyline based post-processing allows combining state-of-the art quantitative performance with an accurate and seamless data processing workflow. The results obtained by this combination have shown that targeted proteomics based on HR-XIC can be a good alternative to SRM or PRM strategies.

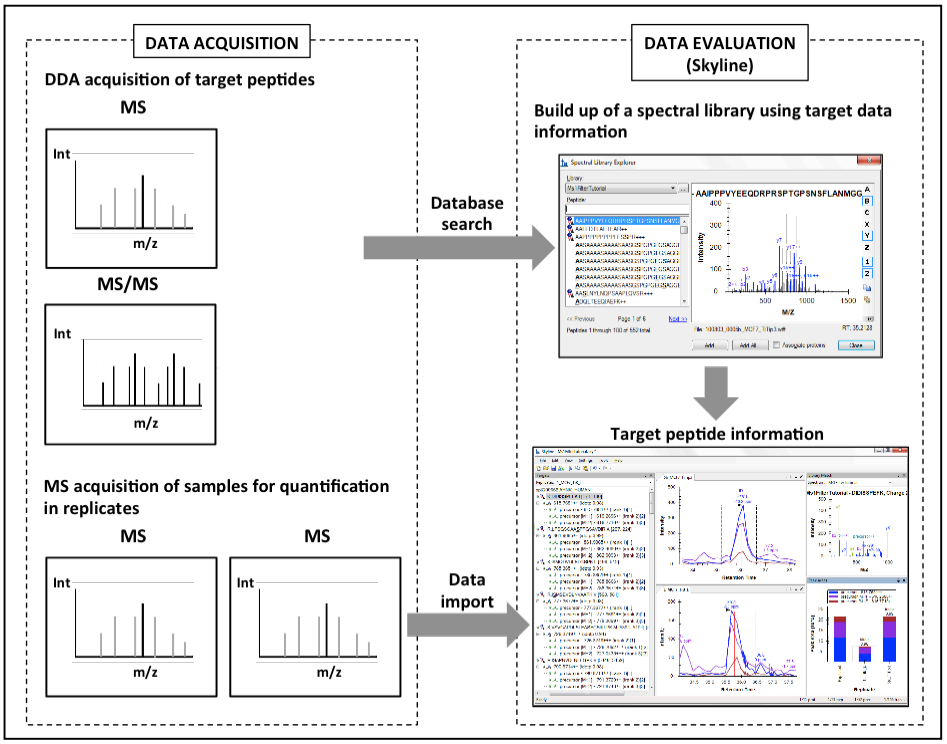

Figure I-29. Workflow for targeted proteomics using HR-XIC for data acquisition and Skyline software for data processing

I.7 CONTEXT OF THE THESIS

I.7.1 Background in the research group

The present work was carried out within the framework of a collaboration started in 2001 by the Biochemistry Laboratory (The Institut Químic de Sarrià - Universitat Ramon Llull, IQS-URL), the University of Porto and the Glycoconjugates Unit (The Institut de Química Avançada de Catalunya - Centro Superior de Investigaciones Científicas, IQAC-CSIC). After the formation of the consortium its members have changed over the years, leading to its current composition: the Drug Discovery Platform, Parc Científic de Barcelona (PCB); the Glycoconjugates Unit (IQAC-CSIC); the PharmacoInformatics Group (PhI), IMIM Hospital del Mar Medical Research Institute, Universitat Pompeu Fabra; the Nephrology and Transplant Unit, Hospital Clínic de Barcelona-IDIBAPS; the Proteomics Laboratory, Vall d'Hebron Institute of Oncology (VHIO); and our group, the Biochemistry Laboratory (IQS-URL).

Initially, the project was aimed to the discovery of new TTR amyloidosis inhibitors based on tetramer stabilization. To this purpose, a kinetic turbidimetric assay was set up in our group, enabling high throughput screening of compounds. The starting point for the screening program by families was the natural TTR ligand, the thyroxin hormone. Hence, studies started with thyroxin analogs, either iodinated or not, leading to the iodination hypothesis. First trials involving iodination of compounds proved the hypothesis in structures derived from salicylic acid, since it was observed that the inclusion of iodine atoms in TTR ligands resulted in an increased tetramer stabilization. A special mention needs to be done regarding the pair diflunisal/iododiflunisal, with the development of a patent by the consortium for the latter. In order to broaden the collection of molecules assayed, different series of diflunisal derivatives (phenyl-salycilates) with inhibitory activity were tested, as well as iodinated structures derived from inactive molecules that ended in new lead compounds. From those studies it was also suggested that iodine location was relevant since iodination was not always effective. Additionally, more structures were assayed in order to complete the screening program with biphenilyc, monocyclic and flavone families, and supplementary information regarding binding constants was obtained by calorimetric techniques. Next step in the selection of inhibitors was the incorporation of bioinformatic drug discovery targeted strategies. Eventually, a large database with around 800 compounds was built, bringing together all the information obtained during the years and making it accessible to the consortium.

Finally, as a result of the studies aiming at shedding light on the mechanism of action of the different compounds, important residues related to binding were defined. Specifically, Lys15 and Glu54 were described as key residues for ligand binding stabilization and Thr119 was defined as a contributor to ligand binding and as a regulator of ligand binding cooperativity. The compounds were also studied from a structural point of view, concluding that the presence of hydrophobic substituents in positions 2', 3' and 5' of diflunisal derivatives enhanced ligand binding to TTR. In addition, we reported that halogenation of TTR ligands may improve their affinity and fibrillogenesis inhibition properties.

In Table I-8 a list of publications referring to the explained milestones of the group is included.

Table I-8. Publications of the TTR Consortium corresponding to the milestones of the group

Year	Title	Journal	Authors
2015 (Submitted)	Optimization of Kinetic Stabilizers of Tetrameric Transthyretin: A Prospective Ligand Efficiency-guided Approach	-	D. Blasi, E.Y. Cotrina, M. Vilà, A. Planas, G. Arsequell, G. Valencia, C. Abad-Zapatero, N.B. Centeno, J. Quintana
2015	Tuning Transthyretin Amyloidosis Inhibition Properties of Iododiflunisal by Combinatorial Engineering of the Nonsalicylic Ring Substitutions.	ACS Comb Sci	M. Vilaró, J. Nieto, J.R. La Parra, M.R. Almeida, A. Ballesteros, A. Planas, G. Arsequell, G. Valencia
2014	TTR Aggregate Specific Antibodies Recognize Cryptic Epitopes on Patient-Derived Amyloid Fibrils	Rejuvenation Res	M. Phay, V. Blinder, S. Macy, M.J. Greene, D.C. Wooliver, W. Liu, A. Planas, D.M. Walsh, L.H. Connors, S.R. Primmer, S.A. Planque, S. Paul, B. O'Nuallain
2013	Modulation of the fibrillogenesis inhibition properties of two transthyretin ligands by halogenation	J Med Chem	E. Cotrina, M. Pinto, L. Bosch, M. Vilà, D. Blasi; J. Quintana, N. Centeno, G. Arsequell, A. Planas, G. Valencia
2012	Methods to evaluate the inhibition of TTR fibrillogenesis induced by small ligands	Curr Med Chem	G. Arsequell, A. Planas
2011	Drug discovery targeted at Transthyretin cardiac amyloidosis: Rational design, synthesis and biological activity of new Transthyretin amyloid inhibitors	Amyloid	D. Blasi, M. Pinto, J. Nieto, G. Arsequell, G. Valencia, A. Planas, N. B. Centeno, J. Quintana
2011	Ligand-binding properties of human transthyretin	Amyloid	M. Pinto, D. Blasi, J. Nieto, G. Arsequell, G. Valencia, A. Planas, J. Quintana, N. B. Centeno
2011	Retrospective mapping of SAR DATE for TTR protein in chemico-biological space using ligand efficiency indices as a guide to drug discovery strategies	Mol Inform	D. Blasi, G. Arsequell, G. Valencia, J. Nieto, A. Planas, M. Pinto, N.B. Centeno, C. Abad-Zapatero, J. Quintana
2009	Isatin Derivatives, a Non-conventional Novel Class of Transthyretin Fibrillogenesis Inhibitors	Bioorg Med Chem Lett	A. González,J. Quirante, J. Nieto, M. R. Almeida, M. J. Saraiva, A. Planas,G. Arsequell, G. Valencia
2009	Iodine Atoms: A New Molecular Feature for the Design of Potent Transthyretin Fibrillogenesis Inhib-itors	PLoS One	T. Mairal, J. Nieto, M. Pinto, M. R. Almeida, L. Gales, A. Ballesteros, J. Barluenga, J. J. Pérez, J. T. Vázquez,N. B. Centeno, M. J. Saraiva, A. M. Damas, A. Planas, G. Arsequell, G. Valencia
2008	Reengineering TTR amyloid inhibition proper-ties of diflunisal	Amyloid and Amyloidosis	M. Vilaró, G. Arsequell, G. Valencia, A. Ballesteros, J. Barluenga, J. Nieto, A. Planas, R. Almeida, M.J. Saraiva
2005	Kinetic assay for high throughput screening of *in vitro* transthyretin amyloid fibrillogenesis inhibitors	J Comb Chem	I. Dolado, J. Nieto., M.J. Saraiva, G. Arsequell, G. Valencia, A. Planas
2004	Selective binding to transthyretin and tetramer stabilization in serum from patients with familial amyloidotic polyneuropathy by an iodinated diflunisal derivative	Biochem J	M. R. Almeida, B. Macedo,I. Cardoso, I. Alves, G. Valencia, G. Arsequell, A. Planas, M. J. Saraiva
2004	Identification of new diflunisal derivatives as potent in vitro transthyretin fibril inhibitors	Amyloid and Amyloidosis	T. Mairal, G. Arsequell, G. Valencia, I. Dolado, J. Nieto, A. Planas, J. Barluenga, A. Ballesteros, R. Almeida, M.J. Saraiva
2004	Effects of a new diflunisal derivative on transthyretin binding and stabilization in serum from FAP patiens	Amyloid and Amyloidosis	M.R. Almeida, B. Macedo, I. Cardoso, G. Valencia, G. Arsequell, A. Planas, M.J. Saraiva

I.7.2 Aims of the thesis

On the basis of the previous work carried out in the group and its trajectory, the present thesis tackles two main branches in the study of TTR amyloidosis: i) Therapeutic interventions and ii) FAP Diagnosis and monitoring. Therefore we continue with the historical research line of the laboratory in the screening of fibrillogenesis inhibitors, in this case, with a repurposing approach for the selection and screening of potential inhibitors. On the other hand, we propose a new research line in the group regarding Cys-10 TTR PTMs and we hypothesize that they may play a role in TTR pathogenicity. Our hypothesis is based on recent findings suggesting that Cys-10 TTR PTMs are relevant in terms of its amyloidogenicity potential and by the fact that they are highly abundant in plasmatic TTR. In addition, it is known that PTMs on most proteins affect their activity and processing. To asses this hypothesis, our first aim is to develop an analytical mass spectrometry method based on targeted proteomics for the quantitative analysis of previously reported Cys-10 TTR PTMs. Secondly, we target the proteomic analysis of individuals carrying TTR mutations in order to gain new evidences on TTR related molecular mechanism, helping in diagnosing, monitoring and finding new therapeutic targets in FAP.

I.8 REFERENCES

Adams D (2013) Recent advances in the treatment of familial amyloid polyneuropathy. *Ther Adv Neurol Disord* 6(2):129–39.

Adamski-Werner SL, Palaninathan SK, Sacchettini JC and Kelly JW (2004) Diflunisal Analogues Stabilize the Native State of Transthyretin. Potent Inhibition of Amyloidogenesis. *J Med Chem* 47(2):355–74.

Aebersold R and Mann M (2003) Mass spectrometry-based proteomics. *Nature* 422(6928):198–207.

Aebersold R, Bader GD, Edwards AM, van Eyk J, Kussman M, Qin J and Omenn GS (2014) Highlights of B/D-HPP and HPP Resource Pillar Workshops at 12th Annual HUPO World Congress of Proteomics: September 14-18, 2013, Yokohama, Japan R. *Proteomics* 14(9):975–88.

Altland K, Winter P and Sauerborn MK (1999) Electrically neutral microheterogeneity of human plasma transthyretin (prealbumin) detected by isoelectric focusing in urea gradients. *Electrophoresis* 20(7):1349–64.

Andersson R (1976) Familial Amyloidosis with Polyneuropathy. A Clinical Study Based on Patients Living in Northern Sweden. *Acta Med Scand* Suppl (590):1–64.

Andrade C (1952) A Peculiar Form of Peripheral Neuropathy. *Brain* 75(3):408–27.

Arsequell G and Planas A (2012) Methods to Evaluate the Inhibition of TTR Fibrillogenesis Induced by Small Ligands. *Curr Med Chem* 19(15):2343–55.

Azoulay D, Salloum C, Samuel D and Planté-Bordeneuve V (2012) Operative risks of domino liver transplantation for the FAP liver donor and the FAP liver recipient. *Amyloid* 19(S1):73–4.

Baures PW, Oza VB, Peterson S a. and Kelly JW (1999) Synthesis and evaluation of inhibitors of transthyretin amyloid formation based on the non-steroidal anti-inflammatory drug, flufenamic acid. *Bioorg Med Chem* 7(7):1339–47.

Benson MD (1996) Leptomeningeal amyloid and variant transthyretins. Am J Pathol 148(2):351–4.

Benson MD, Kluve-Beckerman B, Zeldenrust SR, Siesky AM, Bodenmiller DM, Showalter AD, Sloop KW (2006) Targeted suppression of an amyloidogenic transthyretin with antisense oligonucleotides. *Muscle Nerve* 33(5):609-18.

Benson MD, Smith RA, Hung G, Kluve-Beckerman B, Showalter AD, Sloop KW, Monia BP (2010) Suppression of choroid plexus transthyretin levels by antisense oligonucleotide treatment. *Amyloid* 17(2):43-9.

Bergquist J, Andersen O and Westman A (2000) Rapid method to characterize mutations in transthyretin in cerebrospinal fluid from familial amyloidotic polyneuropathy patients by use of matrix-assisted laser desorption/ionization time-of-flight mass spectrometry. *Clin Chem* 46(9):1293–1300.

Bergström J, Gustavsson A, Hellman U, Sletten K, Murphy CL, Weiss DT, Solomon A, Olofsson BO and Westermark P (2005) Amyloid deposits in transthyretin-derived amyloidosis: Cleaved transthyretin is associated with distinct amyloid morphology. *J Pathol* 206(2):224–32.

Biemann K (1992) Mass spectrometry of peptides and proteins. *Annu Rev Biochem* 61:977–1010.

Bonifacio MJ, Sakaki Y and Saraiva MJ (1996) 'In vitro' amyloid fibril formation from transthyretin: the influence of ions and the amyloidogenicity of TTR variants. *Biochim Biophys Acta* 1316(1):35–42.

Buxbaum J, Anan I and Suhr O (2010) Serum transthyretin levels in Swedish TTR V30M carriers. *Amyloid* 17(2):83–5.

Cardoso I, Martins D, Ribeiro T, Merlini G and Saraiva MJ (2010) Synergy of combined doxycycline/TUDCA treatment in lowering Transthyretin deposition and associated biomarkers: studies in FAP mouse models. *J Transl Med* 8:74.

Chakrabartty A (2001) Progress in transthyretin fibrillogenesis research strengthens the amyloid hypothesis. *Proc Natl Acad Sci USA* 98(26):14757–9.

Coelho T, Adams D, Silva A, Lozeron P, Hawkins PN, Mant T, Perez J, Chiesa J, Warrington S, Tranter E, Munisamy M, Falzone R, Harrop J, Cehelsky J, Bettencourt BR, Geissler M, Butler JS, Sehgal A, Meyers RE, Chen Q, Borland T, Hutabarat RM, Clausen V a, Alvarez R, Fitzgerald K, Gamba-Vitalo C, Nochur S V, Vaishnaw AK, Sah DWY, Gollob J a and Suhr OB (2013) Safety and efficacy of RNAi therapy for transthyretin amyloidosis. *N Engl J Med* 369(9):819–29.

Colomé N (2012) Aplicació de tècniques proteòmiques de quantificació i validació en recerca biomèdica. Ph.D thesis, Autonomous University of Barcelona

Colon W and Kelly JW (1992) Partial denaturation of transthyretin is sufficient for amyloid fibril formation in vitro. *Biochemistry* 31(36):8654–60.

Connors LH, Lim A, Prokaeva T, Roskens V and Costello CE (2003) Tabulation of human transthyretin (TTR) variants, 2003. *Amyloid* 10(3):160–84.

Cotrina EY, Pinto M, Bosch L, Vilà M, Blasi D, Quintana J, Centeno NB, Arsequell G, Planas A and Valencia G (2013) Modulation of the fibrillogenesis inhibition properties of two transthyretin ligands by halogenation. *J Med Chem* 56(22):9110–21.

Coutinho P, da Silva A, Lima J and Barbosa A (1980) Forty years of experience with type 1 amyloid neuropathy: review of 483 cases. *Amyloid and amyloidosis* Excerpta M:88–98.

Dolado I, Nieto J, Saraiva MJM, Arsequell G, Valencia G and Planas A (2005) Kinetic assay for high-throughput screening of in vitro transthyretin amyloid fibrillogenesis inhibitors. *J Comb Chem* 7(2):246–52.

Domon B and Aebersold R (2006) Mass spectrometry and protein analysis. *Science* 312(5771):212–7.

Fändrich M (2012) Oligomeric intermediates in amyloid formation: Structure determination and mechanisms of toxicity. *J Mol Biol* 421(4-5):427–40.

Ferreira N, Cardoso I, Domingues MR, Vitorino R, Bastos M, Bai G, Saraiva MJ and Almeida MR (2009) Binding of epigallocatechin-3-gallate to transthyretin modulates its amyloidogenicity. *FEBS Lett* 583(22):3569–76.

Hamilton J a and Benson MD (2001) Transthyretin: a review from a structural perspective. *Cell Mol Life Sci* 58(10):1491–521.

Haynes PA, Gygi SP, Figeys D and Aebersold R (1998) Proteome analysis: biological assay or data archive? *Electrophoresis* 19(11):1862–71.

Jiang X, Buxbaum JN and Kelly JW (2001) The V122I cardiomyopathy variant of transthyretin increases the velocity of rate-limiting tetramer dissociation, resulting in accelerated amyloidosis. *Proc Natl Acad Sci USA* 98(26):14943–8.

Johnson SM, Wiseman RL, Sekijima Y, Green NS, Adamski-Werner SL and Kelly JW (2005) Native state kinetic stabilization as a strategy to ameliorate protein misfolding diseases: A focus on the transthyretin amyloidoses. *Acc Chem Res* 38(12):911–21.

Kaspar S, Schmit PO, Baessmann C, Percy A and Borchers C (2014). High quantification efficiency in plasma targeted proteomics with a full-capability discovery Q-TOF platform. *Bruker Application Note* #LCMS-89.

Kaspar S, Schmit PO, Jabs W, Baessmann C, MacLean B and Maccoss M (2012) Targeted Proteomics Using HR-XIC Filtering with Skyline. *Bruker Technical Note* #TN-43.

Kim Y, Gallien S, van Oostrum J and Domon B (2013) Targeted proteomics strategy applied to biomarker evaluation. *Proteomics Clin Appl* 7(11-12):739–47.

Kingsbury JS, Théberge R, Karbassi J a., Lim A, Costello CE and Connors LH (2007) Detailed structural analysis of amyloidogenic wild-type transthyretin using a novel purification strategy and mass spectrometry. *Anal Chem* 79(5):1990–8.

Knowles TP, Vendruscolo M and Dobson CM (2014) The amyloid state and its association with protein misfolding diseases. *Nat Rev Mol Cell Biol* 15(7):384–96.

Koike H, Hashimoto R, Tomita M, Kawagashira Y, Iijima M, Nakamura T, Watanabe H, Kamei H, Kiuchi T and Sobue G (2012) Impact of aging on the progression of neuropathy after liver transplantation in transthyretin Val30Met amyloidosis. *Muscle Nerve* 46(6):964–70.

Lai Z, Colon W and Kelly J (1996) The acid-mediated denaturation pathway of transthyretin yields a conformational intermediate that can self-assemble into amyloid. *Biochemistry* 35(20):6470–82.

Law K and Lim Y (2013) Recent advances in mass spectrometry: data independent analysis and hyper reaction monitoring. *Expert Rev Proteomics* 10(6):551–66.

Lim A, Prokaeva T, McComb ME, Connors LH, Skinner M and Costello CE (2003) Identification of S-sulfonation and S-thiolation of a novel transthyretin Phe33Cys variant from a patient diagnosed with familial transthyretin amyloidosis. *Protein Sci* 12(8):1775–85.

Lim A, Sengupta S, McComb ME, Théberge R, Wilson WG, Costello CE and Jacobsen DW (2003) In Vitro and in Vivo Interactions of Homocysteine with Human Plasma Transthyretin. *J Biol Chem* 278(50):49707–13.

Lipman NS, Jackson LR, Trudel LJ and Weis-Garcia F (2005) Monoclonal versus polyclonal antibodies: distinguishing characteristics, applications, and information resources. *ILAR J* 46(3):258–68.

Lladó L, Baliellas C, Casasnovas C, Ferrer I, Fabregat J, Ramos E, Castellote J, Torras J, Xiol X and Rafecas A (2010) Risk of Transmission of Systemic Transthyretin Amyloidosis After Domino Liver Transplantation. *Liver Transpl* 16(12):1386–92.

Magy N, Liepnieks J, Gil H, Kantelip B, Dupond J, Kluve-Beckerman B and Benson M (2003) A transthyretin mutation (Tyr78Phe) associated with peripheral neuropathy, carpal tunnel syndrome and skin amyloidosis. *Amyloid* 10(1):29–33.

Mascarenhas Saraiva MJ, Birken S, Costa PP and Goodman DS (1984) Amyloid fibril protein in familial amyloidotic polyneuropathy, Portuguese type. Definition of molecular abnormality in transthyretin (prealbumin). *J Clin Invest* 74(1):104–19.

McClatchey KD (2002) Clinical laboratory medicine. *Lippincott Williams & Wilkins (2nd Ed).*

Merlini G and Bellotti V (2003) Molecular mechanisms of amyloidosis. *N Engl J Med* 349(6):583–96.

Munar-Ques M, Costa PP, Saraiva MJ, Viader-Farre C and Munar-Bernat C (1988) Familial type I (Portuguese form) amyloidotic polyneuropathy in Majorca. Study using the TTR (Met30) genetic marker. *Med Clin (Barc)* 91(12):441–4.

Nakanishi T, Yoshioka M, Moriuchi K, Yamamoto D, Tsuji M and Takubo T (2010) S-sulfonation of transthyretin is an important trigger step in the formation of transthyretin-related amyloid fibril. *Biochim Biophys Acta* 1804(7):1449–56.

Oza VB, Smith C, Raman P, Koepf EK, Lashuel H a., Petrassi HM, Chiang KP, Powers ET, Sachettinni J and Kelly JW (2002) Synthesis, structure, and activity of diclofenac analogues as transthyretin amyloid fibril formation inhibitors. *J Med Chem* 45(2):321–32.

Picotti P and Aebersold R (2012) Selected reaction monitoring–based proteomics: workflows, potential, pitfalls and future directions. *Nat Methods* 9(6):555–66.

Pires RH, Karsai Á, Saraiva MJ, Damas AM and Kellermayer MSZ (2012) Distinct Annular Oligomers Captured along the Assembly and Disassembly Pathways of Transthyretin Amyloid Protofibrils. *PLoS ONE* 7(9).

Planté-Bordeneuve V (2014) Update in the diagnosis and management of transthyretin familial amyloid polyneuropathy. *J Neurol* 261(6):1227–33.

Poulsen K, Bahl JMC, Tanassi JT, Simonsen AH and Heegaard NHH (2012) Characterization and stability of transthyretin isoforms in cerebrospinal fluid examined by immunoprecipitation and high-resolution mass spectrometry of intact protein. *Methods* 56(2):284–92.

Raz A and Goodman D (1969) The interaction of thyroxine with human plasma prealbumin and with the prealbumin-retinal-binding protein complex. *J Biol Chem* 244(12):3230–7.

Raz A, Shiratori T and Goodman D (1970) Studies on the protein-protein and protein-ligand interactions involved in retinol transport in plasma. *J Biol Chem* 245(8):1903–12.

Redondo C, Damas A and Saraiva M (2000) Designing transthyretin mutants affecting tetrameric structure: implications in amyloidogenicity. *Biochem J* 348 Pt 1:167–72.

Robbins J, Cheng SY, Gershengorn M, Glinoer D, Cahnmann H and Edelnoch H (1978) Thyroxine transport proteins of plasma. Molecular properties and biosynthesis. *Recent Prog Horm Res* 34:477–519.

Roepstorff P and Fohlman J (1984) Proposal for a common nomenclature for sequence ions in mass spectra of peptides. *Biomed Mass Spectrom* 11(11):601.

Samuel D and Adams D (2007) Domino liver transplantation from familial amyloidotic polyneuropathy donors: How close is the damocles sword to the recipient? *Transpl Int* 20(11):921–3.

Saraiva MJ (2001) Transthyretin mutations in hyperthyroxinemia and amyloid diseases. *Hum Mutat* 17(6):493–503.

Saraiva MJ (2002) Hereditary transthyretin amyloidosis: molecular basis and therapeutical strategies. *Expert Rev Mol Med* 4(12):1–11.

Schreiber G, Aldred AR, Jaworowski A, Nilsson C, Achen MG and Segal MB (1990) Thyroxine transport from blood to brain via transthyretin synthesis in choroid plexus. *Am J Physiol* 258(2 Pt 2):R338–45.

Sekijima Y (2014) Recent progress in the understanding and treatment of transthyretin amyloidosis. *J Clin Pharm Ther* 39(3):225–33.

Sekijima Y, Hammarström P, Matsumura M, Shimizu Y, Iwata M, Tokuda T, Ikeda S and Kelly JW (2003) Energetic characteristics of the new transthyretin variant A25T may explain its atypical central nervous system pathology. *Lab Invest* 83(3):409–17.

Soprano DR, Herbert J, Soprano KJ, Schon EA and Goodman DS (1985) Demonstration of transthyretin mRNA in the brain and other extrahepatic tissues in the rat. *J Biol Chem* 260(21):11793–8.

Sousa MM and Saraiva MJ (2003) Neurodegeneration in familial amyloid polyneuropathy: From pathology to molecular signaling. *Prog Neurobiol* 71(5):385–400.

Suhr OB, Svendsen IH, Ohlsson P-I, Lendoire J, Trigo P, Tashima K, Ranlöv PJ and Ando Y (1999) Impact of age and amyloidosis on thiol conjugation of transthyretin in hereditary transthyretin amyloidosis. *Amyloid* 6(3):187–91.

Takaoka Y, Ohta M, Miyakawa K, Nakamura O, Suzuki M, Takahashi K, Yamamura K-I and Sakaki Y (2004) Cysteine 10 is a key residue in amyloidogenesis of human transthyretin Val30Met. *Am J Pathol* 164(1):337–45.

The Human Proteome Project (HPP). Available from: http://www.thehpp.org

Wallace M, Naylor SL, Kluve-Beckerman B, Long GL, McDonald L, Shows TB and Benson MD (1985) Localization of the human prealbumin gene to chromosome 18. *Biochem Biophys Res Commun* 129(3):753–8.

Westermark P, Benson MD, Buxbaum JN, Cohen AS, Frangione B, Ikeda S, Masters CL, Merlini G, Saraiva MJ and Sipe JD (2002) Amyloid fibril protein nomenclature -- 2002. *Amyloid* 9(3):197–200.

Westermark P, Sletten K, Johansson B and Cornwell GG 3rd (1990) Fibril in senile systemic amyloidosis is derived from normal transthyretin. *Proc Natl Acad Sci USA* 87(7):2843–5.

Wilkins M, Pasquali C, Appel R, Ou K, Golaz O, Sanchez J, Yan J, Gooley A, Hughes G, Humphery-Smith I, Williams K and Hochstrasser D (1996) From proteins to proteomes: large scale protein identification by two-dimensional electrophoresis and amino acid analysis. *Biotechnology (NY)* 14(1):61–5.

Yamamoto S, Wilczek H, Nowak G, Larsson M, Oksanen A, Iwata T, Gjertsen H, Söderdahl G, Wikström L, Ando Y, Suhr O and Ericzon B (2007) Liver transplantation for familial amyloidotic polyneuropathy (FAP): a single-center experience over 16 years. *Am J Transplant* 7(11):2597–604.

Zhang Q and Kelly JW (2003) Cys10 mixed disulfides make transthyretin more amyloidogenic under mildly acidic conditions. *Biochemistry* 42(29):8756–61.

Zhang Q and Kelly JW (2005) Cys-10 mixed disulfide modifications exacerbate transthyretin familial variant amyloidogenicity: A likely explanation for variable clinical expression of amyloidosis and the lack of pathology in C10S/V30M transgenic mice. *Biochemistry* 44(25):9079–85.

Zhang Y, Fonslow B, Shan B, Baek M and Yates J (2013) Protein analysis by shotgun/bottom-up proteomics. *Chem Rev* 113(4):2343–94.

OBJECTIVES

According to the general aims presented previously, the current thesis was carried out as a collaboration project within the framework of the TTR Consortium. Specifically, the therapeutic branch of the present work was conducted between the Biochemistry Laboratory (IQS-URL), the Drug Discovery Platform (PCB), and the Glicoconjugates Unit (IQAC-CSIC). The bioinformatic study was performed by the PCB, the molecules to test were provided by the IQAC-CSIC, and the experimental screening of compounds was carried out in our group, the Biochemistry Laboratory (IQS-URL). Regarding the FAP diagnosis and monitoring branch of the current thesis, it was conducted specifically as a collaboration between our group, the Biochemistry Laboratory (IQS-URL), and the Proteomics Laboratory (VHIO). The development of sample preparation methods from serum for unbiased recovery of all Cys-10 TTR PTMs was performed at the former. The development of the analytical mass spectrometry method based on targeted proteomics and the proteomic study of human samples were performed at the latter. Human samples studied in the present work were provided by the Nephrology and Transplant Unit (the Hospital Clínic de Barcelona) and the Centro de Química e Bioquímica (the University of Lisbon).

The specific objectives of this thesis are:

1. *In vitro* screening of a library of possible TTR inhibitors selected by a bioinformatic repurposing study:

    a. Expression and purification of recombinant human TTR and quality evaluation by MALDI-TOF MS
    b. Study of Cys-10 PTMs in the produced recombinant human TTR by MALDI-TOF MS
    c. Primary *in vitro* screening of compounds by means of the previously developed kinetic turbidimetric assay
    d. Preliminary secondary *in vitro* screening of lead compounds by calorimetric techniques

2. Development of an absolute quantitative mass spectrometry method based on targeted proteomics:

    a. Setting up of efficient sample preparation methods from serum and plasma for unbiased recovery of all Cys-10 PTMs
    b. Absolute quantification of the most common Cys-10 PTMs in human TTR
    c. Absolute quantification of human TTR serum levels
    d. Absolute quantification of wt:V30M TTR ratio in human serum and plasma
    e. Comparison of the newly developed analytical method with a relative quantification method available in the literature for the analysis of Cys-10 PTMs based on an intact protein approach

3. Analysis of serum samples of individuals carrying V30M TTR mutation by the absolute and relative quantification methods and correlation of proteomic data with the clinical stage of the individuals

CHAPTER 1. Testing new transthyretin fibrillogenesis inhibitors selected by drug repurposing strategies

C1.1 INTRODUCTION

Human transthyretin (hTTR) is a homotretameric protein that functions as the backup transporter for thyroxine hormone (T_4) in plasma and it is its main transporter across the blood brain barrier. TTR is also the main carrier of retinol by forming a 1:1 complex with the retinol-binding protein (RBP) (Raz et al. 1970, Raz and Goodman 1969). Whereas TTR transports nearly all the circulating RBP in serum and it is the main thyroxin transporter in cerebrospinal fluid (CSF), it only transports around the 15% of the serum circulating thyroxin (Schreiber et al. 1990). It is synthesised in the liver and the choroid plexus of the brain (Soprano et al. 1985), the former being the main responsible for its plasmatic production. hTTR is an amyloidogenic protein associated with senile systemic amyloidosis (SSA), caused by wild-type (wt) TTR (Westermark et al. 1990), affecting up to 25 % of the population older than 80. It is also related with several hereditary amyloidosis classified as rare diseases (Connors et al. 2003, Saraiva 2002): familial amyloidotic polyneuropathy (FAP), produced by single point mutants like V30M or L55P, where the pathology can develop at an early age; familial amyloidotic cardiomyopathy (FAC), mainly associated with V122I and T60A variants; and central nervous system selective amyloidosis (CNSA), the main representatives being the A25T and D18G TTR variants (Arsequell and Planas 2012). Amyloid fibril formation is initiated by TTR tetramer dissociation into dimers and monomers that evolve to misfolded or non-native monomer intermediates that start an intermolecular aggregation process involving a number of states through soluble oligomers and leading to mature fibrils (Colon and Kelly 1992, Quintas et al. 1999, Sousa et al. 2001, Cardoso et al. 2002, Hurshman et al. 2004). Several *in vitro* cell culture studies have shown that toxicity is produced by TTR intermediates (protofibrils and soluble oligomers) rather than by mature fibrils, suggesting its possible role in pathogenesis (Sousa et al. 2001, Sörgjerd et al. 2008).

Therapy for FAP is complex and requires approaches from different perspectives: symptomatic treatment of peripheral and autonomic neuropathy, anti-amyloid treatments and therapies aimed to solve organ insufficiency problems. Until recently, liver transplantation (LT) was the only considered anti-amyloid therapy for FAP patients and it is the current standard therapeutic strategy to ameliorate familial TTR amyloidosis. However, it presents a number of limitations: shortage of donors, requirement of surgery and need for long-term post-transplantation immunosuppressive therapies. In addition, TTR deposition may continue in eye and CNS since the retinal pigment epithelium and choroid plexus also synthesize TTR (Adams 2013). Therefore, there is a need for developing general, convenient, and non-invasive alternative therapeutic strategies to ameliorate TTR amyloidosis (Westermark et al. 1990, Adamski-Werner et al. 2004).

Thanks to the better understanding of the mechanisms related to TTR amyloidosis it has been possible to envisage new therapeutic strategies. A very important one, with a wide variety of chemical families studied over the last decades, is the kinetic stabilization of the TTR tetramer through the binding of small ligands to the T_4 binding sites (Adamski-Werner et al. 2004, Johnson et al. 2005, Wiseman et al. 2005). As a result of that union, an increase in the kinetic barrier associated

with TTR dissociation is observed and hence, amyloid formation is prevented. Even though all those compounds bind to the T_4 binding sites, it is possible to administer them without major side effects since TTR is a T_4 tertiary transporter in blood plasma with more than 99.5% of the two binding sites unoccupied. Many of those small ligands are included in the nonsteroidal anti-inflammatory drugs category (NSAIDS) with the additional positive aspects related to the repurposing of old drugs.

Large libraries of compounds and molecules derived from rational design have been evaluated by means of a great variety of assays (Arsequell and Planas 2012). Among those screening tools, there are *in vitro*, *ex vivo* and *in vivo* assays. A combination of different tests needs to be used, since different properties along the fibrillogenesis pathway need to be evaluated. Usually, *in vitro* assays monitoring protein aggregation or fibril formation are the choice in a primary screening of molecules since they are easily implemented in medium or high throughput format (HTS). *In vitro* assays that monitor the binding to native protein are also performed at early stages of the drug discovery process. As a secondary screening, it is common to perform *ex vivo* studies to evaluate for TTR selectivity in plasma and *in vitro* tests to assess tetramer stabilization. Finally, cellular assays are used for *in vitro* validation of potential drug candidates, with animal models being required later on in the process for the *in vivo* pre-clinical validation of the strongest candidates. Among all the compounds designed and tested for TTR tetramer stabilization, two of them deserve a special mention: Diflunisal and Tafamidis. Regarding Diflunisal, it is a well-known NSAID able to inhibit fibril formation, as shown in phase I and II clinical trials. Clinical efficacy has been demonstrated recently in a randomized double-blind placebo-controlled phase II trial (Sekijima 2014). In the case of Tafamidis (Vyndaquel ®), its efficiency has been tested in a multicenter international clinical phase II/III trial in 128 patients (Fx-005). Tafamidis is preferable for treating early stage symptomatic FAP and it has been approved by the European Medicines Agency in 2011 for early stage I FAP treatment and by the Japanese Pharmaceuticals and Medical Devices Agency in 2013 for all FAP stages (Adams 2013).

In the past decades, the investment of the pharmaceutical industry in R&D has increased, while the incomings derived from such investments have decreased and the number of new chemical entities remains constant. Nowadays, the pharmaceutical industry needs to face a high number of challenges related to the increase of the costs associated to the development of new drugs and clinical trials, harder drug regulations regarding drug safety, expiration of patents and the competition related to generic drugs. It is in this difficult context that the concept of repurposing appears. Drug repurposing is mainly a consequence of two circumstances: the need to extend drug pipelines with new projects and the increasing number of compounds that are abandoned due to strategic reasons (Sleigh and Barton 2010). Thanks to drug repurposing, costs related to drug development decrease and old compounds associated with high economic investments and no benefits (since they never arrived to consumers) are rescued. Examples of drug repurposing are Sildenafil (Pfizer), Raloxifene (Eli Lilly), Viagra (Pfizer) and Thalidomide (Celgene), among many others.

The goal of drug repurposing is the identification of new therapeutic properties for compounds that are (i) in clinical development, (ii) drugs that did not succeed in phase II or III due to low efficacy for a given application (never related to low safety), (iii) drugs abandoned as a consequence of commercial strategies, (iv) drugs under patent near to expiration or with already a generic equivalent and (v) drugs already discovered, developed, and in the market in countries in development but not in Europe or the USA (geographic repurposing). In general, one of the main advantages of drug repurposing is the fact that those drugs have already succeed a great number of tests, among them,

toxicity studies. Therefore, the probability of failure for a given drug due to drug safety or toxicity problems is lower. In addition, since drug safety and toxicity studies were done before, the costs associated to the initial phases of the development decrease, as well as the time required to arrive to the market. However, possible conflicts with intellectual property of those compounds must be taken into account, as well as changes in the regulation between the moment were the compound was developed and the moment when repurposing is considered. In addition, new proof of concept and additional tests related to safety may be required as a result of the new indication (Sleigh and Barton 2010).

There are two main kinds of drug repurposing within the pharmaceutical industry. The first one, based in known compounds-new targets: many drugs act on multiple targets resulting in "off target" effects, enabling companies to pursue a new indication where the secondary target is relevant. The second one, based in known mechanism-new indication: a biological process may be relevant to more than one disease and thus enable a company to establish the relevance of a known drug to a new disease.

Historically, drug repurposing has been related to serendipity, since new indications for existing drugs were discovered without any rational approach. Nevertheless, drug repurposing is changing nowadays thanks to the aid of new technology platforms, allowing the development of new systematic approaches for drug repurposing. Some of those strategies are the high throughput screening technologies and *in vitro* and *in vivo* cellular assays, as well as bioinformatic approaches in the analysis of databases.

It is also believed that drug repurposing will play a critical role within academia. University laboratories as well as public research institutes have been traditionally distant from the development of new drugs because of its associated high costs. In the last years, a great number of projects related to the study of novel therapeutic targets for pre-existing drugs has appeared. The most common strategies within the public sector for drug repurposing are based in the screening of libraries and on the search of new applications for a given molecule (Sleigh and Barton 2010).

We here report the high throughput screening of a library of 41 compounds proposed as possible TTR tetramer stabilizers and thus, fibrillogenesis inhibitors, resulting from a bioinformatic database analysis for drug repurposing.

C1.2 MATERIALS AND METHODS

C1.2.1 Recombinant human TTR (rhTTR) production and purification

Human Y78F rhTTR gene was cloned into a pET expression system (work performed in a previous project in the Biochemistry Laboratory at the IQS) and transformed into *E. coli* BL21DE3 Star. The production of recombinant protein was performed at Erlenmeyer scale; protein production and purification were done as described previously in the group (Dolado et al. 2005).

C1.2.1.1 Expression of rhTTR

Starting from a single *E. coli* colony (BL21DE3 Star transformed with a pET plasmid for the expression of Y78F rhTTR and conferring Kanamicine resistance) a primary inoculum in 2xYT media containing 100 μg/μL of Kanamicine (Sigma) (2xYT+Kn) was performed during 10 h at 37°C, 250 rpm. A secondary inoculum was done by addition of 100 μL of the primary inoculum into 50 mL of 2xYT+Kn media at 37°C, 250 rpm, until an optical density at 600 nm (OD_{600}) of ≈4. Inoculation of 1335 mL of 2xYT+Kn media was performed by addition of 1 mL of the secondary inoculum (from this point, 4 cell culture were run in parallel). After 7 h of incubation at 37°C and 250 rpm, protein expression was induced by addition of 1mM (final concentration) IPTG (Sigma) and continued overnight (ON), 37°C, 200 rpm. Afterwards, *E. coli* cell culture was centrifuged at 4°C, 10000 rpm during 10 minutes. The resulting pellet was resuspended in 250 mL of lysis buffer (Tris·HCl (Sigma) 0.5 M – 1mM PMSF (Roche) pH=7.6).

C1.2.1.2 Purification of rhTTR

French Press was used for cell disruption with a single pass at 20 Kpsi, followed by sonication at 60 % amplitude with cycles of 45 seconds (1 second pause each 3 seconds) until decrease in viscosity was observed. Soluble protein fraction was separated from cell debris by centrifugation at 4°C, 12000 rpm during 30 minutes. The procedure was repeated till a clear supernatant was obtained.

Protein purification steps were started with a fractionated precipitation of proteins from the supernatant previously obtained. A total of three precipitation steps were performed by addition of $(NH_4)_2SO_4$ (Sigma) up to 40%, 55% and 85% saturation, respectively. Each precipitation step consisted in the incubation of the supernatant obtained in the previous step mixed with $(NH_4)_2SO_4$ at 4°C, 8h (or ON), under agitation. Each precipitation was followed by centrifugation at 12°C, 12500 rpm during 30 minutes, obtaining 3 different pellets (protein precipitates).

The different fractions obtained till the moment were analyzed by SDS-PAGE (14% acrylamide gels) in order to determine firstly which of the protein precipitates contained the major quantity of rhTTR and secondly confirm the absence of rhTTR in the cell culture and the third protein precipitation supernatants. In order to analyze cell culture supernatants, 200 μL of each supernatant were concentrated in a Microcon® centrifugal filter (NMWL 10 kDa). For the different pellets studied, a small spatula tip of each pellet was resuspended in 1 mL of deionized H_2O. In the case of the supernatant after the last $(NH_4)_2SO_4$ precipitation, 250 μL of it were diluted in 1 mL of deionized H_2O.

The precipitate or precipitates containing the majority of the rhTTR produced were resuspended by soft pipetting in 50 mL of Tris·HCl 20 mM pH 7.6 – NaCl 0.1 M buffer (Buffer A). Prior to the

chromatographic steps, the resulting solution was dialyzed against Buffer A at 4°C using MWCO 6-8 kDa, 40 mm Cellu·Sep® Regenerated Cellulose Tubular Membranes (Membrane Filtration Products, Inc.).

The first chromatographic step consisted of anion exchange chromatography using a Äkta FPLC system (GE Healthcare Life Sciences) and a 120 mL XK 26/40 column (GE Healthcare Life Sciences) with Q-Sepharaose High Performance resin (GE Healthcare Life Sciences). Buffer A was used for column conditioning (1mL/min) and protein loading (2mL/min). Protein elution (1mL/min) was done by NaCl linear concentration gradient using Tris·HCl 20 mM pH=7.6 – NaCl 0.5 M buffer (Buffer B). The different fractions collected were analyzed by SDS-PAGE (14% acrilamide gels). Fractions containing rhTTR were combined and dialysed against deionized water at 4°C using MWCO 6-8 kDa, 40 mm Cellu·Sep® Regenerated Cellulose Tubular Membranes. The resulting solution was then lyophilized, resuspended in 4 mL of Buffer A and quantified by absorbance at 280 nm (Abs_{280}). The second chromatographic step consisted of a gel filtration chromatography using a Äkta FPLC system and a 440 mL XK 26/100 column (GE Healthcare Life Sciences) with Superdex 75 prep Grade resin (GE Healthcare Life Sciences). Again, Buffer A was used for column conditioning (1 mL/min) and protein loading (2 mL/min). Protein elution was performed with Buffer A at 0.3 mL/min. The fractions collected were analyzed by SDS-PAGE (14% acrilamide gels) and fractions containing rhTTR were combined and dialysed against deionized water at 4°C using MWCO 6-8 kDa, 40 mm Cellu·Sep® Regenerated Cellulose Tubular Membranes.

C1.2.1.3 Storage of the produced rhTTR

The protein solution was quantified by Abs_{280} and aliquoted into tubes for lyophilisation (4 mL/tube). After lyophilisation, tubes were placed in sealed plastic bags and stored at -20°C.

C1.2.2 Analysis of rhTTR by MALDI-TOF MS

Protein solution and sinapinic acid (SA) matrix (saturated solution of SA in 30:70 v/v acetonitrile:0.1% TFA in water) were mixed at 1:1 ratio. A volume of 0.5 μL of the previous mixture was deposited into a polished stainless steel target (Bruker) and allowed to dry. The deposited sample was washed with 0.1% TFA solution and allowed to dry again. Finally, 0.5 μL of SA matrix were deposited into the washed sample and allowed to dry. Same procedure was done for the Protein Standard Calibration I solution (Bruker). The target was introduced in a microflex MALDI-TOF (Bruker), spectra were acquired in lineal mode (Flex Control, Bruker) and processed (Flex Analysis, Bruker). External calibration with Protein Standard Calibration I (Bruker) was performed.

C1.2.2.1 Reduction of rhTTR by 1,4-Dithiothreitol (DTT) treatment

A 4 mg/mL solution of rhTTR was treated with 1 mM DTT during 1h at room temperature (RT). Completion of the reduction reaction was checked by MALDI-TOF MS. The reduced solution was dialysed against 20 mM K_2HPO_4, 100 mM KCl, pH 7.6 buffer at 4°C under soft agitation.

C1.2.3 Kinetic Turbidimetric Assay for the screening of inhibitors

C1.2.3.1 Protein and inhibitors

The Y78F rhTTR used in the screening of inhibitors was produced and purified as described previously. The inhibitors tested were selected by the group of Dr. J. Quintana at the Drug Discovery Platform, Parc Científic de Barcelona (PCB) and provided by the group of Dr. G. Arsequell and Dr. G. Valencia at the Institut de Química Avançada de Catalunya (IQAC-CSIC).

C1.2.3.2 Kinetic Turbidimetric Assay

The selected inhibitors were tested by the Kinetic Turbidimetric Assay, previously reported in our group (Dolado et al. 2005, Arsequell and Planas 2012). The screening of inhibitors was performed in a high throughput-screening (HTS) mode in 96-well plates, allowing the study of up to 14 different compounds per plate. Protein stock solution consisted of a 4 mg/mL (quantified by Abs_{280}) Y78F rhTTR solution in 20 mM K_2HPO_4, 100 mM KCl, pH 7.6. Incubation buffer was a 10 mM K_2HPO_4, 100 mM KCl, 1 mM EDTA, pH 7.6 solution and dilution buffer a solution of 400 mM KAcO, 100 mM KCl, 1 mM EDTA, pH 4.2. The stock solutions for the different inhibitors were prepared at 1.5 mM of each compound in DMSO. For the inhibitor working solutions, a 1:1 dilution with DMSO was performed followed by a 1:1 dilution with DMSO:H_2O (1:1). In order to run the assay, 20 μL of Y78F rhTTR stock solution were added into each well. Different volumes of each working inhibitor solution were added into the 7 corresponding wells to give final concentrations ranging from 0 to 40 μM. The final DMSO content of each well was adjusted up to 5% with DMSO:H_2O (1:1). Incubation buffer was then added up to a volume of 100 μL. The 96-well plate was then introduced into the thermostated microplate reader for 30 minutes at 37°C, with orbital shaking during 15 seconds every minute. Fibril formation was then induced by addition of 100 μL of dilution buffer to each well. The 96-well plate was placed again into the microplate reader and incubated at 37°C with shaking (15 seconds every minute) during 1.5 h. During this last incubation, absorbance at 340 nm was monitored at each minute. All assays were run per duplicate.

C1.2.4 Fibrillogenesis study of the produced rhTTR

C1.2.4.1 Time course fibrillogenesis study at 1.5 h

The assay performed was basically the one described in Section C1.2.3 but in the absence of fibrillogenesis inhibitors. Mainly, 20 μL of rhTTR stock solution were added into each well. The final DMSO content of each well was adjusted up to 5% with DMSO:H_2O (1:1). Incubation buffer was added up to a volume of 100 μL. The 96-well plate was introduced into the thermostated microplate reader for 30 minutes at 37°C, with orbital shaking during 15 seconds every minute. Fibril formation was then induced by addition of 100 μL of dilution buffer to each well. The 96-well plate was placed again into the microplate reader and incubated at 37°C with shaking (15 seconds every minute) during 1.5 h. During this last incubation, absorbance at 340 nm was monitored at each minute. All assays were run per triplicate.

C1.2.4.2 Time course fibrillogenesis study at 72 h

It is an adaptation of the protocol described in Section C1.2.3 in the absence of fibrillogenesis inhibitors and performed in sealed HPLC vials in order to avoid evaporation. Essentially, 40 μL of rhTTR stock solution were added into each vial. The final DMSO content was then adjusted up to 5% with DMSO:H_2O (1:1). Incubation buffer was added up to a volume of 200 μL. HPLC vials were sealed and incubated at 37°C during 30 minutes. Afterwards, fibril formation was induced by addition of 200 μL of dilution buffer to each vial. After soft mixing, 200 μL of each vial were placed into a well in a 96-well plate and absorbance at 340 nm was measured (starting point, t=0). After measurement, the 200 μL were placed again into its corresponding HPLC vial, which was sealed again and placed at 37°C. Measurements were performed at 1, 3, 6, 21, 30, 45, 54, 69 and 72 hours following the same procedure. All assays were run per duplicate.

C1.2.5 Differential Scanning Calorimetry (DSC)

Stock solutions were 100 % DMSO; 0.1 M K_2HPO_4, 0.1 M KCl and 1mM EDTA – pH 7.6 buffer (Buffer 1); protein solution in buffer 1 and inhibitor solution in DMSO at 20 mM. In all cases, solutions were filtered (0.45 um) and degasified previously to its use. Final conditions of the sample to be analyzed were 40 μM of protein and 1 mM of inhibitor, with a final DMSO concentration of 5%. A single scan was performed for each sample with a thermostat temperature of 25°C after each cycle. Initial temperature was set up at 10°C and the final one at 120°C. Scan rate (°C/h) was defined at 90 and the pre-scan's thermostat at 5 minutes.

C1.3 RESULTS AND DISCUSSION

The presented study is summarized in two main goals. First, the recombinant production and mass spectrometry (MS) characterization of Y78F rhTTR, as well as the evaluation of its fibrillogenesis properties. Second, using the produced rhTTR, the screening of fibrillogenesis inhibitors resulting from a new bioinformatic workflow based on drug repurposing. Therefore, it opens a new way of finding compounds with possible anti-fibrillogenesis activity that would arrive faster and in a less expensive way to the market. In all cases, the working hypothesis was tetramer stabilization and thus, the search of T_4 hormone binding analogues.

The method used for evaluation of fibrillogenesis properties of the produced rhTTR and for the *in vitro* screening of selected compounds was the Kinetic Turbidimetric Assay, previously developed in our group (Dolado et al. 2005, Arsequell and Planas 2012). When it was first developed, the Y78F TTR mutant was selected, despite its minor clinical relevance, due to its high amyloidogenic activity. It allowed the study of fibril formation in only 1.5 hours, making it perfect for the high-throughput screening of molecules and for the kinetic study of the initial steps of protein fibrillogenesis. Finally, the high sensitivity achieved by its high amyloidogenicity enables to discriminate between inhibitors without the need for long incubation periods that could lead to experimental artifacts. By means of the described procedure, some promising candidates for the inhibition of TTR fibrillogenesis were found. In addition, we performed a mass spectrometry (MS) analysis of the rhTTR produced in *E. coli*, allowing the identification of several post-translational modifications (PTMs) at the Cys-10.

C1.3.1 Recombinant production of mutant Y78F hTTR

C1.3.1.1 Recombinant Y78F hTTR expression and purification

The Y78F rhTTR was produced and purified as described (see Materials and Methods, section C1.2.1). Protein expression was performed at Erlenmeyer scale even though the optical densities (OD) that can be achieved are low, as compared to bioreactor production scale. The reason for choosing a smaller scale was mainly the easier handling, both upstream and downstream. In addition, it is preferable to use freshly produced protein for the Kinectic Turbidimetric Assay, in order to be sure about the biophysical properties of the protein. Therefore, there was not need for a higher amount of protein than the one produced at the chosen scale.

Briefly, after primary and secondary cultures, a total of 4 Erlenmeyer containing 1335 mL of 2xYT+Kn media were inoculated. Then, after 7 h of culture, protein expression was induced with 1 mM IPTG and let grow overnight. During the production of Y78F rhTTR, optical densities were almost doubled by the use of Erlenmeyer with deflectors, probably due to a better oxygenation of the culture, translated in higher cell growth. After cell culture and protein expression, cell disruption was performed with French Press followed by sonication. Afterwards, 3 serial protein precipitation steps were done by addition of $(NH_4)_2SO_4$ up to 40%, 55% and 85% saturation, respectively. Resuspension of the precipitate containing the majority of rhTTR and dialysis of the resulting protein solution were followed by 2 different chromatographic steps: first, an ionic exchange chromatography and second, a gel filtration. Between the 2 kinds of chromatography, fractions containing rhTTR were combined, dialyzed and lyophilized. After the gel filtration, final fractions containing rhTTR were combined and lyophilized again. Final yields obtained in the production and purification of a Y78F rhTTR batch were

around 65 mg rhTTR/L culture. In Fig. C1-1, the most relevant check-points in the protein purification process are shown.

As shown in Fig. C1-1A, no extracellular proteins were observed in any of the cell culture supernatants, which confirmed no extracellular production of rhTTR or other proteins. In addition, successful total protein precipitation was confirmed by the absence of proteins in the supernatant after the third $(NH_4)_2SO_4$ precipitation. Moreover, it was observed no lose of rhTTR in the cell debris fraction after cell disruption. Finally, the majority of rhTTR precipitated at 85% $(NH_4)_2SO_4$ saturation, this pellet being the selected one to continue with rhTTR purification steps. A small fraction of rhTTR was observed at 55% of saturation; however, this fraction was not considered for further purification since it contained other proteins.

Fig. C1-1B and Fig. C1-1C show the analysis of fractions resulting from the two chromatographic steps. In both cases, fractions covering the whole chromatographic elution, with special interest in the main chromatographic peak boundaries, were analysed by SDS-PAGE. As a result, it was possible to determine the elution volume of rhTTR in the ionic exchange chromatography. Specifically, rhTTR eluted between 424 mL and 688 mL. In the case of the gel filtration chromatography, rhTTR elution was observed between 211 mL and 294 mL.

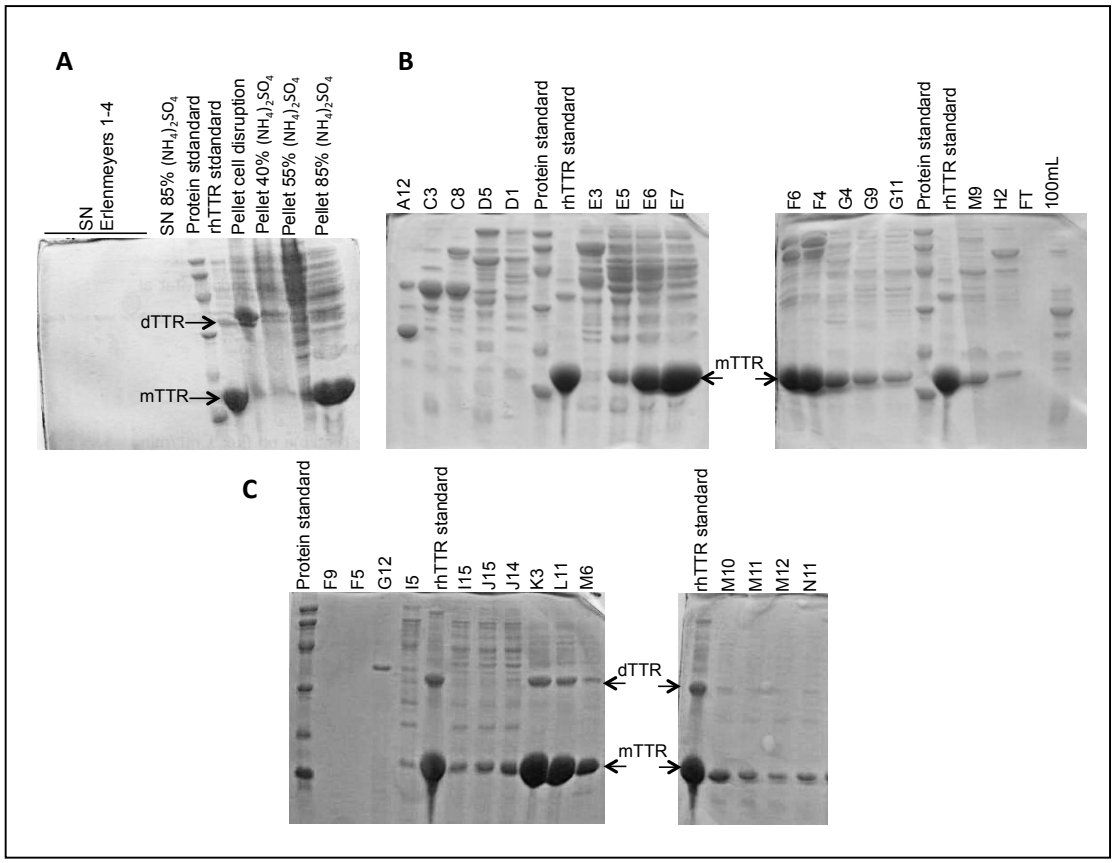

Figure C1-1. Important check-points in rhTTR purification. (A) Initial purification steps. The different supernatants and pellets obtained during protein production were analyzed by SDS-PAGE 14% acrylamide. First 4 lanes correspond to cell culture supernatants; SN 85% $(NH_4)_2SO_4$ corresponds to the analysis of the supernatant obtained after the third protein precipitation step. Pellets after cell disruption and after the 3 precipitations were also analyzed. **(B) Analysis of fractions, ionic exchange chromatography.** Some of the fractions collected were analyzed by SDS-PAGE 14% acrylamide in order to check for presence/absence of rhTTR. FT is the flow through during the column charge step; 100 mL fraction corresponds to the first 100 mL eluted. TTR started eluting in fraction E5 (424 mL) and ended in H11 (688 mL). **(C) Analysis of fractions, gel filtration chromatography.** Some of the fractions collected were analyzed by SDS-PAGE 14% acrylamide in order to check for presence/absence of rhTTR. TTR started eluting in fraction I15 (211 mL) and ended in fraction M12 (294 mL). In all cases, protein standard is the Bio-Rad low range SDS-PAGE standard (from top to bottom, bands correspond to 97.4, 66.2, 45, 31, 21.5, 14.4 kDa); rhTTR standard is a solution of purified rhTTR and TTR monomer and dimer are indicated as mTTR and dTTR, respectively. For each well, 18 µL of the corresponding sample, previously mixed with charge buffer, were charged.

C1.3.1.2 Quality assessment of the Y78F hTTR produced

The quality control and characterization of each of the produced rhTTR batches were performed first, by SDS-PAGE electrophoresis; second, by MALDI-TOF mass spectrometry and third, by a fibrillogenesis assay. With the first technique it was possible to check for protein purity, with the second one, to determine the molecular weight of the produced protein and with the third one, to define the fibrillogenesis capacity of each batch. Thanks to the information obtained from these 3 assays it was possible not only to characterize each batch but also to compare the protein produced between batches.

It is important to highlight that *in vivo* hTTR occurs as a very heterogeneous protein where variability is not only due to point mutations in the encoding gene but also to post-translational modifications (PTMs) at Cys-10, the single Cys residue in the protein sequence (Terazaki et al. 1998, Altland et al. 1999). It has been reported that only around 10-15% of the circulating TTR in plasma remains unmodified at Cys-10, finding S-sulfonation (S-Sulfo), S-glycinylcysteinylation (S-CysGly), S-cysteinylation (S-Cys) and S-glutathionylation (G-GSH) as the most abundant forms. The biological role played by those modifications remains still unknown, though it is suggested that Cys-10 mixed disulfides may reflect the redox balance of the *in vivo* environment, participating somehow in the defence against oxidative stress through thiol conjugation and thus, buffering the redox balance (Poulsen et al. 2012). Nevertheless, the implication of Cys-10 PTMs in the onset and pathological process of the TTR-related amyloidosis is still badly understood and based, mainly, on *in vitro* studies (Altland and Winter 1999, Kishikawa et al. 1999, Suhr et al. 1999, Bergquist et al. 2000, Zhang and Kelly 2003, Nakanishi et al. 2010, Takaoka et al. 2004).

In Fig. C1-2A an example of SDS-PAGE for purity evaluation is shown and in Fig. C1-2B, an example of MALDI-TOF spectra for molecular weight determination. As shown in the SDS-PAGE gel, increasing amounts of the produced rhTTR were charged in a SDS-PAGE, showing virtually 100% of purity. Surprisingly, despite carrying out protein expression in *E. coli*, the produced Y78F rhTTR (Fig. C1-2B) was post-translationally modified in the Cys-10, S-GSH being the main form. In addition, S-Cys, S-Sulfo and cysteic acid forms were found. These results are of high interest, since the Cys-10 forms found are in accordance with the ones reported in the bibliography for plasmatic hTTR *in vivo*. In addition, consistency in the Cys-10 modification pattern was found between batches, finding always S-GSH as the main rhTTR isoform. Nevertheless, the reason explaining why these modifications appear in the recombinant production of hTTR in *E*. coli remains unknown. For chemical structure of the different Cys-10 modifications and its Δ mass see Introduction, Table I-5.

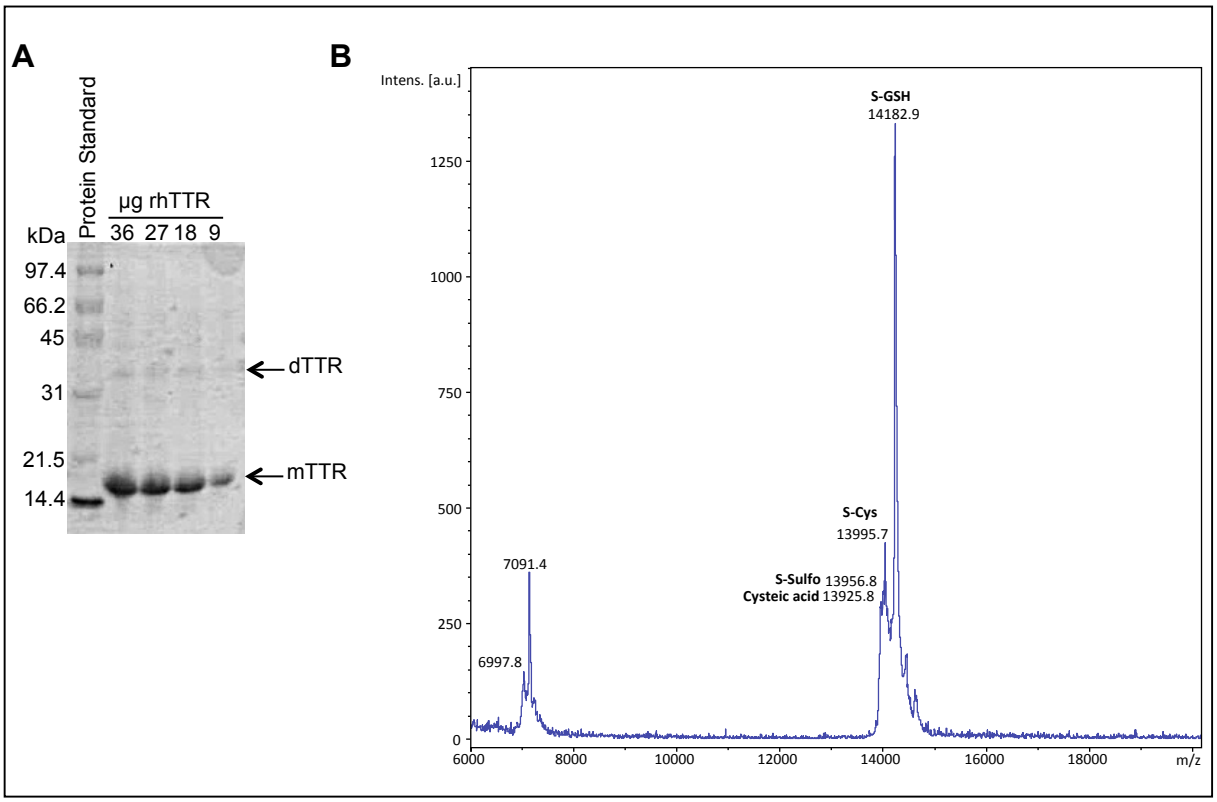

Figure C1-2. Quality assessment of the produced Y78F rhTTR. (A) Verification of protein purity. Increasing amounts of Y78F rhTTR (9 to 36 µg) were charged in a SDS-PAGE 14% acrylamide gel. Protein Standard corresponds to Bio-Rad low range SDS-PAGE standard, with the molecular weight of each band indicated on the left. TTR dimer and monomer are indicated as dTTR and mTTR, respectively. **(B) Checking Y78F rhTTR molecular weight.** MALDI-TOF spectra of one of the batches of Y78F rhTTR. Indicated are the masses of the main peaks as well as the corresponding Cys-10 PTM for each mass. Peaks around 7000 Da correspond to signal $(M+2H)^{2+}$.

Finally, the last step in the quality control of each batch was the determination of the fibril formation capacity. The parameter followed in that kind of assays is turbidity, independently of the formation of fibrils or aggregates. Upon acidification, protein aggregation is observed in the form of fibrils or aggregates, depending on the pH and the rhTTR mutant. Thus, protein precipitation was followed by measuring the absorbance of the solution, as an indicator of turbidity and consequently, fibril formation. The protocol followed is described in Materials and Methods, C1.2.4.1. With the described short-time fibrillogenesis assay it is possible to determine the fibrillogenesis capacity of the highly amyloidogenic variant Y78F rhTTR, by means of the initial rate of fibril formation (V_0, Au/time). First, a solution of Y78F rhTTR at 0.4 mg/mL was incubated at 37°C during 30 minutes, followed by fibril formation induction. After that, absorbance at 340 nm was recorded at each minute during 1.5h. The assay was performed per triplicate and two samples of each protein batch were analyzed. Values of absorbance were represented against time (minutes) and the slope of the linear part of the corresponding exponential curve was defined as V_0 (Au/time). An example of the values obtained for one batch is shown in Table C1-1.

Table C1-1. Determination of the fibrillogenesis capacity for one batch of Y78F rhTTR

	Replicate	$Time_0$ (min)	Abs_0 (Au)	$Time_1$ (min)	Abs_1 (Au)	V_0 (Au/min)	Batch information	
	1	3	0.296	20	0.949	0.0407	**Mean V_0 (Au/min)**	0.040
Sample 1	2	3	0.301	21	1.002	0.0417	**STDV**	0.001
	3	3	0.309	21	1.011	0.0416	**CV (%)**	3.08
	1	3	0.282	20	0.906	0.0389		
Sample 2	2	3	0.284	21	0.96	0.0404		
	3	3	0.293	20	0.916	0.0389		

The delimitation of the linear part of the progress curve is indicated by the subscripts 0 and 1. Values for time and absorbance delimiting the linear region are shown. The fibrillogenesis capacity of the batch is defined as the average V_0 of the triplicates of the two samples analyzed.

C1.3.2 Comparative study of the fibrillogenesis behaviour of S-Glutathionylated and free thiol TTR isoforms

Given the fact that the protein produced corresponded mainly to the isoform S-GSH, and that this isoform is also found *in vivo*, it was considered interesting to compare the fibrillogenesis capacity of this isoform with the Cys-10 free thiol one. Moreover, there is a lot of discussion in the bibliography, as mentioned previously (see Introduction, I.5), about the role of TTR Cys-10 modifications and its possible relation with disease onset or disease progression, emphasizing the importance of comparing Cys-10 modified forms with Cys-10 unmodified TTR in terms of fibrillogenesis capacity.

Two different kinds of fibrillogenesis studies were performed. On the one hand, a short-term fibrillogenesis study (1.5h) and on the other hand, a long term one (72h). In order to obtain the free thiol TTR isoform (see Materials and Methods, C1.2.2.1), the produced Y78F rhTTR was treated with 1mM DTT during 1h at RT. Completion of the reduction was checked by MALTI-TOF MS (Fig. C1-3). As shown in the MALDI-TOF spectra, a significant simplification of TTR heterogeneity was achieved upon DTT treatment (decrease in number of peaks in the mass spectra) and reduction of Cys-10 residue confirmed by a mass shift towards the free Cys isoform. After reduction, and prior to the fibrillogenesis study, the protein solution was dialyzed against 20 mM K_2HPO_4, 100 mM KCl, pH 7.6 buffer.

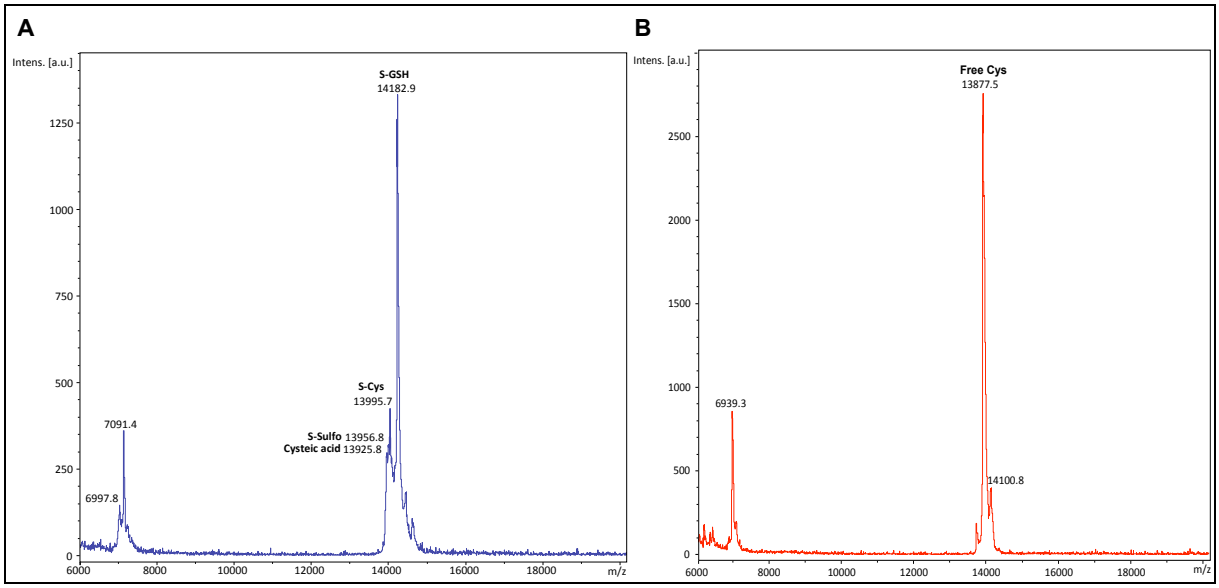

Figure C1-3. Monitoring DTT reduction of Y78F rhTTR by MALDI-TOF MS. (A) Spectra of Y78F rhTTR before reduction. Indicated are the masses corresponding to the main Cys-10 isoforms found. **(B) Spectra of Y78F rhTTR after 1h reaction with 1 mM DTT, RT.** Dramatic simplification of the spectra was observed, as well as a mass shift towards the free Cys isoform, as indicated. Peaks around 7000 Da correspond to signal $(M+2H)^{2+}$.

C1.3.2.1 Fibrillogenesis study at 1.5h

Fibrillogenesis capacity of the two isoforms was determined as described previously (see Materials and Methods, C1.2.4.1). For each isoform, initial rates of fibril formation (V_0, Au/time) were calculated per triplicate; in addition, the whole experiment was carried out per duplicate (Table C1-2). According to the results obtained, the S-GSH Y78F rhTTR isoform is in average 1.26x fold more amyloidogenic than the free Cys isoform, a tendency in accordance with some data found in the literature (Zhang and Kelly 2003) for the wt TTR. Thus, the Cys-10 mixed disulfide S-glutathione would decrease tetramer stabilization at pH 4.2 and could be therefore, a triggering step for fibril formation *in vivo*. However, it was considered of importance to compare this fibrillogenesis capacity with the one at long incubation times (72 h), where the amount of fibrils formed has reached the maximum and remains stable, since there is the possibility that one isoform reaches faster this maximum but that after a certain time, the other isoform reaches it too.

Table C1-2. Evaluation of the fibrillogenesis capacity (1.5 h) of S-GSH and free thiol Y78F rhTTR Cys-10 isoforms

	Cys-10 state	Replicate	$Time_0$ (min)	Abs_0 (Au)	$Time_1$ (min)	Abs_1 (Au)	V_0 (Au/min)	Isoform information	
Experiment 1	S-GSH	1	6	0.207	26	0.52	0.0165	**Mean V_0 (Au/min)**	**0.0167**
		2	7	0.216	27	0.546	0.0165	**STDV**	0.0003
		3	6	0.205	25	0.521	0.0171	**CV (%)**	2.07
	Free thiol	1	7	0.194	29	0.447	0.0120	**Mean V_0 (Au/min)**	**0.0126**
		2	7	0.172	29	0.442	0.0128	**STDV**	0.0005
		3	7	0.185	28	0.447	0.0130	**CV (%)**	4.20
Experiment 2	S-GSH	1	4	0.246	20	0.629	0.0249	**Mean V_0 (Au/min)**	**0.0236**
		2	4	0.224	20	0.576	0.0230	**STDV**	0.001
		3	3	0.226	20	0.594	0.0230	**CV (%)**	4.64
	Free thiol	1	4	0.213	22	0.546	0.0195	**Mean V_0 (Au/min)**	**0.0198**
		2	4	0.211	23	0.563	0.0197	**STDV**	0.0004
		3	4	0.225	24	0.606	0.0203	**CV (%)**	2.10

C1.3.2.2 Fibrillogenesis study at 72h

The fibrillogenesis capacity of the isoforms S-GSH Y78F rhTTR and free Cys Y78F rhTTR was determined according to the protocol described (see Materials and Methods, C1.2.4.2). As shown in Table C1-3 and Fig. C1-4, no differences in terms of fibrillogenesis capacity were found between the S-GSH and the free Cys Y78F rhTTR isoforms. As pointed out before, differences are observed in initial rate of fibril formation, however, those differences disappear at long incubation times, suggesting no significant differences in terms of final fibrillogenesis capacity between this 2 isoforms under the conditions assayed. Therefore, the possible role of the S-GSH PTM in the fibrillogenesis process *in vivo*, if existent, remains still unknown.

Table C1-3. Evaluation of the fibrillogenesis capacity (72 h) of S-GSH and free thiol Y78F rhTTR Cys-10 isoforms

	S-GSH Y78F rhTTR					Free thiol Y78F rhTTR				
Time (h)	**Replicate 1**	**Replicate 2**	**Mean Abs (Au)**	**STDV**	**CV (%)**	**Replicate 1**	**Replicate 2**	**Mean Abs (Au)**	**STDV**	**CV (%)**
0	0.169	0.178	0.174	0.006	3.67	0.175	0.177	0.176	0.001	0.80
1	0.580	0.606	0.593	0.018	3.10	0.491	0.482	0.487	0.006	1.31
3	0.717	0.780	0.749	0.045	5.95	0.708	0.738	0.723	0.021	2.93
6	0.706	0.753	0.730	0.033	4.56	0.718	0.722	0.720	0.003	0.39
21	0.827	0.853	0.840	0.018	2.19	0.775	0.771	0.773	0.003	0.37
30	0.746	0.798	0.772	0.037	4.76	0.781	0.774	0.778	0.005	0.64
45	0.743	0.802	0.773	0.042	5.40	0.726	0.710	0.718	0.011	1.58
54	0.760	0.794	0.777	0.024	3.09	0.709	0.706	0.708	0.002	0.30
69	0.750	0.780	0.765	0.021	2.77	0.742	0.760	0.751	0.013	1.69
72	0.740	0.700	0.720	0.028	3.93	0.735	0.779	0.757	0.031	4.11

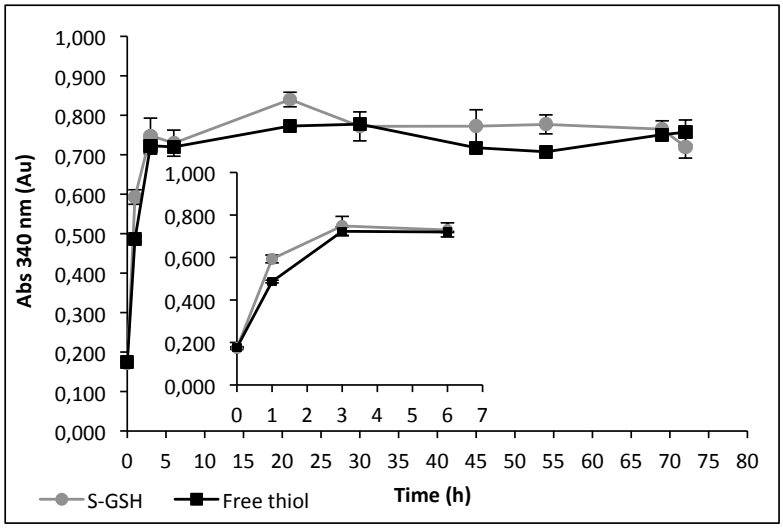

Figure C1-4. Comparative 72 h fibrillogenesis study of isoforms S-GSH and free thiol Y78F rhTTR. A long time fibrillogenesis study was carried out during 72 h and measures were taken at 0, 1, 3, 6, 21, 30, 45, 54, 69 and 72 h. A zoom of the initial region of the graph is shown.

C1.3.3 High Throughput Screening of fibrillogenesis inhibitors selected by drug repurposing

The main purpose of this work is the screening of drug repurposing compounds selected by means of bioinformatic workflows. One of the main advantages of this strategy is the fact that those molecules are closer to the final goal: the commercialization of fibrillogenesis inhibitors for TTR related amyloidosis. As mentioned previously, the test for such screening is the Kinetic turbidimetric assay (Dolado et al. 2005), where upon acidification, the fibrillogenesis of the mutant Y78F rhTTR is followed along time.

C1.3.3.1 Kinetic Turbidimetric Assay

This screening method allows testing up to 14 different compounds per microplate. The parameter followed during the assay is absorbance, and it is measured along the 2 steps of the assay: protein-inhibitor incubation and pH-induced fibrillogenesis. During this last incubation, absorbance is measured at each minute during 1.5 h (see Materials and Methods, C1.2.3.2).

For each compound, a time-course curve is obtained by representing absorbance values against time. From those curves, it is possible to obtain the initial rate of fibril formation (V_0) since it corresponds to the slope of the linear increase of absorbance. When plotting the initial rates against inhibitor concentration, an exponential decay is obtained. Data were fit to equation (1), where V_0 is the initial rate of fibril formation (AU/h) and [I] is the concentration of inhibitor (μM). Fitted parameters are A (AU/h), defined as the residual aggregation rate at high concentration of inhibitor; B (UA/h), amplitude or maximum decrease of initial rate of fibril formation; and C (μM^{-1}), considered as the exponential constant. A+B is equal to the initial rate of fibril formation under the assay conditions in the absence of inhibitor.

$$(1)\quad V_0 = A + B \cdot e^{-C \cdot [I]}$$

Two different parameters were used for the evaluation of compounds: IC_{50} and percent reduction of fibril formation (RA). The first one, IC_{50} (μM), is described as the concentration of inhibitor at which the initial rate of fibril formation is one-half of that one without inhibitor. After the discussed exponential fit, IC_{50} is calculated according to equation (2). RA (%), calculated according to equation (3), is the percent reduction of fibril formation rate at high inhibitor concentration, relative to the rate in the absence of inhibitor.

$$(2)\quad IC_{50}\ (\mu M) = -\frac{1}{C}\cdot \ln\frac{B-A}{2B}$$

$$(3)\quad RA\ (\%) = \frac{B}{A+B}\cdot 100$$

However, the exponential fit of data is just valid for the best inhibitors. For those compounds acting as weaker fibrillogenesis inhibitors, data were adjusted to a lineal model described in equation (4), where A is the initial rate of fibril formation in the absence of inhibitor (AU/h); B, the slope of the curve (AU/(μM·h)); and [I] is the inhibitor concentration (μM). Under this fitting model, IC_{50} is calculated according to equation (5). RA_{40} (%), the percent reduction of fibril formation at 40 μM of inhibitor, is calculated according to equation (6), where C is the initial rate of fibril formation at 40 μM of inhibitor (AU/h).

$$(4)\quad V_0 = A + B\cdot[I]$$

$$(5)\quad IC_{50} = -\frac{A}{2B}$$

$$(6)\quad RA_{40}\ (\%) = \frac{C}{A}\cdot 100$$

According to the described parameters, a good inhibitor will be that one with low IC_{50} values and high RA values. Precisely, valuable inhibitors will be those ones with IC_{50} below 20 μM and RA greater than 80%.

C1.3.3.2 Drug repurposing workflow for the selection of the molecules tested

A set of 41 compounds were selected by a bioinformatic repurposing study and analysed as potential fibrillogenesis inhibitors. The process followed for the prioritization of these 41 molecules is summarized in Fig. C1-5 and was carried out by Dr. D. Blasi and Dr. J Quintana (Drug Discovery Platform). The drug repurposing compounds can be divided into 2 main categories. Firstly, the group of drugs already in the market, in clinical trials (phases I-III) or in advanced pre-clinical studies, containing the most favourable scaffolds for TTR tetramer stabilization (Commercially Available Advanced Compounds, CAAC (Fig. C1-5A)). Secondly, the group of compounds corresponding to already launched drugs (Fig. C1-5B). The database used in the study was the Integrity Prous Science.

In the case of CAAC compounds, after filtering for structural similarity with antranilics, flavones, benzoxazoles and derivative molecules, 312 compounds were selected. The filtering was based in the mentioned structures due to its interest from previous studies in the group (Fig. C1-6). According to

its commercial availability, the group was reduced from 312 to 87 compounds. From these 87 compounds and thanks to the building of a fingerprinting model based in structural similarity to 3 already known strong amyloidogenesis inhibitors (mefenamic acid, iododiflunisal and tafamidis), it was possible to prioritize a total of 20 molecules (Fig. C1-7, numbers in blue).

A fingerprint is a bi- or tri-dimensional structure containing information about the absence or presence of certain characteristics, elements, chemical connectivity or tri-dimensional conformation for a given molecule. The most common applications of this kind of structural information codifier vectors are (i) searches based in structural similarity, (ii) study of the structural diversity of a given chemical space, and (iii) the building of fingerprinting models for the design based in ligand. The developed TTR fingerprinting model was build using the MOE Software (Molecular Operating Environment) from the Chemical Computing Group. The compounds compilated in the database were treated in order to protonate them at the proper pH, their structures were minimized using the force field MMFF9 and their partial charges were computed. Starting from the minimized molecule, the structures of the filtered compounds were transformed into the following fingerprints: the MACCS, based in the molecule's structure; the TAF (TAD, TAT, TGD and TGT), that codify for the properties of a molecule; and the GpiDAH3, that codify for pharmacophoric elements present in a molecule. The 3 chosen references were also vectorized in order to use them as a reference in the search by similitude (based in the calculation of the Tanimoto coeficient) (Blasi 2012).

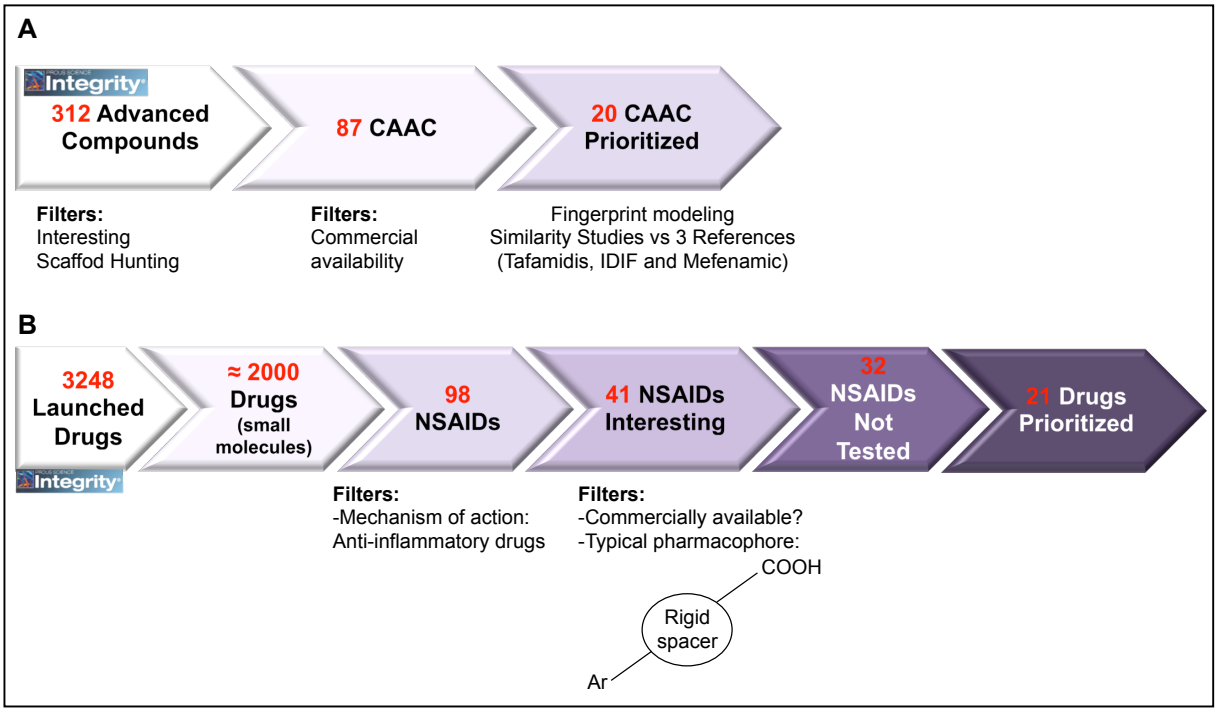

Figure C1-5. Bioinformatic workflow for the selection of compounds. (A) Searching Commercially Available Advanced Compounds (CAAC). **(B)** Searching launched drugs.

In the case of launched drugs, 3248 compounds were available in the Integrity database at the moment of the study. From them, around 2000 compounds corresponded to small molecules with molecular weight <500 Da. It is well reported in the bibliography that anti-inflammatory compounds could be good TTR fibrillogenesis inhibitors. Hence, a first filter was applied according to the mechanism of action of the compounds, selecting the non-steroidal anti-inflammatory drugs

(NSAIDs). After this first filter, the group of selected drugs was reduced from around 2000 to 98. Additionally, 2 more filters were applied: the first one, commercial availability and the second one, correspondence with the typical pharmacophore of TTR stabilizers (two aromatic substructures and a linker) reported in the bibliography (Fig. C1-5B). After these 2 filters, the number of candidates was reduced to 41, of which 32 compounds were not among the previously tested in our group. Again, after a fingerprinting model study against the 3 structures of reference (mefenamic acid, iododiflunisal and tafamidis) it was possible to prioritize a total of 21 drugs (Fig. C1-7, numbers in red).

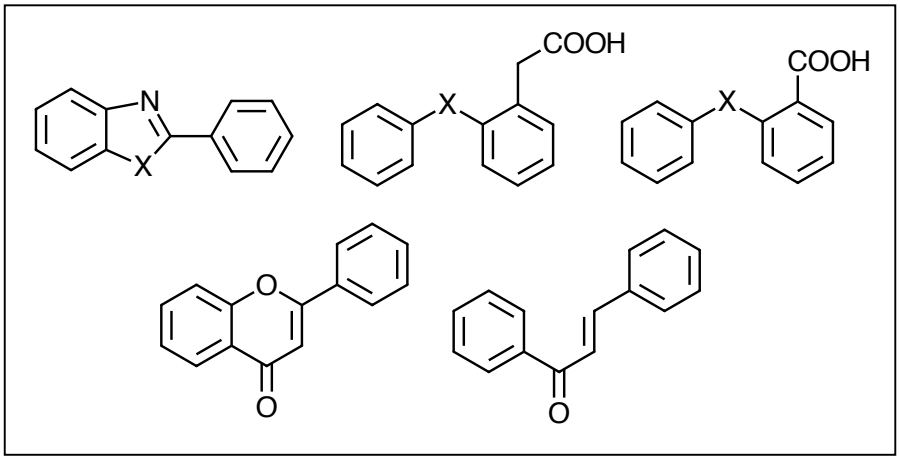

Figure C1-6. Scaffolds previously studied in the group. X = NH, O, S.

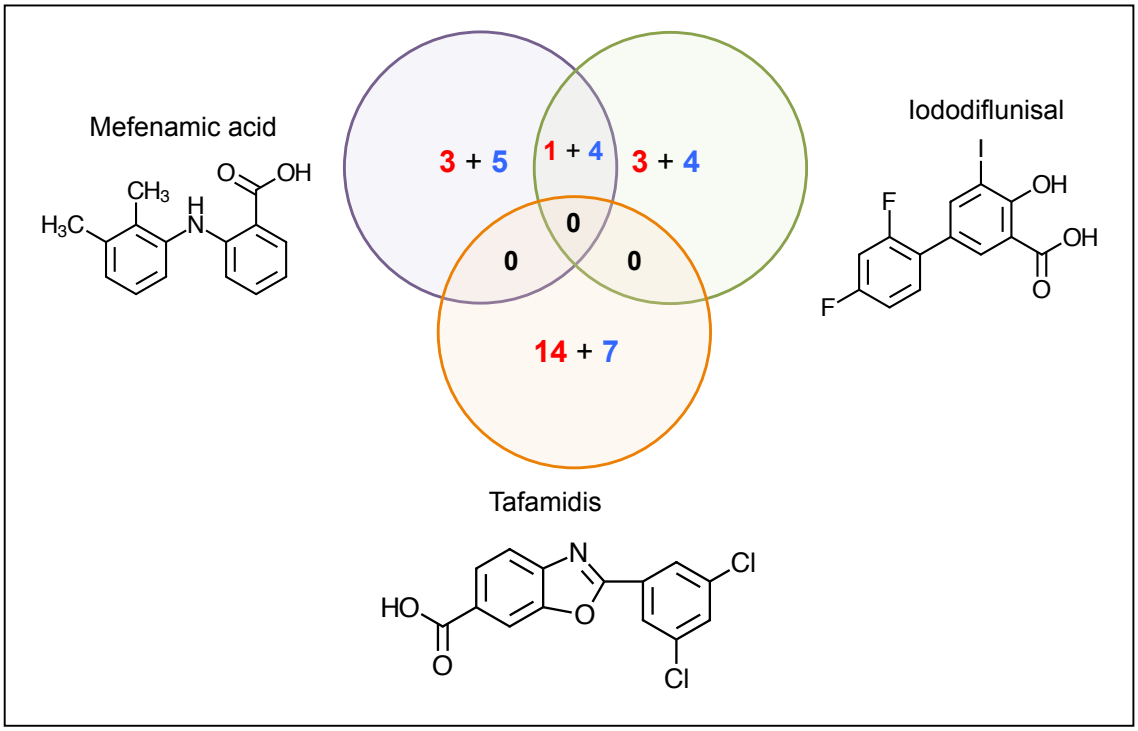

Figure C1-7. Fingerprinting model study for the selection of compound. Numbers in red indicate anti-inflammatory compounds (total of 21) and numbers in blue indicate compounds with interesting scaffolds (total of 20).

In summary, 41 compounds were proposed by the explained bioinformatic workflow to be further tested experimentally by the Kinetic Turbidimetric Assay. The total of 41 molecules assayed are

represented in Fig. C1-8 and Fig. C1-9. It is important to mention that finally, since not all the compounds proposed in the bioinformatic study were commercially available (Fig. 10), alternative compounds were proposed and assayed (Fig. C1-8 and Fig. C1-9: compounds 930, 931, 937, 938, 939, 947, 959, 960, 961) according to its structural similarity with the proposed ones or its interest within the framework of the consortium. It is also important to note that compounds 856 (Lumiracoxib) and 952 (Prexige) are the same ligand. The first one (856) was commercially available and the second one (952), was extracted from the drug Prexige (not available in Spain). The same happens with compounds 942 (extracted from drug, Metamizole) / 950 (commercially available, Dipyron Na salt).

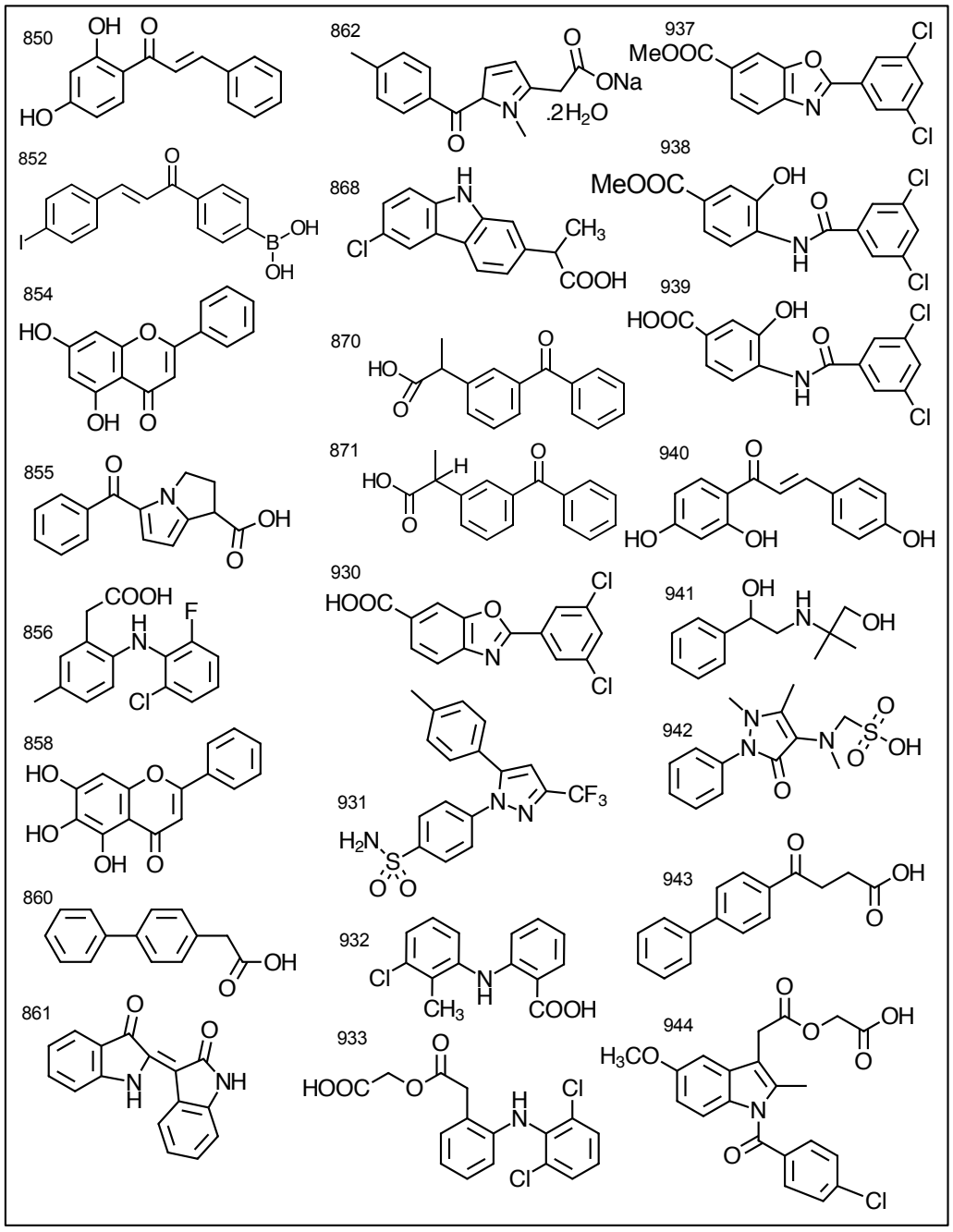

Figure C1-8. Chemical structure of the selected compounds for the drug repurposing screening (part I). Compound 870 (ketoprofen) is a racemic mixture and 871 (dexketoprofen) is the pure right-handed enantiomer.

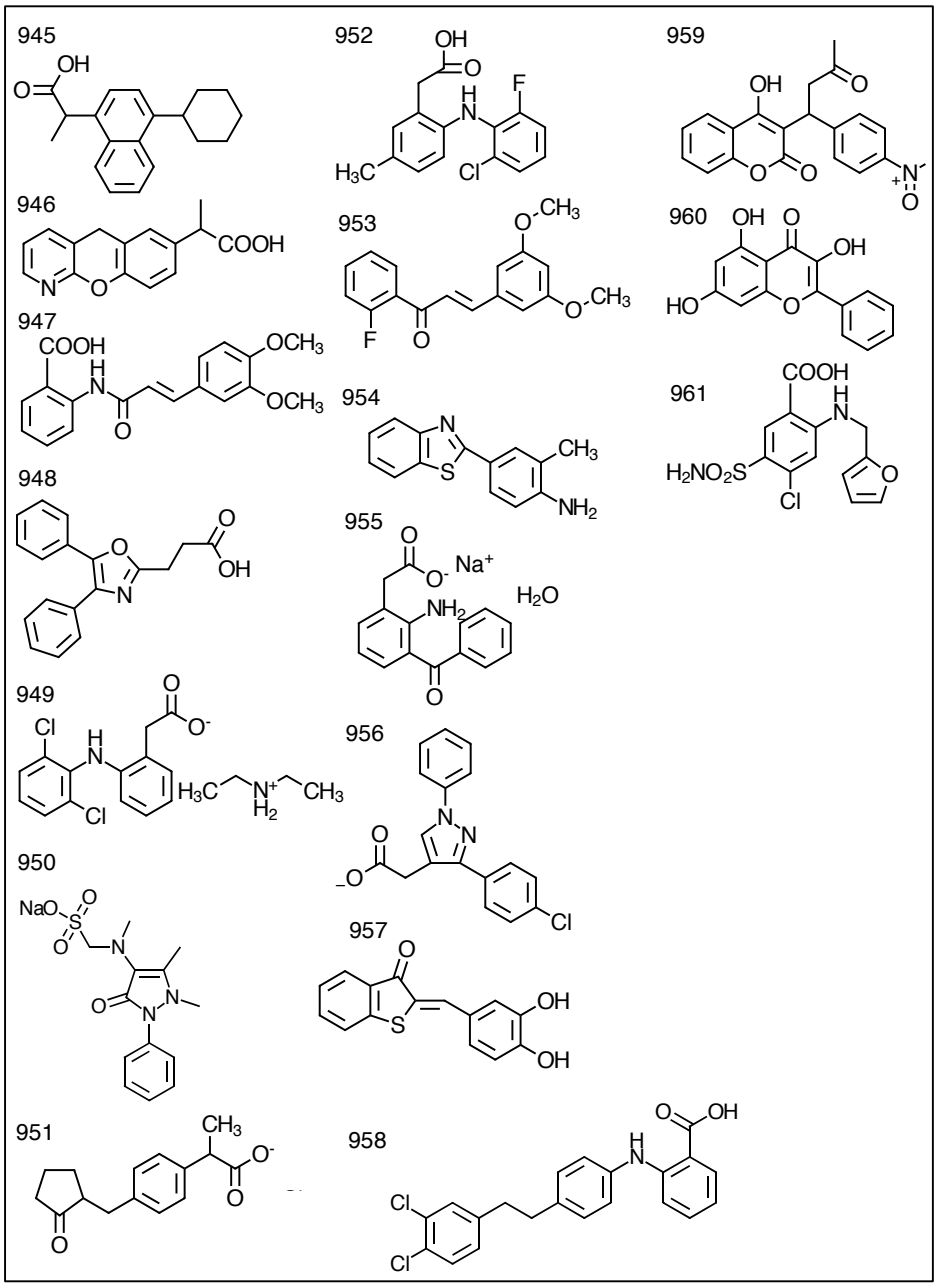

Figure C1-9. Chemical structure of the selected compounds for the drug repurposing screening (part II)

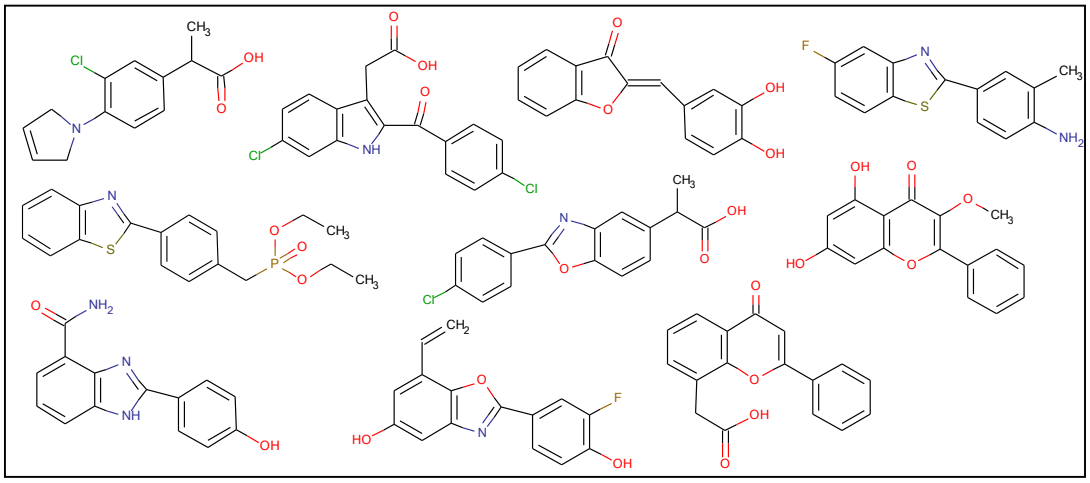

Figure C1-10. Compounds derived from the repurposing workflow not available at the moment of the study

C1.3.3.3 Results from the screening of the selected drug repurposing compounds

The final 41 selected compounds were screened using the Kinetic turbidimetric assay. The results in terms of IC_{50} (μM) and RA (%) are shown in Fig. C1-11A and C1-11B, respectively.

Precisely, among the compounds tested, we found that in terms of IC50 (Fig. C1-11A) there were 7 possible potential anti-amyloid drugs for TTR amyloidosis, with an IC50 < 20 μM. In terms of RA (Fig. C1-11B), the number of compounds was up to 8 (with RA (%) values higher than 80%). However, good TTR stabilizers and thus, anti-fibrillogenesis compounds, are characterized by both parameters. Therefore, taking into account both IC50 and RA, we found a total of 6 compounds with high tetramer stabilization properties: compounds 856 (Lumiracoxib), 932 (Tolfenamic acid), 933 (Aceclofenac), 952 (Prexige), 954 (compound at preclinical stage) and 930 (Tafamidis).

The 5 candidates (856/952, 932, 933, 954, 930) proposed belong to 2 main chemical families: N-aryl-anthranilic acid derivatives (856/952, 932 and 933) and benzoxazole derivatives (930 and 954). According to our results and for the 5 named compounds, anthranilic acid derivatives (mefenamic acid family) are better fibrillogenesis inhibitors when compared to benzoxazole derivatives (tafamidis family), especially in terms of IC_{50}. In addition, unless compound 954, all the other candidates are halogenated drugs. The 5 reported hits are structurally in line with the typical structure of TTR ligands found in the bibliography. Usually, TTR ligands are composed of two aromatic rings either linked directly as a biaryl or separated by linkers of variable chemical structure. In addition, it is common to find one aromatic ring substituted with a polar substituent and the other ring displaying halogenated substituents, aryl groups, or a combination thereof. Polar substituents can make importance electrostatic interactions with the Lys-15 and to some extend with the Glu-54 when positioned in the outer binding site (Adamski-Werner et al. 2004, Cotrina et al. 2013, Johnson et al. 2005). In addition, it is reported in our group (Cotrina et al. 2013) that halogenation of TTR ligands may improve their affinity and fibrillogenesis inhibition properties. Those studies take into account that a relevant feature of TTR binding sites is the presence of 3 symmetry-related depressions termed halogen binding pockets (HBPs) (Fig. C1-12), which naturally accommodate the iodine atoms of the T_4 hormone in their complex with TTR. On this way, the halogenated rings of those small molecules would complement the hydrophobicity of the inner binding pocket by occupying a subset of the HBPs. It could be of special interest for future works to perform a structural bioinformatic analysis with the 5 hits here proposed in order to shed light into their binding with TTR and therefore help to rationalize the design of new and better TTR inhibitors.

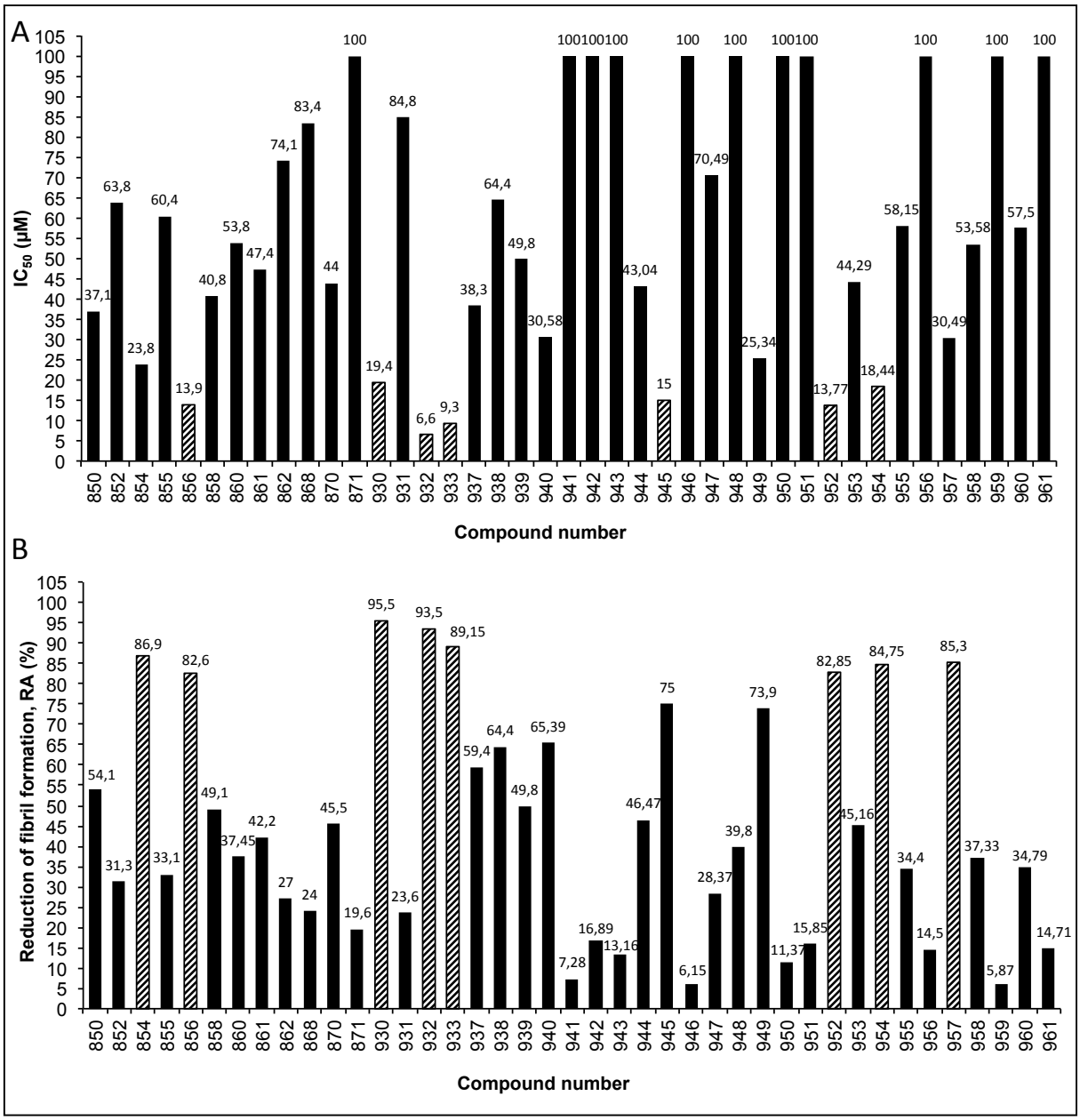

Figure C1-11. Kinetic Turbidimetric screening results of the 41 compounds proposed. (A) Results in terms of IC_{50} (μM) obtained in the Kinetic Turbidimetric Assay. (B) RA (%) results obtained in the same assay. In both cases, striped bars indicate compounds performing the best inhibition properties (IC_{50}<20 μM, RA>80%).

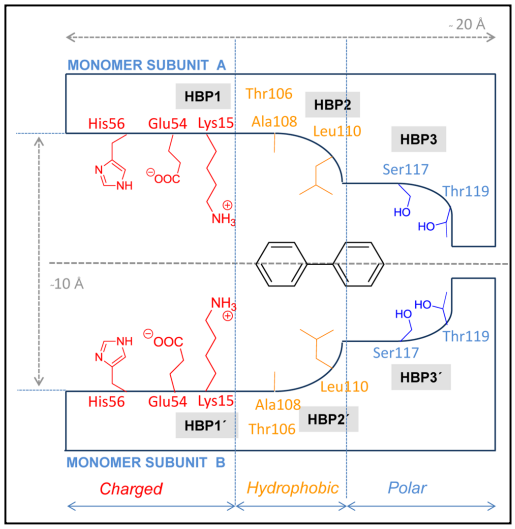

Figure C1-12. Schematic representation of a TTR binding site. The three chemical regions in which TTR binding sites can be divided are shown, as well as the halogen binding pockets (HBPs) location (Cotrina et al. 2013).

Nevertheless, it is of special interest to mention that in 2007 Lumiracoxib/Prexige was withdrawn from several countries such as Australia, Canada and New Zealand due to concerns it may cause liver failure. In addition, in the same year, the European Medicines Agency (EMEA) recommended the withdrawal of the marketing authorizations for all lumiracoxib-containing medicines, because of the risk of serious side effects affecting the liver, suggesting that the risks associated to the drug are greater than its benefits. Thus, before suggesting the repurposing of Lumiracoxib/Prexige for the treatment of FAP it should be well evaluated its associated risks.

Compound 930 (Tafamadis), already approved for FAP therapy, is one of the 5 hits reported. Interestingly, it is important to highlight that the other 4 compounds here reported are promising drug candidates for the treatment of FAP since as proven by our results, they all inhibit fibrillogenesis *in vitro* better than Tafamidis (as seen by their lower IC_{50} values).

C1.3.4 Comparative study of the inhibition of fibril formation by small ligands for the S-Glutathionylated and the free thiol TTR isoforms

In the same way as previously done for the fibrillogenesis capacity, we wanted to check if there were differences in the inhibition of the fibril formation depending on the Cys-10 conjugation state. To this purpose, we assayed by the Kinetic Turbidimetric Assay some of the best inhibitors found (932, 933 and 856) together with Tafamidis (930) as a reference and Iododiflunisal (200) as reference molecule in the group. The free thiol isoform was obtained as previously described (see Materials and Methods, C1.2.2.1). As shown in Table C1-4, no differences were found in the inhibition of fibril formation between the 2 protein isoforms for any of the compounds. Since it is known that in human plasma TTR occurs as a highly heterogeneous protein, it is positive to confirm that the presence of PTMs in the Cys-10 do not interfere with the inhibition by small ligands.

Table C1-4. Comparison of fibril formation inhibition between free thiol and S-GSH Y78F rhTTR isoforms

	Y78F rhTTR			
	Free thiol		S-Glutathionylated	
Inhibitor	IC_{50} (μM)	RA (%)	IC_{50} (μM)	RA (%)
200	5.52	100	5	100
930	17	93.5	19.4	95.5
932	5.6	94.3	6.6	93.5
933	7.7	94.9	9.3	89.15
856	11.3	86.4	13.9	82.6

C1.3.5 Evaluation of TTR tetramer stabilization: Differential Scanning Calorimetry (DSC)

In the attempt to go one step further in the drug validation process, we performed an *in vitro* secondary screening in order to assess TTR tetramer stabilization for the compounds 930, 932, 933, 945, 949 and 952. In addition, and as previously done, Tafamidis (930) and Iododiflunisal (200) were used as references. The technique chosen was Differential Scanning Calorimetry (DSC), a powerful tool for the study of thermal transitions in biological systems. When a macromolecule changes its thermodynamic state upon unfolding, a heat capacity change (ΔCp, cal/°C) is observed. This change is due to the fact that the heat required to raise the temperature of a solution of unfolded protein is greater than that required for a solution of folded protein. The transition is recognized as a sharp

endothermic peak centred at the melting temperature (Tm, °C), where the maximum in Cp (cal/°C) directly occurs (Bruylants et al. 2005). Tm is the temperature at which half of the protein molecules are unfolded. It is directly related with protein stability and it depends on environmental conditions. Based on that principle, we measured the different Tm (°C) associated with Y78F rhTTR mutant in the presence of different ligands (see Materials and Methods, C1.2.5).

As shown in Fig. C1-13, there is a Tm shift towards higher temperatures in the presence of the different ligands. This phenomenon supports the idea of tetramer kinetic stabilization previously explained. An interesting concept is the comparison of the calculated IC_{50} (µM) with the different ΔTm (difference between the Tm of the free protein and that one in the presence of a small ligand). It is expected that the best inhibitors (lower IC50 values) produce higher Tm shifts, since a stronger inhibitor should stabilize more the TTR tetramer. The results from that comparison are shown in Fig. C1-14.

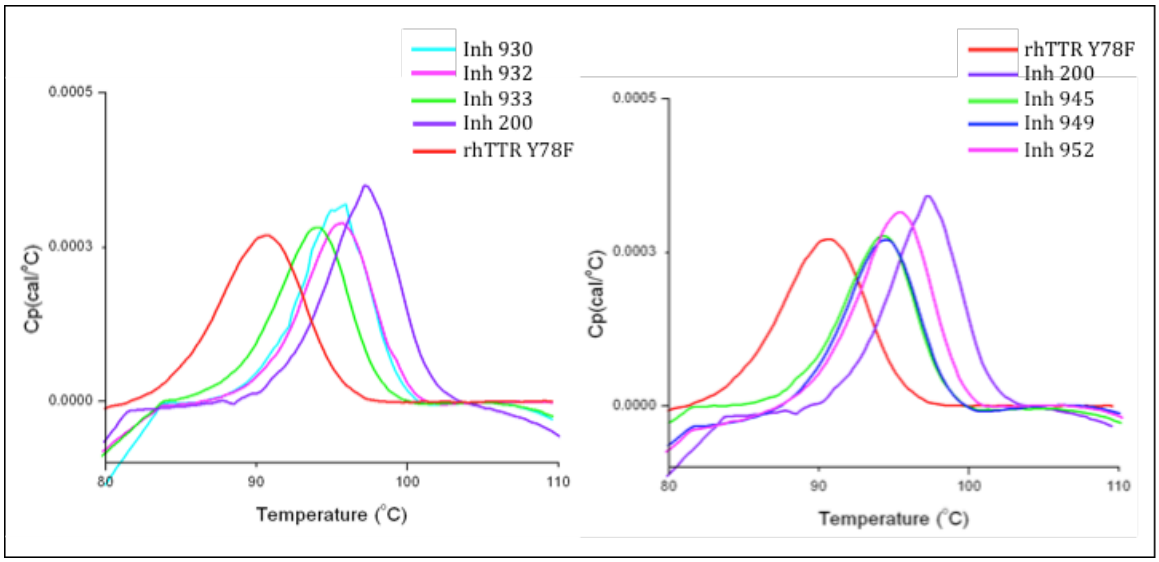

Figure C1-13. Differential Scanning Calorimetry (DSC) results. Each color line indicates the presence of a different inhibitor; in both graphs, red line indicates absence of inhibitor.

Inhibitor	IC_{50} (µM)	Tm (°C)	ΔTm (°C)
200	4.5	97.12	6.29
930	19.4	95.93	5.1
932	6.6	95.72	4.89
933	9.3	93.95	3.12
945	15	94.43	3.6
949	25.34	94.36	3.53
952	13.77	95.27	4.44
TTR Y78F	-	90.83	-

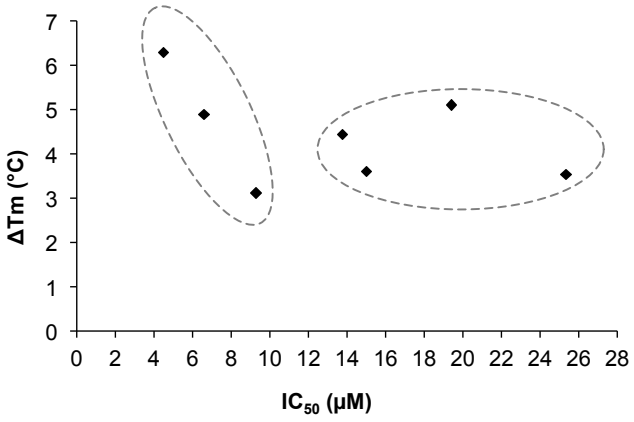

Figure C1-14. Correlation between IC_{50} (µM) and ΔTm (°C). Left, values obtained for each inhibitor; right, representation of those values.

According to the results shown in Fig. C1-14, and as a preliminary study, it seems like there is a trend towards a biphasic system where inhibitors with IC_{50} values <10 μM would produce stronger thermal stabilization. However, those inhibitors with IC_{50} values between 10 and 30 μM, would present similar tetramer stabilization properties, with ΔTm values around 4°C.

C1.4 CONCLUSION

Y78F rhTTR has been recombinantly produced in *E. coli* in a reproducible way, obtaining mainly the S-Glutathionylated (Cys-10) isoform. Upon reduction of rhTTR with DTT its free thiol variant was obtained, allowing the comparison of their fibrillogenesis capacity. From that comparison, it was observed that S-Glutathionylated TTR is 1.3x fold more amyloidogenic at short times (1.5h study), but no differences between the two isoforms are observed for longer incubation periods (72h). The produced S-Glutathionylated Y78F rhTTR was used in a HTS study (Kinetic Turbidimetric Assay) of 41 compounds acting as possible kinetic tetramer stabilizers, proposed by a drug repurposing bioinformatic workflow. As a result, 6 different compounds showed high performance in terms of IC_{50} and 7 different molecules, in terms of RA, the 2 parameters used to evaluate tetramer stabilizers in the selected *in vitro* assay. With a combination of the 2 criteria, a total of 5 different molecules (Fig. C1-15) are here proposed as promising drug repurposing candidates for FAP therapy. Four of them have not been previously reported as TTR tetramer stabilizers and present better performance *in vitro* than the already approved FAP drug Tafamidis (Vyndaquel®). Additionally, the compounds were tested for inhibition capacity against the free thiol isoform, obtaining equivalent results and no selectivity depending on the thiol conjugation state of TTR. Finally, as a secondary screening, Differential Scanning Calorimetry was used to assess the tetramer stabilization properties of some of the best compounds, confirming the thermal stabilization of TTR tetramer by those ligands.

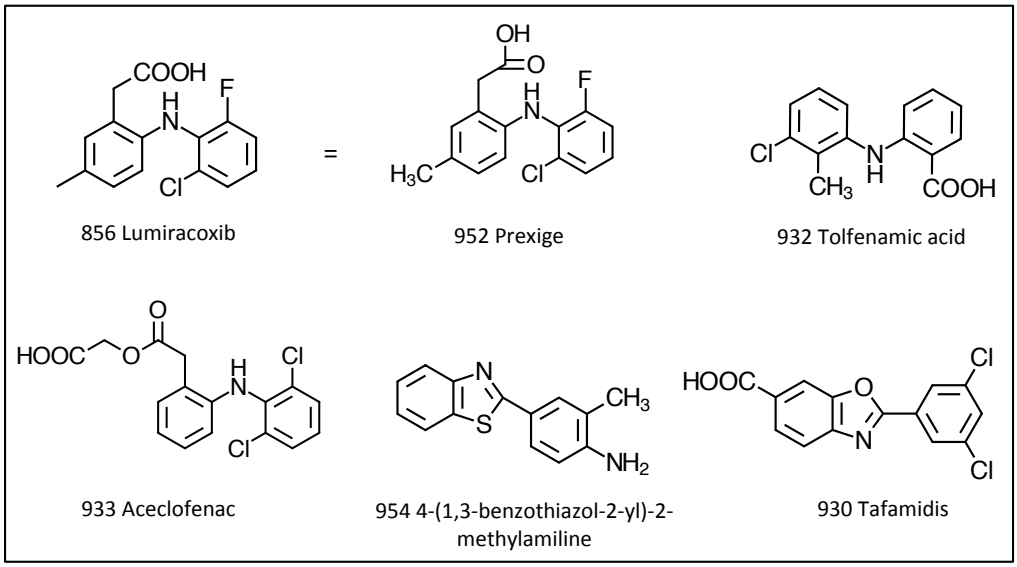

Figure C1-15. Summary of the best compounds assayed. Inhibitors 856 and 952 correspond to the same chemical structure (as previously mentioned). The names of the corresponding drugs are indicated together with the codes of the compounds

C1.5 REFERENCES

Adams D (2013) Recent advances in the treatment of familial amyloid polyneuropathy. *Ther Adv Neuro Disord* 6(2):129–39.

Adamski-Werner SL, Palaninathan SK, Sacchettini JC and Kelly JW (2004) Diflunisal Analogues Stabilize the Native State of Transthyretin. Potent Inhibition of Amyloidogenesis. *J Med Chem* 47(2):355–74.

Altland K and Winter P (1999) Potential treatment of transthyretin-type amyloidoses by sulfite. *Neurogenetics* 2(3):183–8.

Altland K, Winter P and Sauerborn MK (1999) Electrically neutral microheterogeneity of human plasma transthyretin (prealbumin) detected by isoelectric focusing in urea gradients. *Electrophoresis* 20(7):1349–64.

Arsequell G and Planas A (2012) Methods to Evaluate the Inhibition of TTR Fibrillogenesis Induced by Small Ligands. *Curr Med Chem* 19(15):2343–55.

Bergquist J, Andersen O and Westman A (2000) Rapid method to characterize mutations in transthyretin in cerebrospinal fluid from familial amyloidotic polyneuropathy patients by use of matrix-assisted laser desorption/ionization time-of-flight mass spectrometry. *Clin Chem* 46(9):1293–1300.

Blasi D (2012) Drug Discovery Targeted to Transthyretin Related Amyloidosis. Ph.D thesis, University of Barcelona.

Bruylants G, Wouters J and Michaux C (2005) Differential scanning calorimetry in life science: thermodynamics, stability, molecular recognition and application in drug design. *Curr Med Chem* 12(17):2011–20.

Cardoso I, Goldsbury C, Müller S, Olivieri V, Wirtz S, Damas A, Aebi U and Saraiva M (2002) Transthyretin fibrillogenesis entails the assembly of monomers: a molecular model for in vitro assembled transthyretin amyloid-like fibrils. *J Mol Biol* 317(5):683–95.

Colon W and Kelly JW (1992) Partial denaturation of transthyretin is sufficient for amyloid fibril formation in vitro. *Biochemistry* 31(36):8654–60.

Connors LH, Lim A, Prokaeva T, Roskens V and Costello CE (2003) Tabulation of human transthyretin (TTR) variants. *Amyloid* 10(3):160–84.

Cotrina EY, Pinto M, Bosch L, Vilà M, Blasi D, Quintana J, Centeno NB, Arsequell G, Planas A and Valencia G (2013) Modulation of the fibrillogenesis inhibition properties of two transthyretin ligands by halogenation. *J Med Chem* 56(22):9110–21.

Dolado I, Nieto J, Saraiva MJM, Arsequell G, Valencia G and Planas A (2005) Kinetic assay for high-throughput screening of in vitro transthyretin amyloid fibrillogenesis inhibitors. *J Comb Chem* 7(2):246–52.

Hurshman A, White J, Powers E and Kelly J (2004) Transthyretin Aggregation under Partially Denaturing Conditions Is a Downhill Polymerization. *Biochemistry* 43(23):7365–81.

Johnson S, Wiseman R, Sekijima Y, Green N, Adamski-Werner S and Kelly J (2005) Native state kinetic stabilization as a strategy to ameliorate protein misfolding diseases: A focus on the transthyretin amyloidoses. *Acc Chem Res* 38(12):911–21.

Kishikawa M, Nakanishi T, Miyazaki A and Shimizu A (1999) Enhanced amyloidogenicity of sulfonated transthyretin. *Amyloid* 6(3):183–6.

Nakanishi T, Yoshioka M, Moriuchi K, Yamamoto D, Tsuji M and Takubo T (2010) S-sulfonation of transthyretin is an important trigger step in the formation of transthyretin-related amyloid fibril. *Biochim Biophys Acta* 1804(7):1449–1456.

Poulsen K, Bahl JMC, Tanassi JT, Simonsen AH and Heegaard NHH (2012) Characterization and stability of transthyretin isoforms in cerebrospinal fluid examined by immunoprecipitation and high-resolution mass spectrometry of intact protein. *Methods* 56(2):284–92.

Quintas A, Saraiva MJM and Brito RMM (1999) The Tetrameric Protein Transthyretin Dissociates to a Non-native Monomer in Solution: A novel model for amyloidogenesis . *J Biol Chem* 274(46):32943–9.

Quintas A, Vaz DC, Cardoso I, Saraiva MJM and Brito RMM (2001) Tetramer Dissociation and Monomer Partial Unfolding Precedes Protofibril Formation in Amyloidogenic Transthyretin Variants. *J Biol Chem* 276(29):27207–13.

Raz A, Shiratori T and Goodman DS (1970) Studies on the protein-protein and protein-ligand interactions involved in retinol transport in plasma. *J Biol Chem* 245(8):1903–12.

Raz A and Goodman DS (1969) The interaction of thyroxine with human plasma prealbumin and with the prealbumin-retinal-binding protein complex. *J Biol Chem* 244(12):3230–7.

Saraiva MJM (2002) Hereditary transthyretin amyloidosis: molecular basis and therapeutical strategies. *Expert Rev Mol Med* 4(12):1–11.

Schreiber G, Aldred AR, Jaworowski A, Nilsson C, Achen MG and Segal MB (1990) Thyroxine transport from blood to brain via transthyretin synthesis in choroid plexus. *Am J Physiol* 258(2): R338–45.

Sekijima Y (2014) Recent progress in the understanding and treatment of transthyretin amyloidosis. *J Clin Pharm Ther* 39(3):225–33.

Sleigh SH and Barton CL (2010) Repurposing Strategies for Therapeutics. *Pharmaceutical Medicine* 24(3):151–9.

Soprano DR, Herbert J, Soprano KJ, Schon E a. and Goodman DS (1985) Demonstration of transthyretin mRNA in the brain and other extrahepatic tissues in the rat. *J Biol Chem* 260(21): 11793–8.

Sörgjerd K, Klingstedt T, Lindgren M, Kågedal K and Hammarström P (2008) Prefibrillar transthyretin oligomers and cold stored native tetrameric transthyretin are cytotoxic in cell culture. *Biochem Biophys Res Commun* 377(4):1072–8.

Sousa MM, Cardoso I, Fernandes R, Guimarães a and Saraiva MJ (2001) Deposition of transthyretin in early stages of familial amyloidotic polyneuropathy: evidence for toxicity of nonfibrillar aggregates. *Am J Pathol* 159(6):1993–2000.

Suhr OB, Svendsen IH, Ohlsson P-I, Lendoire J, Trigo P, Tashima K, Ranlöv PJ and Ando Y (1999) Impact of age and amyloidosis on thiol conjugation of transthyretin in hereditary transthyretin amyloidosis. *Amyloid* 6(3):187–91.

Takaoka Y, Ohta M, Miyakawa K, Nakamura O, Suzuki M, Takahashi K, Yamamura K-I and Sakaki Y (2004) Cysteine 10 is a key residue in amyloidogenesis of human transthyretin Val30Met. *Am J Pathol* 164(1):337–45.

Terazaki H, Ando Y, Suhr O, Ohlsson PI, Obayashi K, Yamashita T, Yoshimatsu S, Suga M, Uchino M and Ando M (1998) Post-translational modification of transthyretin in plasma. *Biochem Biophys Res Commun* 249(1):26–30.

Westermark P, Sletten K, Johansson B and Cornwell GG (1990) Fibril in senile systemic amyloidosis is derived from normal transthyretin. *Proc Natl Acad Sci U S A* 87(7):2843–5.

Wiseman RL, Green NS and Kelly JW (2005) Kinetic stabilization of an oligomeric protein under physiological conditions demonstrated by a lack of subunit exchange: Implications for transthyretin amyloidosis. *Biochemistry* 44(25):9265–74.

Zhang Q and Kelly JW (2003) Cys10 mixed disulfides make transthyretin more amyloidogenic under mildly acidic conditions. *Biochemistry* 42(29):8756–61.

Zhang Q and Kelly JW (2005) Cys-10 mixed disulfide modifications exacerbate transthyretin familial variant amyloidogenicity: A likely explanation for variable clinical expression of amyloidosis and the lack of pathology in C10S/V30M transgenic mice. *Biochemistry* 44(25):9079–85.

CHAPTER 2. Quantitative analysis of post-translational modifications in human serum transthyretin associated with familial amyloidotic polyneuropathy by targeted LC-MS and intact protein MS

C2.1 INTRODUCTION

Human transthyretin (hTTR; MIM#176300) is a homotetrameric protein that functions as the backup transporter for thyroxine hormone (T4) in plasma and it is its main transporter across the blood brain barrier. TTR is also the main carrier of retinol by forming a 1:1 complex with the retinol-binding protein (RBP) (Raz and Goodman 1969, Raz et al. 1970). It is synthesised in the liver and the choroid plexus of the brain (Soprano et al. 1985), the liver being the main responsible for plasmatic TTR production.Whereas TTR transports nearly all the circulating RBP in serum and it is the main thyroxin transporter in cerebrospinal fluid (CSF), it only transports around the 15% of the serum circulating thyroxin (Schreiber et al. 1990). hTTR is an amyloidogenic protein associated with senile systemic amyloidosis (SSA), caused by wild-type (wt) TTR (Westermark et al. 1990), affecting up to 25% of the population that is more than 80 years old. It is also related to several hereditary amyloidosis classified as rare diseases (Connors et al. 2003, Saraiva 2002): familial amyloidotic polyneuropathy (FAP), produced by single point mutants like V30M or L55P, where the pathology can develop at an early age; familial amyloidotic cardiomyopathy (FAC), mainly associated with V122I and T60A variants; and central nervous system selective amyloidosis (CNSA), the main representative being the A25T and D18G TTR variants (Arsequell and Planas 2012).

Amyloid fibril formation is initiated by TTR tetramer dissociation into dimers and monomers that evolve to a misfolded or non-native monomer intermediate that starts an intermolecular aggregation process involving a number of states through soluble oligomers and leading to mature fibrils (Cardoso et al. 2002, Colon and Kelly 1992, Hurshman et al. 2004, Quintas et al. 1992, 2001). Several studies have shown that TTR intermediates (protofibrils and soluble oligomers), rather than mature fibrils, are the toxic species in cell cultures and that they may play a role in pathogenesis (Sörgierd et al. 2008, Sousa et al. 2001).

TTR is a highly abundant protein in plasma with concentrations around 0.2-0.4 mg/mL in healthy individuals. However, lower TTR levels have been described for TTR-amyloidotic patients (Buxbaum et al. 2010, Saraiva et al. 1983). It occurs as a very heterogeneous protein where variability is not only due to point mutations in the encoding gene but also to post-translational modifications (PTMs) at Cys-10, the single Cys residue in the protein sequence (Altland et al. 1999, Terazaki et al. 1998). Only around 10-15% of the circulating TTR in plasma remains unmodified at this residue and the most common PTMs at Cys-10 are the S-sulfonation (S-Sulfo), S-glycinylcysteinylation (S-CysGly), S-cysteinylation (S-Cys) and S-glutathionylation (S-GSH) (Poulsen et al. 2012). It is thought that PTMs may play an important biological role in the onset and pathological process of the TTR-related amyloidosis, although clinical implications are still badly understood (Altland and Winter 1999,

Hammarström et al. 2002, Jiang et al. 2001, Kingsbury et al. 2007, Kishikawa et al. 1999, Nakanishi et al. 2010, Zhang and Kelly 2003).

Prior studies based on mass spectrometry have addressed the detection and identification of TTR variants in plasma, serum or CSF. In all cases, a common starting step involves the enrichment of TTR by the use of polyclonal antibodies or by SDS-PAGE. Analysis of the immunoprecipitated protein is then performed by MALDI-MS (Bergquist et al. 2000, Trenchevska et al. 2011), MALDI-FTICR-MS (da Costa et al. 2009, Riberio-Silva et al. 2011) or LC-MS (Ando et al. 1996, 1997, Kishikawa et al. 1996, Lim et al. 2003, Poulsen et al. 2012, Suhr et al. 1999) techniques. In most cases, the study of TTR heterogeneity is based on the analysis of the intact protein, where the different TTR variants are assigned on the basis of the mass shift observed in the spectra. An additional digestion step by a combination of different enzymes (trypsin, Arg-C, Asp-N, Glu-C or Lys-C) is often performed to further confirm or determine the location of the modification (Bergquist et al. 2000, da Costa et al. 2009, Lim et al. 2003, Ribeiro-Silva et al. 2011, Suhr et al. 1999, Trenchevska et al. 2011). Few studies are designed to quantify the total amount of TTR and the different TTR variants. These works are based on the study of the intact protein (Ando et al. 1997, Trenchevska et al. 2011) or by mass fingerprinting (da Costa et al. 2009, Ribeiro-Silva et al. 2011) with the assumption that all Cys-10 forms or point mutation variants present the same response factor. However, the presence of a modification or mutation may affect the ionization of the protein resulting in different signal responses.

We here report the development of an analytical mass spectrometry methodology with the aim of quantifying the absolute concentration of the 5 most common TTR Cys-10 PTMs in serum and plasma samples. Additionally, the same methodology will allow the determination of the total amount of TTR in serum and plasma of healthy and FAP individuals bearing V30M mutation, as well as the mutant:wild type (V30M:wt) protein level ratios, which could also play a role in the development of amyloidosis. The strategy is based on targeted LC-MS high resolution analysis (HR-XIC) of a mixture of peptides coming from the digestion of the immunoprecipitated TTR in an Ultra High Resolution-QTOF instrument. For the quantification of wt TTR, V30M TTR, and their PTMs at Cys-10 (free Cys, S-Cys, S-CysGly, S-GSH and S-Sulfo) a set of 7 unique labeled TTR peptides containing the sequence of interest and their modifications were synthesized and added to the samples at known concentrations. In this way, possible changes in response factor due to the presence or absence of modifications are taken into account to determine the percentages of each modification as well as the wt:V30M ratio. In parallel, we used an ESI-MS strategy based on the analysis of the intact protein as described in the bibliography (Poulsen et al. 2012), where the immunoprecipitated TTR was directly infused in an Ultra High Resolution-QTOF instrument, and the relative abundance of each TTR variant was calculated based on the intensity of its corresponding signals in the MS spectra.

C2.2 MATERIALS AND METHODS

C2.2.1 Samples

Human serum samples were kindly provided by the Department of Nephrology and Urology at the Hospital Clínic de Barcelona and had the corresponding informed consent agreement.

Human blood samples were collected and allowed to clot for 30 minutes at room temperature and subsequently centrifuged at 1300 x g for 15 minutes (BD Vacutainer® SST™ Tubes). Serum specimen was extracted from the tube avoiding the fraction closer to the separating gel. Aliquots of 250 µL were then prepared and immediately frozen at -80°C until analyzed.

C2.2.2 Characterization of TTR digestion with different proteases

Recombinant wt TTR (wt rhTTR), obtained as described in (Dolado et al. 2005), was digested with trypsin (Trypsin Gold Mass Spectrometry Grade, Promega), chymotrypsin (Sigma), Asp-N (Sigma), Glu-C (Sigma) and arginine-C (Arg-C, Sigma). 100 µg of protein were digested in each protease test in 1 M urea – 50 mM ammonium bicarbonate (AB) buffer, at 1:10 (trypsin), 1:50 (chymotrypsin, Arg-C, Glu-C) and 1:100 (Asp-N) enzyme:protein ratios, ON at 37°C. Samples of each of the different digests (500 ng) were analyzed on a Maxis Impact Q-TOF spectrometer (Bruker, Bremen), coupled to a nano-HPLC system (Proxeon, Denmark). The samples, dissolved in 5% ACN - 0.1% formic acid in water, were first concentrated on a 100 µm ID, 2 cm Proxeon nanotrapping column and then loaded onto a 75 µm ID, 25 cm Acclaim PepMap nanoseparation column (Dionex). Chromatography was run using a 0.1% formic acid - ACN gradient (5-35% in 20 min; flow rate 300 nL/min). The column was coupled to the mass spectrometer inlet through a Captive Spray (Bruker) ionization source. MS acquisition was set to cycles of MS (2Hz), followed by 3 second cycles of MS/MS (4-16Hz, intensity depending) of a variable number of the most intense precursor ions, with an intensity threshold for fragmentation of 2000 counts, and using a dynamic exclusion time of 2 min, with an automated precursor re-selection when a 3 fold increase in intensity was observed. All spectra were acquired on the range 150-2200 Da. LC-MS/MS data was analyzed using the Data Analysis 4.0 software (Bruker). Peptides were identified using Mascot (Matrix Science, London UK) by search on a database constructed with TTR sequences (wt and V30M). MS/MS spectra were searched with a precursor mass tolerance of 10 ppm, fragment tolerance of 0.05 Da, protease specificity with a maximum of 2 missed cleavages, cysteine modifications (S-Cys, S-Sulfo, S-CysGly and S-GSH) set as variable modifications and methionine oxidation also set as variable modification. Significance threshold for the identifications was set to $p<0.01$, minimum Ions score of 20.

C2.2.3 Targeted LC-MS analysis by high resolution-extracted ion chromatograms (HR-XIC)

C2.2.3.1 Immunoprecipitation with hydrazide-immobilized antibody (IP Ab-ULH)

Polyclonal rabbit anti-human TTR antibody (Dako) was coupled to UltraLink® Hydrazide Resin (Thermo Scientific) following the resin manufacturer's protocol. 225 µg of immobilized antibody (Ab-ULH) were incubated with 25 µL of human serum for 1 hour and 40 minutes at room temperature with soft agitation. After TTR binding to the Ab-ULH, 5 washes with 500 µL PBS were performed. TTR was eluted with 100 mM triethylamine (TEA, Fluka) pH=11.5 solution. Elution was performed in 3 steps by addition of 400 µL TEA followed by 2 minutes of sonication on an ultrasonic bath, and the

total eluted volume was concentrated to 50 µL after 8 M urea-50 mM AB buffer exchange, by diafiltration in an Amicon® Ultra-0.5 mL centrifugal Filter, Ultracel®-3K cut off membrane (Millipore).

C2.2.3.2 Enzymatic digestion of transthyretin

After immunoprecipitation, determination of the total protein amount for each sample was performed using Bio-Rad DC™ Protein Assay Kit (Bio-Rad). Based on the amount of protein quantified, a fraction of the immunoprecipitated TTR (10 µg) was digested with Arginine-C (Endoproteinase Arg-C Sequencing Grade, Roche) during 6 hours, 37°C at a 1:23 ratio enzyme:protein. Another fraction (10 µg) of the immunoprecipitated protein was digested with trypsin (Trypsin Gold Mass Spectrometry Grade, Promega) ON, 37°C at a 1:10 ratio enzyme:protein.

C2.2.3.3 Standard labeled peptides

Labeled (5C13,N15 proline) peptides for the quantification of the 5 Cys-10 forms (>98% purity and quantified by AAA) were purchased from Peptide Synthetics (United Kingdom). The different peptides for the quantification of Cys-10 modifications (Table C2-1) will be referred as N-term heavy peptides. Labeled (6C13,4N15 arginine) peptides for the total TTR determination (99% purity and quantified by AAA) were purchased from AQUA Peptide Sigma-Aldrich. The two different peptides (Table C2-1) used for the total amount of protein determination will be referred as GSPAIN peptides (wt and V30M, for the wt TTR form and the mutant V30M TTR form, respectively). Labeled (6C13,4N15 arginine) GSPAIN V30M peptide carrying methionine-sulfoxide (>95% purity and quantified by AAA) was obtained from Centro Nacional de Biotecnología, Madrid, Spain.

Table C2-1. Summary of the signals monitored and its calculated LOD and LOQ

Peptide	Charge	Label	m/z heavy	m/z light	LOD (fmol)	LOQ (fmol)
(P1) GP*TGTGESKCP*LMVKVLDAVR	4	P 5C13,N15	543.296	540.289	1.38	4.59
(P2) GP*TGTGESKC(C)P*LMVKVLDAVR[a]	4	P 5C13,N15	573.047	570.041	2.49	8.28
(P3) GP*TGTGESKC(GSH)P*LMVKVLDAVR[b]	4	P 5C13,N15	619.563	616.557	0.09	0.29
(P4) GP*TGTGESKC(CG)P*LMVKVLDAVR[c]	4	P 5C13,N15	587.303	584.296	0.44	1.47
(P5) GP*TGTGESKC(S03H)P*LMVKVLDAVR[d]	3	P 5C13,N15	750.712	746.702	23.0	31.6
(P6) GSPAINVAVHVFR*	2	R 6C13,4N15	688.887	683.883	61.7	61.7
(P7) GSPAINVAMHVFR*	2	R 6C13,4N15	704.873	699.869	43.0	44.1

[a] C(C):S-cysteinylation (S-Cys), cysteine on the side chain of cysteine by disulfide bond
[b] C(GSH):S-glutathionylation (S-GSH), glutathione on the side chain of cysteine by disulfide bond
[c] C(CG): S-glycinylcysteinylation (S-CysGly), H-cysteinyl-glycine-OH on the side chain of cysteine by disulfide bond
[d] C(SO3H):S-sulfonation (S-Sulfo)

C2.2.3.4 LC-MS Measurement with UHR-QTOF

TTR from human samples was purified and digested with Arg-C and trypsin as described above. Standard labeled N-term peptides were spiked into Arg-C digested samples after digestion and prior to LC-MS measurement. The same procedure was followed for the standard labeled GSPAIN peptides (P6 and P7 Table C2-1) and the trypsin digested samples. The amount of heavy peptides in column was of 50 fmols for each GSPAIN peptide and of 50, 12.5, 7.5, 200 and 200 fmols for the Free Cys (P1), S-CysGly (P4), S-GSH (P3), S-Cys (P2) and S-Sulfo (P5) N-term peptides (Table C2-1), respectively.

The samples were analyzed on a UHR-QTOF mass spectrometer (Bruker Impact), coupled to a Proxeon Easy nano-LC (Bruker). Samples of the TTR digests (50 ng) spiked with the standard peptides were first loaded into a 100 µm ID, 2 cm Proxeon nanotrapping column and then separated with a 10 minutes 0.1% formic acid – ACN gradient (5-35% in 10 min; flow rate 300 nL/min) on a Acclaim PepMap 75 µm x 25 cm, 3 mm particle size reverse phase nanoseparation column (Dionex) coupled to the mass spectrometer inlet through a Captive Spray (Bruker) ionization source. For quantification, MS acquisition was set to cycles of MS (0.5 Hz). All spectra were acquired on the range 150-2200 Da.

C2.2.3.5 Data analysis

LC-MS data was first processed using Data Analysis 4.1 (Bruker) and then quantified using Skyline Software (MacCoss Lab) to filter and integrate precursor signals of target peptides. Using a HR-XIC Skyline template, extracted ion chromatograms for the m/z corresponding to the main isotope and charge state signal for each target peptide were used for quantification.

C2.2.3.6 Determination of response factor for methionine oxidized GSPAIN peptide

Pure recombinant hTTR protein was quantified based on absorbance at 280 nm (Dolado et al. 2005) and 10 µg of protein were spiked into a 70 µg/µL BSA solution, which was then immunoprecipitated and digested with trypsin according to the above described protocol. The resulting digested protein was used to prepare solutions at 25, 50, 100 and 150 ng/µL of digested rhTTR. A known amount of total V30M GSPAIN peptide (Table C2-1 P7), containing both oxidized and non-oxidized forms at unknown proportions, was added to each solution (total final concentrations of 25, 50, 100 and 150 fmol/µL, respectively). Samples were then analyzed by the described LC-MS strategy. From the results, and taking into account the known concentrations of rhTTR and total GSPAIN peptide, the response factors for the non-oxidized and oxidized forms of the V30M GSPAIN peptide were calculated.

Additionally, a standard curve for the labeled V30M GSPAIN oxidized peptide was performed in triplicate analyzing serial dilutions of the standard labeled peptide in presence of trypsin digest of TTR as matrix. The results were used to calculate the response factor for the oxidized form of the peptide.

C2.2.4 Intact protein analysis

C2.2.4.1 Immunoprecipitation with unconjugated antibody

For TTR immunoprecipitation, 225 µg of the polyclonal rabbit anti-human TTR antibody (Dako) were incubated with 25 µL of human serum over night at 4°C. After incubation, centrifugation at 9000 x g, 10 minutes and 4°C allowed the precipitation of the TTR-Ab complex. The pellet obtained was washed 3 times with 0.1 M AB buffer and finally resuspended in 50% methanol - 1% formic acid (Poulsen et al. 2012) at approximately 4 pmol TTR/µL, according to the reported TTR concentrations in serum.

C2.2.4.2 Intact Protein measurement with UHR-QTOF

TTR immunoprecipitated as described below was analyzed on a UHR-QTOF mass spectrometer (Bruker Impact). Sample was directly infused with a syringe pump at 3 µL/min into an ESI source (Bruker). The MS acquisition method was set up to acquire only MS data during 5 minutes, with MS cycles of 0.5 Hz in the mass range from 50 m/z to 1500 m/z. MS data was analyzed using Data Analysis 4.1 software (Bruker).

Lock mass calibration using Data Analysis 4.1 (Bruker) was performed prior to averaging the spectra. All measurements were done in charge envelope +14, taking into account the intensity of the 5 most intense isotope peaks for each modification. Peak inspection was performed manually and the sum of these 5 isotopes was considered as the total intensity for a given modification. From the total intensity of each form, the percent of each modification with respect to the sum of all forms was calculated, for both wt and V30M TTR.

C2.2.5 Top-down MS analysis

Top-down MS experiments were performed on a 7T LTQ-FT Ultra mass spectrometer (Thermo Scientific). Purified TTR was reconstituted with ESI solution (MeOH, 1% FA (1:1, v/v)) and infused by automated nanoelectrospray using a Triversa Nanomate (Advion BioSciences) as the interface. Full MS spectra (m/z 200-2000) were acquired at 100,000 resolution (m/Δm 50% at 400 m/z) and, after full scan analysis, individual charge state ions of the multiply protonated proteoforms were selected for isolation in the LTQ using isolation widths of 5–10 m/z. Isolated ions were then fragmented by either CID or ECD. CID fragmentation was performed in the trap whereas isolated ions were guided to the FTICR cell for ECD fragmentation. Fragment detection was done in the FTICR cell for both types of fragmentation at 100,000 resolution (m/Δm 50% at 400 m/z) and averaging 200–1000 scans. For CID experiments precursor ions were activated using 30% to 40% normalized collision energy at the default activation q-value of 0.25. For ECD experiments the following settings were used: 3–5 energy (arbitrary units) corresponding to a cathode voltage of 1.5 V to 3.5 V), 127 ms delay (with 0 ms additional delay) and 15-75 ms duration. Fragmentation efficiency was optimized to maximize product ion signal intensity for both CID and ECD. The analyzer charge capacity was set to a target value of 500,000 and 1000,000 counts for CID and ECD MS/MS experiments respectively. Protein masses and zero charged fragments masses were determined by deconvolution using Xtract algorithm integrated in Xcalibur software vs 2.07 (Thermo Scientific). Data validation was done using ProSight PC 2.0 software (Thermo Scientific) in single protein mode using sequence gazer option.

C2.3. RESULTS AND DISCUSSION

C2.3.1 Immunoprecipitation of TTR from serum

The first step of both methodologies consists of immunoprecipitation of serum TTR using a polyclonal antibody. Polyclonal antibodies present several advantages, such as the lack of specificity for a certain modification or the lack of sensitivity in front of point mutations, allowing the use of the same procedure for a wide variety of samples. In addition, they can form precipitating immune complexes with homogeneous monomeric protein antigens, since each antibody can interact with a different epitope on the antigen. In the particular case of TTR, and given its tetrameric nature in plasma, they are able to form precipitating immune complexes without the need of adding immobilized protein A or G. We chose to use this immunoprecipitation with unconjugated antibody for minimal manipulation of the sample for intact protein analysis. However, in the case of the LC-MS HR-XIC strategy the antibody was first immobilized, used to capture TTR from plasma, and then treated with triethylamine, to release antibody-free TTR in order to improve the yield of the enzymatic digestion of the protein.

C2.3.1.1 Immunoprecipitation of TTR with hydrazide-immobilized antibody and TTR recovery

Conditions for the immunoprecipitation with immobilized antibodies (Ab-ULH, see Materials and Methods C2.2.3.1) were set up using solutions of known concentration of recombinant human TTR (rhTTR). rhTTR was prepared either in PBS buffer alone or in the presence of BSA at concentrations similar to plasma, to mimic plasmatic conditions, in case the complexity of the sample could affect the yield of the IP. The recovery from TTR solutions in the concentration range reported for plasma TTR was practically quantitative (Fig. C2-1A). In order to further check that the amount of Ab used is enough to rescue all the plasmatic TTR, solutions ranging from 0.1 to 0.6 mg/mL of rhTTR in PBS or PBS plus 70 mg/mL BSA were immunoprecipitated (Fig. C2-1B). The amount of TTR in the IP fraction was quantified using the standard curve prepared from known amounts of rhTTR in a SDS-PAGE gel (Fig. C2-1C). The results confirmed that recovery was practically quantitative and linear in all the range of concentrations assayed. In addition, two negative controls were performed (Fig. C2-1B, IP BSA and IP PBS). Applying the immunoprecipitation protocol to a solution of BSA or PBS showed no bands interfering with TTR, but some background of BSA, even after extensive washing, or leaking Ab was observed. Finally, immunoprecipitation from human serum samples according to the established protocol was tested (Fig. C2-1B, IP serum), confirming quantitative recovery of serum TTR.

C2.3.1.2 TTR recovery upon immunoprecipitation with unconjugated antibody

In a similar way, we checked the conditions for total recovery of TTR by immunoprecipitation with the antibody in solution, performed essentially as in (Poulsen et al. 2012). Immunoprecipitation from 25 µL solutions containing rhTTR concentrations ranging from 0.2 to 0.6 µg/µL was quantitative, confirming total TTR rescue from the solution after immunoprecipitation (Fig. C2-1D).

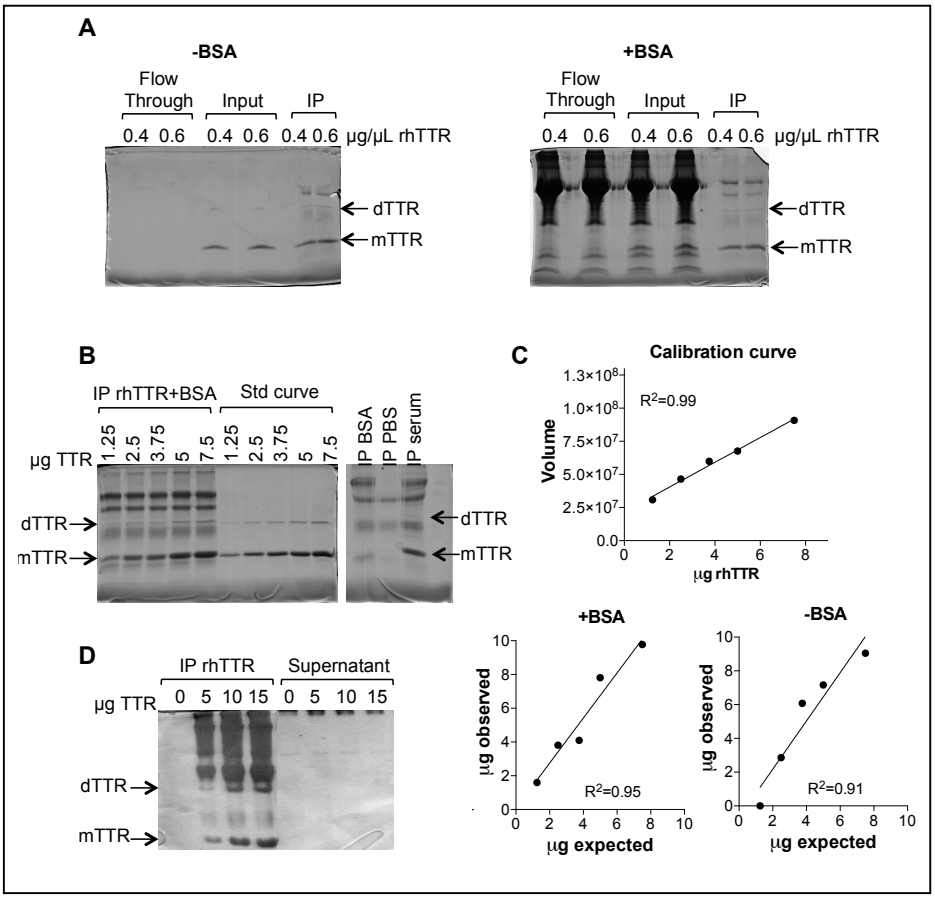

Figure C2-1. Optimization of TTR immunoprecipitation with immobilized (Ab-ULH) and unconjugated anti TTR antibody. **(A)** Immunoprecipitation with ULH-Ab of rhTTR solutions of the indicated concentrations, in the absence and presence of BSA (70 µg/µL). Of each of the indicated fractions (Input, Flow-through and Immunoprecipitate (IP)), 1/10 was loaded in the SDS-PAGE gels; **(B)** Left: Ab-ULH IPs from solutions with increasing amounts of rhTTR, as indicated, in the presence of BSA (70 µg/µL) and rhTTR standard calibration curve. Right: control IPs from a BSA solution and PBS, and IP from serum sample. Half of each IP was loaded in the gel; **(C)** Recovery determination for experiment in (B) and for the same experiment in the absence of BSA; **(D)** Immunoprecipitation using unconjugated Ab from increasing amounts of rhTTR. Equivalent amounts of the IP and supernatant fractions were analyzed. Gels were stained with Coomassie Blue, scanned with LabScan and quantified using ImageQuant software (GE Healthcare). Bands corresponding to monomer and dimer of TTR are indicated with arrows as mTTR and dTTR, respectively.

C2.3.2 Strategy 1: Targeted LC-MS method

C2.3.2.1 Selection of target peptides and digestion optimization

Digestion of purified rhTTR with different enzymes was performed to test the coverage of the TTR sequence by LC-MS/MS analysis (Fig. C2-2). Since we are interested in the study of TTR Cys-10 modifications, digestion with trypsin does not provide a suitable peptide, due to the presence of two Lys residues too close in the sequence (Lys9 and Lys15), which would result in a peptide too short for LC-MS analysis, and with the cleavage site contiguous to the modified residue, which could affect the cleavage efficiency. Suitable peptides were observed in both the Asp-N and Arg-C digests, the later being the one giving the strongest MS signal. Thus, Arg-C digestion was selected for the analysis of the N-term peptides carrying the different modifications at Cys-10. The same digestion produces also the GSPAINVAVHVFR peptide (and its V30M mutant version) that can be used for the quantification of the total TTR amount.

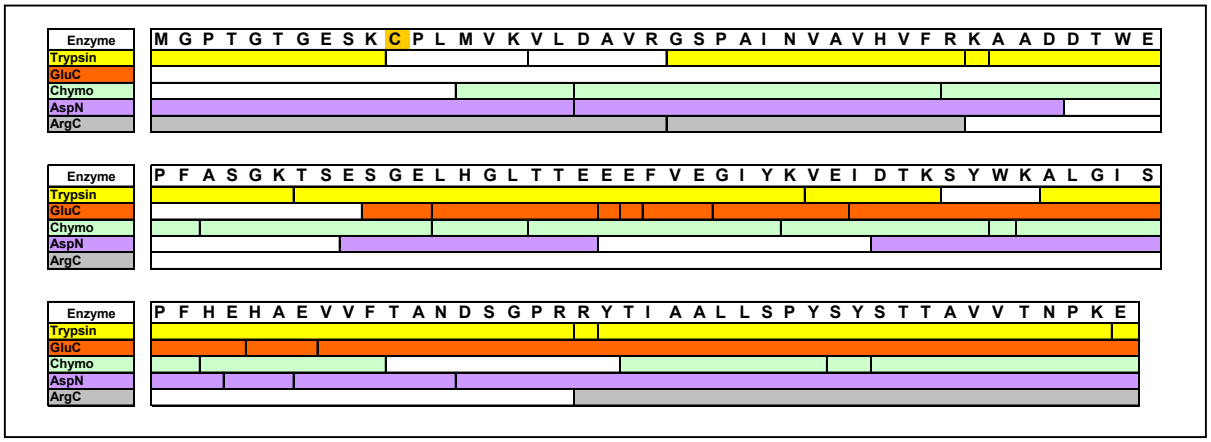

Figure C2-2. Schematic representation of the peptides resulting from rhTTR digestion with several proteases. The different boxes indicate the peptides obtained in a theoretical digestion; coloured boxes indicate the peptides detected by MS/MS.

Since the GSPAIN peptides are also tryptic peptides, they allowed a direct comparison between the efficiency of trypsin and Arg-C digestion of TTR. Experiments to assess the digestion performance were carried out on serum samples having both wt and V30M TTR. After immunoprecipitation with ULH immobilized antibody, the amount of the different peptides obtained was quantified using standard peptides, as detailed below. Different conditions for Arg-C digestion were tested attempting to optimize the yield, as monitored by the GSPAIN peptide quantification (Table C2-1, P6-P7) in comparison to a parallel trypsin digestion of the same sample. Conditions assayed included: different enzyme:protein ratios (1:15 to 1:100), presence of different denaturing agents (10% ACN, 10% trifluoroethanol, 2 M urea, 8 M urea), addition of 10 mM $CaCl_2$, different incubation times (4-16 h), different protein concentration during the digestion, and 3 successive additions of the enzyme, at 2h intervals. It was found (Fig. C2-3A and B) that the yields of the GSPAIN peptides upon Arg-C digestion were 4 to 10-fold lower than the obtained for trypsin digestion. A decrease in the amount of GSPAIN peptide measured at long digestion times was also apparent (Fig. C2-3B). LC-MS/MS analysis of the Arg-C digests showed the presence of some non tryptic peptides, in particular N-terminal truncated forms derived from the GSPAIN peptides (Fig. C2-4), pointing to the presence of some minor proteolytic activity that could explain the observed decrease in the measured amount of GSPAIN peptides. The number of peptide spectrum matches (PSM) corresponding to partially digested peptides (1 missed cleavage) decreased significantly after 3h of digestion, while the amount of tryptic Arg-C GSPAIN peptide matches increased during 5h of digestion. In parallel, the number of non-tryptic peptide matches (N-terminal truncated forms) started increasing after 3h, being up to 20% of the PSMs after 5h of digestion. Similar results were obtained when using other Arg-C enzymes available from different vendors.

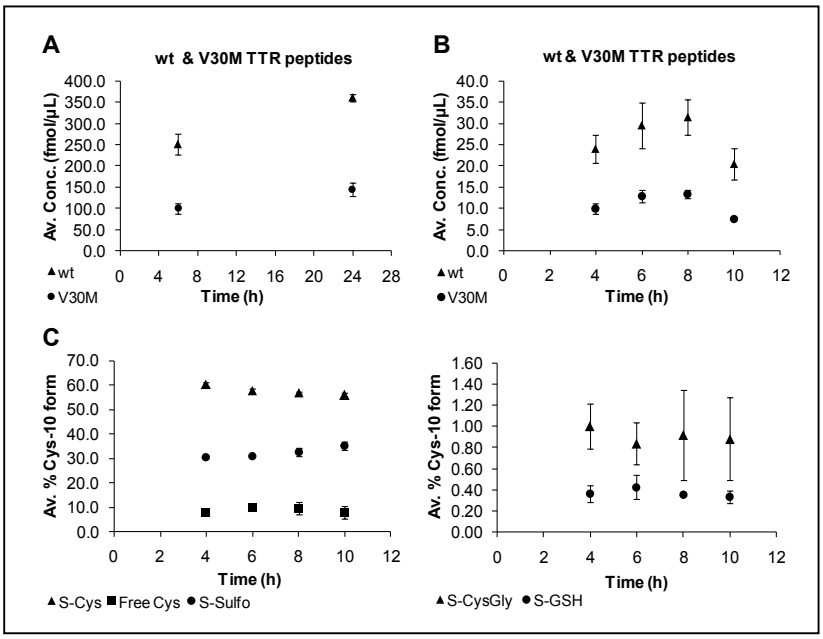

Figure C2-3. Time course of the digestions of immunoprecipitated TTR with trypsin and Arg-C. (A) Trypsin digestion. Measured concentrations of GSPAINVAVHVFR (wt) and GSPAINVAMHVFR (V30M), respectively, as quantified by HR-XIC. (**B) Arg-C digestion.** Measured concentrations of GSPAIN wt and V30M TTR peptides, as in A. **(C) N-term peptides measured along Arg-C digestion.** The percent of each modified N-term peptide, GPTGTGESKC*PLMVKVLDAVR, was quantified by HR-XIC. In all cases, the average values measured at each time point for three replicate digestions are shown. Error bars correspond to the standard deviation. Note that the sample used for digestion was a pool of different serum samples and thus the wt:V30M ratio measured is not representative of a real sample.

Since improving the Arg-C digestion yield was not really possible, and the Arg-C N-term peptide being the best-suited for the study of Cys-10 modifications, we devised an analysis strategy based on two parallel digestions. After immunoprecipitation of serum TTR, an aliquot of the recovered protein was digested with trypsin for the quantification of the total TTR amount in serum through the GSPAIN peptides. A second aliquot was digested with Arg-C for the quantification of the different N-term peptides. Since Arg-C digestion cannot be completed, we checked that the relative amounts of each of the Cys-10 modified forms were constant along the progression of the digestion. As shown in Fig. C2-3C, the proportion of the different forms is constant within experimental error up to 10 hours of digestion. We chose a digestion time of 6 h under these conditions to measure the relative amounts of each Cys-10 form. From those, the absolute amounts of each TTR form were calculated based on the total TTR amount determined from the analysis of the trypsin-digested protein.

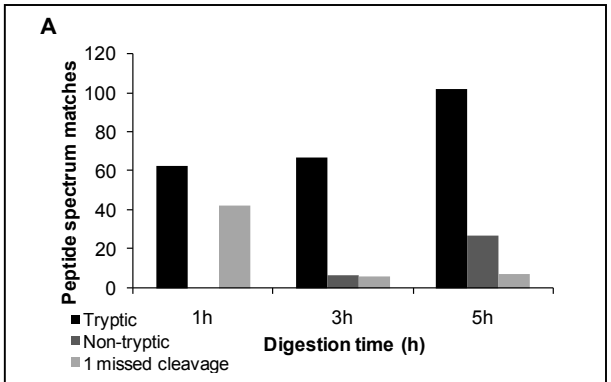

B

	Peptide Spectrum Matches					
	1h		3h		5h	
Sequence	**R1**	**R2**	**R1**	**R2**	**R1**	**R2**
GSPAINVAMHVFR	6	8	10	7	8	11
GSPAINVAM(oxi)HVFR	1	5	2	3	3	2
GSPAINVAVHVFR	35	70	40	72	93	87
SPAINVAMHVFR	0	0	0	0	1	1
PAINVAMHVFR	0	0	0	5	3	5
PAINVAVHVFR	0	0	0	2	6	3
AINVAMHVFR	0	0	0	1	2	2
AINVAVHVFR	0	0	0	1	3	2
INVAMHVFR	0	0	0	0	2	2
INVAVHVFR	0	0	0	0	1	0
NVAMHVFR	0	0	0	1	0	0
NVAVHVFR	0	0	0	0	1	0
MHVFR	0	0	0	0	1	1

Figure C2-4. Peptide spectrum matches (PSM) of the GSPAIN peptides upon Arg-C digestion of TTR. Digestion was performed as described in Materials and Methods. **(A) Number of PSM matching GSPAIN peptides and its N-terminal truncated forms.** Representation at 3 different digestion points: 1h, 3h and 5h. **(B) Sequences of the tryptic GSPAIN peptides** (wt, V30M, and oxidized V30M) **and the non-tryptic ones** (N-terminal truncated forms for both wt and V30M forms) **identified**. It is indicated the number of observed PSMs for each form along the digestion (2 replicas).

C2.3.2.2 Labeled peptide standard curves for quantification

Table C2-1 shows the peptide ions used in the quantification for the HR-XIC strategy, as well as the limits of detection (LOD, S/N=3) and the limits of quantification (LOQ, S/N=10) for the different peptides, derived from their corresponding standard curves (Fig. C2-5). Standard curves for each of the labeled peptides used for quantification were performed by serial dilution of Arg-C (N-term peptides, P1-P5 Table C2-1) or trypsin (GSPAIN peptides, P6-P7 Table C2-1) in the presence of digested immunoprecipitated TTR as matrix. The average heavy/light (H/L) ratio of the three replicates analyzed was represented against the concentration (fmol/µL) of heavy peptide injected. All the peptides presented linear standard curves in the concentration range studied, with R^2 values between 0.957 and 0.998. The charge state and isotopic species giving the strongest signal for each heavy labeled form was used for quantification.

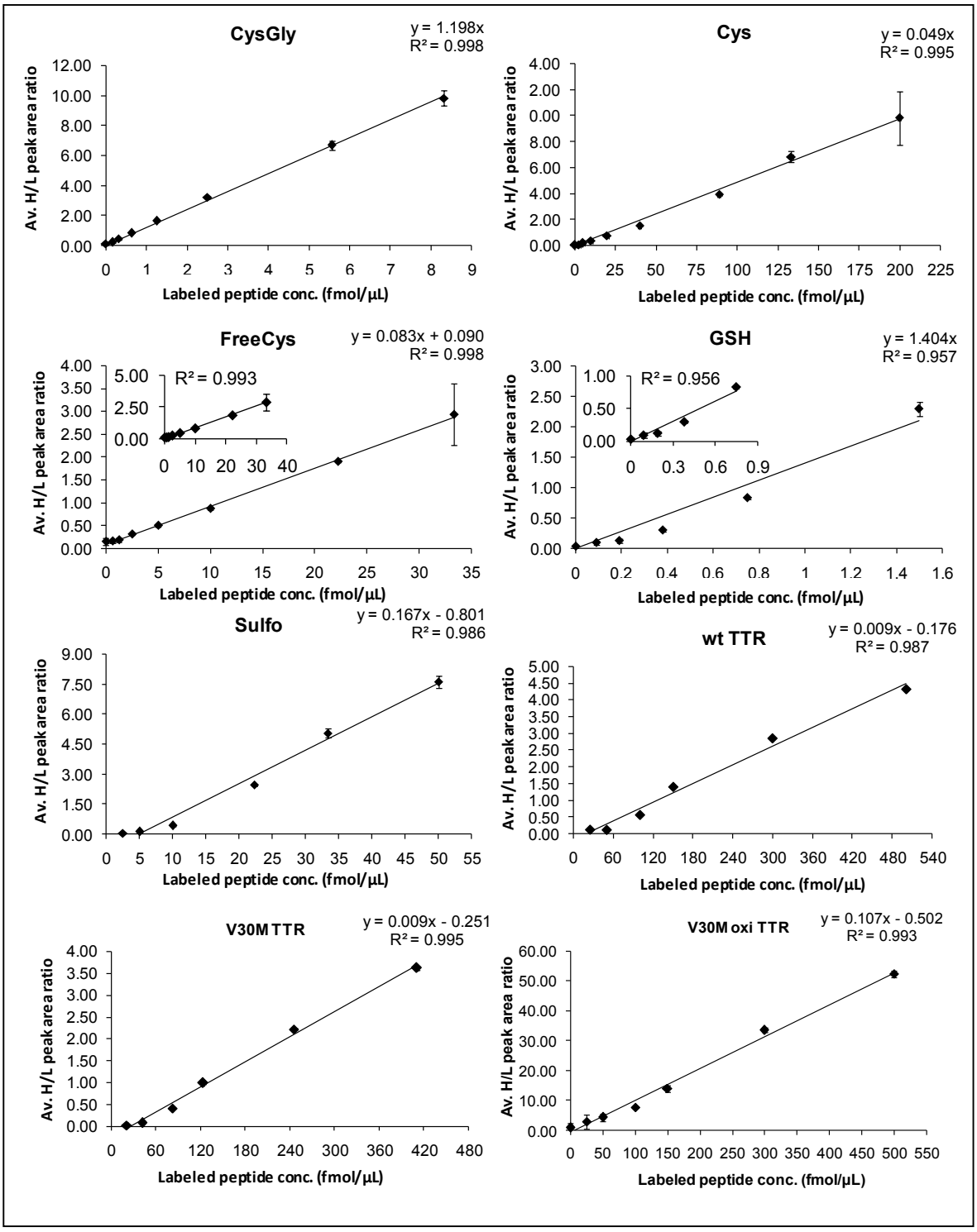

Figure C2-5. Standard curves for the heavy peptides used in the study. Heavy labeled standard peptides were added to an Arg-C (N-term peptides) or trypsin (GSPAIN peptides) digest (50 ng/mL) of immunoprecipitated TTR from serum. The average H/L ratio of three technical replicates is represented versus the fmol/µL of heavy peptide injected. Error bars for the standard deviation between the 3 replicates are shown.

C2.3.2.3 Methionine oxidized peptides

The presence of methionine residues in the peptides used for quantification is normally avoided when designing peptide targeted analysis methods. In this study, however, both the N-terminal peptides used for Cys-10 modifications quantification and the GSPAIN peptides used for total protein quantification have methionine residues. In the first case, methionine 13 is close to the modification site, and cannot be excluded from the targeted peptide by any suitable digestion procedure. In the case of the GSPAIN peptide, methionine is the site of the mutant of interest, and quantifying wt and V30M forms of TTR is one of the goals of the method. Thus, we had to take into account methionine oxidation of the peptides of interest. The signals for the ions corresponding to all possible methionine oxidized forms, both from the endogenous and the labeled peptides, were monitored in the HR-XIC LC-MS analysis.

We found that the signals for the oxidized forms for all the N-term peptides were negligible compared to the non-oxidized forms, and thus they were not further considered in the quantification. However, the standard peptide GSPAINVAMHVFR, used for quantification of total V30M TTR was found particularly prone to oxidation. The standard heavy peptide, of known total concentration derived from the amino acid analysis provided by the manufacturer, contained in fact both oxidized and non-oxidized forms at unknown proportions. Since attempts to convert the standard peptide quantitatively to the reduced or oxidized form were not successful, we devised an indirect strategy to obtain an estimation of the response factors of the oxidized and non-oxidized heavy peptide forms, and their proportions in the standard, based in the use of a rigorously quantified solution of a non-oxidized rhTTR V30M as reference. The recombinant protein was quantified based on absorbance at 280 nm (Dolado et al. 2005) and was used to prepare a solution of known concentration of rhTTR V30M spiked into a 70 mg/mL BSA solution, which was then immunoprecipitated and digested with trypsin according to the established protocol. The resulting digested protein was used to prepare solutions at various known concentrations of digested rhTTR, to which different amounts of total V30M GSPAIN peptide, containing both oxidized and non-oxidized forms at unknown proportions, were added. Analysis of these samples by the described LC-MS strategy was used to derive response factors (signal area/fmol peptide) for the non-oxidized and oxidized forms of the V30M GSPAIN, based on the known concentrations of rhTTR and total GSPAIN peptide. A response factor significantly higher (13.63 fold) for the oxidized peptide was found.

We further confirmed the response factor for the oxidized V30M GSPAIN peptide by an independent, more accurate, measurement using a synthetic labeled standard peptide carrying a Met-sulfoxide. The standard curve for this peptide was determined as in C2.3.2.2, and is shown in Fig. C2-5. Together with the results measured using the mixture of non-oxidized and oxidized forms of V30M GSPAIN, we calculated the ratio of response factors to be 11.11 (oxidized:non oxidized V30M).

The measured response factors were used to quantify the total V30M TTR in samples, as the sum of non-oxidized and oxidized forms. In all serum samples analyzed, the proportion of the Met-30 oxidized form was found to be below 7%.

C2.3.2.4 Intra- and inter-assay precision for the targeted LC-MS strategy

In order to determine intra- and inter-assay precision, a pool of serum from healthy individuals was used. From this pool, the complete sample preparation procedure, including immunoprecipitation

and trypsin and Arg-C digestions, was performed in triplicate. Each of the digests was then analyzed by HR-XIC LC-MS in triplicate. The results obtained for total protein determination (trypsin digestion) and Cys-10 modified forms quantification (Arg-C digestion) are shown in Table C2-2. The reproducibility of the assay was very good, with coefficients of variation ≤2% for the determination of the total amount of protein and variations ≤8% for the quantification of the different Cys-10 forms, both intra- (triplicate sample processing) and inter-assay (triplicate LC-MS analysis). The only exception was for the Free Cys quantification, which presented an inter-assay coefficient of variation of 19%. It is likely that the higher variability observed for the Free Cys form reflects its susceptibility to oxidation during the manipulation of the sample. We have not explored preanalytical issues at this point of the development of the methods, but this is clearly a point to take into account, given the nature of the modifications of interest and in the light of previous reports (Poulsen et al. 2012).

Table C2-2. Determination of the intra- and inter-assay precision for the N-term Cys-10 PTMs quantification and for the determination of the total TTR amount

		Free Cys			S-Cys			S-CysGly			S-GSH			S-Sulfo			Total TTR		
		IP1	IP2	IP3	IP1	IP2	IP3	IP1	IP2	IP3	IP1	IP2	IP3	IP1	IP2	IP3	IP1	IP2	IP3
Intra-assay	STDV	0.085	0.264	0.083	0.329	0.062	0.354	0.073	0.068	0.044	0.008	0.006	0.007	0.354	0.275	0.179	0.950	0.450	0.107
	Mean (% of PTM or ng TTR/µL serum)	4.95	4.13	3.18	70.55	70.80	22.02	2.01	1.85	2.18	0.48	0.46	0.54	22.02	22.76	20.47	55.11	54.99	56.26
	CV (%)	1.71	6.4	2.61	0.47	0.09	1.61	3.65	3.68	2.04	1.66	1.31	1.29	1.61	1.21	0.87	1.72	0.82	0.19
	Av CV (%)		3.57			0.28			3.12			1.42			1.23			0.91	
Inter-assay	STDV		0.779			1.495			0.153			0.039			1.042			0.701	
	Mean (% of PTM or ng TTR/µL serum)		4.09			71.66			2.01			0.49			21.75			55.45	
	CV (%)		19.06			2.09			7.61			7.88			4.79			1.26	

C2.3.3 Strategy 2: Intact protein MS analysis

C2.3.3.1 Relative quantification by intact protein analysis

Analysis of intact immunoprecipitated TTR from serum by direct infusion to the electrospray source on a HR-QTOF instrument (Bruker Impact) allowed to detect signals of m/z values compatible with the main Cys-10 modified forms of wt and V30M TTR, in charge states ranging from z=9 to z=19. Fig. C2-6A shows an example of the spectra obtained for 2 different serum samples, one containing only wt TTR and the other wt and V30M TTR. All the modifications of interest are shown, plus an unknown modification corresponding to a mass shift of +14Da. As shown in Fig. C2-6B, a good agreement between the calculated and observed m/z values was obtained. To further confirm the identity of each of the assigned ions, top-down analysis of each of the TTR forms (example in Fig. C2-7) was performed on a 7T LTQ-FT Ultra mass spectrometer confirming in all cases the structure assigned in Figure 4 (Annex, Tables A-3 – A-19 and Fig. A-1 - A-23).

A

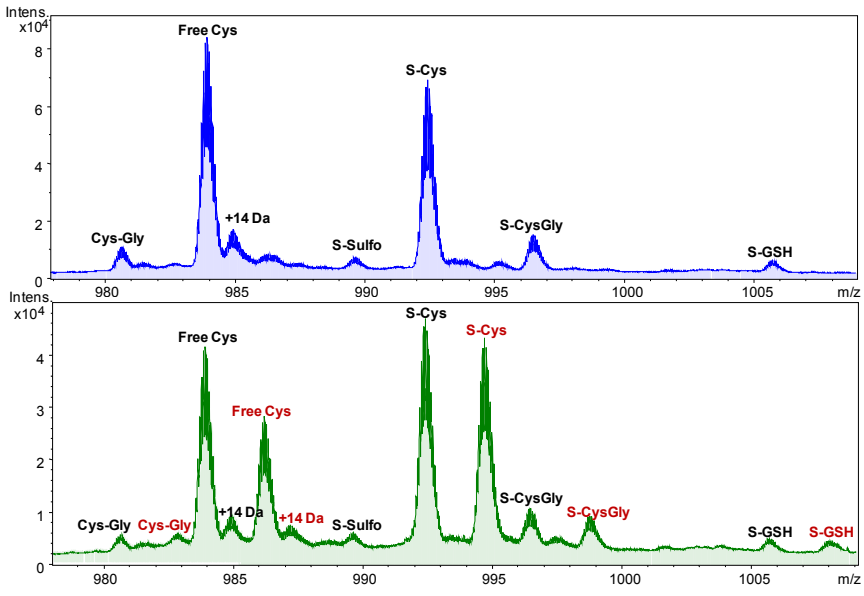

B

	wt TTR			V30M TTR		
	m/z (z=+14)			m/z (z=+14)		
Modification	**Observed**	**Calculated**	**Δ ppm**	**Observed**	**Calculated**	**Δ ppm**
Cys→Gly	980.6508	980.6430	7.95	982.9345	982.9267	7.94
Free Thiol	983.9357	983.9278	8.03	986.2201	986.2116	8.62
wt+14 (unknown)	984.9378	-	-	987.2216	-	-
S-Sulfo (Sulfonate)	989.6472	989.6390	8.29	-	-	-
S-Cys (Cysteinyl)	992.4357	992.4281	7.66	994.7197	994.7119	7.84
S-CysGly (CysteinylGlycine)	996.5076	996.5011	6.52	998.7926	998.7848	7.81
S-GSH (Glutathione)	1005.7259	1005.7184	7.46	1008.0107	1008.0021	8.53

Figure C2-6. TTR spectra obtained by intact protein. (A) wt TTR spectra (blue) and V30M spectra (green) obtained by intact protein strategy in Impact (Bruker); **(B)** Table of m/z values for the different modifications monitored in the charge state +14.

By this methodology it was not possible however to quantify the relative amount of the S-Sulfo form in V30M TTR, since its whole peak is overlapped with part of the S-Cys peak in wt TTR. For comparison purposes, the relative amounts of PTMs determined by this methodology were calculated without taking into account S-Sulfo forms (neither wt, nor V30M).

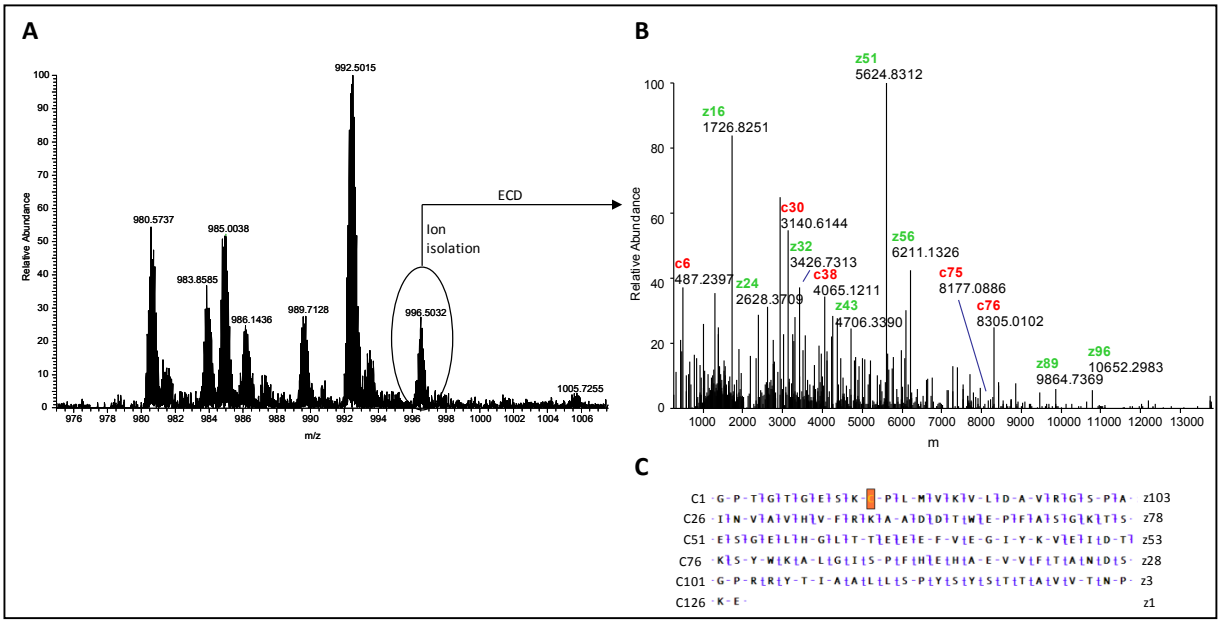

Figure C2-7. Mapping PTM sites in TTR by top-down MS. S-CysGly proteoform characterization. **(A)** Enlarged FT-ICR spectrum of TTR, z=+14; **(B)** Ion deconvoluted ECD spectrum of isolated ion m/z 996.50; **(C)** ECD fragmentation map showing S-CysGly PTM at Cys-10, explained by fragments from C3 to C88 (total of 49 fragments).

C2.3.3.2 Intra- and inter-assay precision for the intact protein strategy

To determine the intra-assay precision we performed four different immunoprecipitations from a pool of human serum, and analyzed them according to the protocol described in Materials and Methods C2.2.4. A second pool was immunoprecipitated and analyzed in 4 different days to assess inter-assay precision. The results are shown in Table C2-3 and Table C2-4. The procedure showed to be highly robust, giving an intra-assay coefficient of variation <8% for the total intensities measured, and <6% for the calculated % of the different PTMs measured. Results of the assay of a sample on different days, after cycles of freezing and thawing, showed a higher variation (<20%) for the total intensities, but still a coefficient of variation ≤4% for the percent of PTMs. The ratio of total wt:V30M TTR was calculated as the ratio of the signals resulting from totalling the peaks corresponding to the modified forms for wt and V30M TTR, respectively. Determination of the ratio total wt:V30M TTR gave also coefficients of variation <0.5% for both intra- and inter-assay.

Table C2-3. Determination of the intra- and inter-assay precision for the total intensity and the % of PTMs in wt and V30M TTR by Intact Protein

	Intra-assay								Inter-assay							
	in wt TTR				in V30M TTR				in wt TTR				in V30M TTR			
	TI		% PTM		TI		% PTM		TI		% PTM		TI		% PTM	
	CV (%)	Mean	STDV	CV(%)	CV (%)	Mean	STDV	CV(%)	CV (%)	Mean	STDV	CV(%)	CV (%)	Mean	STDV	CV(%)
Free Cys	5.59	15.73	0.425	2.70	4.97	22.64	0.599	2.65	17.69	13.63	0.122	0.90	18.48	19.15	0.119	0.62
S-Cys	2.06	55.17	0.911	1.65	1.50	54.90	1.182	2.15	19.00	57.89	0.686	1.19	18.79	54.89	0.477	0.87
S-CysGly	4.29	20.21	0.475	2.35	4.30	13.85	0.250	1.80	16.96	19.83	0.297	1.50	16.84	17.49	0.275	1.57
S-GSH	7.08	8.89	0.415	4.67	6.69	8.60	0.412	4.79	14.92	8.65	0.339	3.92	15.00	8.47	0.296	3.49

Table C2-4. Determination of the intra- and inter- assay precision for the % V30M determination by Intact Protein

	% V30M TTR	
	Intra-assay	**Inter-assay**
STDV	0.053	0.037
Mean (% V30M)	46.70	48.25
CV (%)	0.11	0.08

C2.3.4 Comparison between targeted LC-MS and Intact Protein strategies

In order to compare the results obtained by the two different analytical strategies, a group of 10 human serum samples, five carrying only wt TTR and five carrying both wt and V30M TTR, were analyzed by the two methodologies. The results obtained by the targeted LC-MS strategy for the absolute quantity of TTR are shown in Table C2-5. For V30M samples, in the case of the intact protein strategy, it was also possible to calculate the ratio wt:V30M, by comparing the global intensity for each TTR form (Table C2-5, right).

Table C2-5. Absolute quantification of TTR by HR-XIC and relative abundances of wt and V30M TTR by Intact Protein

	HR-XIC					Intact Protein	
Sample[a]	ng TTR/µL plasma						
	wt TTR	**V30M TTR**	**Total TTR**	**% wt**	**% V30M**	**% wt**	**% V30M**
Sample 1	52.41	0.08	52.49	100	-	100	-
Sample 2	62.14	0.18	62.31	100	-	100	-
Sample 3	118.79	0.16	118.95	100	-	100	-
Sample 4	51.43	0.38	51.81	100	-	100	-
Sample 5	24.42	0.06	24.47	100	-	100	-
Sample 6	51.24	84.54	135.78	37.74	62.26	51.69	48.31
Sample 7	42.73	65.71	108.44	39.4	60.6	52.76	47.24
Sample 8	25.7	52.99	78.69	32.66	67.34	52.58	47.42
Sample 9	28.09	50.44	78.48	35.73	64.27	50.71	49.29
Sample 10	38.08	68.95	107.03	35.58	64.42	56.53	43.47

[a] Samples 1-5 correspond to wt individual human samples and samples 6-10 to V30M individual human samples

Fig. C2-8A shows the comparison of the distribution pattern of the different Cys-10 forms, as determined by the two methods (Annex, Table A-18 and A-19). For this comparison, S-Sulfo form was not considered since as it has been already mentioned, it cannot be properly quantified by the intact protein procedure. As it is clear from the figure, the observed pattern was quite different between both methodologies. By intact protein measurements, Free Cys, S-CysGly and S-GSH fractions appear more abundant than they really are, according to the levels obtained from the absolute quantification. Conversely, the observed proportion for the S-Cys form appears to be much lower by intact protein measurement.

We also compared the % of total V30M and wt TTR in the serum samples, calculated by both strategies (Fig. C2-8B). We observed that both variants appear to be at approximately the same concentration, when looking at the intact protein level. However, absolute quantification shows that wt TTR was less abundant than V30M TTR, with a ratio around 40:60.

Comparison of the results from both techniques demonstrates that indeed, the response factor of the different TTR variants, when analyzed as intact protein, is not the same. Although relative quantification can be a good tool to compare protein forms among different samples, it is not suitable to establish which of those forms are really more abundant in a sample. The results shown here demonstrate the need for absolute quantification using labeled peptide standards to measure the absolute amounts of the different forms and thus have a real evaluation of their distribution in serum. The differences observed between the intact protein analysis and the LC-MS method would result from different response factors of the different proteoforms, which would be a consequence of their different ionization capability upon electrospray ionization. In the LC-MS method, the response of the measurement of each form is corrected by the corresponding internal standard, and therefore the proportions of the different forms measured should be closer to the real composition of the sample.

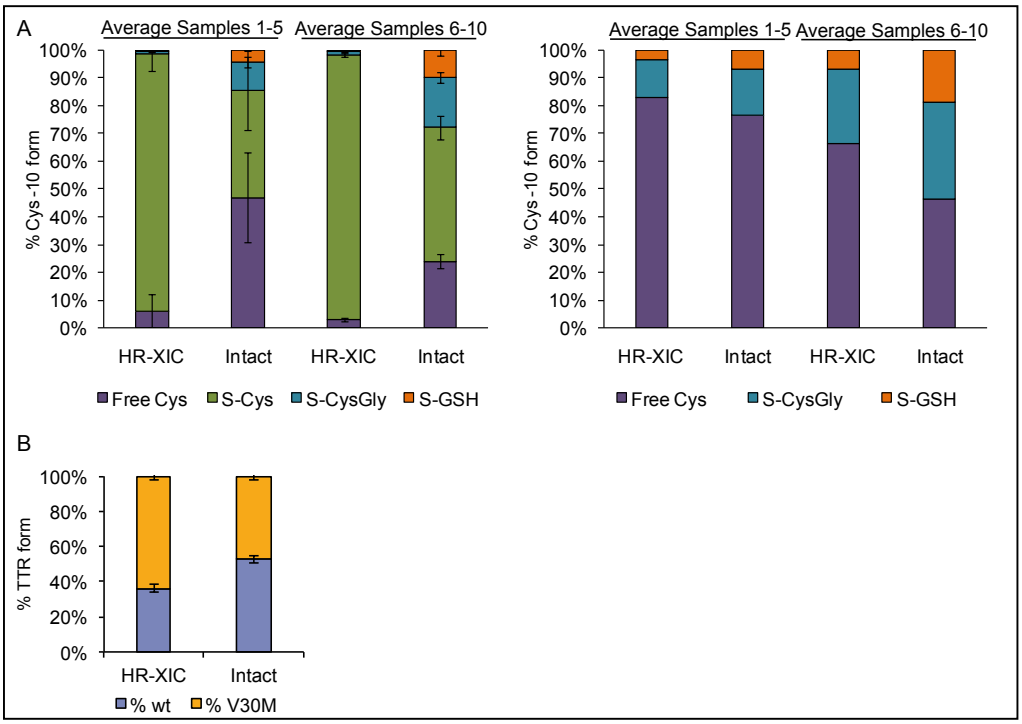

Figure C2-8. HR-XIC and Intact Protein measurements comparison. (A) On the left, distribution of Cys-10 modified TTR forms by both methodologies, error bars show standard deviation between the average of two groups of samples, 1-5 wt TTR, 6-10 V30M TTR; on the right, distribution of Cys-10 modified forms excluding S-Cys. **(B)** Percent proportion of total wt and V30M TTR measured by both methodologies for samples 6-10.

However, it should also be noted that the intact protein analysis method affords information on the relative amounts of the Cys-10 PTM forms of wt and V30M TTR proteins separately, whereas in the targeted LC-MS method the N-term peptides used for PTM quantification measure the total amounts of those PTM forms. On the other hand, as seen in Fig. C2-8, due to the greater response factor for some of the minor PTM forms (S-CysGly, S-GSH), the intact protein method presents a somehow higher sensitivity for their relative quantification.

The most common technique to determine the total amount of TTR in serum samples is the ELISA method. In an attempt to compare the results here obtained for absolute quantification by the targeted LC-MS method, a set of 21 serum samples was analyzed in parallel by both methods (Fig. C2-9). We observed a reasonable correlation between both techniques up to 50 ng TTR/µL serum,

but the ELISA (TTR Human ELISA Kit, KA0495, Abnova) response was saturated at higher concentrations even though the measured absorbances were in the linear range of the standard curve. We also verified, by analyzing solutions of identical concentration of recombinant wt and V30M TTR, spiked into a solution of 75 mg/mL BSA, that the response of the ELISA was identical for both TTR forms. However, the concentration values obtained were significantly higher than the expected from the measured absorbance at 280 nm of the starting solutions. Therefore, it may be suggested that some interference caused by serum components is affecting the ELISA method here tested. On the other hand, the total TTR concentration values measured by our LC-MS method seem to be significantly lower than the established normal range (150-360 ng/µL) (Ritchie et al. 1999). This discrepancy could potentially reflect the presence of modified TTR forms not prone to trypsin digestion, such as glycation or carbonylation derivatives. Troubleshooting of the ELISA procedure assayed, or checking alternative ELISA assays available to clarify these discrepancies is beyond the purpose of this work. Our results show that the LC-MS method developed can be at least as sensitive and robust as the usual immunological methods used, and give a further insight into the detailed composition of different TTR Cys-10 modified forms.

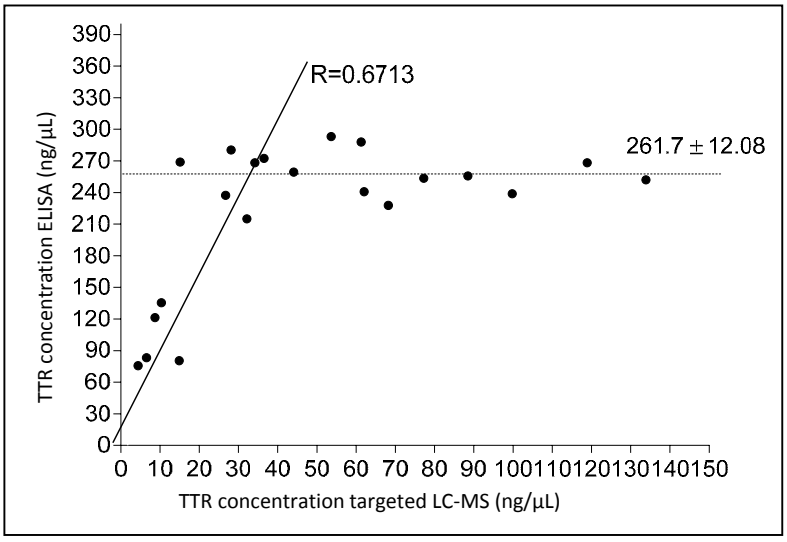

Figure C2-9. TTR concentration determination. Comparison between the targeted LC-MS and ELISA methods

C2.4 CONCLUSION

Two complementary MS based methods for the quantification of the most common Cys-10 PTM isoforms of TTR in plasma or serum have been set up. The targeted LC-MS method developed here, unlike previously described methods, allows the absolute quantification of the levels of each of the Cys-10 modifications, as well as the absolute concentrations of wt TTR and the amyloidotic V30M isoform. Intact protein analysis, on the other hand, provides additional valuable information of the relative distribution of the Cys-10 PTMs for wt and V30M proteins. It is shown that the intact protein ions of the different isoforms display large differences in response factors, which makes the targeted LC-MS analysis, using standard peptides, mandatory for absolute quantification of their levels in serum. Overall, the combined analysis by the two developed strategies constitutes a robust method for the characterization of the PTM forms of TTR in serum, which, when applied to the appropriate clinical samples, can shed light into the relevance of these isoforms on TTR amyloidosis.

C2.5 REFERENCES

Altland K, Winter P, Sauerborn MK. Electrically neutral microheterogeneity of human plasma transthyretin (prealbumin) detected by isoelectric focusing in urea gradients. Electrophoresis 1999;20(7):1349-64.

Altland K, Winter P. Potential treatment of transthyretin-type amyloidoses by sulfite. Neurogenetics 1999;2(3):183-8.

Ando Y, Ohlsson PI, Suhr O, Nyhlin N, Yamashita T, Holmgren G, Danielsson A, Sandgren O, Uchino M, Ando M. A new simple and rapid screening method for variant transthyretin-related amyloidosis. Biochem Biophys Res Commun 1996;228(2):480-3.

Ando Y, Suhr O, Yamashita T, Ohlsson PI, Holmgreen G, Obayashi K, Terazaki H, Mambule C, Uchino M, Ando M. Detection of different forms of variant transthyretin (Met30) in cerebrospinal fluid. Neurosci Lett 1997;238(3):123-6.

Arsequell G, Planas A. Methods to evaluate the inhibition of TTR fibrillogenesis induced by small ligands, Curr Med Chem 2012;19(15):2343-55.

Bergquist J, Andersen O, Westman A. Rapid method to characterize mutations in transthyretin in cerebrospinal fluid from familial mayloidotic polyneuropathy patients by use of matrix-assisted laser desorption/ionization time-of-flight mass spectrometry. Clin Chem 2000;46(9):1293-300.

Buxbaum J, Anan I, Suhr O. Serum transthyretin levels in Swedish TTR V30M carriers. Amyloid 2010;17(2):83-5.

Cardoso I, Goldsbury CS, Muller SA, Olivieri V, Wirtz S, Damas AM, Aebi U, Saraiva MJ. Transthyretin fibrillogenesis entails the assembly of monomers: a molecular model for *in vitro* assembled tranthyretin amyloid-like fibrils. J Biol Chem 2002;317(5):683-95.

Colon W, Kelly JW. Partial denaturation of transthyretin is sufficient for amyloid fibril formation in vitro. Biochemistry 1992, 31(36):8654-60.
Connors LH, Lim A, Prokaeva T, Roskens VA, Costello CE. Tabulation of human transthyretin (TTR) variants, 2003. Amyloid 2003;10(3):160-84.

da Costa G, Gomes R, Correia CF, Freire A, Monteiro E, Martins A, Barroso E, Coelho AV, Outeiro TF, Ponces Freire A, Cordeiro C. Identification and quantitative analysis of human transthyretin variants in human serum by Fourier transform ion-cycloton resonance mass spectrometry. Amyloid 2009;16(4):201-7.

Dolado I, Nieto J, Saraiva MJ, Arsequell G, Valencia G, Planas A. Kinetic assay for high-throughput screening of in vitro transthyretin amyloid fibrillogenesis inhibitors. J Comb Chem 2005;7(2):246-52.

Hammarström P, Jiang X, Hurshman AR, Powers ET, Kelly JW. Sequence-dependent denaturation energetics: A major determinant in amyloid disease diversity. Proc Natl Acad Sci USA 2002;99Suppl 4:16427-32.

Hurshman AR, White JT, Powers ET, Kelly JW. Transthyretin aggregation under partially denaturating conditions is a downhill polymerization. Biochemistry 2004;43(23):7365-81.

Jiang X, Smith CS, Petrassi HM, Hammarström P, White JT, Sacchettini JC, Kelly JW. An engineered transthyretin monomer that is nonamyloidogenic, unless it is partially denatured. Biochemistry 2001;40(38):11442-52.

Kingsbury JS, Klimtchuk ES, Théberge R, Costello CE, Connors LH. Expression, purification, and in vitro cysteine-10 modification of native sequence recombinant human transthyretin. Protein Expr Purif 2007;53(2):370-7.

Kishikawa M, Nakanishi T, Miyazaki A, Shimizu A, Nakazato M, Kangawa K, Matsuo H. Simple detection of abnormal serum transthyretin from patients with familial amyloidotic polyneuropathy by high-performance liquid chromatography/electrospray ionization mass spectrometry using material precipitated with specific antiserum. J Mass Spectrom 1996;31(1):112-4.

Kishikawa M, Nakanishi T, Miyazaki A, Shimizu A. Enhanced amyloidogenicity of sulfonated transthyretin in vitro, a hypothetical etiology of senile amyloidosis. Amyloid 1999;6(3):183-6.

Lim A, Prokaeva T, McComb ME, Connors LH, Skinner M, Costello CE. Identification of S-sulfonation and S-thiolation of a novel transthyretin Phe33Cys variant from a patient diagnosed with familial transthyretin amyloidosis. Protein Sci 2003;12(8):1775-85.

Nakanishi T, Yoshioka M, Moriuchi K, Yamamoto D, Tsuji M, Takubo T. S-sulfonation of transthyretin is an important trigger step in the formation of transthyretin-related amyloid fibril. Biochim Biophys Acta 2010;1804(7):1449-56.

Poulsen K, Bahl JM, Tanassi JT, Simonsen AH, Heegaard NH. Characterization and stability of transthyretin isoforms in cerebrospinal fluid examined by immunoprecipitation and high-resolution mass spectrometry of intact protein. Methods 2012;56(2):284-92.

Quintas A, Saraiva M.J, Brito RM. The tetrameric protein transthyretin dissociates to a non-native monomer in solution. A novel model for amyloidogenesis. J Biol Chem1992;274(46):32943-9.

Quintas A, Vaz DC, Cardoso I, Saraiva MJ, Brito RM. Tetramer dissociation and Monomer partial unfolding precedes protofibril formation in amyloidogenic trasnthyertin variants. J Biol Chem 2001;276(29):27207-13.

Raz A, Goodman DS. The interaction of thyroxine with human plasma prealbumin and with the prealbumin-retinol binding protein complex. J Biol Chem 1969;244(12)3230-7.

Raz A, Shiratori T, Goodman DS. Studies on the protein-protein and protein-ligand interactions involved in retinol transport in plasma. J Biol Chem 1970;245(8):1903-12.

Ribeiro-Silva C, Gilberto S, Gomes RA, Mateus É, Monteiro E, Barroso E, Coelho AV, da Costa G, Freire AP, Cordeiro C. The relative amounts of plasma transthyretin forms in familial transthyretin amyloidosis: a quantitative analysis by Fourier transform ion-cyclotron resonance mass spectrometry. Amyloid 2011;18(4):191-9.

Ritchie RF, Palomaki GE, Neveux LM, Navolotskaia O, Ledue TB, Craig WY. Reference distributions for the negative acute-phase serum proteins, albumin, transferring and transthyretin: a practical, simple and clinically relevant approach in a large cohort. J Clin Lab Anal 1999;13(6)273-9.

Saraiva MJ, Costa PP, Goodman DS.Studies on plasma transthyretin (prealbumin) in familial amyloidotic polyneuropathy, Portuguese type. J Lab Clin Med 1983;102(4):590-603.

Saraiva MJ. Hereditary transthyretin amyloidosis: molecular basis and therapeutical strategies. Expert Rev Mol Med 2002;4(12):1-11.

Schreiber G, Aldred AR, Jaworowski A, Nilsson C, Achen MG, Segal MB. Thyroxine transport from blood to brain via transthyretin synthesis in choroid plexus. Am J Physiol 1990;258(2 Pt 2):R338-45.

Soprano DR, Herbert J, Soprano KJ, Schon EA, Goodman DS. Demonstration of transthyretin mRNA in the brain and other extrahepatic tissues in the rat. J Biol Chem 1985;260(21):11793-8.

Sörgjerd K, Klingstedt T, Lindgren M, Kågedal K, Hammarström P. Prefibrillar transthyretin oligomers and cold stored native tetrameric transthyretin are cytotoxic in cell culture. Biochem Biophys Res Commun 2008;377(4):1072-8.

Sousa MM, Cardoso I, Fernandes R, Guimarães A, Saraiva MJ. Deposition of transthyretin in early stages of familial amyloidotic polyneuropathy: evidence for toxicity of non-fibrillar aggregates. Am J Pathol 2001;159(6):1993-2000.

Suhr OB, Svendsen IH, Ohlsson PI, Lendoire J, Trigo P, Tashima K, Ranløv PJ, Ando Y. Impact of age and amyloidosis on thiol conjugation of transthyretin in hereditary transthyretin amyloidosis. Amyloid 1999;6(3):187-91.

Terazaki H, Ando Y, Suhr O, Ohlsson PI, Obayashi K, Yamashita T, Yoshimatsu S, Suga M, Uchino M, Ando M. Post-translational modification of transthyretin in plasma. Biochem Biophys Res Commun 1998;249(1):26-30.

Trenchevska O, Kamcheva E, Nedelkov D. Mass spectrometric immunoassay for quantitative determination of transthyretin and its variants. Proteomics 2011;11(18):3633-41.

Westermark P, Sletten K, Johansson B, Cornwell GG 3rd. Fibril in senile systemic amyloidosis is derived from normal transthyretin. Proc Natl Acad Sci USA 1990;87(7):2843-5.

Zhang Q, Kelly JW. Cys10 mixed disulfides make transthyretin more amyloidogenic under mildly acidic conditions. Biochemistry 2003;42(29):8756-61.

CHAPTER 3. Familial Amyloid Polyneuropathy: proteomic analysis of transthyretin Cys-10 modifications, searching for biomarkers of disease progression

C3.1 INTRODUCTION

Familial amyloid polyneuropathy (FAP) related to transthyretin (TTR) is an autosomal dominant neurodegenerative and systemic disorder that affects around ~5000-10000 patients worldwide (Planté-Bordeneuve 2014). However, specific endemic areas, where families affected by the disease are found at higher frequency, are Portugal, Japan, Sweden and the Mallorca Island (Andersson 1976, Andrade 1952, Coutinho et al. 1980, Munar-Ques et al. 1988). This progressive neurodegenerative condition is related to mutations in the gene encoding for TTR, with more than 100 amyloidogenic mutations identified worldwide, the V30M TTR being the most common FAP mutation. V30M TTR is virtually the only one found in Portuguese and Swedish populations and has been detected worldwide in nearly 50 % of the FAP cases identified (Planté-Bordeneuve 2014). The age of onset and clinical manifestations of FAP vary across different populations finding an early onset rapidly progressive polyneuropathy in Portugal and Japan (mean age 33 years) whereas an isolated progressive polyneuropathy, apparently sporadic in elder patients, is described in other regions such as Sweden (mean age 56 years) (Planté-Bordeneuve 2014).

TTR is a homotetrameric protein that functions as the backup transporter for thyroxine hormone (T4) in plasma and it is its main transporter across the blood brain barrier. TTR is also the main carrier of retinol by forming a 1:1 complex with the retinol-binding protein (RBP) (Raz and Goodman 1969, Raz et al. 1970). It is synthesised in the liver and the choroid plexus of the brain (Soprano et al. 1985), the liver being the main responsible for plasmatic TTR production. Whereas TTR transports nearly all the circulating RBP in serum and it is the main thyroxin transporter in cerebrospinal fluid (CSF), it only transports around the 15% of the serum circulating thyroxin. TTR occurs as a highly heterogeneous protein not only due to point mutations in the encoding gene but also to post-translational modifications (PTMs) at the Cys-10 residue (Altland et al. 1999, Terazaki et al. 1998). Around 85-90% of the circulating TTR in plasma presents mixed disulfide modifications at Cys-10, the S-sulfonation (S-Sulfo), S-glycinylcysteinylation (S-CysGly), S-cysteinylation (S-Cys) and S-glutathionylation (S-GSH) being the most common proteoforms (Poulsen et al. 2012). Several works suggest that Cys-10 PTMs in TTR may play an important biological role in the onset and pathological process of the TTR-related amyloidosis, although its clinical implications are still badly understood (Altland and Winter 1999, Jiang et al. 2001, Kingsbury et al. 2007, Kishikawa et al. 1999, Nakanishi et al. 2010, Sekijima et al. 2003, Zhang and Kelly 2003, 2005).

FAP symptoms start with numbness and/or spontaneous pains in the feet. Early examination can already detect impaired thermal sensibility over the feet, with decreased pinprick sensation. On the contrary, light touch, proprioception, muscle strength and tendon reflexes are normal (Andrade 1952, Planté-Bordeneuve 2014). This early neurological affection is an indicator of the involvement of unmyelinated and small myelinated fibres. However, at this stage, clinical examination may not be totally realistic, especially in anxious patients aware of the devastating effect of the disease (Planté-

Bordeneuve 2014). At onset, manifestations might be at a focal level due to the random distribution of amyloid in the peripheral nervous system (PNS), where deposits may accumulate locally and induce a focal deficit of a cranial nerve, a nerve trunk or a plexus. A typical and early but nonspecific manifestation of FAP is carpal tunnel syndrome; otherwise, focal lesions are rare in FAP. A prominent life-threatening manifestation of FAP is autonomic neuropathy, which can start at early stages and becomes constant in the course of the disease, especially in early onset cases of FAP. The systems involved in FAP are the cardio-circulatory, the gastrointestinal and the genitourinary, leading to orthostatic hypotension, fatigue, blurred vision or dizziness when standing up, or postural syncope. Other common manifestations are episodic post-prandial diarrhoea, severe constipation or both. As a consequence of gastroparesis and postprandial vomiting, patients present dehydration, increased postural hypotension and progressive weight loss. Finally, in men, another early frequent manifestation that may precede the sensory symptoms of the neuropathy is erectile dysfunction. Regarding the central nervous system (CNS), dementia, stroke and subarachnoid hemorrhage are rare in TTR amyloidosis, in spite of the common finding of leptomeningeal amyloid deposition upon autopsy (TTR mutations affecting CNS have been reported but remain rare). However, 80 % of FAP cases present cardiac involvement and in 10 % of the cases ocular abnormalities take place. Finally, loss of more than 10 % of body weight can be an early sign of the disease, together with cachexia, that becomes inescapable after a few years. With disease progression, patients become also bedridden, develop bedsores, venous thrombosis and pulmonary embolism (Planté-Bordeneuve 2014).

An early detection of clinical manifestations is crucial since the disease modifying treatments currently available must be considered at this stage, before further irreversible neurodegeneration is observed. For this reason, it is important to detect evidences of small fibre involvement in patients with early symptoms and questionable sensory loss through several tests such as neurophysiological tests and skin biopsy with quantitative evaluation of nerve endings. In a matter of months after disease onset, sensory loss extends up to involve the proximal lower limbs. Motor deficits appear in the distal lower limb along with impairment of light touch and deep sensations, in line with involvement of the larger sensory and motor nerve fibres. Walking becomes increasingly difficult with loss of balance and a high stepping gait. Neuropathic pains, usually of a burning type, worse at night and associated with allodynia are common. The sensory deficit then affects the upper limbs, the fingers, forearm gradually, as the anterior trunk is involved. Motor deficits also follow a length dependent progression and walking without aids becomes eventually impossible. A frequent scale used for clinical staging of FAP patients, their follow-up and consideration of therapeutic decisions is the one described by Coutinho (Coutinho et al. 1980), already explained in Introduction I.2. Briefly, it consists of 3 different stages depending on the motor deficits associated with FAP (Planté-Bordeneuve 2014):

- Stage 1: unimpaired ambulation; mild sensory, motor, and autonomic neuropathy in the lower limbs.
- Stage 2: assistance with ambulation required; mostly moderate impairment and progression involving the lower limbs, upper limbs, and trunk.
- Stage 3: wheelchair-bound or bedridden; severe sensory, motor, and autonomic involvement of all four limbs.

Cys-10 PTMs in TTR may play a role in FAP pathogenesis since they could act as a defence against oxidative stress by buffering the redox balance. The presence of oxidative stress has been demonstrated already at early stages of the disease, when no amyloid deposition occurs but soluble aggregates are present (Ando et al. 1997, Sousa et al. 2000, 2001). However, the biological implications of Cys-10 PTMs are still badly understood. Nevertheless, studies about oxidative stress and neurodegenerative diseases reinforce the idea of thiol conjugation as a protective mechanism linked in some cases to disease progression (Mieyal et al. 2008, Sabens Liedhegner et al. 2012).

In the present work we aimed to study whether Cys-10 PTM levels may act as biomarkers of FAP progression. To this purpose we have analyzed samples of FAP patients rigorously classified according to the 3 disease stages, together with asymptomatic V30M carriers and control individuals. We have studied a total of 68 human samples (39 controls, 16 asymptomatic V30M carriers and 13 symptomatic V30M carriers) using our previously developed targeted liquid chromatography-mass spectrometry methodology (targeted LC-MS) (see Chapter 2) and an intact protein MS approach (Poulsen et al. 2012) to measure absolute and relative TTR Cys-10 PTM levels. In addition, we have measured TTR levels and %V30M in the different groups. Finally, we have determined the frequency of the G6S TTR polymorphism in the studied cohort and measured TTR levels in a FAP patient under treatment with siRNA therapy.

C3.2 MATERIALS AND METHODS

C3.2.1 Participants

A total of 68 individuals were included in the study (Table C3-1), corresponding to 16 asymptomatic patients (stage 0 FAP V30M individuals) and 13 symptomatic FAP V30M individuals (5 stage 1, 6 stage 2 and 2 stage 3). In addition, 39 healthy individuals were included in the study as control group (initially, 50 individuals were screened but 11 were discarded since they presented the G6S polymorphism). Both women and men were included with ages ranging from 24 to 82 years old. All individuals gave informed written consent and the study was approved according to the rules of the Ethical Committee of the Hospital Clínic de Barcelona, Barcelona, Spain.

Table C3-1. Summary of data for samples included in the study

	FAP stage	TTR	n (male/female)	Age (years)*
Controls	-	wt	39 (15/24)	42 ± 12
Asymptomatic	0	wt/V30M	16 (8/8)	48 ± 10
	1	wt/V30M	5 (4/1)	61 ± 12
Symptomatic	2	wt/V30M	6 (6/0)	69 ± 7
	3	wt/V30M	2 (2/0)	68 ± 4

* Mean ± SD. Significant differences (Mann-Whitney U test) in age between controls and FAP individuals (all stages) and between asymptomatic and symptomatic.

C3.2.2 Blood and sample handling

Human blood samples were collected and allowed to clot for 30 minutes at room temperature and subsequently centrifuged at 1300 x g for 15 minutes (BD Vacutainer® SST™ Tubes). Serum specimen was extracted from the tube avoiding the fraction closer to the separating gel. Aliquots of 250 µL were then prepared and immediately frozen at -80 °C until analyzed. For TTR immunoprecipitation all samples were unfrozen at the same time and treated identically. For MS analysis, in order to minimize handling artifacts, samples were treated uniformly and as short a handling time and as few thaw-freeze cycles as practically possible were performed.

C3.2.3 Targeted LC-MS analysis by high resolution-extracted ion chromatograms (HR-XIC)

This strategy corresponds to the targeted mass spectrometry method developed in Chapter 2, which enables the absolute quantification of Cys-10 PTMs, wt:V30M ratio and total TTR levels.

C3.2.3.1 Immunoprecipitation with hydrazide-immobilized antibody (IP Ab-ULH)

Polyclonal rabbit anti-human TTR antibody (Dako) was coupled to UltraLink® Hydrazide Resin (Thermo Scientific) following the resin manufacturer's protocol. 225 µg of immobilized antibody (Ab-ULH) were incubated with 25 µL of human serum for 1 hour and 40 minutes at room temperature with soft agitation. After TTR binding to the Ab-ULH, 5 washes with 500 µL PBS were performed. TTR was eluted with 100 mM triethylamine (TEA, Fluka) pH=11.5 solution. Elution was performed in 3 steps by addition of 400 µL TEA followed by 2 minutes of sonication on an ultrasonic bath, and the total eluted volume was concentrated to 50 µL after 8 M urea-50 mM AB buffer exchange, by diafiltration in an Amicon® Ultra-0.5 mL centrifugal Filter, Ultracel®-3K cut off membrane (Millipore).

C3.2.3.2 Enzymatic digestion of transthyretin

After immunoprecipitation, determination of the total protein amount for each sample was performed using Bio-Rad DC ™ Protein Assay Kit (Bio-Rad). Based on the amount of protein quantified, a fraction of the immunoprecipitated TTR (10 μg) was digested with Arginine-C (Endoproteinase Arg-C Sequencing Grade, Roche) during 6 hours, 37°C at a 1:23 ratio enzyme:protein. Another fraction (10 μg) of the immunoprecipitated protein was digested with trypsin (Trypsin Gold Mass Spectrometry Grade, Promega) ON, 37°C at a 1:10 ratio enzyme:protein.

C3.2.3.3 Standard labeled peptides

Labeled (5C13,N15 proline) peptides for the quantification of the 5 Cys-10 forms (>98% purity and quantified by AAA) were purchased from Peptide Synthetics (United Kingdom). The different peptides for the quantification of Cys-10 modifications will be referred as N-term heavy peptides (see Chapter 2, Table C2-1 P1-P5). Labeled (6C13,4N15 arginine) peptides for the total TTR determination (99% purity and quantified by AAA) were purchased from AQUA Peptide Sigma-Aldrich. The two different peptides used for the total amount of protein determination (see Chapter 2, Table C2-1 P6-P7) will be referred as GSPAIN peptides (wt and V30M, for the wt TTR form and the mutant V30M TTR form, respectively). For the quantification of the V30M GSPAIN peptide in its Met oxidized variant we used the calculated (see Chapter 2) ratio of response factors: 11.11 (oxidized:non oxidized V30M).

C3.2.3.4 LC-MS Measurement with UHR-QTOF

TTR from human samples was purified and digested with Arg-C and trypsin as described above. Standard labeled N-term peptides (see Chapter 2, Table C2-1 P1-P5) were spiked into Arg-C digested samples after digestion and prior to LC-MS measurement. The same procedure was followed for the standard labeled GSPAIN peptides (see Chapter 2, Table C2-1 P6-P7) and the trypsin digested samples. The amount of heavy peptides in column was of 50 fmols for each GSPAIN peptide and of 50, 12.5, 7.5, 200 and 200 fmols for the Free Cys, S-CysGly, S-GSH, S-Cys and S-Sulfo N-term peptides, respectively. The samples were analyzed on a UHR-QTOF mass spectrometer (Bruker Impact), coupled to a Proxeon Easy nano-LC (Bruker). Samples of the TTR digests (50 ng) spiked with the standard peptides were first loaded into a 100 μm ID, 2 cm Proxeon nanotrapping column and then separated with a 10 minutes 0.1% formic acid – ACN gradient (5-35% in 10 min; flow rate 300 nL/min) on a Acclaim PepMap 75 μmx25 cm, 3 mm particle size reverse phase nanoseparation column (Dionex) coupled to the mass spectrometer inlet through a Captive Spray (Bruker) ionization source. For quantification, acquisition was set to MS spectra only at a frequency of 0.5 Hz. Spectra were acquired on the range 150-2200 Da.

C3.2.3.5 Data analysis

LC-MS data was first processed using Data Analysis 4.1 (Bruker) and then quantified using Skyline Software (MacCoss Lab) to filter and integrate precursor signals of target peptides. Using a HR-XIC Skyline template, extracted ion chromatograms for the m/z corresponding to the main isotope and charge state signal for each target peptide were used for quantification.

C3.2.4 Intact protein analysis

This strategy corresponds to the method also used in Chapter 2, based on (Poulsen et al. 2012). It allows for the relative quantification of the different Cys-10 isoforms and wt:V30M ratio.

C3.2.4.1 Immunoprecipitation with unconjugated antibody

For TTR immunoprecipitation, 225 μg of the polyclonal rabbit anti-human TTR antibody (Dako) were incubated with 25 μL of human serum over night at 4 °C. After incubation, centrifugation at 9000 x g, 10 minutes and 4 °C allowed the precipitation of the TTR-Ab complex. The pellet obtained was washed 3 times with 0.1 M AB buffer and finally resuspended in 50% methanol - 1% formic acid (Poulsen et al. 2012) at approximately 4 pmol TTR/μL, according to the reported TTR concentrations in serum.

C3.2.4.2 Intact Protein measurement with UHR-QTOF

TTR immunoprecipitated as described below was analyzed on an UHR-QTOF mass spectrometer (Bruker Impact). Sample was directly infused with a syringe pump at 3 μL/min into an ESI source (Bruker). The MS acquisition method was set up to acquire only MS data during 5 minutes, with MS cycles of 0.5 Hz in the mass range from 50 m/z to 1500 m/z. MS data was analyzed using Data Analysis 4.1 software (Bruker). Lock mass calibration using Data Analysis 4.1 (Bruker) was performed prior to averaging the spectra. Quantitation measurements were done in charge envelope +14 signals, taking into account the intensity of the 5 most intense isotope peaks for each modification. Peak inspection was performed manually and the sum of these 5 isotopes was considered as the total intensity for a given modification. From the total intensity of each form, the percent of each modification with respect to the sum of all forms was calculated, for both wt and V30M TTR.

C3.2.4.3 Statistical analysis

For the statistical analysis of data, GraphPad Prism Software was used and for the comparison of the different groups, unpaired t-test with Welch's correction was applied.

C3.3 RESULTS AND DISCUSSION

C3.3.1 Determination of TTR levels and wt:V30M ratio

The 68 samples studied were analyzed by our previously developed HR-XIC strategy and by an intact protein methodology. The complementary use of both methods allows the absolute and relative quantification of TTR concentration and wt:V30M ratio. Thanks to this double approach, an additional comparison between absolute and relative determination of wt:V30M ratio is enabled. In general, absolute quantification gives the real amount of the different parameters measured, taking into account possible differences in response factor. Relative quantification, on the contrary, allows the comparison between samples without taking into account differences in response factor for the different variables measured.

As a rule of thumb, peptides containing methionine residues should be avoided in quantitative mass spectrometry approaches since they can exist in the reduced and the methionine-sulfoxide forms. However, in this particular case, it was impossible to follow this directive since the studied mutation related to FAP is V30M. Hence, the determination of wt:V30M ratio makes compulsory the use of the V30M GSPAIN peptide (Chapter 2, Table C2-1 P7). Consequently, sample handling represents a crucial step in the analysis since oxidation of methionine residues can be introduced *ex vivo* as a result of sample manipulation. For this reason, all samples were treated identically and sample handling and protocol incubations were as short as practically possible, in order to be able to compare the different groups of samples and minimize those *ex vivo* modifications. Nevertheless, the signals corresponding to the Met oxidized peptide were also measured, and their contribution taken into account using a measured ratio for the response factor for the oxidized peptide to the non-oxidized peptide as determined in Chapter 2.

For absolute determination of TTR concentration in the different samples (HR-XIC approach), TTR was immunoprecipitated from plasma and digested with trypsin prior to LC-MS analysis (see Materials and Methods C3.2.3). The labeled peptides (see Chapter 2 Table C2-1 P6-P7) used for quantification (wt and V30M GSPAIN peptides) were spiked into the peptide mixture after digestion at a final amount in column of 50 fmol of each peptide. Samples were then analyzed on an UHR-QTOF mass spectrometer and after integration of precursor signals of target peptides in Skyline Software, values of absolute concentration for each peptide were calculated and hence, total plasmatic TTR concentration and wt:V30M ratio (% of V30M TTR).

As observed in Fig. C3-1A, significant differences in total TTR concentration were found between control and asymptomatic groups ($p=0.0003$), control and stage 1 groups ($p=0.0254$), and control and stage 2 groups ($p=0.0042$). On the contrary, no significant differences were observed between the asymptomatic and the different symptomatic groups, hence, TTR concentration cannot be used as a biomarker of disease progression. Mean ± SEM value of TTR concentration for the control group was 40.61 ± 3.398 ng/μL serum; 76.13 ± 7.457 ng/μL serum for FAP stage 0 group; 66.83 ± 7.959 ng/μL serum for FAP stage 1 group; 79.91 ± 8.572 ng/μL serum for FAP stage 2 group and 66.65 ± 34.06 ng/μL for FAP stage 3 group.

In the case of % V30M TTR (Fig. C3-1B), no significant differences were found between the different FAP stages and therefore, %V30M TTR is not a suitable indicator of disease progression. Mean ± SEM values of %V30M TTR are indicated in the graph for each group.

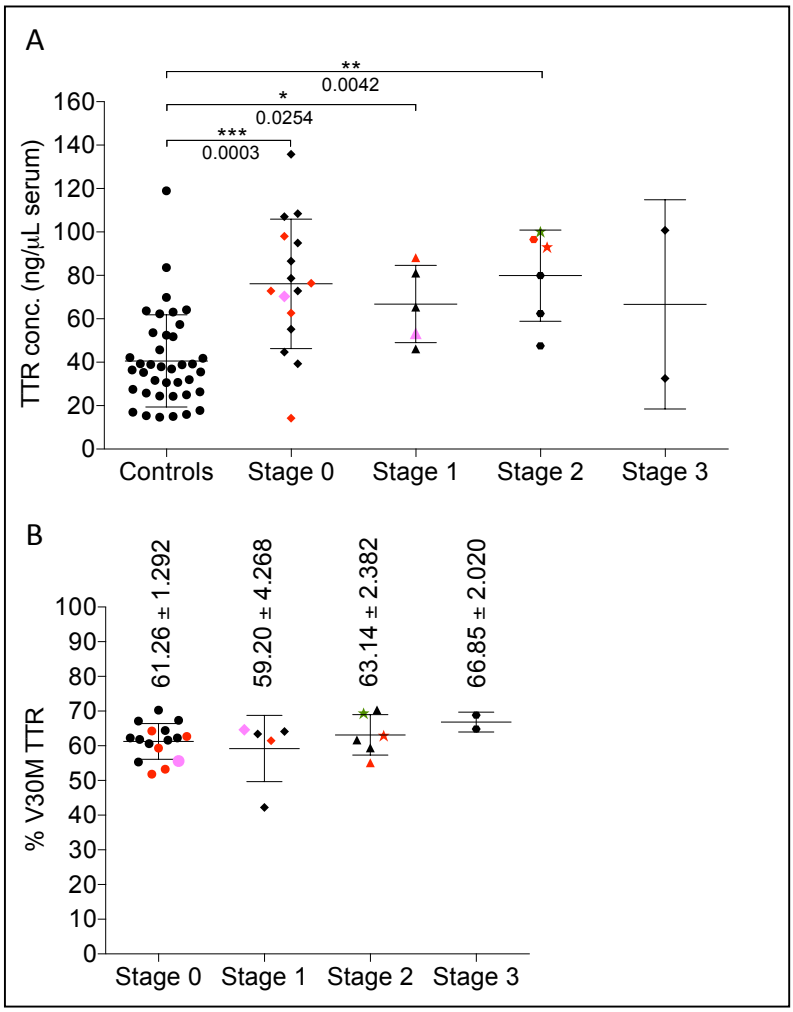

Figure C3-1. LC-MS analysis of TTR in FAP patients. (A) Determination of absolute TTR concentration by HR-XIC. The p-values obtained in the comparison between groups after application of unpaired t-test with Welch's correction are indicated where significant differences were found. **(B) Measurement of %V30M TTR levels in FAP patients by HR-XIC.** Mean ± SEM values for the different groups are indicated. In both graphs, red symbols indicate the presence of an additional mutation in TTR (G6S polymorphism); in pink, samples corresponding to same patient at different stages of the disease; the star symbol indicates samples corresponding to the same patient before (red) and after (green) 2 months of diflunisal treatment.

In general, TTR concentration values reported in the present work are lower than the ones described previously in the bibliography, even for the control group (Ritchie et al. 2000). However, the discrepancy between targeted concentration measurements by LC-MS analysis and ELISA methods is not infrequent (Kim et al 2013, Lin et al. 2013). In the particular case of TTR, even measurements based on ELISA methods that fall outside the established normal ranges, and that agree with our reported concentrations, have been published (Shao et al. 2011). There are a number of conceivable reasons that could account for the observed lower than expected values obtained by the LC-MS method. The most obvious, incomplete recovery of TTR upon immunoprecipitation and incomplete trypsin digestion, have been controlled carefully in our work. Oxidative modifications of lysine and arginine residues, such glycation and carbonylation, are known to occur in TTR and this would

directly affect the amount of protein available to trypsin digestion. On the other hand, TTR can be present in the form of soluble aggregates, which can also present different susceptibility to trypsin digestion. It is plausible that the LC-MS method described is actually measuring a subset of the TTR isoforms present in plasma. However, it is also certain that methods based on immunological detection fail also to capture the complexity of TTR forms in plasma. In addition, since plasma is a high complex body fluid, there is the possibility that other major proteins (e.g albumin) present during the antigen-antibody reaction interfere unspecifically in the assay, giving a higher background in the measure and incrementing the signal for TTR measurement. Moreover, standard curves for most of those techniques are performed with purified recombinant protein and therefore, without the characteristic plasma complexity. Since plasma TTR is highly heterogeneous, investigating what are the forms that are actually measured by different immunological or MS based methods would be of unquestionable interest, but it would exceed clearly the scope of the work here presented. The ultimate purpose of our work is applying the methods developed to the comparative analysis of samples from patients affected by TTR amyloidosis. Hence, it is not really important that the absolute values measured are accurate, but rather that the methodology is robust and reproducible, which we have shown adequately in our work (see Chapter 2).

Another fact that can be drawn from our results is that V30M carriers (asymptomatic or symptomatic) present higher total TTR levels than control individuals (Fig. C3-1). This result is contrary to previous studies reported in the bibliography (Buxbaum et al. 2008, 2010, Nakazato et al. 1984, Saraiva et al. 1985) where lower levels of TTR are associated to FAP individuals. However, in none of those studies patients are classified in detail according to Coutinho FAP stages (Coutinho et al. 1980), the main classification being presence or absence of symptoms. This fact could account for the discrepancy here reported. It is possible that, as suggested by those works, the levels of TTR decrease along disease progression; however, those differences might be just observed at an advanced stage. In our study, we could only analyze 2 samples from patients in FAP stage 3 and therefore, the results obtained for that group are not representative. Hence, since no information about the stage of the disease is given in previous works, it is not fully possible to compare our results with the previously reported. In addition, it is known that TTR levels are directly related to nutritional status (Gofferje and Fekl 1979) and therefore it would be interesting to contrast nutritional status between populations in order to obtain better comparison between groups. Unfortunately there is not enough information available on the different patients studied to allow for such a comparison. Nevertheless, when comparing our results for the asymptomatic group with the ones formerly described the discrepancy cannot be due to classification differences. In this case, we here report incremented levels of total TTR in comparison to the control group while until the moment, lower levels have been described. This quantitative difference may be explained by several reasons. Firstly, previous reports are based on Swedish, Portuguese or Japanese cohorts and our study is based on a Spanish cohort; population differences or particularities may account for the different result obtained. Secondly, several studies report the presence of soluble TTR aggregates even when no FAP symptoms are detected. In this case, methods such as ELISA, nephelometry or radial immunodifusion, techniques used in the previous studies, would fail to quantify all the TTR present in plasma since due to aggregation some of the epitopes involved in the antibody recognition may be hidden. In our case, quantification is not based on antibody recognition and therefore it is possible that we are taking into account a fraction of TTR population not considered in the immunoassays previously used. Despite the relatively limited size of the cohort studied we do not

believe that by incrementing the number of individuals studied the results here reported would be reverted: TTR concentration for the asymptomatic group almost doubles that one of the control group; however, it would be interesting to enlarge the size of this Spanish cohort in order to further confirm our results.

In the previous studies it was not established why serum TTR concentration was lower in the carriers of amyloidogenic mutations than in the control group. In the same way, we do not have any evidence to explain why TTR levels in the Spanish V30M cohort studied are higher than the control group. However, the fact that V30M TTR is less stable than the wt form, with tetramer dissociation into monomers, may be translated in lower amount of functional protein available and therefore it could trigger a feedback loop resulting in increased TTR levels. It is certain that further studies should be performed in order to gain a deeper understanding in the biological mechanisms behind the observed TTR concentration levels.

Finally, we also report a higher presence of V30M TTR than wt TTR in the Spanish FAP cohort studied, with around 60% of mutant protein in serum. On the contrary, the intact protein analysis of the same samples gave levels of V30M TTR around 50% (46.97 ± 3.63, mean ± SD). As previously discussed (see Chapter 2), the difference between techniques is probably due to a different response factor of wt and V30M protein variants. In the case of absolute quantification by LC-MS the two protein forms are quantified based on the relationship between endogenous and labeled GSPAIN peptides, both wt and V30M. Therefore, possible differences in response factor are corrected by means of the corresponding standard labeled peptide. On the contrary, in the intact protein approach, the determination of the percentage of each protein variant is calculated assuming that wt and V30M TTR respond on the same way. Previous works found in the bibliography (da Costa et al. 2009, Ribeiro-Silva et al. 2011, Tsuchiya-Suzuki et al. 2011) report a lower presence of V30M TTR (between 40-50%). Those works are in line with our intact protein strategy results, since no absolute quantification is performed. Therefore, the quantitative discrepancy observed when compared to our LC-MS approach is probably due to the already discussed different response factor for both TTR variants. Our results show the need for absolute quantification using labeled peptide standards in order to measure the absolute amounts of a given form, having a real evaluation of their distribution in serum. However, relative quantification can be still a good tool when the aim is the comparison of protein forms among different samples. Like in the case of increased TTR levels in V30M carriers we do not have any evidence to explain why V30M TTR is more abundant than the wt form and more studies should be conducted before doing any further hypothesis. However, protein aggregation and amyloid deposition in FAP patients may be favored by the fact that V30M carriers present increased TTR levels and that the more unstable V30M variant is indeed the most abundant form. Finally, the difference in TTR variant levels is probably not explained by differences in the allele specific expression since similar mRNA levels have been described for wt and V30M alleles (Norgren et al. 2012).

C3.3.2 Cys-10 mixed disulfide modifications and FAP progression

For this part of the study, those samples corresponding to individuals with the G6S polymorphism (red symbols in Fig. C3-1) were excluded from further analysis since the G6S mutation is present in the N-term peptide used for the quantification of the different Cys-10 PTMs. In the case of the control group, G6S individuals were excluded from the beginning (11 individuals out of 50). The

remaining samples (39 controls, 11 Stage 0, 4 Stage 1, 3 Stage 2 and 2 Stage 3) were analyzed by both our LC-MS strategy and by intact protein. In this case, the complementary use of both methodologies allows the absolute and relative quantification of Cys-10 PTMs in TTR.

Another common directive in targeted proteomics is the exclusion of peptides containing cysteine residues. As it happens for methionine, cysteine is a residue that can suffer oxidation and therefore *ex vivo* modifications can be introduced due to sample handling. For this reason, same considerations as in the previous section were taken into account. All samples were treated identically and sample handling and protocol incubations were as short as practically possible, in order to be able to compare the different groups of samples and minimize those *ex vivo* modifications.

There is a clinical need for an objective classification of FAP patients, especially at the very early stages, when the symptoms are not clear and patients may be suffering anxiety due to their awareness of the devastating effects of the disease. Finding a biomarker defining FAP onset would be highly useful to differentiate between asymptomatic patients and very early Stage 1 patients. It would solve the clinical difficulty to differentiate between the two stages and it would allow a rapid intervention, bringing the possibility of an early treatment either using tetramer stabilizers or considering liver transplantation before major irreversible neurodegeneration is observed. Consequently, in the present work, major interest will be focused in the comparison between Stage 0 and Stage 1 patients.

C3.3.2.1 Relative quantification of Cys-10 PTMs by intact protein

For the relative quantification of Cys-10 PTMs TTR was immunoprecipitated with unconjugated antibody and directly infused on an UHR-QTOF instrument as described (see Material and Methods C3.2.4). Intact protein analysis allows the study of the Cys-10 state of both wt and V30M TTR, information that is not distinguishable by the HR-XIC approach. On this way, Fig. C3-2 – C3-5 show the percentage of each of the modifications studied in wt, V30M and total TTR. As observed, no significant differences were found between stage 0 and stage 1 for any isoform.

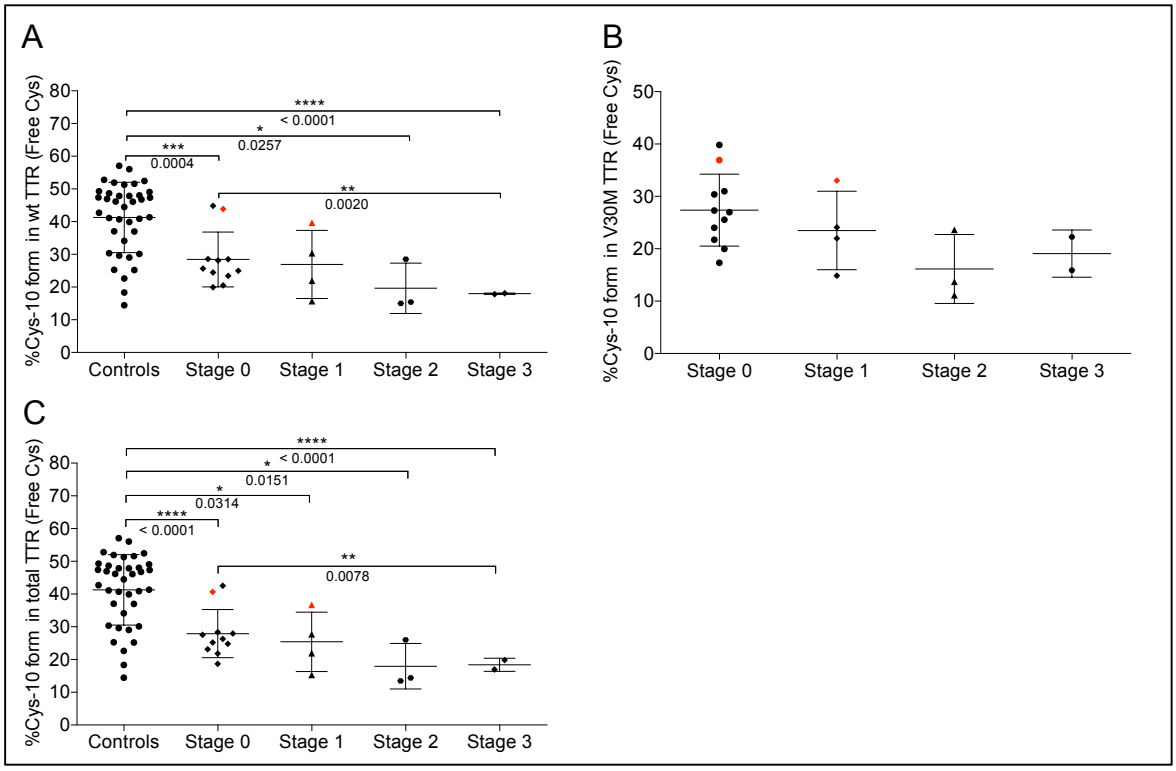

Figure C3-2. TTR intact protein analysis: Free Cys isoform. (A) Percentage of Free Cys in wt TTR. (B) Percentage of Free Cys in V30M TTR. (C) Percentage of Free Cys in total TTR. For all groups, mean ± SEM values are represented. Additionally, p-values are shown when significant differences were found after applying unpaired t-test with Welch's correction. In red, samples from the same patient at different stages.

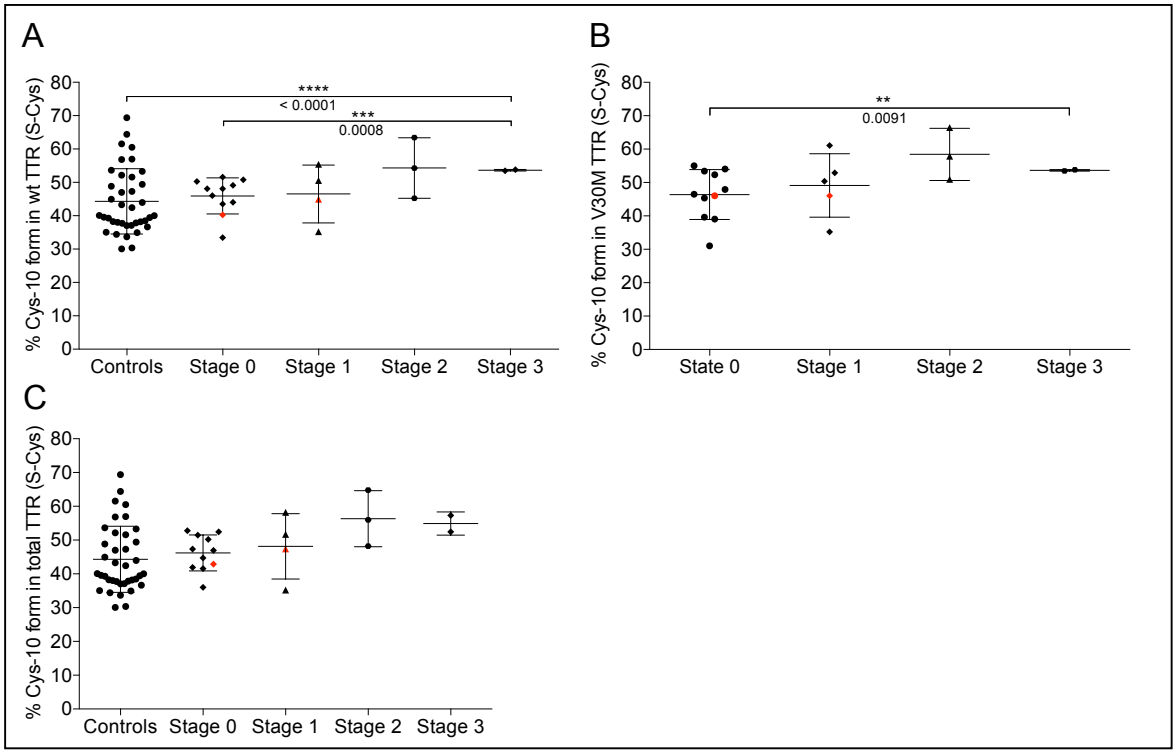

Figure C3-3. TTR intact protein analysis: S-Cys isoform. (A) Percentage of S-Cys in wt TTR. (B) Percentage of S-Cys in V30M TTR. (C) Percentage of S-Cys in total TTR. For all groups, mean ± SEM values are represented. Additionally, p-values are shown when significant differences were found after applying unpaired t-test with Welch's correction. In red, samples from the same patient at different stages.

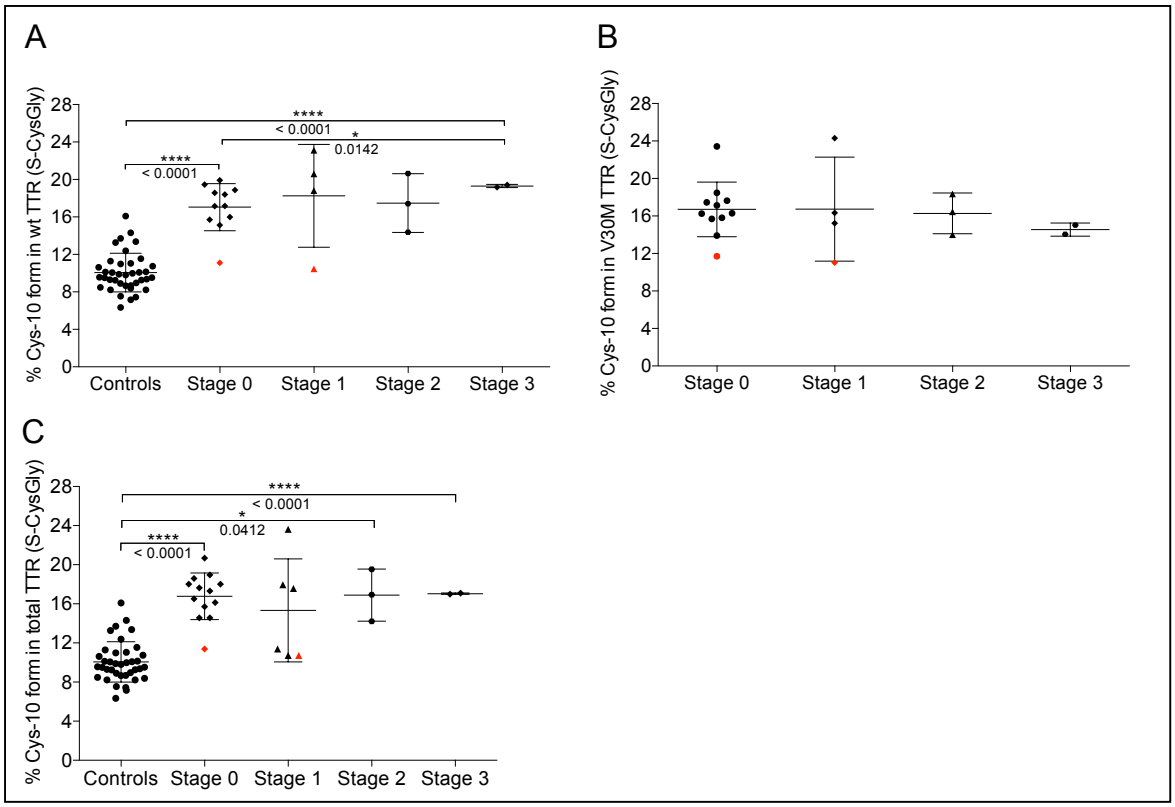

Figure C3-4. TTR intact protein analysis: S-CysGly isoform. (A) Percentage of S-CysGly in wt TTR. (B) Percentage of S-CysGly in V30M TTR. (C) Percentage of S-CysGly in total TTR. For all groups, mean ± SEM values are represented. Additionally, p-values are shown when significant differences were found after applying unpaired t-test with Welch's correction. In red, samples from the same patient at different stages.

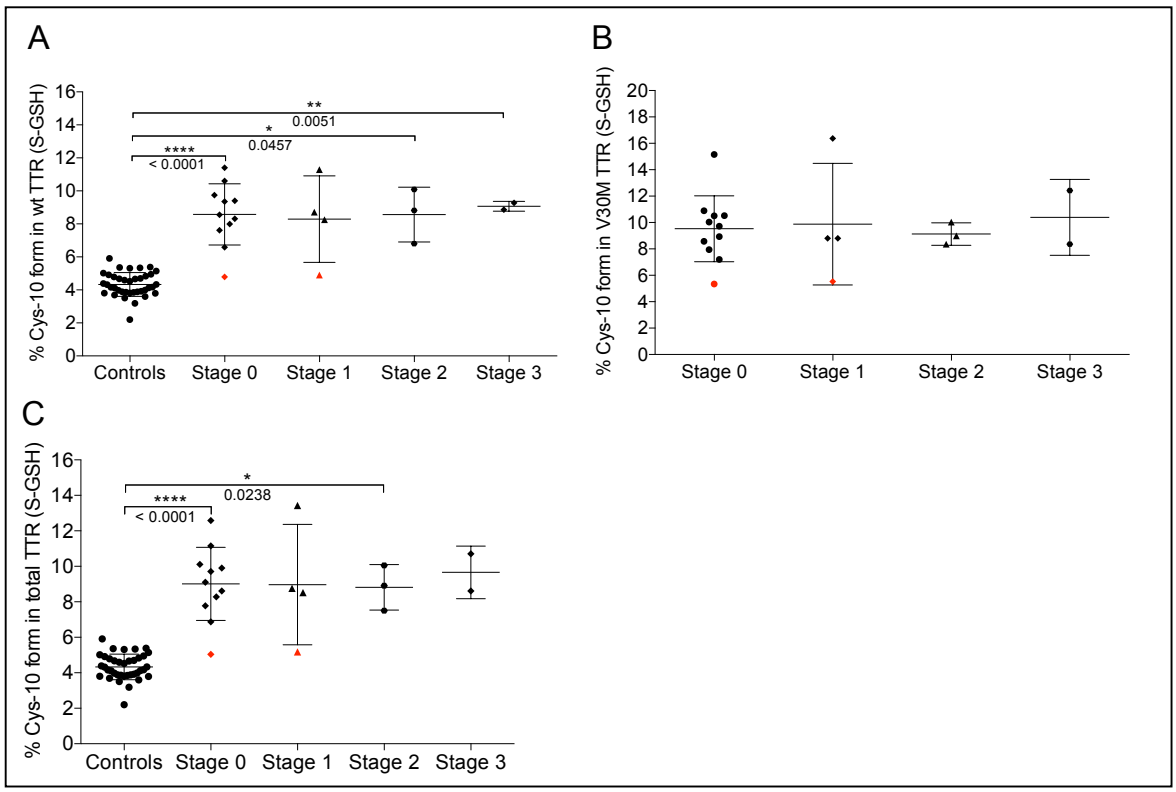

Figure C3-5. TTR intact protein analysis: S-GSH isoform. (A) Percentage of S-GSH in wt TTR. (B) Percentage of S-GSH in V30M TTR. (C) Percentage of S-GSH in total TTR. For all groups, mean ± SEM values are represented. Additionally, p-values are shown when significant differences were found after applying unpaired t-test with Welch's correction. In red, samples from the same patient at different stages.

C3.3.2.2 Absolute quantification of Cys-10 PTMs by HR-XIC

In parallel, absolute quantification of Cys-10 PTMs in the different disease stages was also performed. After TTR immunoprecipitation with immobilized Ab, TTR was digested with Arg-C as described (see Material and Methods C3.2.3). Standard labeled N-term peptides (see Chapter 2, Table C2-1 P1-P5) were spiked into the digested sample at final concentrations in column of 50, 12.5, 7.5, 200 and 200 fmols for the Free Cys, S-CysGly, S-GSH, S-Cys and S-Sulfo Cys-10 isoforms, respectively. Samples were then analyzed on an UHR-QTOF mass spectrometer and after integration of precursor signals of target peptides in Skyline Software, values of absolute concentration for each peptide were calculated. For a better interpretation of the data, the percentage of each Cys-10 form was represented. As seen in Fig. C3-6A (left column), 2 of the Cys-10 PTMs, S-GSH and S-CysGly, happen to be good biomarkers of disease progression, enabling the differentiation between asymptomatic and stage 1 patients. In both cases, the decrease in the corresponding Cys-10 PTM correlates with the appearance of symptoms. In order to increase the size of the groups and therefore increase the reliability of the statistical study, we additionally grouped stage 1 and 2, since no differences were observed between the two groups (Fig. C3-6B, right column). The results obtained after the aggrupation are the same than the previously obtained.

Interestingly, and further confirming our findings, we had the opportunity to analyze one patient in two different disease stages (red symbol in all graphs): asymptomatic and stage 1. In this case, and despite being just one sample, we can see how the levels of S-GSH and S-CysGly decreased at the moment of appearance of the very first symptoms, just a few months after the first sample was taken. In this case, since symptoms appeared early after the first medical checking there was no absolute certainty about the diagnostic. However, from a proteomic point of view, it is clear the change in the Cys-10 PTMs pattern. Future studies should be addressed to collect pairs of samples of patients at different stages to further confirm the changes we are here describing.

Henceforth, and even though it is a preliminary study, we can propose the measurement of S-GSH and S-CysGly levels regularly in V30M carriers as a way to follow disease progression. The mass spectrometry strategy proposed is a non-invasive method since no biopsy is required and just 25 μL of serum are needed to perform the proteomic analysis. Therefore, regular Cys-10 PTMs levels study would allow a rapid, simple and unbiased early classification of patients according to disease progression, permitting a rapid intervention after the appearance of the first symptoms.

We have here studied for the first time TTR Cys-10 pattern distribution across the different stages of FAP. The way Cys-10 mixed disulfides biologically relate with the disease is still unknown. However, there is general knowledge that sulfhydryl chemistry plays a vital role in the defense of cells against oxidants, free radicals and electrophiles. In this sense, modulation of thiol-disulfide status of critical cysteines on proteins is recognized as an important mechanism of signal transduction and an important consequence of oxidative stress (Mieyal et al. 2008, Sabens Liedhegner et al. 2012). Additionally, it is well reported in the bibliography that oxidative stress is associated with many neurodegenerative diseases such as Alzheimer Disease (AD), Parkinson's disease (PD), Huntington's disease (HD) or amyotrophic lateral sclerosis (ALS). An important element in neurodegeneration is neuronal loss through cell death, which it is thought to be caused by protein misfolding, excitotoxicity, activation of cell death pathways, mitochondrial dysfunction, increased iron deposition, and oxidative stress through the overexposure to reactive nitrogen species (RNS) and

reactive oxygen species (ROS) (Mieyal et al. 2008, Sabens Liedhegner et al. 2012). Several enzymes such as catalase, peroxiredoxin and superoxide dismutase, all of them scavengers of reactive oxygen species, are known to protect against oxidative stress. In addition, sulfur-containing aminoacids such as cysteine and methionine in proteins and non-protein cofactors also act as antioxidant mechanisms, especially the Cys-containing tripeptide glutathione (GSH), abundant within cells. Hence, sulfur redox status plays a crucial role in the regulation of several cell functions like signaling, growth, survival or cell death. Protein function or stability is altered by reversible or irreversible modifications of cysteine and methionine residues, which at the same time perturb intracellular sulfhydryl homeostasis, linked to neurodegenerative diseases among many other disorders. Reversible thiol modifications, including intramolecular and intermolecular disulfides, protein sulfenic acids, and protein-glutathione mixed disulfides (protein-SSG), protect proteins from irreversible overoxidation, allowing for a return to normal function after the oxidant challenge has subsided (Jones et al. 2000, Mieyal et al. 2008, Sabens Liedhegner et al. 2012).

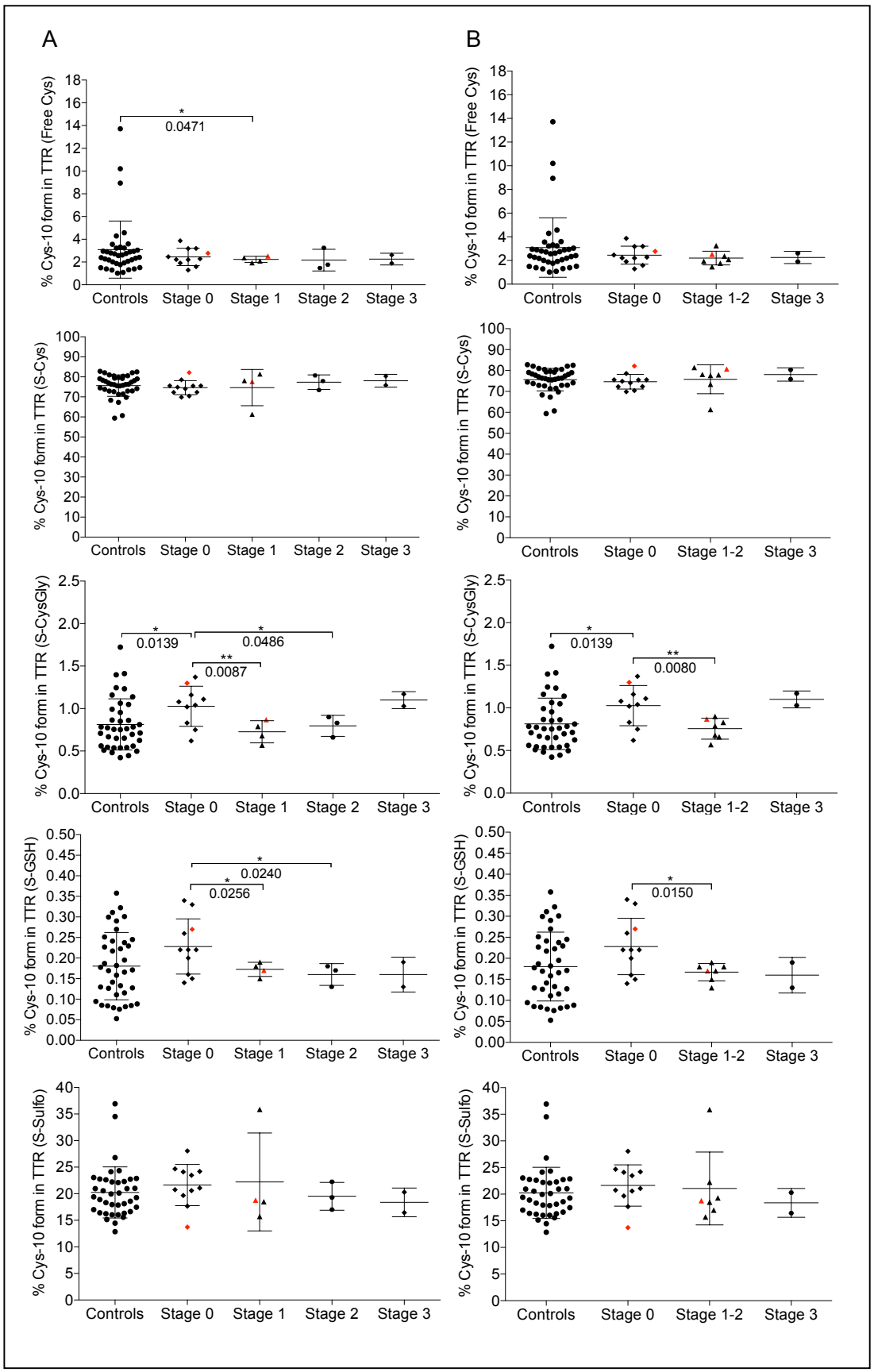

Figure C3-6. HR-XIC analysis of TTR. (A) Left column. Percentage values for the 5 most common TTR Cys-10 PTMs in human serum. Study of control group, asymptomatic group and the 3 different FAP stages. **(B) Right column. Percentage values for the 5 most common TTR Cys-10 PTMs in human serum.** Stages 1 and 2 are shown as a single group. For all groups, mean ± SEM values are represented. Additionally, p-values are shown when significant differences were found after applying unpaired t-test with Welch's correction. In red, samples from the same patient at different stages.

In the particular case of TTR and FAP it has also been suggested that oxidative stress may be a consequence of protein aggregation and that it could be related with cellular toxicity. Precisely, it has been reported that the presence of TTR soluble aggregates induces the production of RNS in human epidermoid and Schwannoma cell lines (Fong and Vieira 2012). Furthermore, there are evidences for the involvement of ROS in cellular toxicity due to TTR aggregates in a Schwannoma cell line. TTR aggregates increased cellular hydrogen peroxide production (about 125% increment) and promoted depletion of antioxidant factors such as glutathione and catalase and, more generally, diminished the cellular antioxidant capacity (Fong and Vieira 2013). There are also *in vivo* evidences for oxidative stress as oxidatively modified lipids and proteins have been reported in colon tissues and protein nitration has been observed in nerves of FAP patients (Ando et al. 1997, Sousa et al. 2001).

Finally, in neurodegenerative diseases, a decrease in GSH (reduced glutathione) levels has been reported. For example, in brain samples of AD patients, lower levels of GSH, together with higher GSSG (oxidized glutathione) levels, have been reported when comparing with a control group. A similar behavior has been described for PD samples. For this reason, GSH loss is thought to be one of the early changes responsible for the increased oxidative stress associated with onset of PD. Hence, changes in the GSH/GSSG ratio and conditions that produce ROS and RNS can promote modifications on protein cysteine residues and on glutathione that serve as precursors to the formation of proteine-SSG. The product of degradation of GSH by the enzyme γ-glutamyltranspeptidase (γ-GT) is CysGly, which can be degradated to Cys by the enzyme dipeptidase (Jones et al. 2000).

Therefore, the increased S-GSH levels in the asymptomatic group in comparison to the control group could be suggesting the presence of soluble TTR aggregates despite FAP symptoms are not evident yet at this moment. Deposition of TTR in the form of small toxic nonfibrillar aggregates, occurring locally before amyloid formation, has been already described (Sousa et al. 2001). Individuals with this nonfibrillar form of TTR deposition are asymptomatic, have normal fiber density and no fiber degeneration. Given the demonstrated toxic nature of these small aggregates, the mechanism by which axons are able to survive this injury should be further addressed in the future (Sousa et al. 2001). The presence of such aggregates would induce ROS and RNS production and diminish the cellular antioxidant capacity, thus, protein S-Glutathionylation would act in redox signal transduction and serve as a protective mechanism against irreversible cysteine oxidation. The various ways that protein thiol moieties could be converted to protein-SSG include thiol disulfide exchange if the GSSG concentration is high enough; reaction of GSH with protein-sulfenic acid or protein-SNO precursors, or recombination of protein and glutathione thiyl radicals (Sabens Liedhegner et al. 2012). Since S-CysGly is the product of degradation of S-GSH, it is normal to find an increase in S-CysGly when S-GSH is also augmented. Finally, since in plasma the major low-molecular weight sulphydryl/disulphide pool is CysSH/$(CysS)_2$, extracellular proteins are predominantly S-Cysteinilated (Jones et al. 2000), as it is also seen in our results.

Reversal of protein S-glutathionylation is catalyzed specifically by glutharedoxin (Grx), which thereby plays a critical role in cellular regulation. The reaction catalyzed by Grx is appropriately depicted as a thiol-disulfide exchange reaction involving nucleophilic displacement reactions rather than single electron transfer reactions that would involve radical intermediates. There are two forms of Grx that have been characterized in mammals, Grx1 and Grx2, and five forms of Grx (Grx1-5) have been identified in *E. coli* and yeast, and the gene for a mammalian form of Grx5 has also been reported.

Grx1 is the best characterized isoform in mammalian systems. The deglutathionylating activity of Grx has been implicated in regulation of many vital functions, including actin polymerization, vasodilation, and propagation of apoptosis (Mieyal et al. 2008). Recent studies show that dysregulation of redox signaling and sulfhydryl homeostasis likely contributes to onset or progression of neurodegeneration. The main function of Grx is to deglutathionylate proteins and therefore, to restore the reduced state (protein-SH), contributing to sulfhydryl homeostasis. It has been previously described in two FAP mouse models that increased Grx1 activity is associated with TTR deposition in the stomach and the peripheral nervous system (Macedo et al. 2007). This increased Grx activity upon TTR deposition could explain the decrease in S-GSH TTR levels described in the present work for FAP stage 1 patients. However, despite the importance of Grx1 as regulator of oxidative stress and apoptosis, its role in FAP is completely unknown. It is suggested that overexpression of Grx1 may have a protective role, acting to detoxify FAP tissues as it does the frontal cortex and hippocampal neurons of the brain in AD.

C3.3.3 Analysis of G6S TTR polymorphism frequency in the studied Spanish cohort

TTR is a highly heterogenic protein, with more than 100 point mutations described (see introduction I.3.1). For this reason, the finding of other mutations different from the variant initially considered (TTR V30M) is not surprising. Particularly, we have detected by our intact protein strategy, and further confirmed it by top-down MS, the presence of the common G6S polymorphism. The G6S polymorphism is described as a benign mutation with a frequency of 4% worldwide and more precisely, of 15% in Europe and the Iberian Peninsula according to the 1000 genomes database (The 1000 Genomes Project Consortium 2012). However, our results describe a higher frequency for the population here studied with a frequency of 31% (9 out of 29) in the V30M FAP patients and of 20% (11 out of 50) in the control group. In addition, we have found two patients heterozygous for V30M and homozygous for G6S, a condition that to our knowledge has not been previously described.

In previous works (Sikora et al. 2014), a possible protective role for the G6S polymorphism has been suggested in wt TTR amyloidosis. Nevertheless, this would not be the case for the present cohort since a higher G6S frequency was observed in FAP patients when compared to the control group. It would be highly interesting to perform a genomic or proteomic study in a much larger Spanish cohort in order to define more accurately the frequency of the G6S polymorphism in the Spanish population and hence, determine if there is a correlation between G6S polymorphism and a higher tendency to develop FAP.

C3.3.4 siRNA treatment for FAP: a case study of a stage 2 FAP patient

Several therapeutic strategies are nowadays available for FAP patients (see Introduction I.4). Some of those treatments are already approved by the EMEA, like the tetramer stabilizer Tafamidis; others, however, are still in clinical trials, like the tetramer stabilizer Diflunisal or the siRNA Patisiran (Coelho et al. 2013). In the present work we had the opportunity to study the case of a stage 2 FAP patient who entered Patisiran phase III clinical trial. The patient was under Tafamidis treatment for 8 months and with evident progression of the disease prior to enrollment in the clinical trial. In order to obtain TTR basal levels in the patient, treatment with Tafamidis was stopped for 15 days and then TTR levels were measured by our HR-XIC strategy. Afterwards, plasma samples were taken after the first siRNA

dose and prior to additional doses. In all cases, total TTR amount in plasma was determined as well as the ratio wt:V30M (Fig. C3-7).

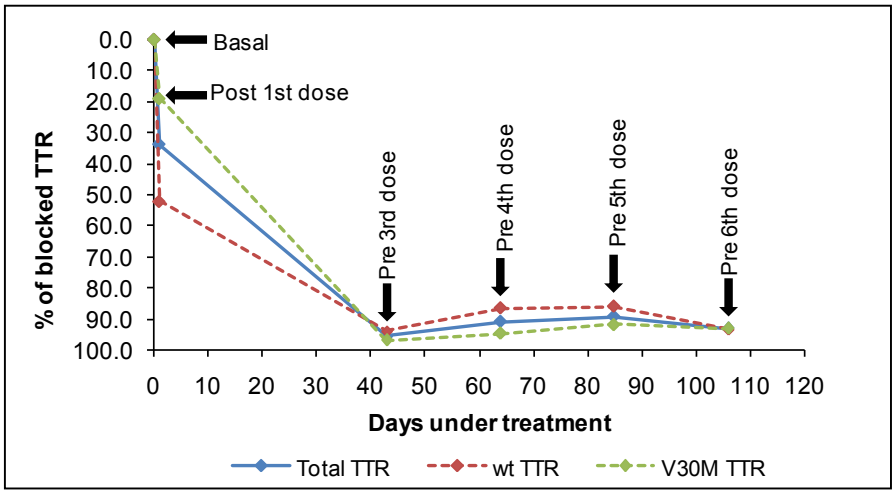

Figure C3-7. Analyzing TTR levels during siRNA treatment. TTR concentration was measured by our HR-XIC strategy. For interpretation of the data, % of blocked TTR referred to basal level was represented. The moment of sample extraction is indicated for each case.

As observed, just after the first siRNA dose, TTR levels decreased in approximately 20% for the V30M TTR and up to 50% for wt TTR, the total TTR decrease being of around 30%. In addition, just with a second dose TTR levels decreased up to 90% of the basal levels for all TTR forms, confirming the efficiency of siRNA in the TTR gene silencing *in vivo*. In addition, TTR suppression was maintained along the siRNA treatment.

Routinely, TTR levels in siRNA clinical trials are measured based on immunoassay techniques. However, the use of our HR-XIC methodology allows the study of both wt and V30M TTR levels, information that is not available by such techniques. Indeed, thanks to the independent measure of wt and V30M TTR we have been able to describe a possible differential suppression of both variants after the first dose. We do not know why the used siRNA suppresses preferentially wt TTR but it might be an interesting point to study in order to improve the efficiency of the therapy.

C3.4 CONCLUSION

After analyzing a Spanish cohort of asymptomatic and symptomatic FAP patients as well as control healthy individuals, by both HR-XIC and intact protein methodologies, we have been able to measure TTR levels and absolutely/relatively quantify Cys-10 PTMs. As a result, we here propose S-GSH and S-CysGly TTR levels as biomarkers of disease progression. Precisely, we have observed significant increased levels of these two PTMs in asymptomatic patients when compared to controls, which could be associated with the presence of soluble TTR aggregates. In addition, we have found significant differences in terms of S-GSH and S-CysGly TTR levels between asymptomatic and stage 1 FAP patients, possibly associated to an increase in Grx activity upon TTR deposition. Therefore, the measure of S-GSH and S-CysGly TTR levels could be used as an indicator of disease onset. Despite being preliminary, the results here presented are highly promising since they offer a non-invasive objective measure of disease stage and they enable an early intervention in the treatment of FAP after the very first symptoms. Additionally, we have described an anomalously higher G6S frequency in the studied Spanish population that should be further analyzed in order to determine a possible relationship between this polymorphism and FAP. Finally, we have shown the utility and suitability of our developed HR-XIC technique in the study of the efficiency of TTR gene silencing by siRNA therapy, providing new information and suggesting a possible initial differential suppression between variants.

C3.5 REFERENCES

Altland K and Winter P (1999) Potential treatment of transthyretin-type amyloidoses by sulfite. *Neurogenetics* 2(3):183–8.

Altland K, Winter P and Sauerborn MK (1999) Electrically neutral microheterogeneity of human plasma transthyretin (prealbumin) detected by isoelectric focusing in urea gradients. *Electrophoresis* 20(7):1349–64.

Andersson R (1976) Familial Amyloidosis with Polyneuropathy. A Clinical Study Based on PAtients Living in Northern Sweden. *Acta Med Scand* Suppl 590:1–64.

Ando Y, Nyhlin N, Suhr O, Holmgren G, Uchida K, el Sahly M, Yamashita T, Terasaki H, Nakamura M, Uchino M and Ando M (1997) Oxidative stress is found in amyloid deposits in systemic amyloidosis. *Biochem Biophys Res Commun* 232(2):497–502.

Andrade C (1952) A peculiar form of peripheral neuropathy. *Brain* 75(3):408–27.

Buxbaum J, Anan I and Suhr O (2010) Serum transthyretin levels in Swedish TTR V30M carriers. *Amyloid* 17(2):83–5.

Buxbaum J, Koziol J and Connors LH (2008) Serum transthyretin levels in senile systemic amyloidosis: effects of age, gender and ethnicity. *Amyloid* 15(4):255–61.

Coelho T, Adams D, Silva A, Lozeron P, Hawkins PN, Mant T, Perez J, Chiesa J, Warrington S, Tranter E, Munisamy M, Falzone R, Harrop J, Cehelsky J, Bettencourt BR, Geissler M, Butler JS, Sehgal A, Meyers RE, Chen Q, Borland T, Hutabarat RM, Clausen V a, Alvarez R, Fitzgerald K, Gamba-Vitalo C, Nochur S V, Vaishnaw AK, Sah DWY, Gollob J a and Suhr OB (2013) Safety and efficacy of RNAi therapy for transthyretin amyloidosis. *N Engl J Med* 369(9):819–29.

Da Costa G, Gomes R, Correia CF, Freire A, Monteiro E, Martins A, Barroso E, Coelho a V, Outeiro TF, Ponces Freire A and Cordeiro C (2009) Identification and quantitative analysis of human transthyretin variants in human serum by Fourier transform ion-cyclotron resonance mass spectrometry. *Amyloid* 16(4):201–207.

Coutinho P, da Silva A, Lima J and Barbosa A (1980) Forty years of experience with type 1 amyloid neuropathy: review of 483 cases. *Amyloid and amyloidosis* Excerpta Med:88–98.

Fong V and Vieira A (2012) Transthyretin aggregates induce production of reactive nitrogen species. *Neurodegener Dis* 11(1):42–8.

Fong V and Vieira A (2013) Pro-oxidative effects of aggregated transthyretin in human Schwannoma cells. *Neurotoxicology* 39:109–13.

Gofferje H and Fekl W (1979) Diagnosis of malnutrition. *Infusionsther Klin Ernahr* 6(2):95–9.

Jiang X, Buxbaum JN and Kelly JW (2001) The V122I cardiomyopathy variant of transthyretin increases the velocity of rate-limiting tetramer dissociation, resulting in accelerated amyloidosis. *Proc Natl Acad Sci USA* 98(26):14943–8.

Jones D, Carlson J, Mody V, Cai J, Lynn M and Sternberg P (2000) Redox state of glutathione in human plasma. *Free Radic Biol Med* 28(4):625–35.

Kim Y, Gallien S, van Oostrum J and Domon B (2013) Targeted proteomics strategy applied to biomarker evaluation. *Proteomics Clin Appl* 7(11-12):739–47.

Kingsbury JS, Klimtchuk ES, Théberge R, Costello CE and Connors LH (2007) Expression, purification, and in vitro cysteine-10 modification of native sequence recombinant human transthyretin. *Protein Expr Purif* 53(2):370–7.

Kishikawa M, Nakanishi T, Miyazaki A and Shimizu A (1999) Enhanced amyloidogenicity of sulfonated transthyretin. *Amyloid* 186(6):183–6.

Lin D, Alborn W, Slebos R and Liebler D (2013) Comparison of protein immunoprecipitation-multiple reaction monitoring with ELISA for assay of biomarker candidates in plasma. *J Proteome Res* 12(12):5996–6003.

Macedo B, Batista AR, do Amaral JB and Saraiva MJ (2007) Biomarkers in the Assessment of Therapies for Familial Amyloidotic Polyneuropathy. *Mol Med* 13(11-12):584–91.

Mieyal J, Gallogly M, Qanungo S, Sabens E and Shelton M (2008) Molecular mechanisms and clinical implications of reversible protein S-glutathionylation. *Antioxid Redox Signal* 10(11):1941–88.

Munar-Ques M, Costa PP, Saraiva MJ, Viader-Farre C and Munar-Bernat C (1988) Familial type I (Portuguese form) amyloidotic polyneuropathy in Majorca. Study using the TTR (Met30) genetic marker. *Med Clin (Barc)* 91(12):441–4.

Nakanishi T, Yoshioka M, Moriuchi K, Yamamoto D, Tsuji M and Takubo T (2010) S-sulfonation of transthyretin is an important trigger step in the formation of transthyretin-related amyloid fibril. *Biochim Biophys Acta* 1804(7):1449–56.

Nakazato M, Kurihara T, Kangawa K and Matsuo H (1984) Diagnostic radioimmunoassay for familial amyloidotic polyneuropathy. *Lancet* 2(8414):1274–5.

Norgren N, Hellman U, Ericzon BG, Olsson M, Suhr OB (2012) Allele specific expression of the transthyretin gene in swedish patients with hereditary transthyretin amyloidosis (ATTR V30M) is similar between the two alleles. *PLoS One* 7(11):e49981.

Planté-Bordeneuve V (2014) Update in the diagnosis and management of transthyretin familial amyloid polyneuropathy. *J neurol* 261(6):1227–33.

Poulsen K, Bahl JMC, Tanassi JT, Simonsen AH and Heegaard NHH (2012) Characterization and stability of transthyretin isoforms in cerebrospinal fluid examined by immunoprecipitation and high-resolution mass spectrometry of intact protein. *Methods* 56(2):284–92.

Raz A and Goodman D (1969) The interaction of thyroxine with human plasma prealbumin and with the prealbumin-retinal-binding protein complex. *J Biol Chem* 244(12):3230–7.

Raz A, Shiratori T and Goodman D (1970) Studies on the protein-protein and protein-ligand interactions involved in retinol transport in plasma. *J Biol Chem* 245(8):1903–12.

Ribeiro-Silva C, Gilberto S, Gomes R, Mateus E, Monteiro E, Barroso E, Varela-Coelho A, da Costa G, Ponces-Freire A and Cordeiro C (2011) The relative amounts of plasma transthyretin forms in familial transthyretin amyloidosis: A quantitative analysis by Fourier transform ion-cyclotron resonance mass spectrometry. *Amyloid* 18(4):191–9.

Ritchie R, Palomaki G, Neveux L, Navolotskaia O, Ledue T and Craig W (2000) Reference distributions for the positive acute phase serum proteins, alpha1-acid glycoprotein (orosomucoid), alpha1-antitrypsin, and haptoglobin: a practical, simple, and clinically relevant approach in a large cohort. *J Clin Lab Anal* 14(6):284–92.

Sabens Liedhegner E, Gao X and Mieyal J (2012) Mechanisms of Altered Redox Regulation in Neurodegenerative Diseases—Focus on S-Glutathionylation. *Antioxid Redox Signal* 16(6):543–66.

Saraiva M, Costa P and Goodman D (1985) Biochemical Marker in Familial Amyloidotic Polyneuropathy , Portuguese Type. *J Clin Invest* 76(6):2171–7.

Sekijima Y, Hammarström P, Matsumura M, Shimizu Y, Iwata M, Tokuda T, Ikeda S-I and Kelly JW (2003) Energetic characteristics of the new transthyretin variant A25T may explain its atypical central nervous system pathology. *Lab Invest* 83(3):409–17.

Shao J, Xin Y, Li R and Fan Y (2011) Vitreous and serum levels of transthyretin (TTR) in high myopia patients are correlated with ocular pathologies. *Clin Biochem* 44(8-9):681–5.

Sikora JL, Logue MW, Chan GG, Spencer BH, Prokaeva TB, Baldwin CT, Seldin DC and Connors LH (2014) Genetic variation of the transthyretin gene in wild-type transthyretin amyloidosis (ATTRwt). *Hum Genet* 134(1):111–21.

Soprano DR, Herbert J, Soprano KJ, Schon E a. and Goodman DS (1985) Demonstration of transthyretin mRNA in the brain and other extrahepatic tissues in the rat. *J Biol Chem* 260(21):11793–8.

Sousa M, Cardoso I, Fernandes R, Guimarães A and Saraiva M (2001) Deposition of transthyretin in early stages of familial amyloidotic polyneuropathy: evidence for toxicity of nonfibrillar aggregates. *Am J Pathol* 159(6):1993–2000.

Sousa M, Du Yan S, Fernandes R, Guimaraes A, Stern D and Saraiva M (2001) Familial amyloid polyneuropathy: receptor for advanced glycation end products-dependent triggering of neuronal inflammatory and apoptotic pathways. *Journal Neurosci* 21(19):7576–86.

Sousa M, Yan S, Stern D and Saraiva M (2000) Interaction of the receptor for advanced glycation end products (RAGE) with transthyretin triggers nuclear transcription factor kB (NF-kB) activation. *Lab Invest* 80(7):1101–10.

Terazaki H, Ando Y, Suhr O, Ohlsson PI, Obayashi K, Yamashita T, Yoshimatsu S, Suga M, Uchino M and Ando M (1998) Post-translational modification of transthyretin in plasma. *Biochem Biophys Res Commun* 249(1):26–30.

The 1000 genes Project Consortium (2012) An integrated map of genetic variation from 1,092 human genomes. *Nature* 135(V):0–9.

Tsuchiya-Suzuki A, Yazaki M, Kametani F, Sekijima Y and Ikeda S (2011) Wild-type transthyretin significantly contributes to the formation of amyloid fibrils in familial amyloid polyneuropathy patients with amyloidogenic transthyretin Val30Met. *Hum Pathol* 42(2):236–43.

Zhang Q and Kelly JW (2003) Cys10 mixed disulfides make transthyretin more amyloidogenic under mildly acidic conditions. *Biochemistry* 42(29):8756–61.

Zhang Q and Kelly JW (2005) Cys-10 mixed disulfide modifications exacerbate transthyretin familial variant amyloidogenicity: A likely explanation for variable clinical expression of amyloidosis and the lack of pathology in C10S/V30M transgenic mice. *Biochemistry* 44(25):9079–85.

CHAPTER 4. Proteomic characterization of wt and V30M transthyretin after liver and domino liver transplantation

C4.1. INTRODUCTION

Amyloidosis is the process wherein soluble extracellular proteins become insoluble due to folding problems, resulting in protein deposition in form of aggregates in different organs and tissues throughout the body. Amyloidosis can be acquired or hereditary and they are defined according to their precursor protein. There are three main kinds of familial amyloid polyneuropathy (FAP) according to the responsible protein: transthyretin (TTR), apolipoprotein A-1 or gelsolin. In the present work we focus on TTR-related FAP (further referred as simply FAP), the most common and devastating disease in the group (Planté-Bordeneuve and Said 2011).

FAP is an autosomal dominant neurodegenerative disorder associated to point mutations in the TTR gene, mainly V30M and L55P. Andrade first described the disease in 1952 in Porto, Portugal. FAP presents endemic character in specific geographical areas such as Portugal, Sweden, Japan and Mallorca Island (Andersson 1976, Andrade 1952, Coutinho et al. 1980). The main clinical manifestation is the systemic extracellular deposition of amyloid fibrils throughout the connective tissue, with the exception of the brain and the liver parenchyma and with special affection of the peripheral nervous system (PNS), ending in organ dysfunction and lastly, death (Sousa and Saraiva 2003). FAP is characterized by presenting an important heterogeneity both in age of onset and clinical manifestation, the former varying geographically. In the case of Portugal, an early age of onset is observed (<50 years) whereas a late age of onset is found in Sweden and Japan (Coutinho et al. 1980, Koike et al. 2012).

Since the liver is the main responsible of TTR synthesis (production of 90-80% of TTR), liver transplantation (LT) was proposed 20 years ago in Sweden (Holmgren et al. 1991, 1993) in order to suppress the main source of mutant TTR and thus prevent formation of amyloidosis and stop disease progression. It was seen that after LT, mutant TTR was reduced by 98% in the following days, finding almost exclusively wt TTR. In addition, in up to 70% of the patients, most of the symptoms presented at the time of transplantation remained but no further progression, or at a very low speed, was observed (Adams 2013, Samuel and Adams 2007). According to data in the Familial Amyloidotic Polyneuropathy World Transplant Registry (FAPWTR), more than 2000 LT were performed until 2012 in 19 countries, half of them in Portugal. Success of LT is tightly related to the TTR gene mutation, the age of the patient and the stage of the disease progression. The main causes of death after LT are cardiac related affections (21%), septicemia (21%) and liver related complications (14%), according to FAPWTR data. After the first year, however, patients die from progress of the amyloid disease (50%), affecting specially the heart or peripheral nervous system. In addition, the rate of survival at 5 years for V30M FAP patients is 20% higher than for other FAP mutations. In some cases, worsening of walking ability is possible after LT, explained by the fact that wt TTR may continue accumulating in the nerve after LT. It is recommended to perform LT as soon as possible in the disease progression, and thus, acting before the onset of walking difficulties that require aid. Finally, regarding renal function and ocular manifestations, while the former remains stable in most patients after LT, the

latter presents the risk of developing glaucoma or vitreous opacities in 8% and 12% of the patients respectively, due to the retinal source of mutated TTR (Adams 2013).

Until recently, LT was the only considered anti-amyloid therapy for FAP patients. Nowadays, new therapies such as Tafamidis (Vynidaquel®), Diflunisal or small interfering RNA (siRNA) are being considered. While Tafamidis and Diflunisal are tetramer stabilizers, siRNA therapies aim to abolish TTR synthesis. Tafamidis has already been approved by the European Medicines Agency (2011) and the Japanese Pharmaceuticals and Medical Devices Agengy (2013) for the treatment of FAP. However, Diflunisal and ALN-TTR02 (a specific siRNA) are still in clinical trials (Adams 2013).

In 1995 and in parallel to LT, domino liver transplantation (DLT) was introduced in Portugal as a way to mitigate the organ shortage. The procedure consists in the use of livers from FAP patients as a subsequent graft in a second liver transplant. The basis of this strategy is that livers from FAP patients are anatomically and functionally normal, being the production of mutant TTR the only problem associated to them. In addition, donors are usually young and the ischemic time is short. Since then, more than 1000 DLT have been performed worldwide in 63 hospitals from 21 different countries, according to the Domino Liver Transplantation Registry (DLTR). Short-term and long-term graft and patient survival rates have been shown to be similar to those of standard LT with cadaveric donors (Azoulay et al. 2012). The main indications for DLT are patients with primary hepatic malignancy, metastatic hepatic malignancy, cirrhosis secondary to hepatitits B and C, alcoholic cirrhosis and retransplantation. In fact, since FAP livers are considered as marginal livers, they are offered to patients with marginal indications for liver transplantation or to patients over 60 years old (Samuel and Adams 2007). The main causes of death after DLT are tumor recurrence (24%), septicemia (16%), cardiac related deaths (7%), and peroperative deaths (5%) (DLTR data).

Despite all the advantages discussed previously, the main drawback of DLT is the risk of developing acquired amyloid neuropathy, since the mutant TTR is produced by the liver. Nevertheless, since FAP is usually not symptomatic during the first 20 years of life, it was considered that the FAP liver recipient was not supposed to develop FAP symptoms before 20 years after transplantation. On the contrary, in a prospective study to assess the risk-benefit ratio of DLT, systemic amyloidosis developed surprisingly earlier than expected, with amyloid deposits on labial salivary gland 5 years after DLT in half of patients or on rectal biopsy in one third of patients (Adams 2013). On this way, *de novo* amyloid neuropathy mimics FAP of early onset putting into question DLT transplantation. Those recipients developing acquired polyneuropathy may require a retransplantation with wt liver (Lladó et al. 2010, Samuel and Adams 2007). The reason explaining why those patients develop symptoms earlier than expected is not known, although several explanations have been proposed. It is thought that the recipient's age may have a possible role, since amyloid deposition may depend on unknown age-related mechanisms that promote amyloid fibrillogenesis. Other proposed factors are, for instance, the fact that the presence of amyloid fibers in the graft may trigger the disease or the fact that inflammatory reactions related to the liver transplantation may promote the production of amyloid, accelerating the development of the disease (Lladó et al. 2010). Despite all the problems related to *de novo* amyloid neuropathy, it is considered that the shortage of graft from cadaveric donors still justifies the DLT in selected patients.

TTR, the main protein related with FAP, occurs as a highly heterogeneous protein not only due to point mutations in the encoding gene but also to post-translational modifications (PTMs) at the Cys-

10 residue (Altland et al. 1999, Terazaki et al. 1998). Around the 85-90% of the circulating TTR in plasma present modifications at Cys-10, being the S-sulfonation (S-Sulfo), S-glycinylcysteinylation (S-CysGly), S-cysteinylation (S-Cys) and S-glutathionylation (S-GSH) the most common PTMs (Poulsen et al. 2012). Several works suggest that Cys-10 PTMs in TTR may play an important biological role in the onset and pathological process of TTR-related amyloidosis, although its clinical implications are still badly understood (Altland and Winter 1999, Jiang et al. 2001, Kingsbury et al. 2007, Kishikawa et al. 1999, Nakanishi et al. 2010, Sekijima et al. 2003, Zhang and Kelly 2003, 2005).

In the present work, using our previously developed targeted liquid chromatography-mass spectrometry methodology (targeted LC-MS) (see Chapter 2) and an intact protein MS approach (Poulsen et al. 2012), we have studied a time series of samples from FAP patients having undergone LT and samples from DLT recipients. We have simultaneously characterized for the first time both groups in terms of wt:V30M ratios, Cys-10 PTMs and TTR levels by a relative and an absolute quantitative proteomic approach. In particular, we have studied the progression of the wt:V30M ratios (from transplantation and up to 9 years after) and the total amount of TTR in plasma, as well as the different levels of the most important Cys-10 PTMs in the two groups by means of its relative and absolute quantification. We hypothesize that Cys-10 PTMs in TTR and/or total TTR levels may play a role in the development of acquired amyloidosis in DLT patients.

C4.2. MATERIALS AND METHODS

C4.2.1 Participants

A total of 38 patients (Portuguese cohort) were included in the study (Table C4-1), corresponding to 19 FAP V30M individuals after liver transplantation and 19 individuals after domino liver transplantation. Both women and men were included with ages ranging from 23 to 66 years old. Samples were additionally classified according to time of extraction: short after surgery or long after it (from 0 hours and up to 11 years after transplantation). The first group gives information about changes in the wt:V30M ratios as well as V30M/wt TTR clearance/appearance rates. The second group, once protein levels reach steady values, allows the comparison of the Cys-10 PTMs pattern and the total amount of protein between groups. All individuals gave informed written consent and the protocol was approved according to EEC ethic rules at Hospital de Curry Cabral, Lisboa.

Table C4-1. Summary of data for samples included in the study

		n (male/female)	Age (years)[d]	Time post-surgery
Liver transplantation (LT)	Time course	0/4[a]	38 ± 13	0h - 72h
	Time course/Long period post-surgery*	3/1	-	1 month - 9 years
	Long period post-surgery	6/5	43 ± 14	11 months - 9 years
Domino liver transplantation (DLT)	Time course	4/0[b]	59 ± 5	24h - 96 h
	Time course/Long period post-surgery*	4/1[c]	-	120h - 3 years
	Long period post-surgery	7/3	54 ± 11	2 months - 4 years

a Samples corresponding to same individual

b Samples corresponding to same individual

c One of the male samples corresponds to same individual as in b

d Mean ± SD. Significant difference with $p<0.05$ between LT and DLT groups in the time course (Mann-Whitney U test)

* Samples used in both the time course and the long period post-surgery studies

C4.2.2 Blood and sample handling

Blood samples were collected to citrate containing tubes (Sarstedt) and were readily centrifuged at 18000 x g for 5 minutes at 4°C to obtain cell free plasma. Plasma aliquots were prepared and stored at -80 °C until its analysis. For TTR immunoprecipitation all samples were unfrozen at the same time and treated identically. For MS analysis, in order to minimize handling artifacts, samples were treated uniformly and as short a handling time and as few thaw-freeze cycles as practically possible were performed.

C4.2.3 Targeted LC-MS analysis by high resolution-extracted ion chromatograms (HR-XIC)

This strategy corresponds to the targeted mass spectrometry method developed in Chapter 2, which enables the absolute quantification of Cys-10 PTMs, wt:V30M ratio and total TTR levels.

C4.2.3.1 Immunoprecipitation with hydrazide-immobilized antibody (IP Ab-ULH)

Polyclonal rabbit anti-human TTR antibody (Dako) was coupled to UltraLink® Hydrazide Resin (Thermo Scientific) following the resin manufacturer's protocol. 225 µg of immobilized antibody (Ab-ULH) were incubated with 25 µL of human serum for 1 hour and 40 minutes at room temperature

with soft agitation. After TTR binding to the Ab-ULH, 5 washes with 500 μL PBS were performed. TTR was eluted with 100 mM triethylamine (TEA, Fluka) pH=11.5 solution. Elution was performed in 3 steps by addition of 400 μL TEA followed by 2 minutes of sonication on a ultrasonic bath, and the total eluted volume was concentrated to 50 μL after 8 M urea-50 mM AB buffer exchange, by diafiltration in an Amicon® Ultra-0.5 mL centrifugal Filter, Ultracel®-3K cut off membrane (Millipore).

C4.2.3.2 Enzymatic digestion of transthyretin

After immunoprecipitation, determination of the total protein amount for each sample was performed using Bio-Rad DC ™ Protein Assay Kit (Bio-Rad). Based on the amount of protein quantified, a fraction of the immunoprecipitated TTR (10 μg) was digested with Arginine-C (Endoproteinase Arg-C Sequencing Grade, Roche) during 6 hours, 37°C at a 1:23 ratio enzyme:protein. Another fraction (10 μg) of the immunoprecipitated protein was digested with trypsin (Trypsin Gold Mass Spectrometry Grade, Promega) ON, 37°C at a 1:10 ratio enzyme:protein.

C4.2.3.3 Standard labeled peptides

Labeled (5C13,N15 proline) peptides for the quantification of the 5 Cys-10 forms (>98% purity and quantified by AAA) were purchased from Peptide Synthetics (United Kingdom). The different peptides for the quantification of Cys-10 modifications will be referred as N-term heavy peptides (see Chapter 2, Table C2-1 P1-P5). Labeled (6C13,4N15 arginine) peptides for the total TTR determination (99% purity and quantified by AAA) were purchased from AQUA Peptide Sigma-Aldrich. The two different peptides (see Chapter 2, Table C2-1 P6-P7) used for the total amount of protein determination will be referred as GSPAIN peptides (wt and V30M, for the wt TTR form and the mutant V30M TTR form, respectively). For the quantification of the V30M GSPAIN peptide in its Met oxidized variant we used the calculated (see Chapter 2) ratio of response factors: 11.11 (oxidized:non oxidized V30M).

C4.2.3.4 LC-MS Measurement with UHR-QTOF

TTR from human samples was purified and digested with Arg-C and trypsin as described above. Standard labeled N-term peptides (see Chapter 2, Table C2-1 P1-P5) were spiked into Arg-C digested samples after digestion and prior to LC-MS measurement. The same procedure was followed for the standard labeled GSPAIN peptides (see Chapter 2, Table C2-1 P6-P7) and the trypsin digested samples. The amount of heavy peptides in column was of 50 fmols for each GSPAIN peptide and of 50, 12.5, 7.5, 200 and 200 fmols for the Free Cys, S-CysGly, S-GSH, S-Cys and S-Sulfo N-term peptides, respectively. The samples were analyzed on a UHR-QTOF mass spectrometer (Bruker Impact), coupled to a Proxeon Easy nano-LC (Bruker). Samples of the TTR digests (50 ng) spiked with the standard peptides were first loaded into a 100 μm ID, 2 cm Proxeon nanotrapping column and then separated with a 10 minutes 0.1% formic acid – ACN gradient (5-35% in 10 min; flow rate 300 nL/min) on a Acclaim PepMap 75 μmx25 cm, 3 μm particle size reverse phase nanoseparation column (Dionex) coupled to the mass spectrometer inlet through a Captive Spray (Bruker) ionization source. For quantification, MS acquisition was set to cycles of MS (0.5 Hz). All spectra were acquired on the range 150-2200 Da.

C4.2.3.5 Data analysis

LC-MS data was first processed using Data Analysis 4.1 (Bruker) and then quantified using Skyline Software (MacCoss Lab) to filter and integrate precursor signals of target peptides. Using a HR-XIC Skyline template, extracted ion chromatograms for the m/z corresponding to the main isotope and charge state signal for each target peptide were used for quantification.

C4.2.4 Intact protein analysis

This strategy corresponds to the method also used in Chapter 2, based on (Poulsen et al. 2012). It allows for the relative quantification of the different Cys-10 isoforms and wt:V30M ratio.

C4.2.4.1 Immunoprecipitation with unconjugated antibody

For TTR immunoprecipitation, 225 μg of the polyclonal rabbit anti-human TTR antibody (Dako) were incubated with 25 μL of human serum over night at 4 °C. After incubation, centrifugation at 9000 x g, 10 minutes and 4 °C allowed the precipitation of the TTR-Ab complex. The pellet obtained was washed 3 times with 0.1 M AB buffer and finally resuspended in 50% methanol - 1% formic acid (Poulsen et al. 2012) at approximately 4 pmol TTR/μL, according to the reported TTR concentrations in serum.

C4.2.4.2 Intact Protein measurement with UHR-QTOF

TTR immunoprecipitated as described below was analyzed on a UHR-QTOF mass spectrometer (Bruker Impact). Sample was directly infused with a syringe pump at 3 μL/min into an ESI source (Bruker). The MS acquisition method was set up to acquire only MS data during 5 minutes, with MS cycles of 0.5 Hz in the mass range from 50 m/z to 1500 m/z. MS data was analyzed using Data Analysis 4.1 software (Bruker). Lock mass calibration using Data Analysis 4.1 (Bruker) was performed prior to averaging the spectra. All measurements were done in charge envelope +14, taking into account the intensity of the 5 most intense isotope peaks for each modification. Peak inspection was performed manually and the sum of these 5 isotopes was considered as the total intensity for a given modification. From the total intensity of each form, the percent of each modification with respect to the sum of all forms was calculated, for both wt and V30M TTR.

C4.2.5 Statistical Analysis

For the statistical analysis of data, GraphPad Prism Software was used and for the comparison of the different groups, unpaired t-test with Welch's correction was applied.

C4.3. RESULTS AND DISCUSSION

C4.3.1 Time course of V30M TTR levels after transplantation

A total of 17 samples (Portuguese cohort), 8 corresponding to time series from liver transplanted patients (from 0 hours and up to 9 years after transplantation) and 9 to domino liver transplanted patients (from 24 hours and up to 3 years after transplantation), were analyzed by our previously developed targeted LC-MS strategy (see Chapter 2) and by intact protein (Poulsen et al. 2012). Sample handling is a crucial step in the analysis of post-translational modifications since oxidation of methionine residues and oxidation/modifications of Cys-10 can be introduced *ex vivo* as a result of sample manipulation, as it has been well reported in the bibliography (Poulsen et al. 2012, 2014). For this reason, all samples were treated identically and sample handling and protocol incubations were as short as practically possible, in order to be able to compare both groups of samples and minimize those ex vivo modifications.

For the targeted LC-MS strategy, TTR was immunoprecipitated from plasma samples using immobilized Ab. After elution, a fraction of TTR was digested with trypsin and 50 fmols (amount in column) of each standard labeled GSPAIN peptide (wt and V30M) were spiked into TTR digests (see Chapter 2, Table C2-1 P6-P7). The samples were then analyzed on the UHR-QTOF mass spectrometer (see Materials and Methods, C4.2.3). After integration of precursor signals of target peptides in Skyline software, values of absolute concentration for each peptide were calculated. For the representation of the data, percentages of each peptide were considered. As a result of studying the time course of samples corresponding to LT and DLT patients during a short period after transplantation, we were able to follow the evolution of the V30M TTR form in both kinds of patients, as shown in Fig. C4-1. As a result, we determined that for LT patients the half-life of V30M TTR was of 61.20 hours. In addition, we observed that only 37.80 hours after surgery, DLT patients presented already 50% of the V30M TTR final levels, that to the best of our knowledge, has not been previously reported in the bibliography. These results show that the V30M TTR appearance in DLT patients is 1.6-fold higher than its clearance rate in LT patients. The V30M TTR half-life reported here is slightly higher than the ones previously reported, 2.1 and 2.25 days (Ando et al. 1995, Schmidt et al. 1999), but still lower than the 2.67 days reported for wt TTR in humans (Socolow et al. 1965). In the previous works, non-mass spectrometric techniques (nephelometry and radioimmunoassays) were used for the quantification of TTR, a possible reason to explain the slight differences obtained, since different techniques may account for differences in the TTR measurements. In addition, some variances may come from blood and abdominal fluid loss related to surgery. The fact that V30M TTR presents a shorter half-life than its wt variant it is probably explained by its lower stability, as it is suggested from studies in mouse models (Longo Alves et al. 1997), where more rapid clearance of amyloidogenic variants has been observed.

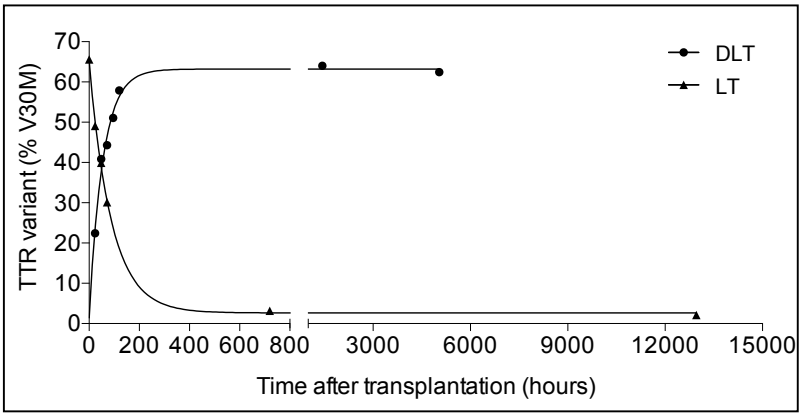

Figure C4-1. Levels of V30M TTR variant after liver or domino liver transplantation (LT, DLT). Initial measures correspond to the same patient. Final measures, when TTR V30M levels are stable, correspond to different patients.

In parallel, for the intact protein strategy, TTR was immunoprecipitated from plasma samples with unconjugated antibody. The TTR-Ab complex obtained was then centrifuged, washed and resuspended in 50% methanol - 1% formic acid at approximately 4 pmol TTR/µL, according to the reported TTR concentrations in serum. The complex TTR-Ab was then directly infused into the UHR-QTOF, where MS spectra were obtained (see Materials and methods, C4.2.4). After manual peak inspection of the spectra, the total intensity of wt and V30M TTR variants was calculated as the sum of intensities of all the TTR isoforms (Cys-10 modifications) for each variant. For the representation of the data, percentages of each variant were calculated. By this strategy it was also possible to establish TTR half-life in LT patients (72.55 hours) and the time to reach 50% of V30M TTR final levels in DLT patients was of 29.26 hours.

Comparing both strategies allowed us to see that, in general, percentage values for V30M are underestimated in the intact protein strategy (final levels reached, 42.50% ±0.86 V30M TTR) when compared with the values obtained by the absolute quantification with labeled standards (final levels reached, 63.23% ±1.15 V30M TTR). This underestimation is translated into higher values for TTR half-life and lower TTR appearance rates in DLT patients, due to differences in the response factor of the two variants (wt and V30M). Since in the targeted approach we are comparing the endogenous peptide with its equivalent synthetic one, those differences in response factor do not affect quantification and thus, the determination of wt:V30M ratio is more precise. Therefore, our results show the need for absolute quantification using labeled peptide standards in order to measure the absolute amounts of a given form, having a real evaluation of their distribution in serum. However, relative quantification can be still a good tool when the aim is the comparison of protein forms among different samples.

C4.3.2 Comparison between LT and DLT patients: total TTR amount, wt:V30M ratios and Cys-10 PTMs levels after long periods post-transplantation

Patients who undergo domino liver transplantation produce both wt and V30M TTR and it has been observed that the development of acquired amyloidosis occurs early than expected, mimicking FAP of early onset. The reason why this happens is still poorly understood and we here hypothesize that Cys-10 PTMs may play a role in the process. To this purpose, we compared a group of LT patients (n=15, Portugal) with a group of DLT patients (n=15, Portugal) once their protein levels were stable and long after the surgery (up to 11 years after). In addition, we determined the wt:V30M ratio in DLT patients and compared the total amount of protein between the two groups. Again, the

comparison was performed with the 2 methodologies described, our targeted LC-MS approach and an Intact Protein strategy.

Firstly, TTR was immunoprecipitated with both immobilized and unconjugated Ab. For the former, used in the targeted approach, TTR was eluted and two different digestions were performed in parallel. A fraction of the protein was digested with Arg-C (for the absolute quantification of the different N-term Cys-10 peptides) and another fraction with Trypsin (for the determination of the wt:V30M ratio and the total amount of TTR). After digestion, the required standard labeled peptides were added (see Chapter 2, Table C2-1 P1-P7). In the case of the N-term Cys-10 labeled peptides, added to the Arg-C digest, the amount of peptide in column was of 50, 12.5, 7.5, 200 and 200 fmols for the Free Cys, S-CysGly, S-GSH, S-Cys and S-Sulfo N-term forms, respectively. For the GSPAIN analysis performed from the Trypsin digestion, 50 fmols in column of each variant were spiked into the samples (see Materials and Methods, C4.2.3). In the case of immunoprecipitation with unconjugated antibody, used in the intact protein study, the complex TTR-Ab was directly infused into an UHR-QTOF as described previously (See Materials and Methods, C4.2.4).

Interestingly, in terms of total amount of TTR, we found that the total amount of TTR in DLT patients (mean ± SEM, 64.91 ± 5.305 ng TTR/μL plasma) was higher than in the LT ones (mean ± SEM, 42.20 ± 3.377 ng TTR/μL plasma), with a significance of p=0.0014 (unpaired t test with Welch's correction), as shown in Fig. C4-2A. In addition, we were able to determine the ratio wt:V30M in the DLT cohort (Fig. C4-2B), obtaining an average value of % V30M of 59.11 ±5.87 (mean ± SD).

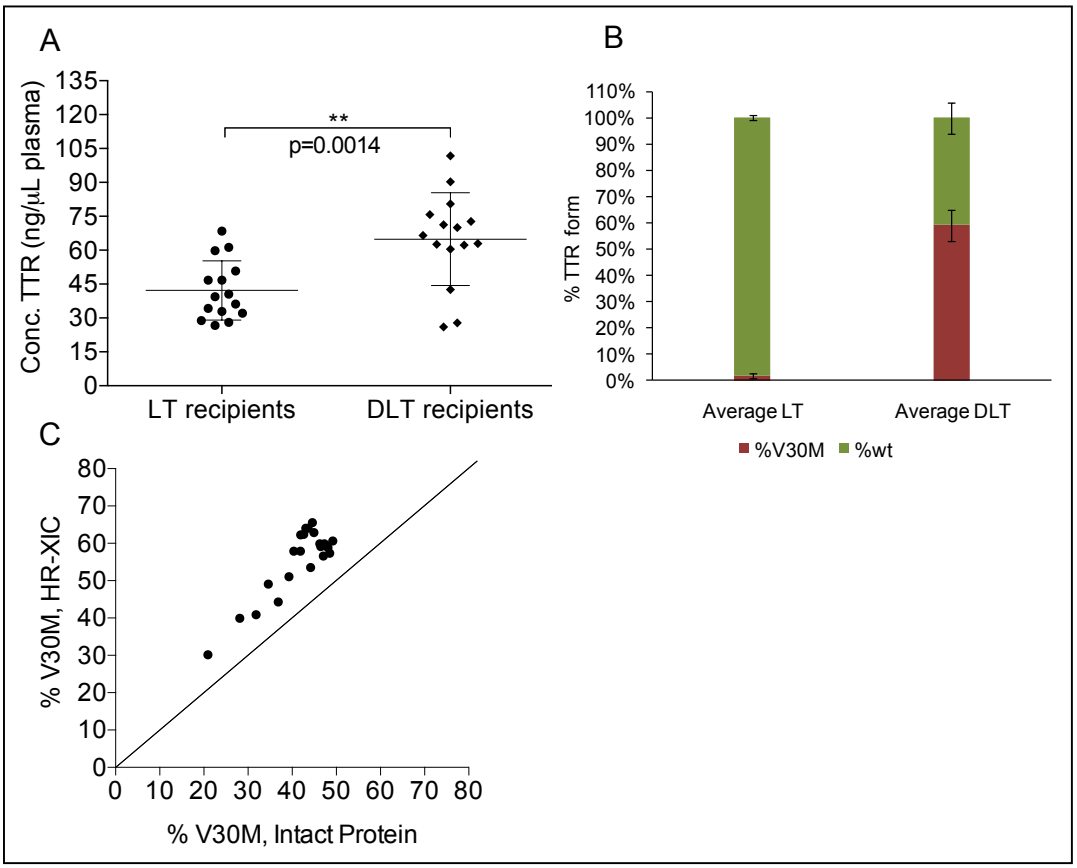

Figure C4-2. Absolute quantification of total TTR and wt:V30M ratio determination by HR-XIC methodology. (A) Absolute quantification of total TTR in LT and DLT patients. The p-value obtained in the comparison between groups after application of unpaired t-test with Welch's correction is indicated. **(B) Determination of wt:V30M ratio.** Mean values for each TTR variant are shown in the graph, error bars indicate standard deviation. **(C) Comparison between absolute and relative quantification of % V30M.** The y-axis represents values of % V30M in the absolute quantification (HR-XIC) and the x-axis the values in the relative quantification (Intact protein).

It has been described that V30M TTR tetramer is less stable than the wt; hence, it is more prone to dissociation into monomers. Despite the mechanism of fibril formation *in vivo* is not known, it is accepted that TTR monomers give rise to the formation of soluble aggregates and finally, fibril formation and deposition (see Introduction I.1.3.3). Therefore, the higher amounts of circulating TTR, together with a higher presence of its V30M amyloidogenic variant here described, could explain why DLT patients develop amyloidosis earlier than expected, mimicking FAP of early onset. This is the first time where it is found that TTR levels in DLT patients are increased. However, it might be due to the limited size of the previously studied cohort (Ribeiro-Silva et al. 2011), with just 4 LT and 4 DLT subjects, which has been increased in the present work. More studies should be conducted in order to shed light into the biology of the results here described. A higher cohort should be analyzed and studies about protein expression levels and degradation rates could be helpful to understand the results here reported.

In general, the values of TTR concentration (in both LT and DLT patients) found in this work are lower than the ones described in the bibliography by other techniques such as ELISA, nephelometry or radial immunodifusion. As it has already been discussed in detail in Chapter 2, different techniques can give different values, since the response of each method is different. In addition, the previous quantification techniques used are based on the recognition antigen (TTR) – antibody (polyclonal) directly in plasma. Therefore, since plasma is a high complex body fluid, there is the possibility that other major proteins (e.g albumin) present during the antigen-antibody reaction interfere in the assay, giving a higher background in the measure and incrementing the signal for TTR measurement. Moreover, standard curves for most of those techniques are performed with purified recombinant protein and therefore, without the characteristic plasma complexity. The fact that standard curves and samples are not measured under the same conditions may explain part of the differences observed. Finally, it is extensively reported in the bibliography that mass spectrometry techniques do not always correlate with immunoassays such as ELISA, without always finding the reason for such a lack of correlation (some examples: Kim et al. 2013, Lin et al. 2013).

There are not many works found in the bibliography addressing the determination of the wt:V30M ratio in FAP or DLT patients, however, among the few found, the amount of V30M TTR is described to be between 40 and 50% (da Costa et al. 2009, Tsuchiya et al. 2008, Tsuchiya-Suzuki et al. 2011). This quantitative discrepancy between our work and the previous ones may be explained by the different approaches used for quantification. In the previously reported works, determination of wt:V30M ratio was performed in terms of relative quantification (either by LC-MS/MS either by MALDI-FTICR MS). And in fact, as shown in our own comparison between absolute and relative quantification, differences in the response factor of the two variants are translated in an underestimation of %V30M (Fig. C4-2C). In addition, another fact that could contribute to the differences observed is that in (da Costa et al. 2009) quantification was performed based on the relative intensity of the wt peptide and a common peptide between the two TTR variants. Hence, quantification was based in the comparison of two different peptides that might present different ionization properties, which could lead to over or underestimation of the real % of wt and V30M. Despite the utility of relative quantification as a tool for protein forms comparison among different samples, it is not suitable to establish which of those forms are actually more abundant, as seen in the present study. The results shown here highlight the importance of using labeled peptide standards to measure the absolute amounts of the different forms and thus have a real evaluation of their serum distribution. Nevertheless, it should also be noted that intact protein analysis affords information on the relative

amounts of the Cys-10 PTM forms of wt and V30M TTR proteins separately, while this information is lost in the targeted LC-MS approach since N-term peptides used for quantifications are common between the two variants.

On the contrary, in terms of percent distribution of Cys-10 PTMs, no statistically significant differences were found between the two groups after the analysis of the two populations by HR-XIC, (Fig. C4-3). However, as seen in Table C4-2 and Fig. C4-4, due to the greater response factor for some of the minor PTM forms (S-CysGly and S-GSH), the intact protein method presents a somehow higher sensitivity for their relative quantification, allowing to observe significant differences between LT and DLT patients in terms of Cys-10 PTMs. Precisely, we have found that S-GSH and S-CysGly levels are significantly increased in DLT patients when compared to LT subjects, while Free Cys levels are decreased in DLT compared to LT patients, for both wt and V30M TTR.

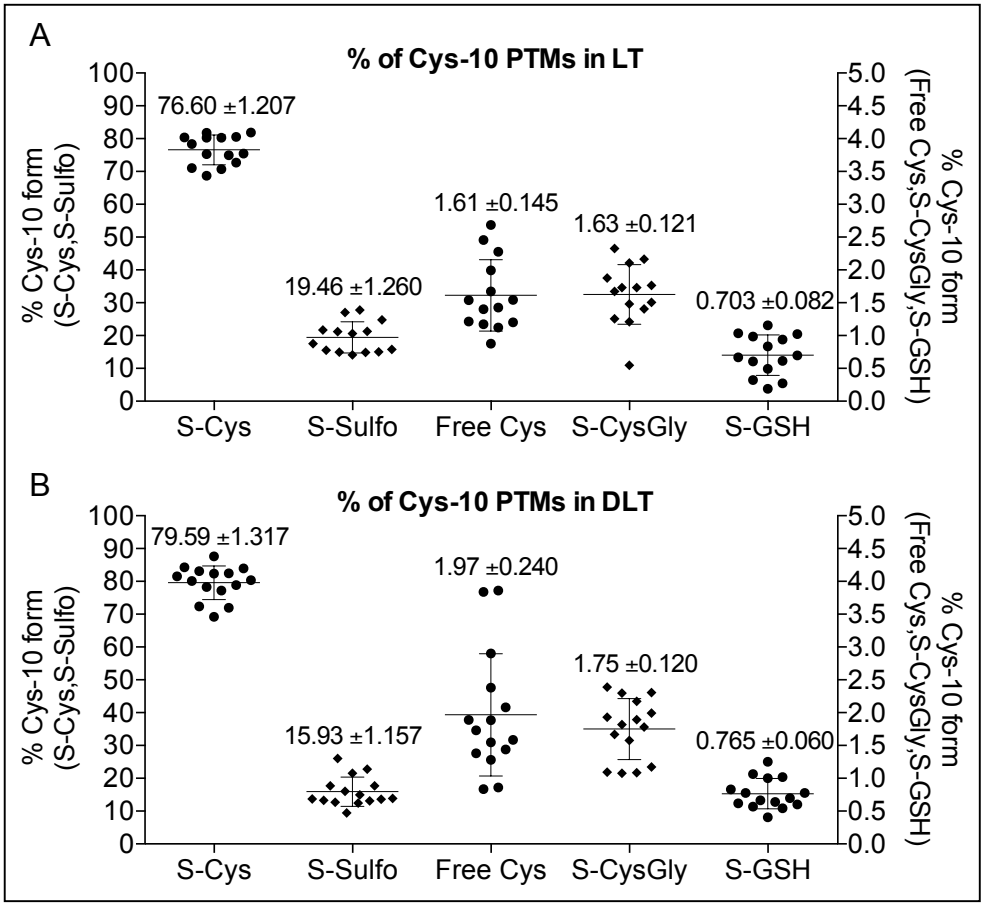

Figure C4-3. Absolute quantification of Cys-10 PTMs in TTR by HR-XIC methodology. (A) Percent distribution of Cys-10 PTMs in TTR from LT patients. Mean ±SEM values for each modification are indicated. **(B) Percent distribution of Cys-10 PTMs in TTR from DLT patients.** Mean ±SEM values for each modification are indicated.

Table C4-2. Mean Cys-10 TTR PTMs values for LT and DLT groups (relative quantification by Intact protein)

	% Cys-10 form (Mean ±SEM)		
	LT (wt TTR)	**DLT (wt TTR)**	**DLT (V30M TTR)**
Free Cys	29.86 ±1.577	21.53 ±1.301	20.73 ±1.312
S-Cys	50.36 ±1.330	51.74 ±2.135	53.99 ±1.997
S-CysGly	12.91 ±0.447	17.43 ±0.778	16.60 ±0.958
S-GSH	6.873 ±0.367	9.295 ±0.673	9.354 ±0.408

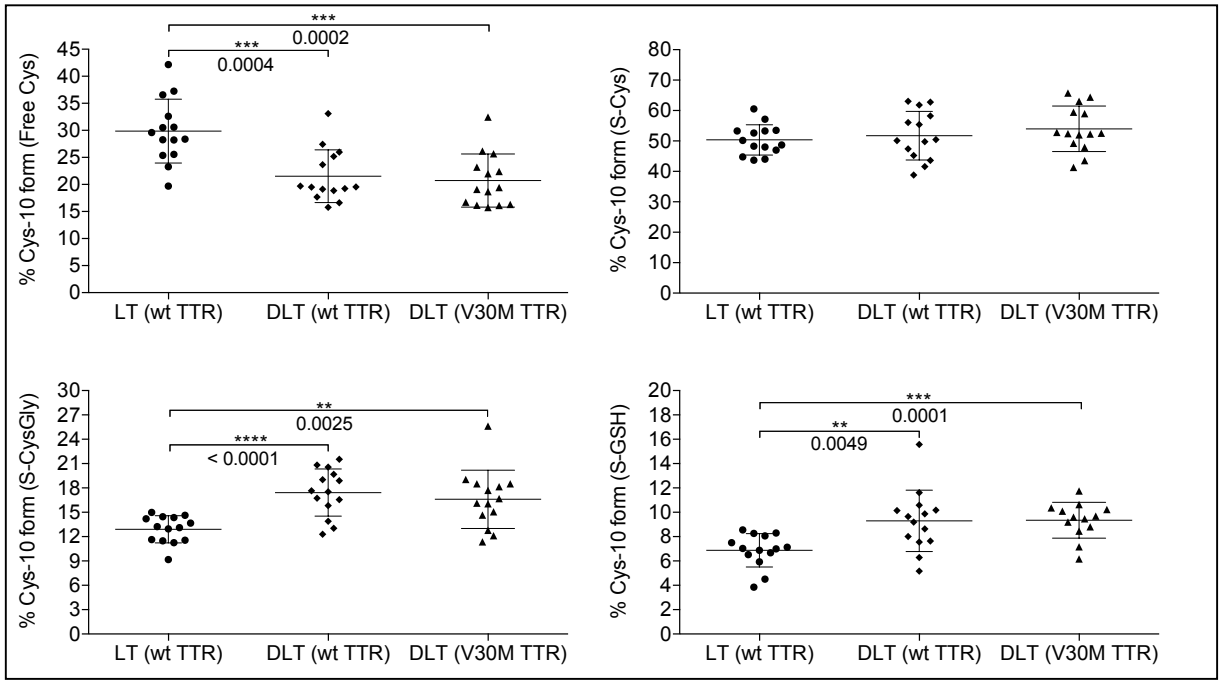

Figure C4-4. Relative quantification of Cys-10 PTMs in LT and DLT recipients by Intact protein. Percentages of each Cys-10 form are represented, comparison between groups was performed by the unpaired t-test with Welch's correction and p-values are indicated when significant differences where found.

This is the first time that both groups have been compared in terms of Cys-10 PTMs and the results here reported are highly promising since they confirm our previous findings suggesting S-GSH and S-CysGly Cys-10 PTMs as possible biomarkers of FAP onset (see Chapter 3). As previously explained in Chapter 3, it is well reported in the bibliography that oxidative stress is associated with many neurodegenerative diseases such as Alzheimer Disease (AD), Parkinson's disease (PD), Huntington's disease (HD) or amyotrophic lateral sclerosis (ALS). Multiple factors have been thought to contribute to neuronal loss through cell death including protein misfolding, excitotoxicity, activation of cell death pathways, mitochondrial dysfunction, increased iron deposition, and oxidative stress through the overexposure to reactive nitrogen species (RNS) and reactive oxygen species (ROS) (Mieyal et al. 2008, Sabens Liedhegner et al. 2012). Modulation of thiol-disulfide status of critical cysteines on proteins is recognized as an important mechanism of signal transduction and an important consequence of oxidative stress (Mieyal et al. 2008, Sabens Liedhegner et al. 2012). Hence, sulfur redox status plays a crucial role in the regulation of several cell functions like signaling, growth, survival or cell death. Protein function or stability is altered by reversible or irreversible modifications of cysteine and methionine residues, which at the same time perturb intracellular sulfhydryl homeostasis, linked to neurodegenerative diseases among many other disorders. Reversible thiol modifications, including intramolecular and intermolecular disulfides, protein sulfenic acids, and protein-glutathione mixed dissulfides (protein-SSG), protect proteins from irreversible overoxidation, allowing for a return to normal function after the oxidant challenge has subsided (Jones et al. 2000, Mieyal et al. 2008, Sabens Liedhegner et al. 2012). Finally, in neurodegenerative diseases, changes in GSH (reduced glutathione) levels have been reported (see Chapter 3). Hence, changes in the GSH/GSSG ratio and conditions that produce ROS and RNS can promote modifications on protein cysteine residues and on glutathione that serve as precursors to the formation of proteine-SSG. The

product of degradation of GSH by the enzyme γ-glutamyltranspeptidase (γ-GT) is CysGly, which can be degradated to Cys by the enzyme dipeptidase (Jones et al. 2000).

In the particular case of TTR and FAP, it has been reported that the presence of TTR soluble aggregates induces the production of RNS in human epidermoid and Schwannoma cell lines (Fong and Vieira 2012). Furthermore, there are evidences for the involvement of ROS in cellular toxicity due to TTR aggregates in a Schwannoma cell line. TTR aggregates increased cellular hydrogen peroxide production (about 125% increment) and promoted depletion of antioxidant factors such as glutathione and catalase and, more generally, diminished the cellular antioxidant capacity (Fong and Vieira 2013). There are also *in vivo* evidences for oxidative stress as oxidatively modified lipids and proteins have been reported in colon tissues and protein nitration has been observed in nerves of FAP patients (Ando et al. 1997, Sousa et al. 2001). Therefore, the increased levels of S-GSH TTR that we here report could be suggesting the presence of soluble TTR aggregates in DLT patients, which would induce ROS and RNS production and diminish the cellular antioxidant capacity. The various ways that protein thiol moieties could be converted to protein-SSG include thiol disulfide exchange if the GSSG concentration is high enough, reaction of GSH with protein-sulfenic acid or protein-SNO precursors, or recombination of protein and glutathione thiyl radicals (Sabens Liedhegner et al. 2012). Since S-CysGly is the product of degradation of S-GSH, it is normal to find an increase in S-CysGly when S-GSH is also augmented. Finally, since in plasma the major low-molecular weight sulphydryl/disulphide pool is CysSH/$(CysS)_2$, extracellular proteins are predominantly S-Cysteinilated (Jones et al. 2000), as it is also seen in our results. The fact that DLT patients might present soluble TTR aggregates in such a short time after transplantation, as indirectly suggested by the increase in the TTR isoforms S-GSH and S-CysGly, would be a possible explanation for the observed early onset of FAP. However, future studies should aim to confirm the presence of soluble TTR aggregates in the DLT cohort in order to further confirm if there is a correlation between its presence and the levels of S-GSH and S-CysGly.

C4.4.CONCLUSION

By means of our previously developed targeted mass spectrometry technique, together with the complementary intact protein approach, we have analyzed a total of 38 human plasma samples, corresponding to LT and DLT recipients at different time points after transplantation. We have been able to determine V30M TTR half-life in LT patients as well as its rate of appearance in DLT recipients by both an absolute and a relative quantification approach. Finally, we have found statistical significant differences between the two groups compared in terms of total amount of TTR and in its Cys-10 PTMs distribution. In particular, we have found that DLT recipients present higher TTR levels and increased amounts of S-GSH and S-CysGly modified TTR, suggesting a situation of higher oxidative stress in those patients, which, at the same time, could be an indicator of the presence of soluble TTR aggregates. The preliminary results here reported are highly promising since S-GSH and S-CysGly TTR levels in plasma could serve as an indirect measurement of the presence of soluble TTR aggregates before FAP onset and therefore, as a biomarker of disease progression.

C4.5.REFERENCES

Adams D (2013) Recent advances in the treatment of familial amyloid polyneuropathy. *Ther Adv Neuro Disor* 6(2):129–39.

Altland K and Winter P (1999) Potential treatment of transthyretin-type amyloidoses by sulfite. *Neurogenetics* 2(3):183–8.

Altland K, Winter P and Sauerborn MK (1999) Electrically neutral microheterogeneity of human plasma transthyretin (prealbumin) detected by isoelectric focusing in urea gradients. *Electrophoresis* 20(7):1349–64.

Andersson R (1976) Familial Amyloidosis with Polyneuropathy. A Clinical Study Based on Patients Living in Northern Sweden. *Acta Med Scand* Suppl 590:1–64.

Ando Y, Nyhlin N, Suhr O, Holmgren G, Uchida K, el Sahly M, Yamashita T, Terasaki H, Nakamura M, Uchino M and Ando M (1997) Oxidative stress is found in amyloid deposits in systemic amyloidosis. *Biochem Biophys Res Commun* 232(2):497–502.

Ando Y, Tanaka Y, Nakazato M, Ericzon BG, Yamashita T, Tashima K, Sakashita N, Suga M, Uchino M and Ando M (1995) Change in variant transthyretin levels in patients with familial amyloidotic polyneuropathy type I following liver transplantation. *Biochem Biophys Res Commun* 211(2):354–8.

Andrade C (1952) A peculiar form of preipheral neuropathy. *Brain* 75(3):408–27.

Azoulay D, Salloum C, Samuel D and Planté-Bordeneuve V (2012) Operative risks of domino liver transplantation for the FAP liver donor and the FAP liver recipient. *Amyloid* 19(S1):73–4.

Da Costa G, Gomes R, Correia CF, Freire A, Monteiro E, Martins A, Barroso E, Coelho AV, Outeiro TF, Ponces Freire A and Cordeiro C (2009) Identification and quantitative analysis of human transthyretin variants in human serum by Fourier transform ion-cyclotron resonance mass spectrometry. *Amyloid* 16(4):201–7.

Coutinho P, da Silva A, Lima J and Barbosa A (1980) Forty years of experience with type 1 amyloid neuropathy: review of 483 cases. *Amyloid and amyloidosis* Excerpta Med: 88–98.

Fong V and Vieira A (2012) Transthyretin aggregates induce production of reactive nitrogen species. *Neurodegener Dis* 11(1):42–8.

Fong V and Vieira A (2013) Pro-oxidative effects of aggregated transthyretin in human Schwannoma cells. *Neurotoxicology* 39:109–113.

Holmgren G, Ericzon B, Groth C, Steen L, Suhr O, Andersen O, Wallin B, Seymour A, Richardson S, Hawkins P and Pepys M (1993) Clinical improvement and amyloid regression after liver transplantation in hereditary transthyretin amyloidosis. *Lancet* 341(8853):1113–6.

Holmgren G, Steen L, Ekstedt J, Groth C, Ericzon B, Eriksson S, Andersen O, Karlberg I, Nordén G, Nakazato M, Hawkins P, Richardson S and Pepys M (1991) Biochemical effect of liver transplantation in two Swedish patients with familial amyloidotic polyneuropathy (FAP-met30). *Clin Genet* 40(3):242–6.

Jiang X, Buxbaum JN and Kelly JW (2001) The V122I cardiomyopathy variant of transthyretin increases the velocity of rate-limiting tetramer dissociation, resulting in accelerated amyloidosis. *Proc Natl Acad Sci USA* 98(26):14943–8.

Jones D, Carlson J, Mody V, Cai J, Lynn M and Sternberg P (2000) Redox state of glutathione in human plasma. *Free Radic Biol Med* 28(4):625–35.

Kim Y, Gallien S, van Oostrum J and Domon B (2013) Targeted proteomics strategy applied to biomarker evaluation. *Proteomics Clin Appl* 7(11-12):739–47.

Kingsbury JS, Klimtchuk ES, Théberge R, Costello CE and Connors LH (2007) Expression, purification, and in vitro cysteine-10 modification of native sequence recombinant human transthyretin. *Protein Expr Purif* 53(2):370–7.

Kishikawa M, Nakanishi T, Miyazaki A and Shimizu A (1999) Enhanced amyloidogenicity of sulfonated transthyretin. *Amyloid* 186(6):183–6.

Koike H, Hashimoto R, Tomita M, Kawagashira Y, Iijima M, Nakamura T, Watanabe H, Kamei H, Kiuchi T and Sobue G (2012) Impact of aging on the progression of neuropathy after liver transplantation in transthyretin Val30Met amyloidosis. *Muscle Nerve* 46(6):961–4.

Lin D, Alborn W, Slebos R and Liebler D (2013) Comparison of protein immunoprecipitation-multiple reaction monitoring with ELISA for assay of biomarker candidates in plasma. *J Proteome Res* 12(12):5996–6003.

Lladó L, Baliellas C, Casasnovas C, Ferrer I, Fabregat J, Ramos E, Castellote J, Torras J, Xiol X and Rafecas A (2010) Risk of Transmission of Systemic Transthyretin Amyloidosis After Domino Liver Transplantation. *Liver Transpl* 16(12):1386–92.

Longo Alves I, Hays M and Saraiva M (1997) Comparative stability and clearance of [Met30]transthyretin and [Met119]transthyretin. *Eur J Biochem* 249(3):662–8.

Mieyal J, Gallogly M, Qanungo S, Sabens E and Shelton M (2008) Molecular mechanisms and clinical implications of reversible protein S-glutathionylation. *Antioxid Redox Signal* 10(11):1941–88.

Nakanishi T, Yoshioka M, Moriuchi K, Yamamoto D, Tsuji M and Takubo T (2010) S-sulfonation of transthyretin is an important trigger step in the formation of transthyretin-related amyloid fibril. *Biochim Biophys Acta* 1804(7):1449–56.

Planté-Bordeneuve V and Said G (2011) Familial amyloid polyneuropathy. *Lancet Neurol* 10(12):1086–97.

Poulsen K, Bahl JM, Simonsen AH, Hasselbalch SG and Heegaard NH (2014) Distinct transthyretin oxidation isoform profile in spinal fluid from patients with Alzheimer's disease and mild cognitive impairment. *Clin Proteomics* 11(1):12.

Poulsen K, Bahl JMC, Tanassi JT, Simonsen AH and Heegaard NHH (2012) Characterization and stability of transthyretin isoforms in cerebrospinal fluid examined by immunoprecipitation and high-resolution mass spectrometry of intact protein. *Methods* 56(2):284–92.

Ribeiro-Silva C, Gilberto S, Gomes R, Mateus E, Monteiro E, Barroso E, Varela-Coelho A, da Costa G, Ponces-Freire A and Cordeiro C (2011) The relative amounts of plasma transthyretin forms in familial transthyretin amyloidosis: A quantitative analysis by Fourier transform ion-cyclotron resonance mass spectrometry. *Amyloid* 18(4):191–9.

Sabens Liedhegner E, Gao X and Mieyal J (2012) Mechanisms of Altered Redox Regulation in Neurodegenerative Diseases—Focus on S-Glutathionylation. *Antioxid Redox Signal* 16(6):543–66.

Samuel D and Adams D (2007) Domino liver transplantation from familial amyloidotic polyneuropathy donors: How close is the damocles sword to the recipient? *Transpl Int* 20(11):921–3.

Schmidt H, Nashan B, Pröpsting M, Nakazato M, Flemming P, Kubicka S, Böker K, Pichlmayr R and Manns M (1999) Familial Amyloidotic Polyneuropathy: domino liver transplantation. *J Hepatol* 30(2):293–8.

Sekijima Y, Hammarström P, Matsumura M, Shimizu Y, Iwata M, Tokuda T, Ikeda S-I and Kelly JW (2003) Energetic characteristics of the new transthyretin variant A25T may explain its atypical central nervous system pathology. *Lab Invest* 83(3):409–17.

Socolow EL, Woeber K a., Purdy RH, Holloway MT and Ingbar SH (1965) Preparation of I-131-labeled human serum prealbumin and its metabolism in normal and sick patients. *J Clin Invest* 44(10):1600–9.

Sousa M, Du Yan S, Fernandes R, Guimaraes A, Stern D and Saraiva M (2001) Familial amyloid polyneuropathy: receptor for advanced glycation end products-dependent triggering of neuronal inflammatory and apoptotic pathways. *Journal Neurosci* 21(19):7576–86.

Sousa MM and Saraiva MJ (2003) Neurodegeneration in familial amyloid polyneuropathy: From pathology to molecular signaling. *Progr Neurobiol* 71(5):385–400.

Terazaki H, Ando Y, Suhr O, Ohlsson PI, Obayashi K, Yamashita T, Yoshimatsu S, Suga M, Uchino M and Ando M (1998) Post-translational modification of transthyretin in plasma. *Biochem Biophys Res Commun* 249(1):26–30.

Tsuchiya A, Yazaki M, Kametani F, Takei Y and Ikeda S (2008) Marked Regression of Abdominal Fat Amyloid in Patients with Familial Amyloid Polyneuropathy During Long-Term Follow-Up After Liver Transplantation. *Liver Transpl* 14(4):563–70.

Tsuchiya-Suzuki A, Yazaki M, Kametani F, Sekijima Y and Ikeda S (2011) Wild-type transthyretin significantly contributes to the formation of amyloid fibrils in familial amyloid polyneuropathy patients with amyloidogenic transthyretin Val30Met. *Hum Pathol* 42(2):236–43.

Zhang Q and Kelly JW (2003) Cys-10 mixed disulfides make transthyretin more amyloidogenic under mildly acidic conditions. *Biochemistry* 42(29):8756–61.

Zhang Q and Kelly JW (2005) Cys-10 mixed disulfide modifications exacerbate transthyretin familial variant amyloidogenicity: A likely explanation for variable clinical expression of amyloidosis and the lack of pathology in C10S/V30M transgenic mice. *Biochemistry* 44(25):9079–85.

GENERAL CONCLUDING REMARKS

The current thesis aimed to address TTR related amyloidosis from two different perspectives by combining a therapeutic and a diagnostic approach. Particularly, we have worked on the search of new fibrillogenesis inhibitors and in the search of biomarkers of FAP progression.

Towards the aim of finding new therapeutic solutions for TTR amyloidosis, we have performed an *in vitro* screening of a library of 41 compounds selected by a new bioinformatic repurposing workflow. As a result, we have found 4 new TTR tetramer stabilizers with superior *in vitro* fibrillogenesis inhibition properties than the already approved drug Tafamidis. Those results assert the newly developed workflow in the search of new TTR fibrillogenesis inhibitors and confirm the usefulness of drug repurposing strategies.

Based on the clinical need stated by physicians regarding FAP onset diagnosis, we envisaged a new methodology for Cys-10 TTR PTMs analysis in order to look for biomarkers of disease onset and/or progression. Our newly developed targeted LC-MS methodology proved to be highly reproducible and allowed for absolute quantification of TTR and its Cys-10 PTMs levels. We have described a different response factor of the peptides analyzed when compared to relative quantification, proving the need for absolute quantification in the determination of Cys-10 PTMs levels in serum or plasma. Subsequently to development and set up of the analytical tools, we have analyzed samples of V30M TTR mutation carriers at different stages of disease and after liver and domino liver transplantation, together with wt TTR control individuals. As a result of the human samples analysis, we preliminary point out S-GSH and S-CysGly isoforms as biomarkers of disease progression. Particularly, we suggest that S-GSH and S-CysGly could be good indicators of the presence of soluble aggregates and a consequence of a situation of increased oxidative stress. We have observed increased levels of the two Cys-10 PTMs in asymptomatic patients when compared to controls or in domino liver transplanted patients when compared to liver transplanted ones. More importantly, we propose that S-GSH and S-CysGly levels may be good indicators of FAP onset, since the levels of the two isoforms are decreased after the first FAP symptoms appearance. The decrease in S-GSH and S-CysGly levels could be related to an increase in Grx activity upon TTR deposition. Therefore, and despite being preliminary, the results presented are highly promising since they offer a non-invasive and objective measure of disease stage, which could enable an early intervention in FAP treatment.

CONCLUSIONS

1. The protocol for recombinant production of Y78F rhTTR is highly reproducible and leads to the production of the TTR S-Glutathionylated form, as detected by MALDI-TOF MS, which is between 20-30% more amyloidogenic than wt TTR at short term fibrillogenesis studies and equally amyloidogenic at long term studies.

2. A library comprising 41 compounds selected by a bioinformatic repurposing workflow has been tested by means of our Kinetic Turbidimetric Assay, finding a total of 4 new TTR tetramer stabilizers. Moreover, these 4 compounds present greater *in vitro* fibrillogenesis inhibition than Tafamidis.

3. Two complementary mass spectrometry based methods for the quantification of the most common Cys-10 PTM isoforms of TTR in plasma or serum have been set up. The targeted LC-MS method developed here, unlike previously described methods, allows the absolute quantification of the levels of each of the Cys-10 modifications, as well as the absolute concentrations of wt TTR and amyloidotic V30M isoforms.

4. The intact protein ions of the different isoforms display large differences in response factors, which makes the targeted LC-MS analysis using standard peptides, mandatory for absolute quantification of their levels in serum. Nevertheless, the combined analysis by the two developed strategies constitutes a robust method for the characterization of Cys-10 PTM forms of TTR in serum and plasma.

5. After the intact protein analysis of all samples included in the Spanish cohort, an anomalous high frequency for the G6S TTR polymorphism has been found, with values of 31% in V30M TTR carriers and of 20% in the control group. In addition, we have found two patients heterozygous for V30M and homozygous for G6S, a condition not described previously.

6. Asymptomatic FAP individuals present significant increased levels of S-GSH and S-CysGly TTR isoforms when compared to a control group in the Spanish cohort studied. Additionally, this same TTR isoforms are significantly increased in domino liver transplanted patients when compared to liver transplanted patients in the analyzed Portuguese cohort.

7. Levels of S-GSH and S-CysGly TTR were significantly lower for FAP stage 1 patients when compared to asymptomatic patients in the Spanish cohort studied. Hence, the measure of S-GSH and S-CysGly TTR levels could be used as an indicator of disease onset, offering a non-invasive objective measure of disease stage and enabling an early intervention in the treatment of FAP after the very first symptoms.

ANNEX